JULY 2017

Ph. D. in Civil Engineering

GHASSAN SUBHI JAMEEL

UNIVERSITY OF GAZİANTEP
GRADUATE SCHOOL OF
NATURAL AND APPLIED SCIENCES

EXPERIMENTAL AND NUMERICAL STUDY ON STEEL FIBER REINFORCED SCC AND THOSE FILLED CIRCULAR STRUCTURAL STEEL TUBES

Ph. D. THESIS
IN
CIVIL ENGINEERING

BY
GHASSAN SUBHI JAMEEL

JULY 2017

Experimental and Numerical Study on Steel Fiber Reinforced SCC and Those Filled Circular Structural Steel Tubes

Ph. D. Thesis
in
Civil Engineering
University of Gaziantep

Supervisor
Assoc. Prof. Dr. Esra METE GÜNEYİSİ

by
Ghassan Subhi JAMEEL
July 2017

REPUBLIC OF TURKEY
UNIVERSITY OF GAZİANTEP
GRADUATE SCHOOL OF NATURAL & APPLIED SCIENCES
CIVIL ENGINEERING DEPARTMENT

Name of the thesis: Experimental and Numerical Study on Steel Fiber Reinforced SCC and Those Filled Circular Structural Steel Tubes

Name of the student: Ghassan Subhi JAMEEL

Exam date: July 10, 2017

Approval of the Graduate School of Natural and Applied Sciences

Prof. Dr. A. Necmeddin YAZICI

Director

I certify that this thesis satisfies all the requirements as a thesis for the degree of Doctor of Philosophy.

Prof. Dr. Abdulkadir ÇEVİK

Head of Department

This is to certify that we have read this thesis and that in our opinion it is fully adequate, in scope and quality, as a thesis for the degree of Doctor of Philosophy.

Assoc. Prof. Dr. Esra METE GÜNEYİSİ

Supervisor

Examining Committee Members:	Signature
Prof. Dr. Hanifi ÇANAKCI	....
Assoc. Prof. Dr. Esra METE GÜNEYİSİ	....
Assoc. Prof. Dr. Kasım MERMERDAŞ	....
Asst. Prof. Dr. Hatice Öznur ÖZ	....
Asst. Prof. Dr. Ayşe Y. GÜNAL	....

I hereby declare that all information in this document has been obtained and presented in accordance with academic rules and ethical conduct. I also declare that, as required by these rules and conduct, I have fully cited and referenced all material and results that are not original to this work.

Ghassan Subhi JAMEEL

ABSTRACT

EXPERIMENTAL AND NUMERICAL STUDY ON STEEL FIBER REINFORCED SCC AND THOSE FILLED CIRCULAR STRUCTURAL STEEL TUBES

JAMEEL, Ghassan Subhi

Ph.D. in Civil Engineering

Supervisor: Assoc. Prof. Dr. Esra METE GÜNEYİSİ

July 2017

168 pages

The present study aims firstly to investigate experimentally material behavior of steel fiber reinforced self-compacting concrete (SFRSCC) and secondly to introduce a numerical investigation regarding the structural performance of circular structural steel tube columns infilled with SFRSCC. To this purpose, twelve different mixtures were designed. Hooked ends steel fiber was used to produce SFRSCC. Some engineering properties in terms of workability, compressive and flexural strength, fracture energy and steel-concrete bond strength were tested. Thereafter, to simulate the behavior of SFRSCC filled steel tubular short column under concentrically compression load, the experimental results obtained in the first part of the study were utilized in the evaluation of ultimate axial capacity of concrete filled steel tube column. In this context, different diameter to tube thickness ratio and steel grade were utilized. Based on the predicted column axial capacity, a comparative analysis was made by means of international design codes such as Eurocode 4, ACI, AIJ and DL/T. At each code, a total of 216 column capacity results were assessed and discussed herein. The results revealed that the experimental parameters significantly affected the fresh and mechanical performance. Furthermore, the analytical study presented in this thesis showed that the codes assessed a rational capacity for such special composite column.

Keywords: Axial capacity; Concrete; Composite column; Mechanical property; Steel fiber

ÖZET

ÇELİK FİBER TAKVİYELİ KYB VE BUNUNLA DOLGULU DAİRESEL YAPISAL ÇELİK TÜPLER ÜZERİNE DENEYSEL VE NÜMERİK BİR ÇALIŞMA

JAMEEL, GHASSAN SUBHI

Doktora Tezi, İnşaat Mühendisliği Bölümü

Tez Yöneticisi: Doç. Dr. Esra METE GÜNEYİSİ

Temmuz 2017

168 sayfa

Bu çalışma, ilk olarak çelik fiber takviyeli kendiliğinden yerleşen betonun (ÇFTKYB) malzeme davranışının deneysel olarak incelenmesini; ikinci olarak ise bu betonlarla doldurulmuş dairesel yapısal çelik tüplerin yapısal performansı üzerine nümerik bir incelemeyi içerir. Bu amaçla, 12 farklı karışım tasarlandı. Üretimde uçları kancalı çelik fiber kullanıldı. İşlenebilirlik, basınç ve eğilme dayanımı, kırılma enerjisi ve çelik-beton aderans dayanımı gibi bazı mühendislik parametreleri incelendi. Daha sonra, merkezi olarak basınç yüküne maruz bırakılan ÇFTKYB ile doldurulmuş çelik tüp şeklindeki kısa kolonu simüle etmek için, çalışmanın birinci kısmında elde edilen deneysel sonuçlar kolonun maksimum eksenel kapasitesinin değerlendirilmesinde kullanıldı. Bu bağlamda farklı çap-tüp cidar kalınlığı oranı ve çelik sınıfları kullanıldı. Tahmin edilen kolon eksenel kapasitesini temel alarak, Eurocode 4, ACI, AIJ ve DL/T standartları kullanılarak karşılaştırmalı analizler yapıldı. Her bir standartta, toplam 216 kolun kapasite değeri hesaplandı ve irdelendi. Sonuçlar deneysel parametrelerin taze ve mekanik performansı büyük ölçüde etkilediğini gösterdi. Bunun da ötesinde, tez kapsamında sunulan analitik çalışma, standartların bu şekilde hazırlanmış özel kompozitlerin kapasitesini anlamlı olarak değerlendirdiğini gösterdi.

Anahtar Kelimeler: Eksenel kapasite, Beton, Kompozit kolon, Mekanik özellik, Çelik fiber.

To My Parents.........

ACKNOWLEDGEMENTS

I would like to express my highest appreciation to my supervisor, Assoc. Prof. Dr. Esra METE GÜNEYİSİ, for her continual encouragement and supervision. She offered me so much advice and always guiding me in the right direction. I have learned a lot from her, without her help, I could not have finished my PhD dissertation successfully. It is not sufficient to express my gratitude with only a few words.

Special thanks also given to Assoc. Prof. Dr. Erhan GÜNEYİSİ. He is directly or indirectly involved in the process of producing this research report, for their generous assistance.

I also appreciate the advice of the committee members, Prof. Dr. Hanifi ÇANAKCI Assoc. Prof. Dr. Hatice Öznur ÖZ, Assoc. Prof. Dr. Kasım MERMERDAŞ and Assoc. Prof. Dr. Ayşe Y. GÜNAL for their critical comments, which enabled me to notice the weaknesses of my dissertation and make the necessary improvements according to their comments.

I am very grateful for my parents, brothers and sister. Their understanding and their love encouraged me to work hard and to continue pursuing a Ph.D. project abroad. Their firm and kind-hearted personality has affected me to be steadfast and never bend to difficulty. They always let me know that they are proud of me, which motivates me to work harder and do my best.

I am greatly indebted to my devoted wife and my daughter and son. They form the backbone and origin of my happiness. Their love and support without any complaint or regret has enabled me to complete this Ph.D project.

Finally, I would like to thank to those who took part in completion of this thesis.

TABLE OF CONTENTS

Page

LIST OF TABLES

LIST OF FIGURES

Page

LIST OF SYMBOLS/ABREVIATIONS

ACI	American Concrete Institute
A_c	Cross-sectional area of the concrete specimen core
A_{sc}	Area of composite section
A_s	Cross sectional area of steel
ASTM	American Society for Testing and Materials
BS	British standard
CH	Hydroxide Calcium
C-S-H	Calcium-Silicate-Hydrate
CFST	Concrete Filled Steel Tubular
D	Outer diameter of concrete filled steel tube
D/t	Diameter to Thickness
E_{c2}	Elastic modulus of concrete
E_s	Elastic modulus of steel
$(EI)_{eff^2}$	Effective flexural stiffness of CFST
f_c'	Compressive strength of concrete cylinders (150×300 mm)
f_{cu}	Compressive strength of 150 mm cube
f_y	Yield stress of steel
f_{ck}	Characteristic concrete strength
f_{scy}	Nominal yielding strength of the composite section

f_{flex}	Flexural Strength
FRC	Fiber Reinforced Concrete
Fst	Splitting Tensile Strength
G_F	Fracture Energy
ITZ	Interfacial Transition Zone
LVDT	Linear Variable Displacement Transducer
MK	Metakaolin
nS	Nano Silica
N_{cr}	Euler buckling load of the pin-ended CFST column
N_{pIR}	Cross-section plastic resistance of the CFST column
SCC	Self-compacting Concrete
SF	Steel Fiber
SFRSCC	Steel Fiber Reinforced Self-compacting Concrete
T	Thickness of steel tube
τ_b	Bond Strength
w/b	Water per binder ratio
w/c	Water per cement ratio
$\bar{\lambda}$	Relative slenderness of the CFST column
ξ	Confinement factor

CHAPTER 1

INTRODUCTION

1.1 General

To be used more efficiently in the steel-concrete structures, various types of structural concrete have been tried to develop. Among them, the relatively new concrete, that does not require any form of external vibration to compact, is the self-compacting concrete (SCC). SCC causes a great change in concrete alignment as it runs through the self-mass. Researches in Japan launched it towards the end of the1980s (Nagamoto and Ozawa, 1997). Since it can move under its own mass within the limited portions, SCC works effectively without exhibiting any form of separation or the bleeding. The concrete that has the aforementioned characteristics ought to have less yield value relatively so as to obtain higher running capability and an average viscosity since separation and bleeding should be prevented. It is essential for the stractural concrete to be in a homogenous state that can help in placing, transportation, and curing in order to be durable and have satisfactory structural functions. In the process of developing SCC the balance between deformity and stability should be kept (Nagamoto and Ozawa, 1997).

Researchers laid some instructions for the structural SCC mixture proportions as follows: (1) The volume of the aggregate should be reduced in congruence with the paste volume (2) The volume of the powder should be increased with lower ratio of water with cement (3) The minimisation of the coarse aggregate quantity balanced with its maximum size (4) And different viscosity enhancing admixtures should be used (VEA) (Nagamoto and Ozawa, 1997). It is required to improve a method for the SSC mixture because the proportions of the SSC mixture and the properties of its matter influence SCC compatibility. Okamura and Ozawa (1995) proposed such a design for the mixture of SCC that includes the certain known quantity of contents from the fine aggregate and coarse aggregate. In addition, the mixture became compatible by balancing the ratio of water and dry contents as well as the amount of superplasticizer. The quantity of the coarse and fine aggregate is designed in accordance with the volume of the total solid. Thus, the coarse contents constitute half of the total solid volume and sand ought to be about 40% in comparison to the mortar volume. Furthermore, the proportion by volume between the water and powder is considered within the range of 0.9-1.0 whereas, keeping the powder properties and amount of superplasticizer in mind. However, many experiments may help in assessing the ratio between the water and powder. Conversely, the absence of a constructed method for the mixture of SSC is one of the restrictions.

In structural applications, In the last ten years the was a surge in the importance and the desirability of self-compactible cementitious materials. Traditional fiber reinforced concrete needs a great level of vibration effort to achieve complete compaction and for that reason the advancement of steel fiber reinforced self-compacting concrete shows many economical and technical advantages. Self-compactibility of fibred cementitious materials can so improve the behavior of the fibred composites through attaining best regular fiber dispersion (Ozyurt, 2005).

Steel fiber is the most usually used type of fiber in most structural and non-structural sorts of work (Mehta, 2006; Dvorkin, 2011). It is popular for economical, production facilities, strengthening effects, and resilience in adverse environments (Barros, 2011). The concrete's properties and eventually performance of the structures are affected by several variables like orientation, distribution, concentration, and fiber geometry.

An important strategy to develop SCCs further is to boost the properties to a stage similar with that of bulk paste, which can be done by using another essential mineral cementing materials ultra fine particles as nano level. For instance, nano silica (nS) seems to be the most prevalent nano-particle for the researchers since it involves minute particles (10^{-9} m) that can fill the gaps between cement and particles. nS be able to produce from the adjustment of molecules and atoms so as to generate somewhat larger scale of materials (Shaikh and Supit, 2014). The main properties of nS, such as the specific density, pore structure, specific surface area, and particle size distribution, are thought of as an quintessential factor in speeding up the pozzolanic reaction of pozzolanically since it compensated for the early increase in strengths (Li, 2004; Shaikh and Supit, 2014; Supit et al., 2013).

To understand how nano particles work, two useful contribution reactions of silica in SCC should be viewed as a central roadmap. First of all, the silica surface works as a nucleation center for the development of C–S–H phases formed by hydration known as seeding effect (Deschner et al., 2011; Thomas et al., 2009; Land and Stephan, 2012). Afterward, the silica particles react pozzolanically with CH which is formed before by the hydration of alite (Korpa et al., 2008; Qing et al., 2007; Jo et al., 2007).

The resulting minuscule nano silica particles may frequently form a compressed microstructure by reducing gaps between particles of cement and other constituents and increasing particle packing density, which is called the filler effect (Krauss and Budelmann, 2011; Kumar et al., 2012; Oertel et al., 2013). Moreover, Seeding effect is one of the main mechanisms in the filler effect (Lothenbach et al., 2011).

Since the middle of 1990s, many researchers have been interested in the use of metakaolin (MK) as a supplementary cementitious material to improve concrete performance (Caldoarone et al., 1994; Badogiannis et al., 2005; Hubertova and Hela, 2007; Güneyisi et al., 2012a; Güneyisi et al., 2012b; Güneyisi et al., 2013).

MK is different from other natural or artificial mineral admixtures in that it needs a series of processes to achieve pozzolanic property. MK is activated by thermal process known as calcination in a temperature range of 650–800 ^{o}C (Wild et al., 1996). Thermal activation of the kaolin essentially depends on the mineralogical structure (Sabir et al., 2001; Shvarzman et al., 2003). MK tends to react with portlandite (CH) produced by the hydration process resulting cementitious products that change the micro-structure of concrete and thus improve its total mechanical and durability performance (Barnes et al., 2003; Güneyisi et al., 2008).

1.2 Steel-concrete composite members

Steel-concrete considered as a composite structure and is commonly used in the construction of modern bridges and buildings, even in areas under the risk of seismic. Generally, the concrete sections characterized by its high compressive strength and stiffness whereas the steel sections possess high ductility and superior tensile strength. The composite elements throughout the structural system combine the favorable properties of concrete and steel (Uy et al., 2001; Varma et al., 2002; Giakoumelis and Lam, 2004). The modern improvement of concrete constructions started in the 1800s. With the enhancement of concrete industry approached an era of investigations which also involved the use of iron with concrete, and yielded the first iron-concrete composite structures (Collings, 2008). In more modern times there was a duration of experimentation in the end of 1950s to 1960s where composite construction with embedded steel elements, pre-stressed beams, as well as the first pre-casting of deck components, were first introduced (Cracknell, 1963; Svensson, 2005).

The main members in composite construction can be constructed as slabs, beams and columns. The composite slab can be defined as a slab system containing concrete (normal weight concrete or lightweight concrete) placed over cold-formed steel deck. The steel deck behaves as a formwork for the fresh concrete during casing process and as additional reinforcement for the slab during its life service, Figure 1.1. A composite beam is a steel beam connected to the slab of reinforced concrete slab in such a way they act together as a single section. Such member has the advantage that the reinforced concrete slab takes most of the compression action whereas the steel beam supports the overall system for tension actions, Figure 1.2. Typically, the composite column of steel and concrete generally utilized as a load bearing element in a composite structure. Such column consists of earthier a concrete encased steel section or concrete filled steel tubular (CFST) column, Figure 1.3 (Şamhâl, 2005).

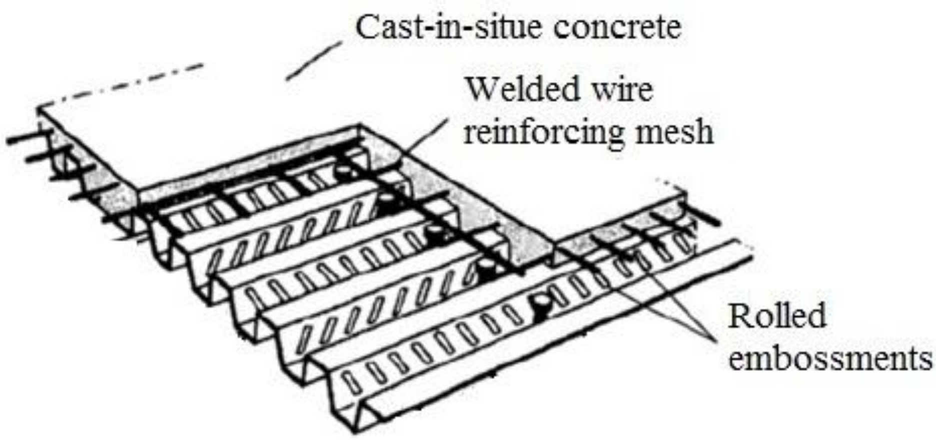

Figure 1.1 Composite slab (Crisinel and Marimon, 2004)

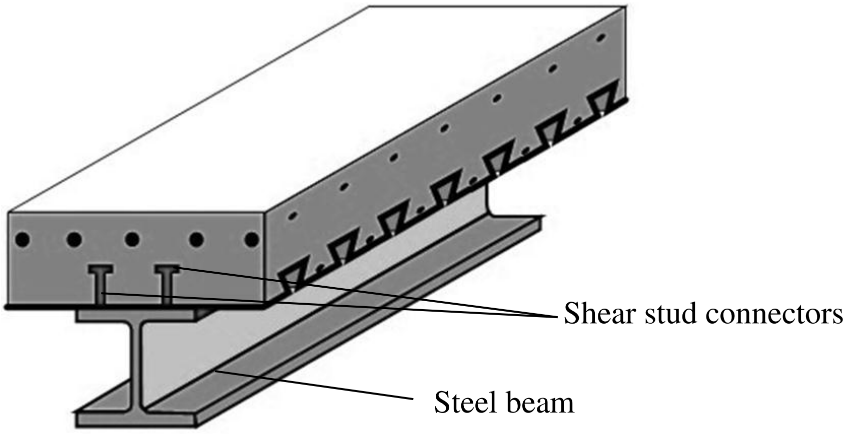

Figure 1.2 Composite beam (Choudhary, 2017)

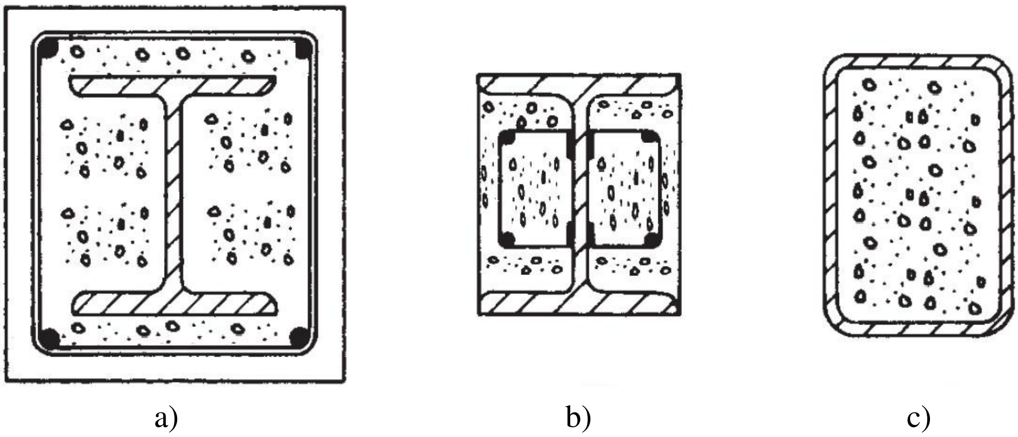

Figure 1.3 Composite column, a) for concrete-encased H-section, b) for concrete encased I-section and c) for concrete filled steel tube (Johnson, 2004)

The use of CFST columns in building construction has been received a great attention in the recent years due to its superior structural performance. The CFST column characterized by significant advantages such as its capability to provide higher confinement in the concrete, fire and earthquake resistance, the concrete in-filled the steel tube is delayed local buckling, extra construction cost can be avoided, etc. Normally, it was utilized in different composite frame constructions such as buildings, stadiums, bridges, subway stations, workshops, electricity pylons and poles for example, Figure 1.4 presents the Canton Tower in Guangzhou, China. The structure involves of a space lattice composite frame and a reinforced concrete core. The height of the main structure is reached to 454 meters, and the height of its pinnacle is 600 meters. As can be seen the CFST columns constructed in inclined forms. The numbers of inclined concrete filled steel circular tube columns are 24 and the maximum diameter and wall thickness reached to about 200 and 5 centimeters, respectively (Han et al., 2014; Huang, 2015). Another example on the use of CFST columns in the real constructions is given in Figure 1.5. This is utilized as industrial building columns. CFST laced columns provide a large cross-sectional moment of inertia with a relatively small section (Han, 2007; Cui et al., 2013).

Figure 1.4 Canton Tower completed in 2010, China (Han et al., 2014)

Figure 1.5 CFST laced columns used in real constructions (Han, 2007)

The use of hybrid fiber-reinforced cementitious composites is of particular interest, due to its noteworthy potential in successful enhancing the structural performance through rather modest variations in constructional and manufacturing technologies (Chen, 1997). Regarding this concept, the hybrid concrete infilled the steel tube must satisfy the quality of high performance concrete so as to yield high ductility and strength composite column. Generally, there are different materials can be used to achieve this objective (i.e. steel fibers). The utilization of fiber to reinforce concrete has attracted the interest of the investigators due to the improvement of tensile strength of concrete (Nili and Afroughsabet, 2012; Güneyisi et al., 2014). The improvement of structural performance of concrete can lead to produce composite column having higher ductility and absorption energy capacity.

The scientific research related to CFST column infilled with SCC is a relatively new research area on which a very limited investigation has been conducted (Jamaluddin et al., 2013; Aslani et al., 2017). It can be expected that due to the favorable rheological properties of SCC, new structural applications can be recognized and various benefits can be definite. The main benefit from a practical point of view regarded the utilization of SCC involves in employing the steel tube as a formwork to cast concrete without the need of vibration directly inside it. Besides the absence of vibration process, other factors such as dense reinforcement, complex sections, cost saving (i.e reduced labor cost) and environmental conditions encourage the use of SCC instead of ordinary concrete (Muciaccia et al., 2011). Thus, it can be stated that the high performance of steel fiber reinforced SCC filled steel tube is a motivation for further investigations in this topic.

1.3 Aim and objectives

The first topic of this study is to examine the properties of hooked end steel fiber reinforced SCC (SFRCC) with nS and MK and estimate the ability of production of such structural SCC mixtures. Also, the aim is to evaluate combined effect of two or three of additives which used in this study on the SCC mixtures (nS blended MK, nS blended steel fiber, MK blended steel fiber, and nS/MK blended steel fiber). The fresh, hardened, and fractured capability of SCC in the presence of such additives were tested. It should be noted that the efficient utilization of nS or MK and also other power full materials will serve as a replace part of cement or a new source of cementless materials. This reduces considerably the environmental impact of cement industries. Another important issue that the concrete with fibres, as already found by a several researchers, can improve the toughness of SCC by arrest propagation of cracks.

The second objective of this thesis is to investigate the structural behaviour of CFST columns infilled with SFRCC under the action of compression. To this goal, three ratios of diameter to thickness (D/t) and yield strengths of the steel tube were used. Moreover, so as to take the advantage of the experimented compressive strength on the structural performance of CFST column, the axial capacity of the composite columns were evaluated by using the experimental test results for 28 and 90 days through four international design provisions, namely, Eurocode 4 (EC4), American Concrete Institute (ACI), Japanese Code (AIJ) and Chines Design Code for Steel Concrete Composite Structures (DL/T). It is worthy to mention that the development of the high performance and low cost as well as environmentally friendly concrete-filled tubular structural member is particularly important for the designer so as to make and design the high performance and sustainable composite structures. On this issue, the mixture properties of concrete infill and its interaction with surrounding steel are the key factors.

1.4 Organization of thesis

The organization of the dissertation includes six chapters.

Chapter 1- It encloses the introduction, steel-concrete composite members and aims and objectives of the dissertation.

Chapter 2- This section is composed of the literature review and contains the general background knowledge regarding SCC and its theoretical and experimental aspects. Furthermore, this chapter includes the introduction of nS, MK and steel fibers. Additionally, their influences on the SCC fresh, fracture, and mechanical attributes. Also, the definition, types and structural performance of the CFST column as well as the main differences between such composite column and conventional reinforced concrete column and its applications are described.

Chapter 3- This chapter discusses the protocol of the dissertation. It includes the characteristics of the materials which are used in concrete manufacture. Moreover, it involves the test conducted on fresh and hardened traits of SCCs. On the other side, the section related to the numerical study which includes the design code and formulas for examining the ultimate capacity of the CFST columns having steel fibers reinforced SCC are presented in this chapter.

Chapter 4- In this chapter, test results and discussion are covered which includes evaluation, indication and discussion related to the test.

Chapter 5- Presents the results of analytical study to examine the behavior of steel fiber reinforced SCC filled steel tube columns subjected to compressive load. The design code of comparisons on the calculated axial capacity of such structural members were adopted by utilizing of four provisions of EC4, ACI, AIJ and DL/T.

Chapter 6- This section comprises of the conclusion drawn from the experimental and analytical study.

CHAPTER 2

LITERATURE REVIEW

2.1 Fiber reinforced concrete

2.1.1 History of FRC

The utilization of fiber in construction is not a modern innovation as Egyptians and Babylonians improved the quality of adobe bricks by reinforcing them with hay (ACI Committee 544, 1996). Metal waste was used to reinforce concrete in 1874 (Minelli, 2005) and in the 1900s, asbestos was added to concrete. However, the research community has only started to focus on fiber reinforced concrete (FRC) in the 1950s. As of the 1960's FRC using glass, synthetic, and steel fiber had been experimented with, and in the same period straight steel fiber was utilized for the first time to reinforce concrete and mortar (Balaguru and Shah, 1992). Manufacturing steel fiber reinforced concrete (SFRC) began in Europe in the late 1970's; however, it was without standards or recommendations for utilization by engineers. The implementation of SFRC was slow in part because of the absence of standards (Ross, 2008).

2.1.2 Steel fiber

Due to the fast development in concrete technology, high strength concrete may be produced easily (Balaguru et al., 1992). As the strength of concrete increases, ductility is reduced, which is the main concern regarding high strength concrete: it becomes more brittle as it becomes stronger. However, the problem of the inverse relationship between ductility and strength may be handled by through the addition of fiber (Wafa and Ashour, 1992).

FRC was first scrutinized academically in the united states in the year 1963 (Nanni, 1998) even though it was steel fiber was first used in concrete in 1910 by Porter (Naaman 1985). It is a composite material that contains the traditional hydraulic cement, sand, gravels, water in addition to small fiber. To increase

Flowability, superelasticizers may be added as well. The fiber utilized to manufacture FRC could be made of steel, plastic, glass and other materials and the engineering specifications of fiber are the shape, raw material, length, diameter and type of cross-section. By definition, Steel fiber is steel with an aspect ratio (proportion of length to diameter) ranging 20 and 100 with small, discrete lengths and various cross sections. It should also be small enough to be randomly dispersed with ease in fresh concrete mixture by conventional mixing methods (ACI 544.1R, 1996). Steel fiber can be produced in various shape (Figure 2.1) and these geometries are shaped in the production process (Figure 2.2).

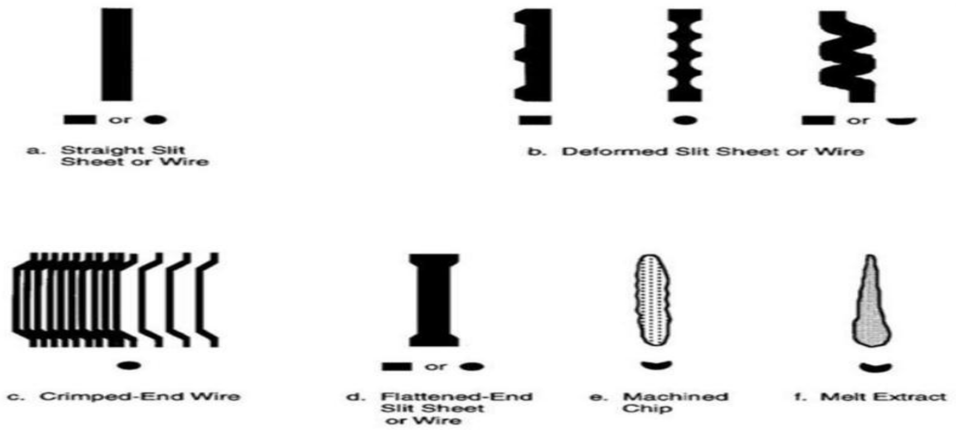

Figure 2.1 Different steel fiber geometries (ACI 544.1R, 1996)

Figure 2.2 Different types of steel fiber (Weiler and Grosse, 2010)

As steel fiber is mixed into the concrete, it improves several mechanical properties like ductility, toughness, tensile strength, and alters the macro and micro cracking. The extent of this enhancement is based on steel fiber sort, form, length, cross-section, bond property of fiber, fiber quantity (Shah and Naaman, 1976; Altoubat and Lange, 2001; Bayramov et al., 2004). The tensile strength improves considerably when steel fiber is added, through the resulting crack arresting process (Nanni, 1998). Researchers found that using steel fiber improves the flexural strength due to high strain value (Shah and Naaman, 1976). Adding steel fiber to concrete increases considerably the splitting tensile strength and gives an rise in the energy needed for fracture because of the crack block effect of the fiber, Further, splitting tensile strength and fracture energy are greatly influenced by both aspect ratio and fiber volume fraction (Bayramov et al., 2004).

Steel fiber is categorized by ASTM A820 according to the materials utilized in its production. The four various types of steel fiber according to ASTM A820 are as follows: Cold-drawn wire, cut sheet, melt-extracted, and other fiber.

- Type I (Cold wire fiber): This kind is made of drawn steel wire, and it is the most available type on the market.
- Type II (Cut sheet fibers): This type is produced by laterally shearing off steel sheets.
- Type III (Melt-extracted fiber): It is produced through a comparatively complicated technique. Liquid metal is lifted from a molten metal surface through a wheel. Then, the lifted molten metal is frozen quickly to form fibers and taken off the wheel though centrifugal force. Thus, Crescent-shaped cross section fibers are produced.
- Type IV (Other fiber): This type is produced for tolerances to length, diameter, aspect ratio, lowest tensile strength and bending request (ASTM, 2011).

The volume for using steel fiber ranges from 0.25% to 2%. In general, using over 2% decreases fiber dispersion and the workability, and required distinct mix design and concrete placement method (UM, 2012).

It was recommended by Bekaert, a major producer of steel fiber, that steel fiber may be added along with aggregates and sand, or in freshly mixed concrete, but never used as the initial ingredient in the mixer (Bosfa, 2012). Since the use of steel fiber, especially at large percentages, reduce the workability, it is advised to use superplasticizer in order to maintain workability (MWM, 2012).

2.1.3 Studies on steel fiber reinforced concrete

Various materials, such as steel, polypropylene, and glass … etc., have been used to manufacture fiber, which spread progressively to other applications, particularly to manufacturing FRC (ACI Committee 544, 1996). Concrete is viewed as a building material with strong heterogeneous behaviour, with high compressive strength and a little tensile strength normally about 5–8% of the compressive strength (Eurocode 2, 2004). Furthermore, the strain capacity of concrete is small and brittle in fracture. At present, special attention is paid to utilizing FRC, particularly to structures with high standards of performance and durability. The behaviour of FRC is largely affected by the binding matrix characteristics and by its interaction with the reinforcing fiber. The most prevalent fiber that can enhance the characteristics of plain concrete is manufactured from steel, glass or polypropylene (Buratti et al. 2011; Wang et al. 2012).

Most studies regarding FRC have concentrated on steel fiber. This sort of fiber is normally utilized in industrial pavements (Sorelli et al., 2006), precast industry (Ferrara and Meda, 2006) and tunnel linings (Bernard, 2001). Research accentuates the fact that mode of failure of steel fiber reinforced concrete (SFRC) alters from fragile to ductile and that the post-cracking response becomes considerably better (Thomas and Ramaswamy, 2007; Olivito and Zuccarello, 2010). Several studies indicate the improved toughness, ductility and flexural strength of the SFRC, whose values range from 30 to 125% in comparison to plain concrete and based on concrete strength and the amount of fiber (Buratti et al., 2011; Thomas and Ramaswamy, 2007; Olivito and Zuccarello, 2010; Song and Hwang, 2004; Ahin and Köksal, 2011; Banthia and Sappakittipakorn, 2007). Nonetheless, there are contrary outcomes regarding the expectation of material characteristics even with this fiber. For instance, some researchers found that the compressive strength of SFRC (Thomas and Ramaswamy, 2007; Song and Hwang, 2004) rises to 10% in comparison with plain concrete; whereas, other research maintains that the alteration is merely marginal or not even related with the incorporation of fiber (Olivito and Zuccarello, 2010; Ahin and Köksal, 2011).

Simoes et al. (2017) tested the mechanical behaviour of SFRC. Four volumetric proportions were adopted, ranging from 0.5% to 2% in 0.5% increments. The influence of fiber and dosage on the properties of the SFRC, including compressive strength, bending behaviour, cracking and maximum loads and ductility was analysed. it was found that the compressive strength generally improves with the reinforcement dosage, and that this growth is greatly affected by the characteristics of the fiber. The steel fiber is the ones impacting more significantly on the compressive strength with a gain increasing proportionally up to a 1.5% volume of fiber. It then decreases for 2.0% of fiber as shown in Figure 2.3. Generally, the compressive strength of SFRC tends to increase with the fiber addition. This property is enhanced by the confinement provided by the fiber to the matrix. In compression, the latter tends to expand by Poisson’s effect and the fiber oppose to this effect, thus increasing the strength. Steel fiber provide the composite material a better capacity to withstand high deformations. An increase in the load capacity is also observed, with a maximum of 160% for addition of 2.0% of steel fiber. The deformation capacity increases significantly when comparing with that of the reference. The response also changes from fragile to ductile. For steel fiber mixtures, the maximum load is always higher than that of the reference. This behaviour was expected, since more fiber in the tension zone mean more material to resist to the load (Figure 2.4). The mixtures reinforced with steel fiber exhibited a ductile behaviour. For these mixtures, with the increase in fiber addition, cracks have more fiber linking their boundaries, this way showing more energy absorption capacity and, thus, the toughness index grow.

In the case of addressing the dual impact of steel fiber with other material in term of behavior and properties of concrete, the study performed by Güneyisi et al. (2014) reported the findings of an study of hardened properties of plain and fiber concrete with and without metakaolin (MK). To improve SFRC mixtures contaning MK, MK was added with 10% by weight of cement. Two kinds of steel fiber with hooked ends were used to make FRCs. The activity of MK and various sorts of fiber on the compressive, flexural, splitting, and bonding strength were investigated. The outcomes showed that utilization of MK and incorporation of various kinds of steel fiber claerly influenced the mechanical property of the concretes as shown in Figure 2.5.

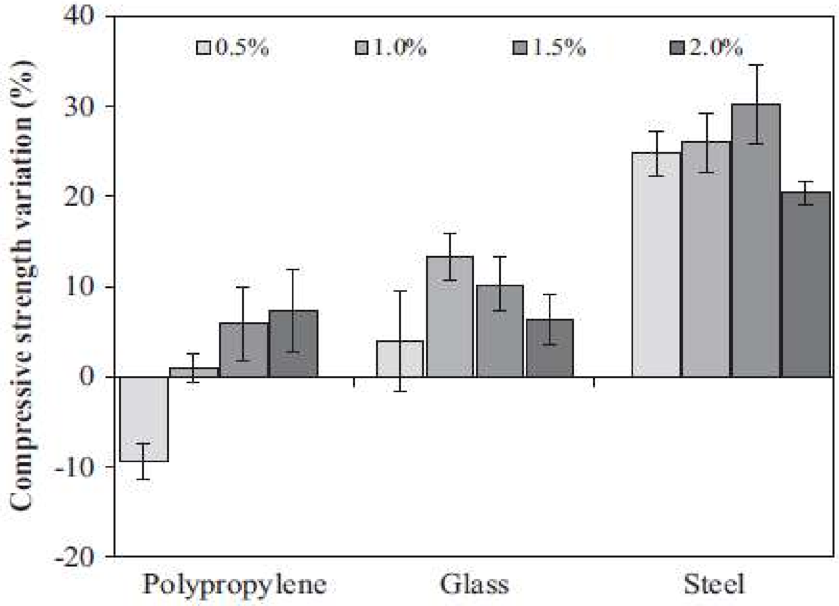

Figure 2.3 Compressive strength variation in relation to the reference mixture (Simoes et al., 2017)

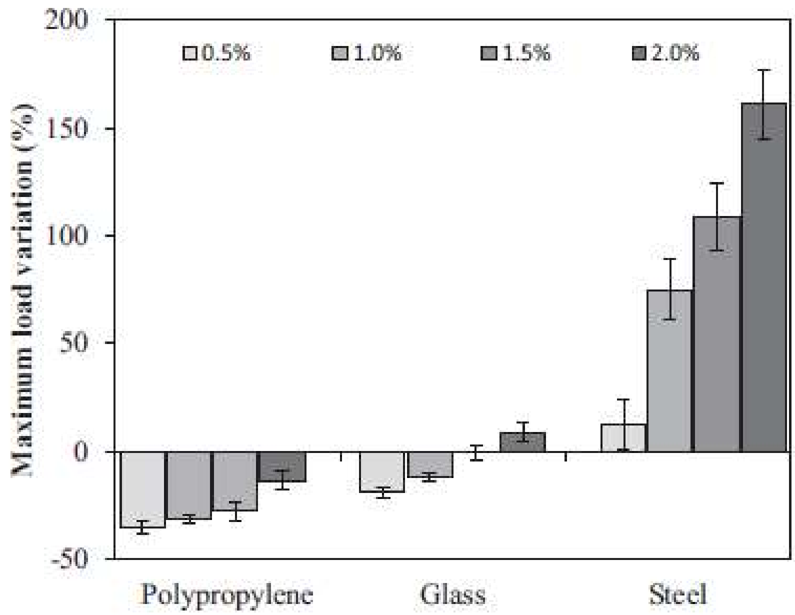

Figure 2.4 Maximum load variation in relation to the reference mixture (Simoes et al., 2017)

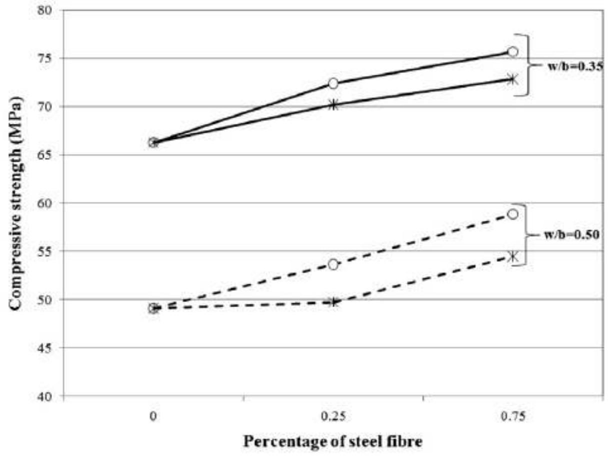

(a)

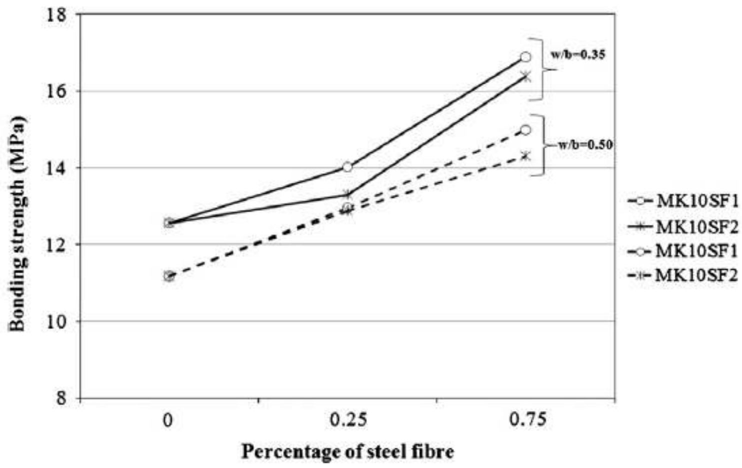

(b)

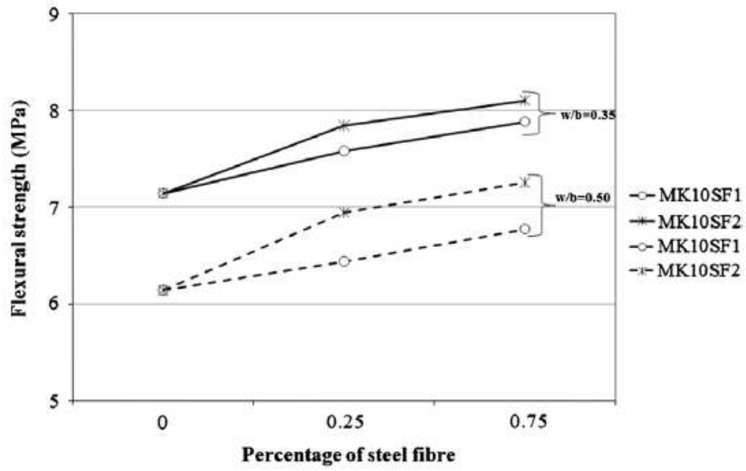

(c)

Figure 2.5 Influence of percentage of steel fiber on a) compressive strength, b) bonding strength, and c) flextural strength of MK concretes (Güneyisi et al., 2014)

It can be shown qualitatively by drawing a comparison between flexural failure forms of beams with and without fiber (Figure 2.6). This expression of toughness or energy absorption ability is important in some applications, such predicted earthquake exposure where conservation of structural integrity even with extensive damage is the main purpose. In several additional applications in which the serviceability conditions are lower intense and disastrous structural harm is not predicted, performance up to a specified allowable stage of serviceability denoted by deformation or cracking might be more pertinent. In cases like this, reserved strength at this serviceability stage might be a more valuable and satisfactory design criterion than toughness. Accordingly, most of the criterion tests estimate the toughening impacts of fiber to reach specified deformation or load limits rather than to complete failure of the sample (Lemond and Pielert, 2006).

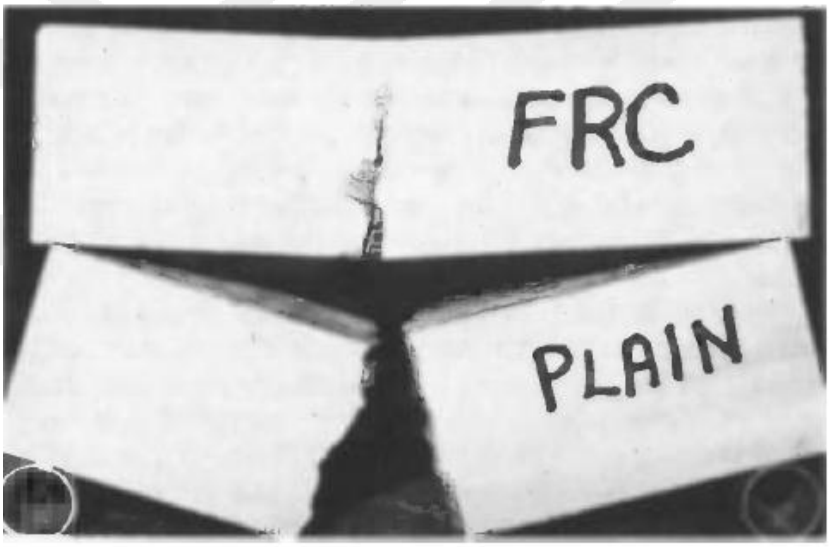

Figure 2.6 Toughness of FRC in flexure compared with plain concrete (Lemond and Pielert, 2006)

2.1.4 Application of SFRC in structures

The use of SFRC has been so various and so prevalent recently, which renders the classification of SFRC uses hard. Pavements, linings, slabs, tunnel, shotcrete, airport pavements and slabs, bridge deck slab repairs, etc. are the most popular applications of SFRC.

1. Shotcrete application: Shotcrete is a highly fluid kind of concrete which may be sprayed onto most surfaces. Shotcrete is normally sprayed onto irregular or vertical

surfaces. Prior to shotcrete spraying on the application surface, steel mesh may be set up to offer an adhesive substrate for the shotcrete. Steel fiber are commonly utilized to reinforce the shotcrete and rovide cohesion, thus cancelling the need for a steel mesh (eHow, 2012). A thin plain layer of shotcrete is applied monolithically on the fiber shotcrete to cover it, which can inhibit external staining due to rusting. Common applications of steel fiber shotcrete include bridge repair, rock slope stabilization, and tunnel lining (Gambhir, 1985).

2. Hydraulic structures application: Due to SFRC is resilient to cavitations or erosion wear and tear from high velocity water currents, it may be used in the hydraulic structures (Gambhir, 1985).

3. Tunnel application: Precast concrete elements, cast-in elements, shotcrete or their combination are utilized to create tunnel linings. Tunnels must be resilient to soil or water which poses as a fixed load on it. As SFRC provides extra flexural strength, decreasing shrinkage cracking and permeability, it is generally utilized in tunnel construction (eHow, 2012).

4. Precast application: Precast concrete elements are fabricated before they are transported and set up on location. Their uses include apartment buildings, offices, bridges, substructures and tunnels. SFRC usage in manufacturing precast delivers extra flexural and impact strengths (Gambhir, 1985; eHow, 2012).

5. Industrial ground slabs: In the industrial ground slabs, SFRCs, with great durability and flexural strength, are utilized to resist repeated loading and impact load. Repeated loads are produced from forklifts in warehouses, cranes in plants, and traffic loads in airport runways. SFRC also brings the thickness of slabs to the minimum. SFRC has a higher tensile strain capacity than plain concrete, which leads to lower maximum crack widths (Gambhir, 1995; eHow, 2012).

In structural applications, according to ACI Committee 544's recommendations, SFRC ought to be utilized solely in a supplementary role to increase impact resistance or repeated load, to prevent cracking, and to resist material fragmentation. The reinforcing steel needs to have the capacity to bear the whole tensile load, in structural members in case of tensile or flexural loads are present. Therefore, although the strength of beams reinforced can be predicted merely with steel fiber through some techniques, there are not any equations for prediction for large SFRC beams because such beams are expected to include traditional reinforcement bars, too. The American Concrete Institute issued an comprehensive instructor for design limitations for SFRC. The usage of SFRC will be presented in this section mainly in structural members that include also traditional reinforcement (Craig, 1984).

For beams with fiber and reinforcing bars together, the condition is complicated because the fiber has two effects:

1. They enable the use of the tensile strength in design as the matrix will lose little amount from its load-carrying capbility at initial crack; and

2. They increase the bond property between the reinforcing bars matrix by preventing the development of cracks resulting form the deformations on the bars.

The beam analysis focuses mainly on the increase of the tensile strength of SFRC because the increase of bond strength is a great deal harder to measure. It was demonstrated that steel fiber increases the maximum deflection and maximum moment of traditionally reinforced beams; the greater the tensile stress because of the fiber, the greater the maximum moment (Craig, 1984).

- New application areas for SFRC (Rilem TC 162; G C S C, 2010):

1. big surfaces, dense utilization, jointless joints:

Seamless manufacturing floor is progressively supplanting no joint floor. While jointless floors contain contraction joints at each 40 meters or lesser, seamless floors do not contain any joints at all, regardless of how big the area of the floor is. The better crack monitoring and perfect resistance against to impact of the steel fiber series along with a mere top mesh offers a scheme with heavy use, and decreased keep and reparation costs.

2. Fluid tight floors, water tight structures and coated slabs:

Steel fiber was designed specifically to influence cracks between 0.1 and 0.3mm, which makes it possible to build durable fluid and/or water tight structures with the sternest serviceability necessities. Combined reinforcement may be utilized as the substrate for very thin toppings like epoxy layers and other coatings. In addition to a single top mesh a crack width limitation designed for the exact SLS prerequisites may be used. Figure 2.7 demonstrates a characteristic drawing of a fluid tight floor. A covering was utilized to ensure tightness. An extremely tight crack width limitation The slab is employed to enable the coating to keep intact (The slab is subject to a very stringent crack width limitation in order to allow the coating to remain undamaged). A combined method with only a top mesh + high performing SFRC is a most feasible, inexpensive and time-efficient approach for building.

Figure 2.7 Typical illustration of a fluid tight floor made with SFRC (Structurae, 2017)

3. Structural floors and seismic floors

Industrial floors are typically ground-supported and they do not affect the reliability of the actual structure. Yet, the whole construction is supported by structural floors, which act in addition as foundation slab bracing and bearing the whole construction load.

Figure 2.8 demonstrates the raft foundation of a production facility that is 30 meter high. The entire building is established on the slab with cantilever columns exercising more than 5 MN and 2 MNm loads onto the slab. An added requirement was a unified building with crack width limit to 0.2 mm. Without the dual reinforcement of design and execution about 60% of the conventional reinforcement would have been mandatory. The great influence of this solution was the time efficient output and the practicability (e.g. usage of meshes enabled).

In seismic region, floors work similar to a tie beam for structural elements like columns and pad foundations. Remarkable uplift forces, and in plane forces during a seismic incident need to be handled. A mutual solution presents a feasible, inexpensive and time-efficient solution. By utilizing better performing fiber such as the Dramix® 5D fiber a substantial quantity of conventional reinforcement may be substituted.

Figure 2.8 The raft foundation for 30 m building (Structurae, 2017)

4. Floor on piles

SFRC floors on piles have already been implemented from time to time still with stricter limits regarding pile distances, slab thickness and extra quantity of reinforcement. As of the current time, all carried out SFRC piled floors were typically solutions with added reinforcement beside the pile grid or having a piece of mesh on top of the piles. Due to its extraordinary load bearing capacities, Dramix® 5D steel fiber allow the construction of floors on piles with no conventional reinforcement. This also grants new potentials for floors on piles and saves construction time.

5. Clad Rack foundations

A Clad Rack warehouse is a sort of storage with the built-in shelves in building structure, thus no civil works are required unlike a traditional building. In this kind of warehouses, the shelving facility supports the load of the building cover, addition actions (snow, wind and seismic tremors), and the load of the seismic forces.

Therefore, the foundation of this racking system is a real raft foundation which needs also to meet the conditions for a floor. The raft is implemented prior to the erection of the rack system and that means that temperature has to be taken into consideration for a monolithic slab kind. A characteristic method with SFRC may be combined with or even without a mesh or any other conventional reinforcement approaches. Due to the unique capacity of the steel fiber, it affords maximum strength and durability to reserve the reliability of the clad rack structure from descending forks, uplift from wind loads and seismic action. The removal of conventional reinforcement may accomplish remarkable savings.

6. Raft foundations

SFRC has been utilized for years in foundation slabs of domiciliary buildings. The legal leeway to design this sort of load bearing structure received the support of local general approvals. Yet, foundation slabs were restricted to certain loads and size measurements. Thus, the raft foundations for constructions with several floors of any sort may be implemented with SFRC, or binary reinforcement. As these, mostly, are hefty loaded rafts, large and subjected to a stringent crack width limits binart reinforcement is typically used. Generally speaking, around 50% of the conventional reinforcement is substituted. This is obviously contingent on the SFRC performance wherefore the usage of steel fiber is especially useful and will produce higher savings.

The raft foundation of the construction exemplified in Figure 2.9 was executed in dual reinforcement. A chief reason for the deciding to utilize SFRC was to reduce shear studs and shear reinforcement, both of which were accomplished through the method using dual reinforcement. Bending reinforcement and reinforcement for crack width requirement have essentially been decreased. Most importantly, the binary reinforcement skipped most predicted shears studs and shear reinforcement entirely. Thus, the most important reason to adopt this method was cost-efficiency time-efficiency and constructability. Figure 2.10 demonstrates the main uses of the comprehensive application area for SFRC. Certainly other Elements, in addition to the ones presented here, are also conceivable.

Figure 2.9 The raft foundation of the building was carried out in combined reinforcement (Structurae, 2017)

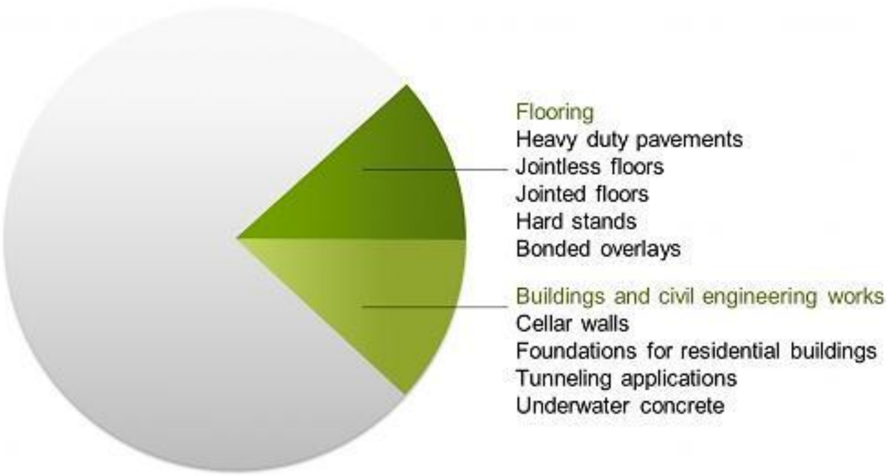

Figure 2.10 Application area for SFRC (Structurae, 2017)

2.1.5 Development of steel fiber reinforced self-compacting concrete

Novel groups of added components like superplasticizers (SP), which enhance concrete plasticity, and viscosity modifying agent (VMA), which alter concrete viscosity and stop segregation, have been created and incremented successfully to steel fiber self-compacting concrete (SFRSCC). The new supplements make it viable to reach high strength concrete without any decrease in concrete workability. Fine cementitious materials such as blast furnace slag, fly ash, silica fumes, and limestone fines were also created to enhance SFRSCC. Adding fine cementitious materials, for instance, decreases voids, which has tendency to increase the fiber-matrix bond (Banes, 2017).

The addition of fiber to cementitious composites decreases the matrix flowability, particularly in case of presence coarse aggregates. The effect of the addition of steel fiber on workability of concrete was examined by Rtche and Raman (1937). They established that workability deteriorated progressively as the added steel fiber increased, and that a 3% of fiber reduced the slump by 12%, whereas 8% of steel fiber decreases the slump by 70%.

SCCs are strongly impacted by the mixing procedure and the period given to every step. Moreover, slight alterations in the mixing process and the order of mixing can meaningfully impact the fresh property (Lio et al., 2000). Academics conducted a great deal of research to advance SCC manufacturing procedures. Conventionally, the use of basic mixing methods and normal fiber (smoth and straight) resulted in fiber separation and fiber agglomerate. The use of glued steel fiber, particular mixing procedures, and distinctive placing systems to curtail segregation and to disperse fiber consistently, are viewed as remarkable developments in FRC (Namn, 2003).

2.1.6 Studies on SFRSCC

Akcay et al. (2012) studied the workability, orientation and dispersion of fiber, mechanical property and fracture conduct of hybrid SFRSCC. Three various sorts of steel fiber (hooked-ends and non-hooked ends) were used in the mixtures using different ratios. These ratios were 0.75 and 1.5% of the total volume of concrete. Results of fresh properties have demonstrated that rising the fiber quantity of the concretes somewhat lowered the fluidity of hybrid SFRSCC, and the major effecting term on fluidity is the fiber geometry. Additionally, the experimental results demonstrated that both compressive strength and modulus of elasticity had marginal change, while the using of fiber had noticeable action on flexural and tensile strengths. The authors stated that both the mechanical property and the fracture energy were enhanced using of hybrid steel fibers. This is in particular after the initiation of the first crack. Moreover, strain hardening in the second part of the load deflection curve is a ideal for high performance concrete designation. Increase of fiber quantity highly enhanced the fracture energy. The small fiber had a slight influence on the first part of load-deflection curve, while impact was substantial in the case of long fiber used, which caused in substantial increasing in fracture energy. It was also proved that fiber dispersed uniformally in all mixtures with no clumping. With mounting the quantity of fiber, the fiber was oriented vertically more than that of bending loading path, causing an improvement of mechanical performance.

Yardimci et al. (2014) used two kinds of steel fibres with hooked ends at three several ratios were used in self-compacting concrete having same paste quantities but no same sand to gravel (FA/CA) proportions. Mechanical characteristics of concrete in term of fracture absorption energy in addition to the workability and passing capability of fresh concrete were examined. The outcomes demonstrated that steel fiber with hooked ends using in the mixtures adversely affected the workability and passing capability of the fresh concrete. The results of compressive strength indicate the change because of fiber incorporation is about 10% or low in the SFRSCC groups in case of FA/CA proportion is above 1.72. It has been found that the ratio of FA/CA above 1.72 is preferable to achieve good stage of fracture absorption energy at fiber quantity are 40 or 60 kg/m^3. A good relation occurs in term of fiber number in both flexural parameters and unit area. SFRSCC's fracture absorption energy improves with increment of the orientation number.

The mechanical property in term of modulus of elasticity is so substantial because it indication to structures rigidity. By comparing plain SCC to FRSCC, it can be observe that raising in the modulus of elasticity with using fiber. Growth of compressive strength by 16% was found when end hooked steel fiber utilized in SCC. Development of elastic modulus and flextural strength was claer. There was an improvement in the mechanical characteristics of SCC by the using of artificial and metallic fiber without changing its fresh property limited through the standards.

Various concretes were manufactured. Four types of fibers were used. Straight and hooked end metalic, Micro artifitial Polypropylene and Macro artificial Copolymer. the finding demonstrate that: (1) with using of metallic fibers that respects the fresh property of SCC, the flexural strength is only marginally influenced; (2) With the high capability of macro synthetic fibers to distributed in the cementitious matrix, flexural strength is highly enhanced; (3) The use of a high quantity of micro synthetic fibers raises the fiber segregation in fresh state so self-compacting properties are disrupted (Benaicha et al., 2013).

Orbe et al. (2012) focuses on the structural using of SFRSCC. A SFRSCC mix, prepared to enhanced performance, was utilized to make wall at (height equal to 3 m, length equal to 6 m, and thickness equal to 0.15 m) as in Figure 2.11. The empirical assessments performed on 380 samples take from the wall comprised non destructive and mechanical checking methods. The compressing test was performed on 11 samples taken from several parts of the wall. a rate of result of 61 MPa was observed with a coefficient divergence of 9.4%. Moreover, the height of the sample is pointed have no impact the compressive force. Tensile strength pointed at a 1/3 of the height gave well value. Failure location was pointed at a plane normal to the predominant fiber directions in the 63 bending tests. The material was therefore able to improve its full capacity between the compressed zone and tensile zone.

The research of El-Deib. (2016) was about the conduct of axially loaded short columns produced using ultra-high-strength SFRSCC. The research goal was the influence of fiber incorporation , fiber ratio and the transverse steel ratio (i.e. stirrups). The conduct of the columns was assessed in term of strain of concrete, maximum load, transverse and axial reinforcement, and failure mode of the columns tested. It is believed that the incorporation of steel fiber might improve the load carrying capacity as well as axial deformation, particularly at high ratio of fiber. The raised deformability of the concrete might activate the captivity used by the stirrups at high level of fiber volume fraction. Figure 2.12 explains the failure characteristics columns tested.

Figure 2.11 SFRSCC wall (Orbe et al., 2012)

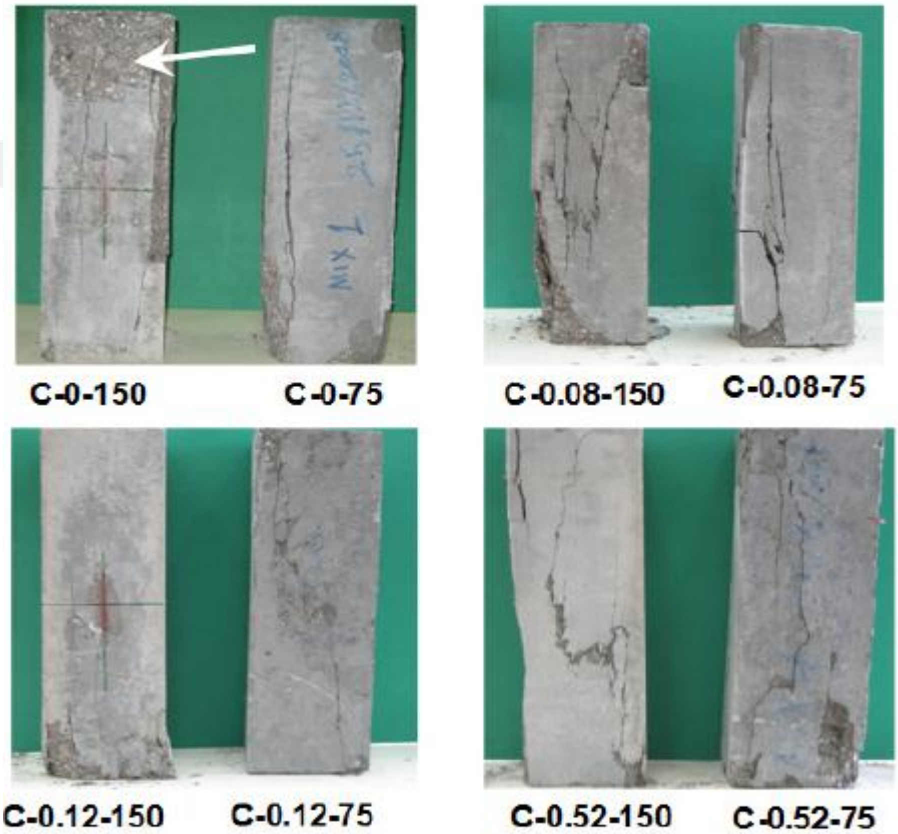

Figure 2.12 Failure modes of tested columns (El-Deib., 2016)

The outcomes in Table 2.1 show the compressive strength and fracture energy of plain and SFRSCC beams. The studied material is a concrete reinforced with two types and three volume ratios of steel fiber. It might clear that inclusion of steel fiber gave very high value of fracture energy. The fracture energy of reference mixture is 296 N/M while it was ranged between 743-3532 N/M in mixtures containing steel fiber (Sucharda et al., 2017).

Table 2.1 Strength and fracture energy of plain and SFRSCC beams (Sucharda et al., 2017)

Code	Fiber [%]	(beam/cubes)	Fiber type	Marking	$f_{cu,28}$d [Mpa]	G_f [N/M]
C00	0	3/6	-		73.4	296
H05	0.5	3/6	Hooked	H	98.2	1487
H10	1	2/6	Hooked	H	96.5	2669
H15	1.5	3/6	Hooked	H	88.6	3532
A05	0	3/6	Straight	A	80.1	743
A10	1	3/6	Straight	A	84.6	1237
A15	1.5	3/6	Straight	A	88.6	1502

2.1.7 Application of SFRSCC in structures

Applying structural concrete with no vibration in highway bridge manufacturing is not novel. Mass concrete and seal concrete underwater. In general, these concretes have less strength, lower than 34.5 MPa and it is hard to give regular characteristics. Yet, contemporary application of structural SCC concentrates on high performance, dense and regular surface texture, superior and more dependable quality, better durability, high strength, and quicker use. Further uses of SCC in structures were mentioned in Japan. Up to the year 2000, the quantity utilized for ready-made products (cast in place) and pre produced concrete (precast elements) in Japan was approximately 400,000 m^3. The pre-stressed, precast concrete fabrication and forecasting place building proved to have several advantages through the structural SCC: lower work required, more strength, fast building, superior type and stability, fewer difficulties related to vibration and more quiet building locations (CRC, 2000; 2002).

Getting rid of vibration for the compaction of fresh state and of the traditional reinforcement renders the utilization of SFRSCC useful in regards to saving costs and supporting the work environment. In China, because of the thriving infrastructure development in the recent decades, the uses of SCC have made more rapid. A compressive strength of 60 MPa for SFRSCC was utilized in building the modern China Central TV station. The project consists of two 234 m high towers, sloped at 6 degrees in a convergent manner. The tower is supported with 190×150 cm columns. The columns are constructed with C60 SFRSCC to fulfil the pre-requisites of crack control and to suit the intricate figure (Yan and Yu, 2009).

Figure 2.13 shows a distinctive application of the SCC with steel fiber is in fas wall method. This method is utilized to construct walls with amvic system as a frame to construct new inexpensive structure with great isolation (Amvic company, 2017).

a)

b)

c)

Figure 2.13 Fas wall system (Amvic company, 2017)

2.2 Steel-concrete bond mechanisms in structural members

While concrete bears loads constantly, these loads are not born at present by the bars in reinforced concrete structures. The concrete tends to crack because of the lack of strength in tension portion. At the area cracked, the loads are conveyed to the bars and in this condition a part of the tension forces is come back to the concrete. The foundation of the reinforced concrete concept is depend on the simple stress convey system. The concrete-steel bond stresses result from the stress convey. The significance of the concrete-steel bond received the attention of engineers and academics since 1877 (ACI Committee 408, 2003).

Bond design calculations depend on sufficient bond strength which may be described as quantity of conveyed load between steel and concrete (ACI committee 408, 2003; Rteil, 2007). Since conveying adequate force by sufficient bond strength yields the steel and that will give ductility for a reinforced concrete element (Rteil, 2007). Shape of bar and cross section area, concrete characteristics, bar surface situation, and the confinement on the steel affect the bond strength. Shear and compressive stresses of the concrete touch surfaces balance the forces occurred on the surface of steel. They are transformed, and result in tensile stress that is parallel and normal to the steel bars. They induce cracks in planes as demonstrated figures 2.14a and 2.14b. Creation of narrowed failure surface for bars anticipated from concrete may result in the cracks shown in Figure 2.14a which is also identified as Goto (1971) cracks. When the span between steel or concrete overlay is minor, the cracks illustrated in

Figure 2.14b take place and cause splitting cracks as demonstrated in Figure 2.14c. A pullout failure, as demonstrated in Figure 2.14d is caused by the failure of the group because of shearing alongside a surface on the ribs surrounding the steel. This state of affairs only takes place when splitting failure is barred or postponed by the adequate concrete overlay, bar layout or transverse reinforcement (ACI committee 408, 2003).

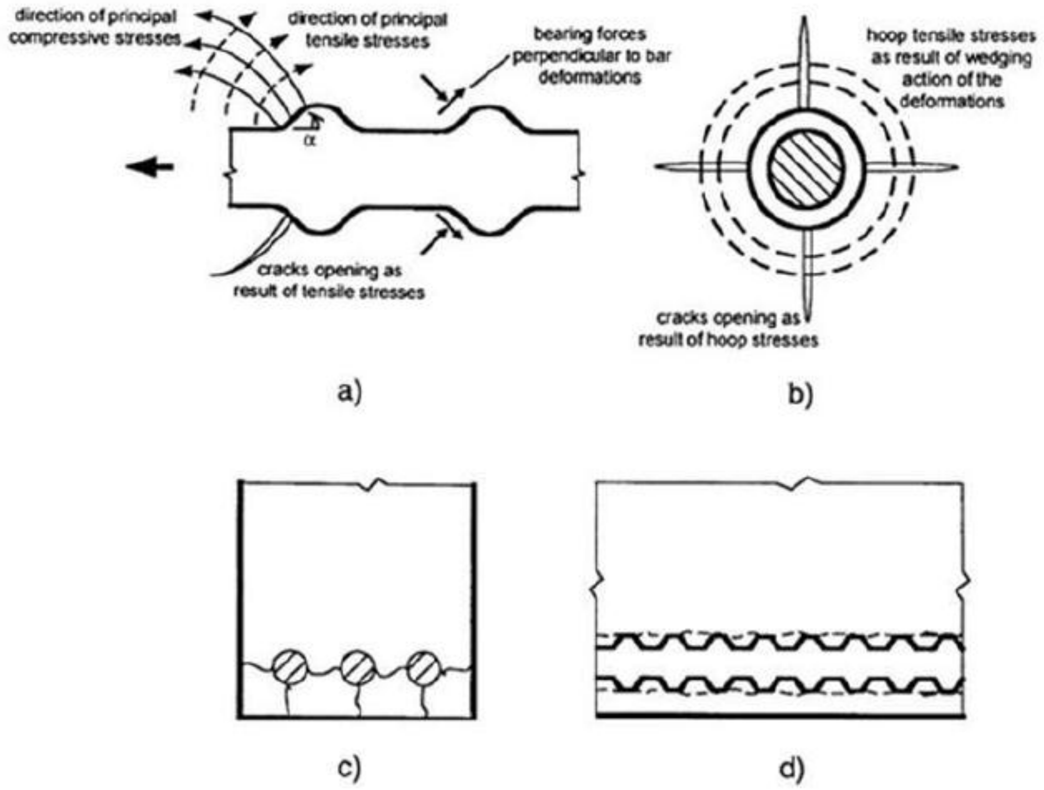

Figure 2.14 Loss of bond mechanism and cracking a) a deformed bar, b) formation of splitting cracks, c) a structural member showing splitting cracks, and d) shear crack in a member with local concrete crushing (ACI committee 408, 2003)

2.2.1. Load transfer

Bond strength defined as a transmission of axial forces from reinforcement to the adjacent concrete, and by relocating the forces result in the growth of lateral stress components alongside the touch external area (Pillai and Kirk, 1983). if the reinforcement are attached to the adjoining concrete well, the reinforced concrete will function as composite material. Slip of the steel in the concrete may be minimized or eliminated only if a decent connection is made between the concrete and the steel and achieving this condition entails that the stress is transmitted through the concrete and steel (Warner et al., 1998). The transmission of forces from deformed steel bars by concrete is demonstrated in figure 2.15 and it happens in the subsequent conditions; chemical adhesion of the concrete to the reinforcement, slip and friction of the reinforcement from the adjacent concrete and mechanical anchorre/ ribs bearing against the concrete surface (ACI committee 408, 2003).

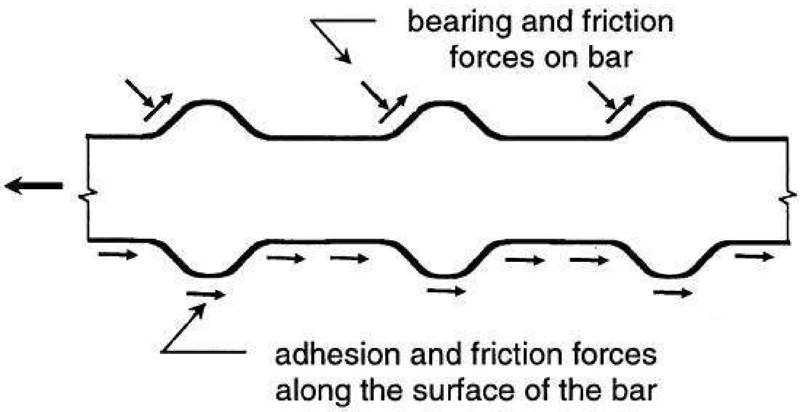

Figure 2.15 Bond force transfer mechanism (ACI committee 408, 2003)

The adhesion between the concrete and reinforcement the primary loads, and the adhesion stops the slipping of the steel bar from the adjacent concrete. When the load on the reinforcement greater than the cohesion resistance, the surface adhesion is eliminated. After the failure of the adhesion resistance, slip starts and the mast of the force is transmitted by bearing forces on the ribs and friction forces between the concrete and bar ribs has a vital duty in transfer of the force. The main mechanism of force transfer results from bearing forces and friction forces which are affected on the ribs. Slip upsurges due to of raising the load, which results in a decrease in friction forces on the surface area of the bar (ACI committee 408, 2003). The relation (Figure 2.16) between the bond stress and slip is specified by Eligehausen et al. (1983).

Several test sample formations are available to find out the bond between steel reinforcement and concrete. The formations, demonstrated in Figure 2.17, are the four most prevalent kinds. The particulars of the sample influence both the calculated bond strength and the type of the bond reaction (ACI committee 408, 2003).

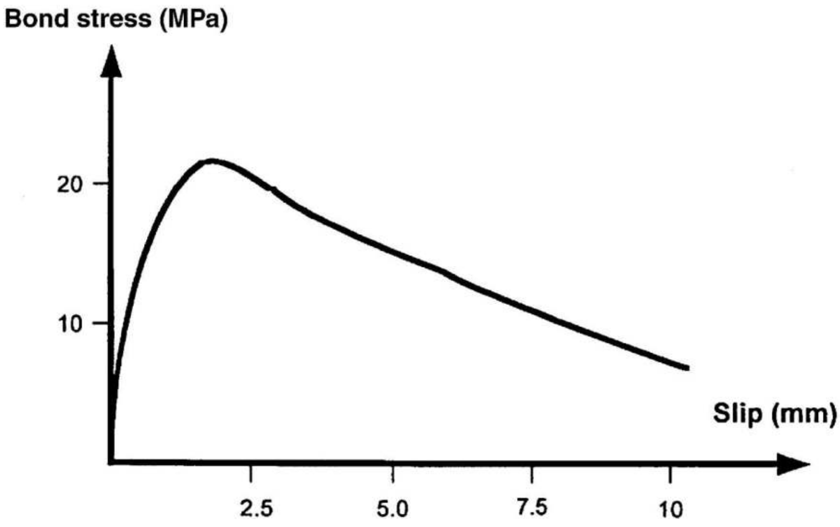

Figure 2.16 Bond stress-slip curve for bar loaded monotonically and failing by pullout (Eligehausen et al., 1983)

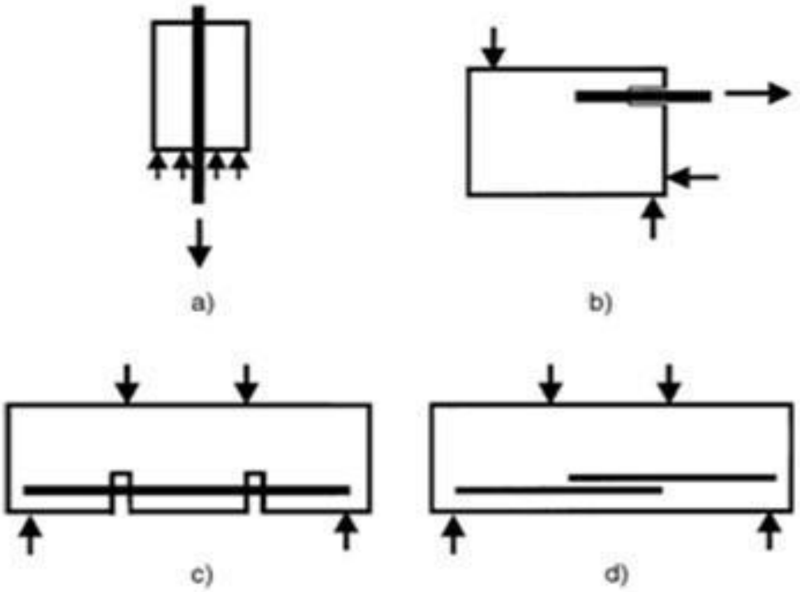

Figure 2.17 Schematic of: a) pullout specimen; b) beam-end specimen; c) beam anchorage specimen; and d) splice specimen (ACI committee 408, 2003)

Due to the concordant stress fields in the sample with limited instances in real situations, the most accurate test samples among the four, demonstrated in Figure 2.17, is pullout sample and it is extensively utilized sort of bond strength identifying the test arrangement because of its easy production and as it is a simple test. In the pullout test sample, the tension is exerted on the bar while the concrete is compressed. In addition, the bar surface is compressed by the creating the compressive struts between the upholding points for the surface of the steel bar and the concrete (ACI committee 408, 2003).

2.2.2. Factor affecting bond strength

Many terms influence the bond strength of reinforcement in concrete such as:

- Development length
- Bar location
- Size of the bar
- Geometry of the bar
- Situation of the bar surface
- Concrete tensile and compressive strength
- Confinement

The study of Dehn et al. (2000) is focused on the behaviour of the bond between the SCC and steel bars as compared to conventional concrete. To guarantee the manufacturing of better SCC, a mix design ought to be done to achieve the pre-defined characteristics of fresh and hardened concrete. Each component should be coordinated to prevent bleeding and segregation and because of these influences, their know-how from Netherlands, Japan, Sweden, and France was employed of to create the design mix. The following factors were taken into consideration as the reinforced concrete capacity to bearing has considerably impacted by the behaviour of the bond between concrete and the steel reinforcement.

- The reinforcement bar anchorage
- Control of crack width
- Lapped reinforcing bars

Accordingly, tests on behaviour of the bond between the SCC and the steel bars were vital, especially distinguishing the time development of the bond strength. These tests showed that the main parameters which influence the bond behaviour are the re-bars surface, the quantity of load cycles, the course of cementing, the design mix, and the (pull out) examination specimens geometry. The bond behaviour was determined under unchanging static loading using pullout samples with a uniform concrete blanket surrounding the fortifying bar. The bar diameter for the whole examination procedure was 10 mm and the concrete blanket it had a 10 cm diameter and length too. It was stated that many conditions that influence bond strength between concrete and reinforcement like location of bar manufacturing, development length, bar size, bar geometry, surface state of the bar, concrete’s compressive and tensile strength and confinement (Dehn et al., 2000).

2.3 Fracture mechanics

Fracture mechanics is a discipline which explores the stress surrounding the crack and strain replacement. The characteristics and mechanical conduct of substances utilized in structures considerably impact the mechanical conduct of the structure. Designing of concrete in application based on the theory of compressive strength, and the concrete brittleness is neglected in this theory. Thus, the description of the fracture terms of concrete with its brittleness needs to be conducted (Akçay, 2007). The fracture mechanics explore the locations, creation and conditions of failure and the influence before spread of existing cracks. Linear Elastic Fracture Mechanics (LEFM) and Nonlinear Fracture Mechanics (NFM) were improved for this goal. LEFM may be used to consistent and brittle materials like glass and NFM is the advance status of LEFM because it is not effective for quasi-brittle and heterogeneous substances similar to concrete (Taşdemir et al., 1996).

2.3.1 Linear elastic fracture mechanics

The stress concentration occurs at the tip of space in the material, which contain a space and is under the load, due to discontinuity. Being obliged of the stress flow, taking place due to loading, to move around the cracks causes the concentration of the stress at the tip of crack and the stress relaxation at the upper and lower faces of crack. According to LEFM, the stress, occurs the tip of crack, goes infinity as the crack becomes sharper. Griffith was introduced LEFM for brittle and homogeneous materials and this introducing was landmark for the theory of fracture mechanics (Akçay, 2007). The fundamental contributions to develop this theory were done by

Irwin for non-brittle materials (Irwin, 1957). Concrete is a quasi-brittle material and the theory of fracture mechanics was connected to concrete firstly by Kaplan (1961). Likewise, he confirmed that the LEFM may not be utilized for the extracting of fracture terms of concrete due to the inclusion of concrete the fracture process zone which was described as the inelastic zone surrounding the crack tip (Mindess and Diamond, 1982; Taşdemir and Karihaloo, 2001).

The presence of minor cracks and other crack-like imperfections in stiff brittle materials results in a huge difference between the theoretical and real tensile strengths of these materials (Griffith, 1920). A sheet shows this theory. When the constant remotely stress was applied to a sheet of brittle material with a narrow crack, the stresses around the crack tip reaches infinity (Karihaloo, 1995). In addition, the types of crack surface displacement, demonstrated in figure 2.18 which take place at a crack tip influence the nonconformity of the stresses adjoining a sharp crack tip. Thus, the load capacity of the sheet becomes vital at the stress status in the vicinity of the sheet (Akçay, 2007).

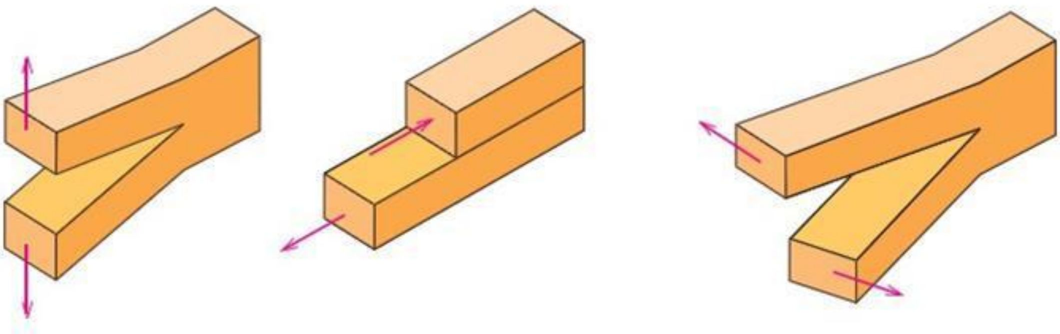

a) b) c)

Figure 2.18 Crack surface displacement mods: a) Opening or tensile mode (mode I), b) Sliding mode (mode II), and c) Tearing mode (mode III) (Karihaloo, 1995)

2.3.2. Nonlinear fracture mechanics

Several studies have been conducted to render LEFM feasible to concrete and to confirm the theories of NFM (Akçay, 2007). Figure 2.19 concisely shows the variances between notions. The figure, L, N, and F show the linear elastic, nonlinear, and fracture behaviour, respectively.

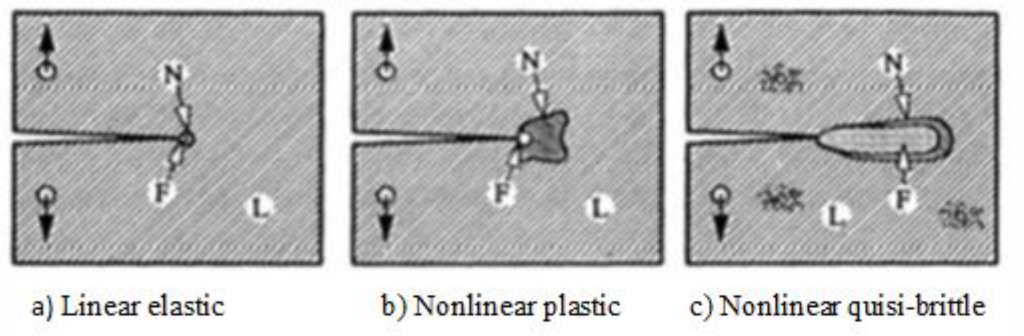

Figure 2.19 Linear and nonlinear models (Dugdale, 1959 ; Karihaloo, 1995)

Based on the predominant fracture mechanics, there are six approaches: fictitious crack model (Hillerborg et al., 1976), the crack band model (Bažant and Oh, 1983), the size effect law (Bažant, 1984), the two parameter fracture model (Jenq and Shah, 1985), the effective crack model (Nallathambi and Karihaloo, 1990), and the recently proposed concepts of boundary effect and local fracture energy distribution (Hu and Wittmann, 2000; Duan et al., 2003). These approaches have been recommended for the determination of the parameters regarding fracture of concrete, and the fictitious crack model, both the law of size effect, and the two parameters model are among RILEM recommendations (1985).

Fictitious crack model (FCM), introduced by Hillerborg et al. (1976), is the first non-linear theory of fracture mechanics. There are resemblances between cohesive crack models and fictitious crack model. Nevertheless, the closing stresses are not consistent and they surge along with tensile strength of material and this happens at the tip of the fictitious crack. The model of Hillerborg et al. established in 1976 is moderated by Bažant and Oh (1983). They exhibited the fracture process zone with a limited width of consistently and continuously distributed micro cracks in lieu of happening separately as in FCM.

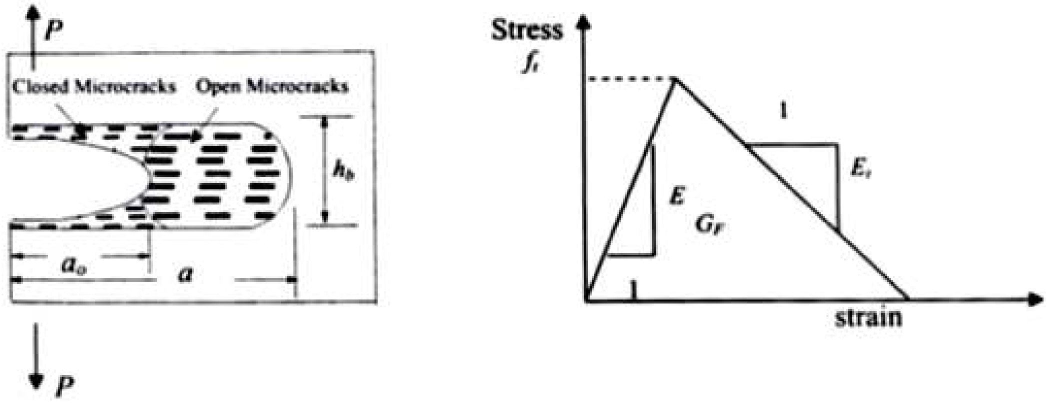

Figure 2.20 Crack band model for fracture member: a) a microcrack band fracture and b) stress-strain curve (Bažant and Oh, 1983 ; Shah et al., 1995)

Two fracture parameters, the critical energy release rate and the effective crack length, might mainly require to deduce the lab size samples to real-size engineering structures. In the Bažant's size effect law (1984), the critical energy release rate can be considered as the unit fracture energy needed for the crack initiation in an infinite sample and the critical effective crack length. The factor of critical stress intensity and the critical crack tip opening displacement are defined through the only one size three-point bending samples which are loaded up to ultimate stress, and then subjected to an unloading and reloading cycle (Shah et al., 1985). This is called a two parameter fracture model (TPM) and this is the suggestion of Jeng and Shah in1985. Nallathambi and Karihaloo (1990) also suggested the effective crack model (ECM) in which the basic notion of effective crack is comparable to the TPM. The ECM depends on the effective-elastic crack method as in the TPM.

2.4 Steel tubular columns with concrete infill

It is well known that the concrete filled steel tubular (CFST) columns are utilized to take the advantages of both concrete and steel properties and nowadays widespread in the worldwide. Concrete supplies its potential mass, rigidity, damping, and cost efficiency, while steel contributes its speed of construction, strength, long-span competences, and light weight. With CFST columns, the steel section serves as formwork during casting, therefore, offer the advantage to erect the steel frame of building and subsequently fill the hollow column by pumping in the concrete. By so doing the erection time can be lessened (Tao and Han, 2006; Lu et al., 2007). Figure 2.21 illustrates the most commonly utilized types of CFST columns. As can be seen from a, there are three types of hollow section namely circular, square and rectangular. The outer dimensions of steel tube are designated as D and B while the thickness of steel tube is t. Polygon, round ended-rectangular and elliptical shapes are the other cross sections normally utilized for aesthetical purposes, Figure 2.21b.

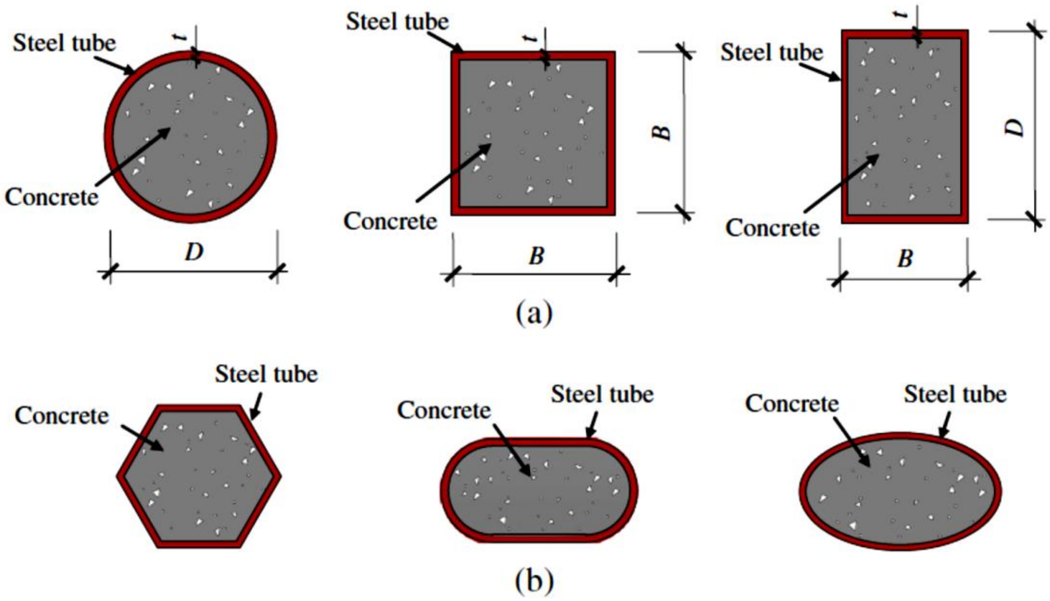

Figure 2.21 Cross section of CFST column (Han et al., 2014)

2.4.1 Structural performance of CFST column

The CFST column is a composite member made of two different materials. The most commonly forms of CFST column in construction sectors consist of circular or rectangular structural hollow steel tube infilled with concrete, as depicted in Figure 2.22. In the figure, D is the diameter of circular cross section, L is the total length of column and t is the thickness of steel tube. For the rectangular cross section b and d is the breadth and depth of the composite column, respectively. The sophisticated structural behavior of CFST column yields from the cooperation of concrete as a brittle material and steel as a ductile material. Advantages of CFST columns start at the stage of construction, as such columns are easy to fabricate and no formwork during casting fresh concrete. The steel tube protects hardened concrete core from adverse environmental actions. On the other hand, concrete increases the resistance of fire of column by performing as a heat sink. The structural behavior of CFST columns is significantly depends on steel grade and quality of concrete, confinement action, and interface condition between concrete and steel and local buckling of steel tube (Pires et al., 2012; Moliner et al., 2013).

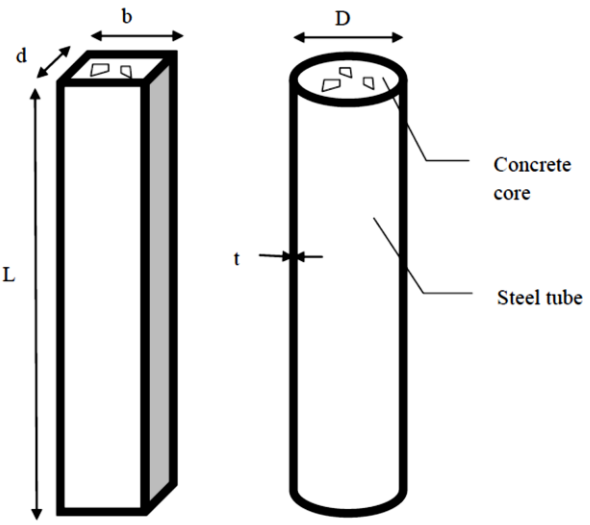

Figure 2.22 Typical geometrical details of CFST column (Chu, 2014)

It is well known that the type of concrete significantly affects the structural performance of composite members. Recently, advancement in concrete technology has allowed developing special concrete type, i.e. high performance concrete (HPC). Compared to conventional concrete the HPC has superior behavior in terms of fresh, strength and durability aspects. Use of HPC such as fiber reinforced concrete, lightweight aggregate concrete and SCC, can add to the strength and ductility of CFST columns. Han and Yao (2004), Han et al. (2005) and Lachemi et al. (2006) examined the structural behavior of CFST columns inflled with SCC having compressive strength between 50 to 90 MPa. Yu et al. (2008) went farther in their study regarded the ultimate strength of concrete filled circular and square steel tube structural columns. The study used SCC with 600 mm slump flow, slenderness ratio varied from 12 to 120, 1.6 mm for steel tube thickness and load eccentricity ratios altered from 0.0 to 0.6. They reported that the normal strength CFST columns generally having higher ductility than columns infilled with ultra-high strength SCC. Therefore particular consideration should be paid when utilized in seismically active regions HPC. Moreover, as presented in Figure 2.23 a and b, the square specimens post-peak curves are steeper than those of circular columns. They related this behavior to the relation of circular and square shapes on the confinement effects. As a result the square columns were less ductile than circular ones.

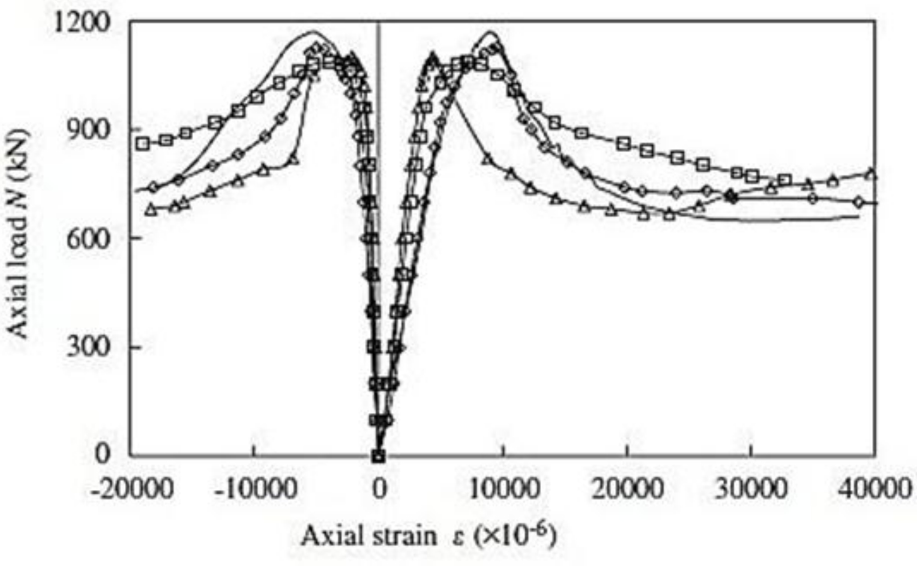

a)

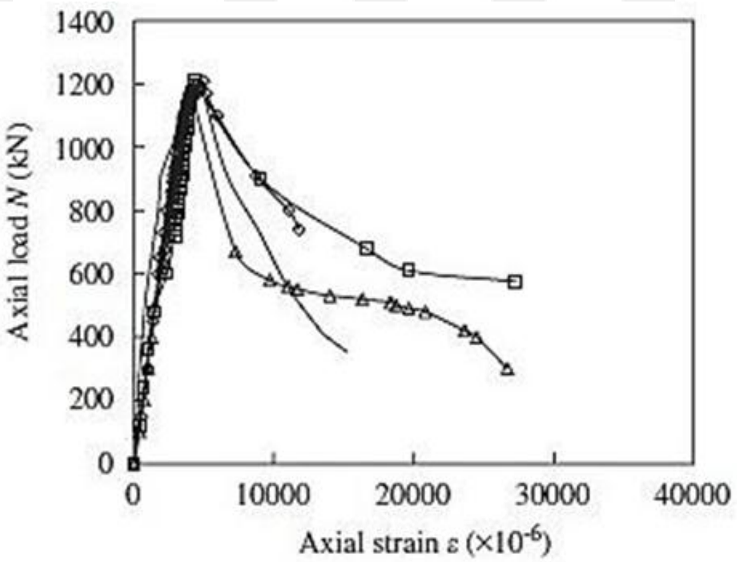

b)

Figure 2.23 Axial load vs. strain curves: a) circular section and b) square section (Yu et al., 2008)

The ratio of diameter-to-thickness (D/t) of steel tube can be considered the key factor for assessing the structural performance of CFST columns. In fact, D/t ratio is the most important parameter effecting the providing of confining action, hence the axial load capacity and ductility of CFST columns. In this regard, the steel tube would buckle first before yielding when D/t ratio surpassed a definite limit. The relation between the diameter ratio to thickness and confinement stress is considered as an inverse relationship. This is why ductility and strength of CFST column reduces when D/t ratio increases. Furthermore, the strain corresponding to peak load also affects by the diameter-to-thickness ratio. It is believed that the smaller D/t ratio provides larger peak strain Sakino et al. (2004). Hu et al. (2003) performed an analytical modeling study about CFST columns. Their study reviled that when D/t ratio of circular tube more than 40 insufficient confinement effects of circular steel tube can be resulted, while for square section it must be 30 or less. Huang et al. (2010) and Hassanein et al. (2013) found that for concrete filled double skin steel tubular short columns the internal diameter to thickness ratio had no influence on the strength of such columns. This is due to the internal steel tube contributes relatively slight to the strength of column. However, Han et al. (2003), Uenaka et al. (2010), Huang et al. (2010) and Hassanein et al. (2013) understood that for the concrete filled double skin steel tubular short columns the axial capacities significantly defined by confinement effect of the external steel tube rather than that of the internal tube. Thus, they stated that the ratio of D/t -D is the external diameter of steel tube- is the key factor affects the strength of such columns. Figure 2.24 illustrates the cross section of CFST column and the double skin column.

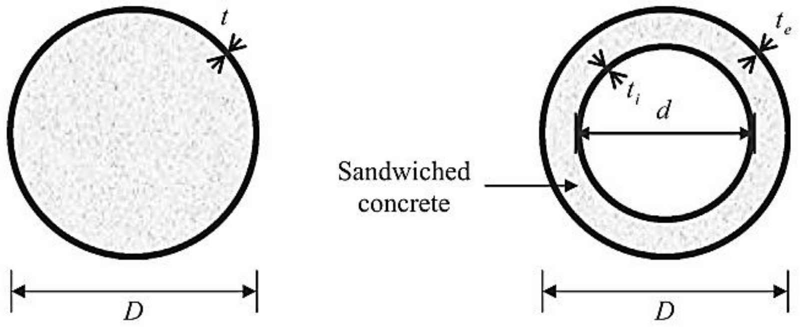

a) CFST column b) double skin CFST column type

Figure 2.24 Details of CFST columns having circular cross section (Hassanein and Kharoob, 2014)

Generally the effect of concrete confinement at high strain levels enhances the stress-strain response of concrete. It is well known that the strength, ductility and stiffness of concrete are dramatically improves by the lateral confinement of axially loaded conventional reinforced concrete columns. This is because the confinement effect decreases the tendency for cracking and extension of concrete (Jaffry, 2001).

Richart et al. (1928) were the first to detect the performance of confined and unconfined concrete. They reported that the confined concrete has the remarkable influence to enhance the ultimate compressive strength, stiffness and extended strain at which the maximum stress was achieved. The unconfined concrete can withstand sustain smaller deformation than confined concrete. Moreover, the confined concrete characterize by the ability to save its load-bearing capacity and to fail gradually in a ductile way. The typical stress- strain response of unconfined and confined concrete is presented in Figure 2.25. The figure depicts how the confined concrete tends to achieve higher strain than unconfined concrete and the enhancement in the compressive strength of these two types of concrete (Hatzigeorgiou, 2008).

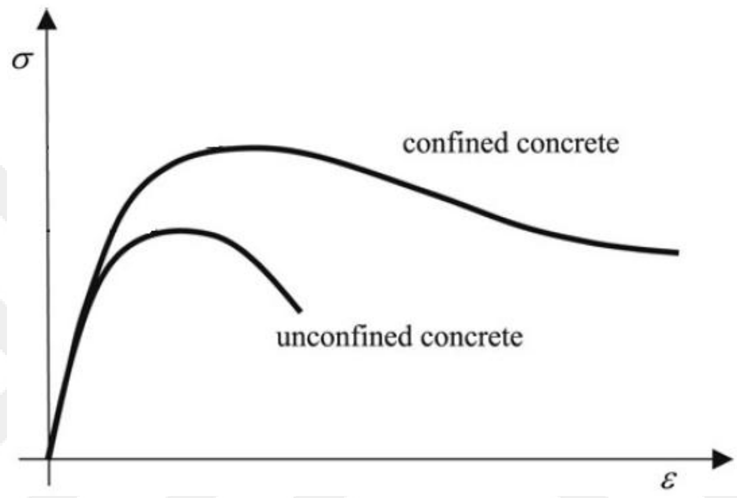

Figure 2.25 Stress-strain response of confined and unconfined concrete (Hatzigeorgiou, 2008)

The mechanism aspects of confinement in conventional steel spirals or hoops concrete columns are similar to that occurs in CFST columns. The confinement mechanism of the concrete in normal reinforced concrete column can be drawn below (Park and Paulay, 1975):

- At the low concrete stress levels, the concrete can be considered in unconfined whereas the lateral spirals or hoops are hardly stressed.
- As the stress increases toward the uniaxial strength, the progressive internal cracking cause extensive lateral strains.
- The concrete starts to bear out against the spirals or hoops inside the concrete and hence apply confining action to concrete.

The most useful structural performance of CFST columns is the confinement of steel tube to the concrete core. At the same approach adopted above the mechanism of confinement of CFST column can be simplified below:

- At early stage of axial loading the steel tube of CFST column has no restraining actions toward the concrete due to the difference between the Poisson's ratio of concrete and steel. Hence, in this stage the concrete and steel behave independently (Tu et al., 2014).
- As the axial load increases, the longitudinal strain increases. It can be explain such behavior by considering Poisson’s ratio. The Poisson’s ratio of concrete in this stage approached or exceeded that of steel and the steel tube began to offer confinement to the concrete core (Lai and Ho, 2013).

There are many factors affect the confinement stresses of CFST columns under axial load. The following factors are relevant:

The CFST column with appropriate slenderness ratio and D/t ratio exhibits adequate axial capacity as the triaxial confinement effects cause to increase strength of concrete, whereas the high slenderness ratios lead to yield local buckling before reaching the required strains necessary to provide concrete confinement (Prion and Boehme, 1989; Giakoumelis and Lam, 2004; Gupta et al., 2007).

Matsui et al. (1995) reported that the circular and most of the octagonal cross sections can offer confinement for concrete core, whilst the square and rectangular tube provide confinement only on the corners and this is because the walls resists the concrete pressure.

At the same line, Schneider (1998) examined analytically and experimentally the structural behavior of concentrically loaded CFST columns having different sections such that five square, three circular, and six rectangular sections were experimented so as to study the effect of section type and thickness of steel on the behavior of CFST short columns. Their study revealed that the CFST column with rectangular or square section had the lower strength, stiffness and ductility comparing to the circular column. The better performance of circular CFST column is related to the confinement stress generated by the circular cross section is higher and more uniform than square and rectangular sections.

Sakino et al. (1985) observed that the effect of confinement depends on the condition of applying the load. That is if the concrete and steel tube are loaded at the same conditions, the steel tube offers confinement after yielding and if the load is applied only for concrete core the confinement effect is invisible.

Ding et al. (2011) studied the effect of yield strength of steel tube on the performance of CFST columns in terms of ultimate axial capacity, ductility and confinement effect. The increase of yield strength of steel tube significantly enhanced structural performance of composite columns. On the other side, they also reported that the use of high strength concrete increases the ultimate load capacity and reduces ductility of CFST columns.

Typically, buckling is a mode of failure normally yielding from structural elastic instability due to high compressive action on the structural member involved. Its behavior is considered by developing deformations in a direction normal to that of loading. Although the tensile strength of steel is high, steel tube under compression loads may buckle locally. The presence of concrete inside the CFST column significantly increases the local buckling resistance of steel tube. The mode of failure of steel tube, concrete and CFST column are schematically depicted in Figure 2.26. It can be seen that the failure mode for steel tube is outward and inward buckling whereas the plain concrete stub column fail in brittle fashion by shear. However, outward buckling is found in steel tube of CFST column and the concrete core exhibits more ductility until overall failure (Giakoumolis and Lam, 2004; Han et al., 2014).

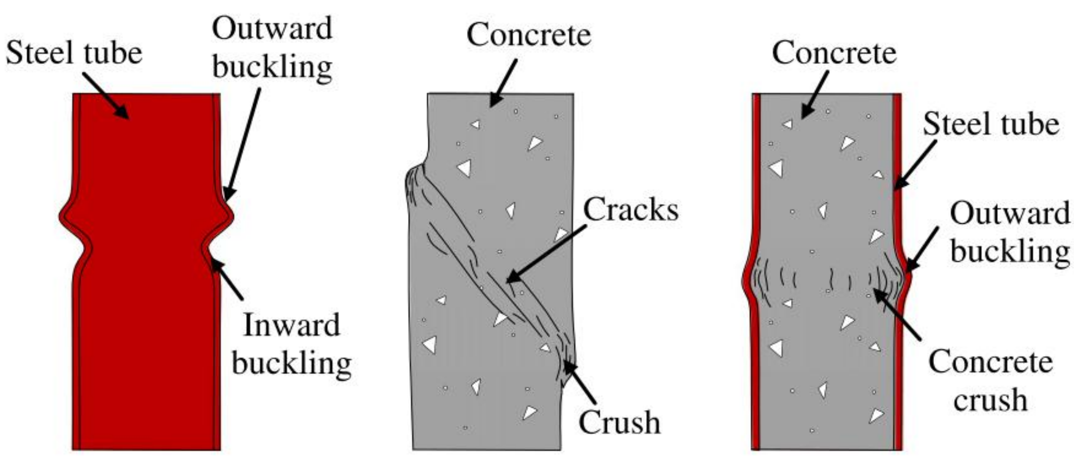

Figure 2.26 Typical mode of failure for steel tube, plain concrete and CFST column (Han et al., 2014)

The use of circular cross section of steel tube improves the buckling resistance CFST column while the local buckling is more expected to happen in rectangular or square cross sections. The increase of D/t ratio increases local buckling event of CFST columns even at the low deformation stage (Gupta et al., 2007). The structural steel tube infilled with softer concrete can lead to create higher axial loads on the steel tube and resulting in buckling failure. The length to diameter ratio of CFST column greatly influences local buckling resistance. That is to say, column with length to diameter ratio of ≤ 4 can be considered as short column since the confinement stress created from the steel can be completely derived without global buckling. Thus, in order to avoid global buckling to take place before maximum column strength, it is important to specify a practical factor when computing the strength of slender CFST column (Han et al., 2005; Uy et al., 2011).

As indicated in previous studies the simultaneously application of load to concrete and steel at the end of columns offers the strain continuity in the composite system (Kilpatrick and Rangan, 1999). Accordingly, the performance of CFST column does not influence too much by the bond quality between the inner wall of steel tube and concrete core. However, strong bonding forces are structurally required where longitudinal shearing stresses are probably to be predominant such as connections and foundation supports. In this case the applied forces are transferred to the concrete or the steel tube. Thus adequate bond stress capacity needs to be provided (Roeder et al., 1999: Tao et al., 2016). The diameter of steel tube is one of the most factors affecting concrete-steel interlocking. In this regard, the large D/t ratio contributes to deformation and develops lower bond stresses due to the insufficient effect of interlocking between steel and concrete. On the other hand, higher D/t ratio lowers contact forces as well as ductility. In practice stiffening method can be used to offer satisfactory bond between the steel and concrete in CFST columns. In this method, steel bars are welding to the inner wall of steel tube. Taking into account the specification of bars influences the efficiency of this method. Novel is another method also can be applied but depends on the increase of contact area between steel and concrete, Figure 2.27. Longitudinal symmetric stiffeners are welding to the inner side of steel tube along the column length of column (Huang et al., 2002; Abedi, 2008).

Figure 2.27 Steel tube of novel CFST column (Petrus et al., 2010)

2.4.2 Use of steel fiber in CFST columns

The brittle concretes yield CFST columns with uncomplimentary structure performance, i.e., unfavorable axial load capacity (Tao et al., 2008). In order to eliminate inherent brittleness of concrete, fiber reinforced concrete can be introduced (Güneyisi et al., 2015). Khaloo et al. (2014) evaluated the effect of incorporation different volume fraction of steel fiber on the flexural toughness of beams made of SCC had medium and high strength. They concluded that the steel fiber can be used to enhance the ductility of SCC significantly up to volume fractions of 2.0%. The mechanism of steel fiber behavior in conventional concrete was explained earlier by (El-Dieb, 2009; Cattaneo et al., 2012). The steel fiber serves as a bridge between the cracks formed in concrete; consequently hold materials together. Thus it can be expected that the use of steel fiber reinforced concrete to fill hollow steel tube enhances the ductility of CFST columns.

Recently, the structural behavior of fiber reinforced CFST columns at normal temperature has been an increasing concern. The behavior of steel tube columns filled with fiber reinforced low and normal strength concrete have been investigated by Tao et al., (2009) and Ellobody (2013). In these researches, the CFST columns were of slender columns or/and examined with eccentrically load and the use of fiber were achieved to increase strain intensity accompanying with flexure strength increment as fiber reinforced concrete possesses favorable flexural and tensile strengths. As a result, several beneficial effects of composite behavior in terms of strengths are achieved. In addition, the ductility and the energy absorption capability of CFST columns made with fiber reinforced concrete are significantly enhanced because the use of fiber contributes to stiffness which delays the growing of lateral deflection.

Lu et al. (2015) investigated the structural performance steel fiber reinforced CFST columns under axial compression. The main objective of the study is to examine the effect of steel fiber, concrete strengths and thicknesses of steel tube on the behavior of CFST columns. For this purpose they tested thirty six specimens by considering steel fiber volume percentages of 0%, 0.6%, 0.9% and 1.2%, steel tube thicknesses of 3, 4 and 5 mm and concrete strengths from 50 to 70 MPa. The effect of these parameters used to analyze the structural behavior of CFST columns in terms of ultimate load and ductility. The results of strength index of steel fiber reinforced CFST column specimens were above that of free of fibers as shown in Figure 2.28a. Therefore they concluded that the steel fiber had a beneficial effect on composite action between steel tube and concrete. Moreover, the study also presented that the addition of steel fibers can substantially enhance the ductility index of the specimens, Figure 2.28b. One of the most significant highlight concluded from their study was the use of steel fiber reinforced CFST column is a more effective method to improve the ductility index of such columns than using thicker steel tube.

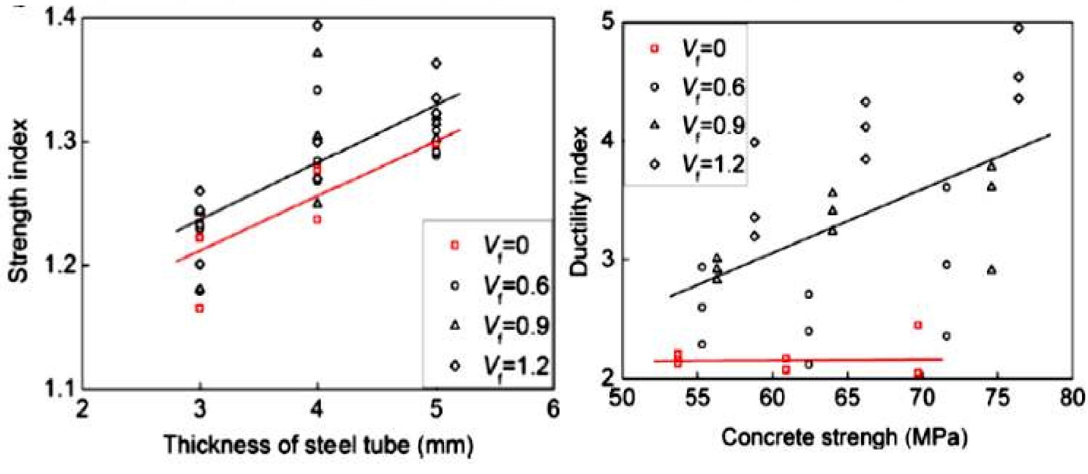

a) b)

Figure 2.28 a: Strength index in terms of thickness of steel tube, b: Ductility index vs. concrete strength (Lu et al., 2015)

Guler et al. (2013) carried out an experimental research program on the behavior of steel fiber reinforced concrete filled steel tube (SFRCFST) columns under axial load. They aimed to study the influence of D/t ratio and the composite action in terms of bond strength between steel tube and concrete core on the structural performance of SFRCFST columns. To this aim, the experimental work involved the use of 100 mm*100mm square steel tube having different D/t ratios of 20, 25 and 33. The length of each tube was 400 mm to prevent the slenderness effect. The mixture proportions of the steel reinforced concrete used to fill steel tube are given in Table 2.2. They founded that the bond strength of steel tube which had small D/t ratio is lower than that of those with high D/t ratio (thinner steel tube). The study also reported that the improvement in the ultimate axial capacity due to the provided confinement effect by the steel tube for the core concrete is affected by the strength of concrete itself. Moreover, their experimental results were compared with provided design international codes, Table 2.3. They found that all the codes (Eurocode 4 (2004), ACI318R (2005) and AISC (1999)) overestimated axial load capacity with respect to thinner steel tube. From this finding they advised to use a reduction coefficient in the axial load capacity calculation for the SFRCFST columns with thinner steel tube so as to consider the weak confinement action.

Table 2.2 Mixture proportion of steel fiber reinforced concrete (kg/m^3) (Guler et al., 2013)

Item	Weight (kg)
Cement	1000
Siliceous sand (0.5-2 mm)	325
Siliceous powder (0-0.5 mm)	500
Silica fume	250
Super plasticizer	130
Water	165
ZP 305 Dramix steel fiber	160
Total	2530

Table 2.3 Computed and evaluated ultimate axial capacity (kN) (Guler et al., 2013)

Column type	D/t ratio	$N_{u, Eexperimental}$	$N_{u, EC4}$	$N_{u, ACI}$	$N_{u, ASCI}$
SFRCFST column	33.3	856	1370	1218	1047
SFRCFST column	33.3	902	1370	1218	1047
SFRCFST column	25	990	1440	1294	1114
SFRCFST column	25	980	1440	1294	1114
SFRCFST column	20	1481	1309	1369	1187
SFRCFST column	20	1474	1309	1369	1187

An experimental investigation on the structural behavior of steel tubular columns infilled with plain and steel fiber reinforced concrete is performed by Tokgoz and Dundar (2010). The volume fraction of the end hooked RC 65/35 BN-type steel fibers was 0.75%. The SF incorporated in concrete mixtures had a length, diameter, aspect ratio and density of 35 mm, 0.55 mm, 64 and 7850 kg/m^3. Their study showed that the use of steel fibers in core concrete had considerably developed ductility and deformations, Figure 2.29. On the hand, they also observed that the addition of SF into concrete core does not enhance the ultimate strength capacity of composite columns.

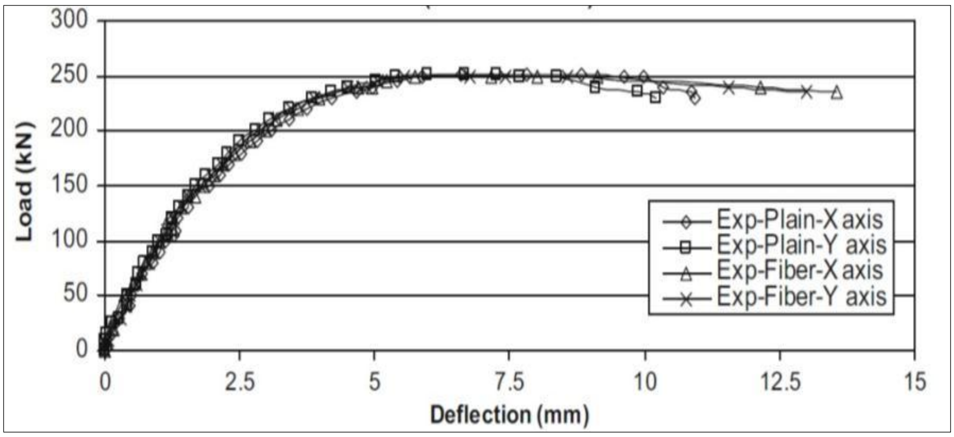

Figure 2.29 Experimental load-deflection curves for CFST and SFRCFST columns (Tokgoz and Dundar, 2010)

Yi-yan et al. (2015) studied the shear reinforcing effect of SF on CFST short column by the use of high strength concrete. In their study, 9 plain CFST and 27 SFRCFST columns were produced in order to test them under axial load. Their study interested with various parameters to evaluate the ultimate axial capacity of CFST column; concrete strength, thickness of steel tube and steel fiber volume fraction. The tested columns revealed that the presence of steel fiber had no effect on the failure mode of CFST column as they observed a shear failure plane in plain CFST and SFRCFST columns, Figure 2.30. Another conclusion reported in there study showed that the SF has no effect on the transverse strain of steel tube when the applied load is comparatively low. However, when the applied load increases to a certain level, the transverse strain of plain CFST columns increases with a much higher rate than the corresponding SFRCFST columns. They justified such behavior to the ability of SF to control the development of concrete cracks, thus delay the lateral expansion of concrete.

Figure 2.30 Shear failure plane in concrete core (Yi-yan et al., 2015)

2.4.3 Conventional reinforced concrete and CFST columns

A reinforced concrete column is a structural member consists of a combination of concrete and an embedded steel frame (reinforcement bars). The ability of plain concrete column to withstand lengthwise shortening and laterally expansion is quantified by using of longitudinal bars and lateral restraint - ties or helical spirals - for these longitudinal bars. In this regard, the reinforced concrete columns are classified to tied and spiral column. Spirals can be considered more effective to increase column strength than ties. The use of closely spaced spirals significantly increases the ability of holding the longitudinal bars in place, and they also confine the concrete inside and enhance its resistance to axial compression (McCormac and Brown, 2014).

Although no one can deny the favorable performance of conventional reinforced concrete columns, but recently with a sharp increase in labor costs, the on-site temporary works involving formworks of concrete require high costs in construction market. Particularly for the projects like building with high story heights, the time of construction and costs for the temporary works have considerably increased, and thus the competitiveness of the reinforced concrete construction method has been adversely affected. Obviously, construction process of columns in typical reinforced concrete frame constructions is one of the challenges, therefore, absolutely advantageous to minimize the on-site temporary works for reduction of the construction time (Oh et al., 2016).

The concrete filled steel tube column as discussed earlier is a composite member made by filling steel tube with concrete. Concrete inside the steel tube enhances the performance of the steel tube column, and the stainless steel tube in turn offers lateral confinement or lateral reinforcement to the concrete. Unlike conventional reinforced concrete column and thin walled steel tube column, the CFST column has higher load-carrying capacity, toughness, and ductility. For a specified load, the required cross sectional area for CFST column smaller and the ratio of strength to weight higher than that of a conventional reinforced concrete column. However, the external material of CFST column is steel which can be represented the main disadvantage of such column because causing to a lower fire resistance compared with conventional reinforced concrete column (Yin et al., 2006; Jamaluddin et al., 2013).

CFST columns have become the preferred form for many earthquake-resistant structures. Subjected to severe earthquakes, concrete encasement cracks resulting in reduction of stiffness but the steel core provides the shear capacity and ductile resistance to subsequent cycles of overload. Moreover, due to the fast erection and optimum design, the construction costs could be reduced (Huang, 2015).

2.4.4 Applications of CFST columns in structures

Nowadays, the composite structural columns are widely applied in the construction of multi-storey buildings, and other types of structures all around the world. In fact, there are several other applications of composite construction including multi-storey car parks, industrial and residential buildings, metro station buildings and apartments (Han et al., 2014). Moreover, CFST columns have been successfully utilized in bridge members. Figure 2.31 illustrates the applications of CFST columns in the form of built-up sections adopted in piers the beam bridges-Ganhaizi bridge, located in Sichuan Province, China (Huang, 2015).

Figure 2.31 CFST built-up columns utilized for continuous beam bridge (Huang, 2015)

In China CFST columns have been extensively utilized in construction. For example SEG Plaza in Shenzhen, which is the 21st tallest building in China and the 72nd tallest in the world, Figure 2.32. The building constructed by using C60 concrete and Φ 1600 mm × 28 mm steel section profile. The roof height of the building is 292 m. There are a total of 71 stories above ground (72 when counting the helipad) and 4 stories underground (Han et al., 2014; Wikipedia, 2016).

Normally, the towers of electrical transmission throughout the world involved angle sections and normal bolted connections. At the present time, an important challenges in this endeavour are architectural appearance becomes more required and maintenance is more expensive. These issues motivate designs made of hollow sections has good prospects of application in the construction sectors (Wardenier et al., 2010). For instance, Figure 2.33 depicts a long-span electrical transmission tower built in 2009, Zhoushan, China. It is the largest electrical transmission towers in the world. The height of these pylons are 370 meters and the diameter of CFST column is 2 meter (Han et al., 2014; Huang, 2015).

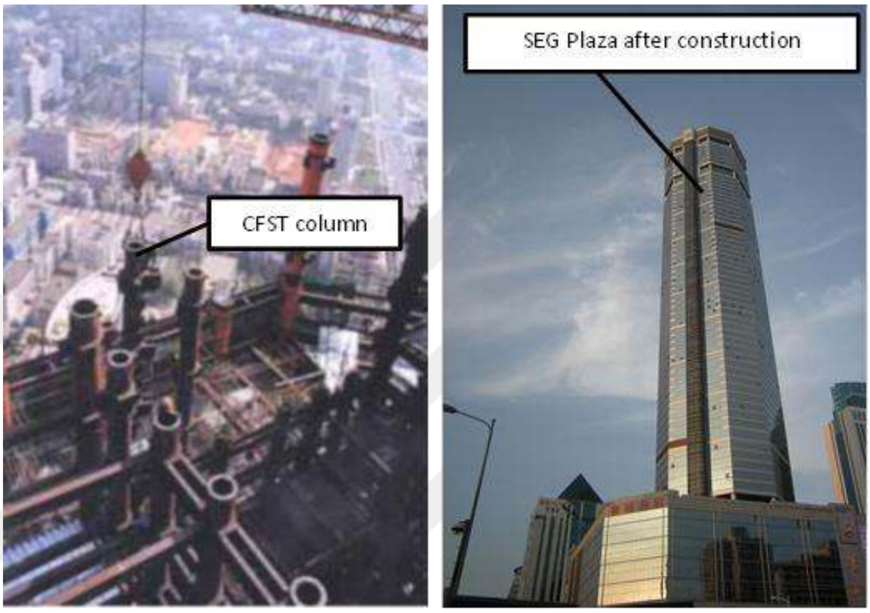

Figure 2.32 SEG Plaza constructed with CFST column (Wang, 2014)

Figure 2.33 Zhoushan electricity tower, China (Huang, 2015)

CHAPTER 3

METHODOLOGY

In this thesis, we undertake a sequence of experiments and numerical investigations to test the properties of steel fiber reinforced self-compacting concrete (SFRSCC) and to assess the composite column's behaviour made with SFRSCC under compression. For experimental program, hooked end steel fiber, nano silica (nS) and metakaolin (MK) were used. Fresh properties of SFRSCC were first measured and then their mechanical performance were studied through compressive strength, splitting tensile strength, bonding strength, elastic modulus, fracture energy and net flexural. After that, a detailed numerical analysis was conducted to recognize the structural response of SFRSCC filled steel tubular columns subjected to compressive loading. For this, the capacity of such composite columns were evaluated by using four international design codes; Eurocode 4, ACI, AIJ, and DL/T. The main experimental and numerical parameters of the study were nS and MK content, strength level of core concrete, diameter of column, and yield strength of steel tube used. The details of the study are given below.

3.1 Experimental study

3.1.1 Materials

We used (CEM I 42.5R) Portland cement (PC) having 3.15 g/cm^3 specific gravity and Blaine fineness of 326 m^2/kg in this study conforming to TS EN197-1 (which mainly based on the European EN197-1). The fly ash (FA) utilized in the current study was type F following ASTM C- 618 (2000) criteria and taken from the thermal power plant of Yumurtalik- Sugozu with commercial quality. The specific gravity of FA was 2.25 g/cm^3 and that of the Blaine fineness was 287 m^2/kg. MK is a white color, it has a specific gravity of about 2.6. Chemical and physical characteristics of PC, FA, MK, and nS are shown below. In this study, hooked end steel fiber with length, diameter, and aspect ratio equal to 30 mm, 0.6 mm, and 50, respectively as in Figure 3.1, was used to produce SFRSCC. High range water reducing admixture

(HRWRA) having 1.07 specific gravity and 5.7 pH was utilized in all mixes. HRWRA characteristics are given in Table 3.2 as reported by the local supplier. Limestone was crushed to be used as coarse aggregate with an maximum size equal to 16 mm and we utilized natural river sand as the fine aggregate having ultimate size of 4 mm. Sand, as well as gravel, had a specific gravities of 2.39, and 2.69, respectively. The gradation of particle size acquired by means of the sieve analysis of the sand and gravel is shown in Figure 3.2. For reinforced concrete sample preparation for testing the strength of bonding, reinforcing ribbed steel bars having 16 mm diameter and minimum yield strength of 420 MPa was utilized.

Table 3.1 Properties of PC, FA, MK and nS

Analysis report (%)	Cement	FA	MK	nS
CaO	62.12	2.24	0.5	-
SiO_2	19.69	57.2	53	99.8
Al_2O_3	5.16	24.4	43	-
Fe_2O_3	2.88	7.1	1.2	-
MgO	1.17	2.4	0.4	-
SO_3	2.63	0.29	-	-
K_2O	0.88	3.37	-	-
Na_2O	0.17	0.38	-	-
Loss on ignition(%)	2.99	1.52	0.4	≤ 1.0
Specific gravity	3.15	2.04	2.6	2.2
Fineness (m^2/kg)	327	379	18,000	-
Surface-volume ratio (m^2/gm)	-	-	-	150 ± 15
Average particle size (nm)	-	-	-	14

Table 3.2 Properties of HRWRA

Properties	HRWRA
Name	Glenium 51
Color tone	Dark brown
State	Liquid
Specific gravity (kg/l)	1.07
Chemical description	Modified Polycarboxylic type polymer
Recommended dosage	1-2% (binder content%)

Figure 3.1 Steel fiber utilized in this research

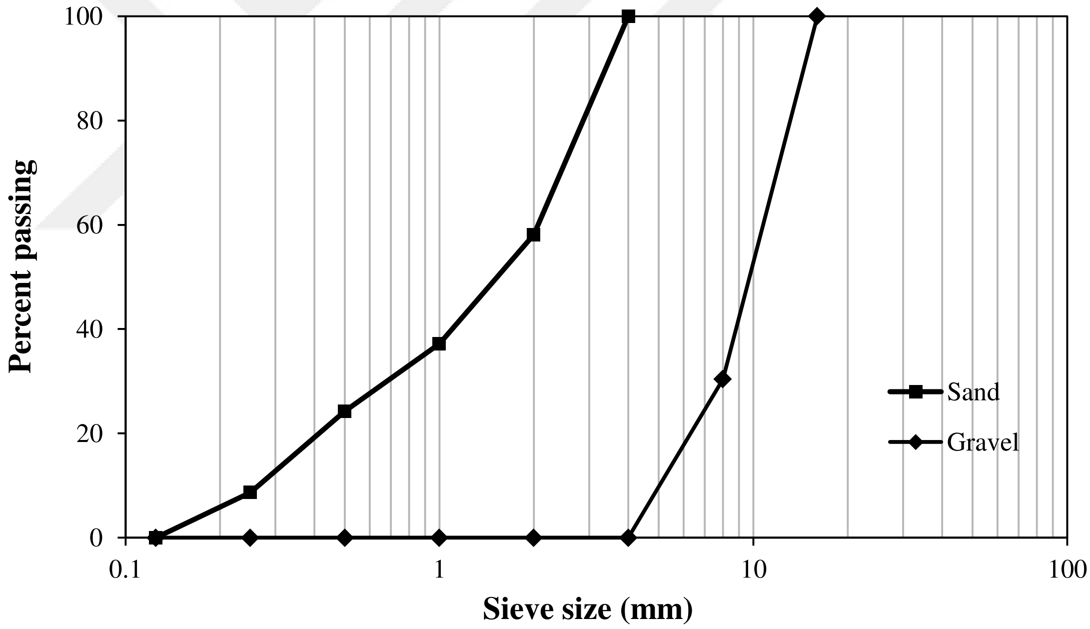

Figure 3.2 Fine and coarse aggregates sieve analysis

3.1.2 The design of the mixture

We have designed the SFRSCC mixtures with 550 kg/m^3 total binder amount and at 0.37 w/b percentage. The number of SCC groups manufactured in this research was 4 and in every SCC group; 0%, 2% and 4% nS, as well as 0% and 10% MK substitution degrees by weight was used instead of the PC. The mixtures in both of the first and second groups were made without SF while in third and fourth groups

SF had been added at a ratio of 1% , by volume. Totally 12 mixtures were made based on the aforementioned factors. The mix ratios are shown in detail in Table 3.3. In mixture ID, nano silica, metakaolin and steel fiber are abbreviated as nS, MK and SF. For instance, nS2MK10SF1 denotes that the SFRSCC mix has nS ratios of 2%, MK 10% as well as steel fiber 1%. The mixes have been designed based on 700 ± 50 mm slump flow diameter and this was realized by using the HRWRA at different quantities.

3.1.3 Casting and curing

During casting, powder materials were first mixed while still dry in the mixture. Then, the aggregate was introduced and blended together. About halves of water and HRWRA were blended in a container and introduced to the mix. The second halves of the water and the HRWRA was slowly introduced into the mix to attain uniformity. Fibers were dispersed in the mix and meticulously blended to attain a homogeneous dispersion. Following the completion of fresh laboratory checks, the fresh concrete was cast in the mold. Samples were taken out of the molds after one day from being poured and submerged in water for a curing period up to testing day. The medium strength of compression of three 150 mm cubes at 28 and 90 days of age were calculated as indicators of compression strength. Additionally, 100x200 mm cylindrical mold was filled from the SFRSCC mixture to measure splitting tensile strength at 28 and 90 days. For each mixture, three 150x300 mm cylinder specimens were casting to attain a modulus of elasticity. The bond strength measurement was taken on a 150 mm cubes specimen inserted bar steel at the age of 90 days. Finally, net flexural and fracture energy were examined on 100x100x500 mm beam at the age of 90 days.

3.1.4 Testing procedure

3.1.4.1 Fresh properties

The slump flow diameter, T_{50} slump flow time, L-box height ratio, L-box T_{20} and T_{40} flow time, and V-funnel flow time tests were carried out based on EFNARC (2005) committee (European Federation for Specialist Construction Chemicals and Concrete Systems) recommendations.

.

Table 3.3 Mix proportions for SFRSCC (kg/m^3)

Mix ID	(w/b)%	cement	FA	nS	MK	SF	water	HRWRA	Coarse agg.	Medium agg.	Natural sand
nS0MK0SF0	0.37	385	165	0	0	0	203.5	4.67	374.4	374.4	748.7
nS2MK0SF0	0.37	374	165	11	0	0	203.5	9.62	373.4	373.4	746.8
nS4MK0SF0	0.37	363	165	22	0	0	203.5	13.73	372.5	372.5	744.9
nS0MK10SF0	0.37	330	165	0	55	0	203.5	6.05	372.0	372.0	744.1
nS2MK10SF0	0.37	319	165	11	55	0	203.5	10.45	371.1	371.1	742.2
nS4MK10SF0	0.37	308	165	22	55	0	203.5	15.12	370.1	370.1	740.3
nS0MK0SF1	0.37	385	165	0	0	39.25	203.5	4.67	374.4	374.4	748.7
nS2MK0SF1	0.37	374	165	11	0	39.25	203.5	9.62	373.4	373.4	746.8
nS4MK0SF1	0.37	363	165	22	0	39.25	203.5	13.73	372.5	372.5	744.9
nS0MK10SF1	0.37	330	165	0	55	39.25	203.5	6.05	372.0	372.0	744.1
nS2MK10SF1	0.37	319	165	11	55	39.25	203.5	11	371.1	371.1	742.2
nS4MK10SF1	0.37	308	165	22	55	39.25	203.5	15.4	370.1	370.1	740.3

The value of slump flow, the initial test for the consistence of concrete in the fresh state to fulfill the required specification, is an accurate test. It is utilized to describe the flowability of a fresh concrete in free circumstances. Therefore, it may naturally be determined for all. T_{50} time is the time measured for concrete flow to 500 mm diameter. EFNARC (2005) gives extra information related to the resistance of segregation, and concrete homogeneity, which may be observed visually at the moment of testing and/or the measurement of T_{50} time. This test showed in Figure 3.3. The viscosity may be measured by the T_{50} slump flow time and V-funnel flow time. The flow rate associated with viscosity may be defined by the outcomes of these checks although the actual viscosity may not be realized through these checks. The V-funnel flow time is measured by using a V-shaped funnel. We pour concrete in fresh state in it to the brim and then allow the concrete to pass out of the funnel, the time it takes for the concrete to completely pass through is noted down as the V-funnel flow time as shown in Figure 3.4. The fresh concrete passing ability to pass through restricted spaces and tight holes like congested reinforcement areas without inducing blockage, homogeneity loss, or segregation may be measured by being subjected to the L-box examination. A known amount of concrete in fresh state is caused to flow on a horizontal path through the spaces between perpendicular, unruffled reinforcing bars and then we measure the height of the concrete behind the reinforcement as shown in Figure 3.5.

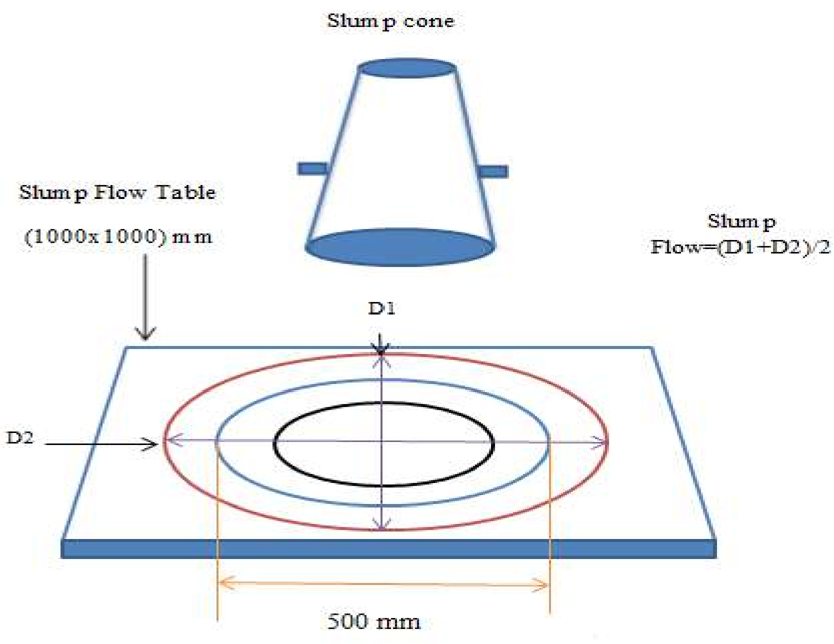

Figure 3.3 Measurement of slump flow diameter

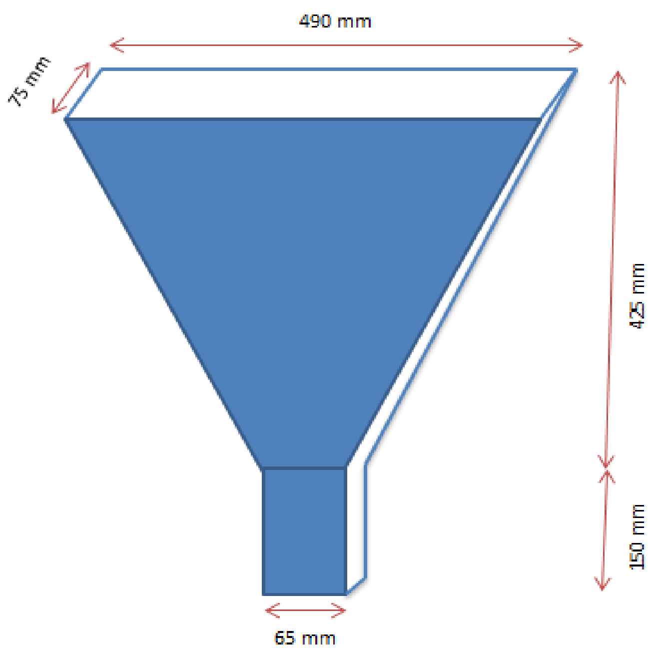

Figure 3.4 V-funnel apparatus

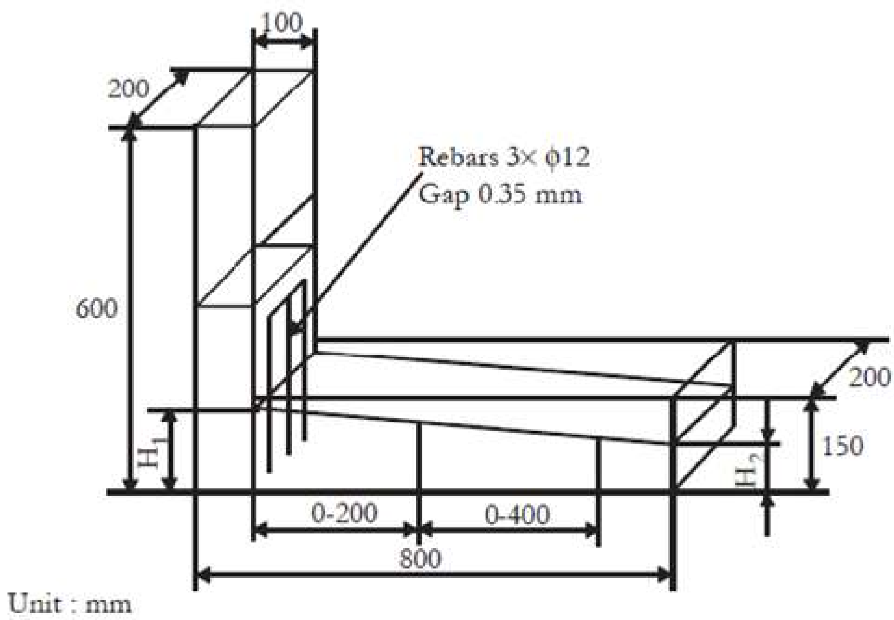

Figure 3.5 L-box test

3.1.4.2 Mechanical properties

The examination of compression was conducted on cubical samples (150x150x150 mm) through an examination machine with a capacity of 2000 kN with respect to ASTM C39 (2012) as shown in Figure 3.6. Three samples were used in the test for every mixture at two ages, 28 and 90 days. According to ASTM C496 (2011), by using the cylinder specimens of 100x200 mm at 28 as well as 90 days, one can determine the concrete splitting tensile strength. By calculating the average of the outcomes from the three examined cylinder specimens, the strength in terms of splitting tensile is determined. Finally Equation (3.1) can be used to calculate this examination.

$$f_{st} = \frac{2P}{\pi h \phi} \tag{3.1}$$

Where P is the ultimate load, h is the length of the cylindrical sample, and Φ is diameter of the cylindrical sample.

Figure 3.6 Compressive strength test machine

Static elastic modulus was calculated through testing cylinders with a dimension of Φ150x300 mm based on ASTM C469 (2010). Every sample was provided with a compress meter including a dial gage which can measure deformation down to 0.002 mm as shown in Figure 3.7 and then loaded to 40% of the maximum load. The ultimate load was determined based on the compressive strength test results for each mix. The first group of recordings for every sample was ignored and the modulus of elasticity was calculated as the rate of the second two groups of recordings. For each parameter, three samples were used.

The test to determine the fracture energy (G_f) was carried out with respect to the standard of RILEM 50-FMC Technical Committee (RILEM 50-FMC, 1985). The displacement was read at the same time by utilizing a linear variable displacement transducer (LVDT) at the centre of the sample's length. An examination machine (Instron 5590R) with a closed-loop, having a 250 kN maximum load was utilized for loading. The description of the examination machine and specimen in addition to placing (LVDT) were illustrated in Figures 3.8 and 3.9.

Figure 3.7 Modulus of elasticity test setup

The beams, which were 500 mm long and had a cross-section of 100x100 mm, were manufactured for testing fracture energy. The proportion between the notch and the depth (a/D) for samples was 0.4 and the notch opening was attained by decreasing the original cross section to 60x100 mm by cutting so as to accommodate large aggregates in more abundance, and the distance between supports was 400 mm. Load vs. deflection at the center of distance (δ) curve was measured for every sample and area within the load vs. displacement at the center of distance (Wo) was utilized in the fracture energy determination. To calculate the fracture energy, the equations given by RILEM 50-FMC Technical Committee (RILEM 50-FMC, 1985) can be used.

$$G_F = \frac{WO + mg\frac{s}{u}}{B\,(W-a\,)}\,\delta s \qquad (3.2)$$

Where B is width, W is depth, a is notch depth, S is the span, U is length, m is mass, and δs is specified deflection of the beam.

Notched beams were used to calculate the net flexural strength by means of the subsequent formula on the assuming the absence of notch sensitivity, given that Pmax stands for the ultimate load.

$$f_{flex} = \frac{3\mathrm{P\ maxS}}{2\mathrm{B(W-a)\ 2}} \qquad (3.3)$$

Figure 3.8 Universal testing devices for three point flexural testing

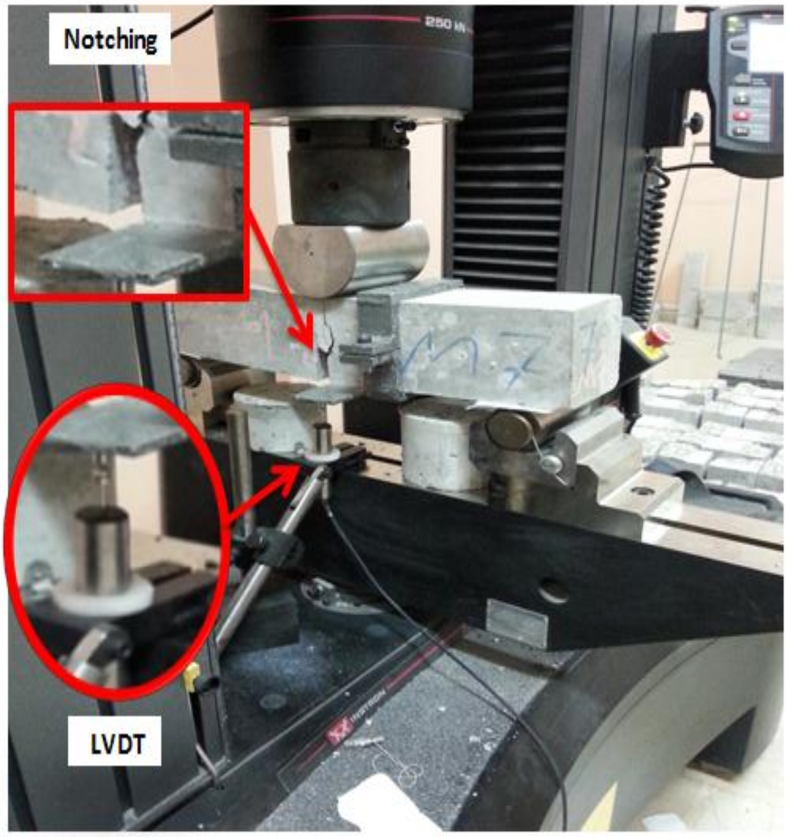

(a)

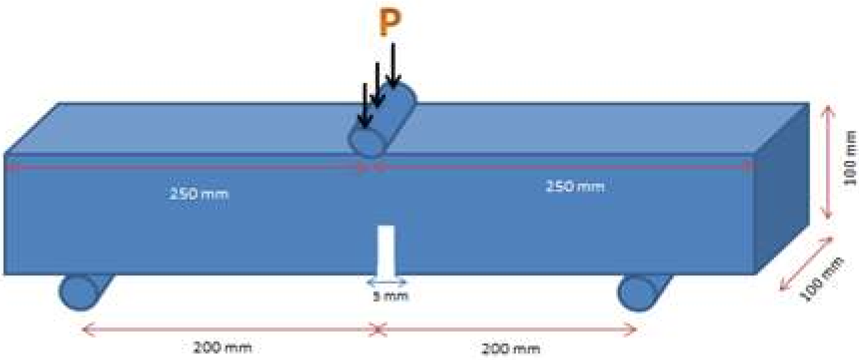

(b)

Figure 3.9 Beam specimens under flextural test

Bar steel-concrete bonding strength was measured based on RILEM RC6 (1996)**.** The strength of bonding, τ_b is determined by the formula below:

$$\tau_b = \frac{F}{\pi L d} \tag{3.4}$$

Where F is the tensile load at failure (N), d is the diameter (mm) and L is the development length (mm) of the reinforcing steel bar. Because steel bar with 16-mm diameter and cubic samples with 150-mm dimensions are utilized in this research, d and L are taken as 16 mm and 150 mm. The description of the bonding strength test sample can be seen in Figure 3.10. A 600 kN universal testing machine was utilized to load by installing a specially altered test tool into it as can be seen in Figure 3.11.

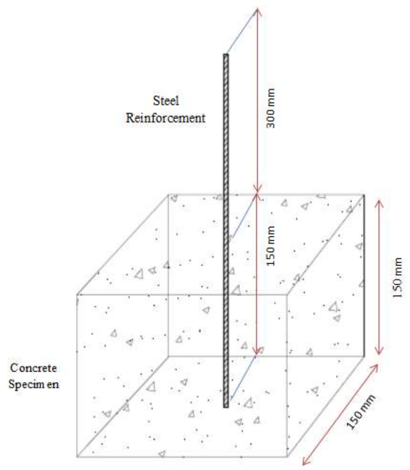

Figure 3.10 Details of the sample used to conduct the test of bond strength

Figure 3.11 Pullout test system during testing

3.2 Numerical study

3.2.1 Introduction to CFST column

The application of concrete-filled steel tubular (CFST) columns as composite members in construction sectors have been extensively increasing day by day. Nowadays, industrial plants, subways, multi-storey construction and arch bridges construct with these composite members. The CFST columns characterized by several advantages in terms of structural performance such as superior strength and stiffness, proper ductility, low brittleness and good strain energy absorption abilities. CFST columns construction has established to be cost-effective in building resources materials as well as satisfying for rapid construction and therefore its application has been developed in construction building industries worldwide (Yuan and Yang, 2013).

The performances of concrete and steel with the presence of new innovative materials have significantly enhanced and the cross section with these materials becomes lighter, hence, the load carrying capability of the column is significantly influenced (Güneyisi et al., 2016). The main benefits of CFST columns can be illustrated as follows (Chang et al., 2013):

- The confinement effect of surrounding steel as well as contribution in load carrying capacity of CFST columns represent the main structural advantages resulting from the use of such columns.
- Inhibition or delay of local buckling of the steel tube infilled with concrete.
- The construction period is also diminished by excluding the permanent formwork usually used for conventional concrete steel column.

From the above, the use of concrete-filled steel tubes in various areas of constructions is becoming an attractive solution. Moreover, as a result of the increase in the load carrying capacity, stiffness, and ductility as well as economy and rapid construction, use of CFST columns has become prevalent (Chang et al., 2013; Güneyisi et al., 2016).

In order to dependably predict the strength and ductility of circular CFST columns, correct constitutive models must be developed for confined concrete. However, it has been found that there are inconsistencies in empirical models projected by investigators for confined concrete (Liang and Fragomeni, 2009). On the other hand, there are also inconsistencies in the capacity prediction of axially loaded CFST column given in current design codes such as Eurocode 4 (2004) and ACI 318 (2005).

3.2.2 Details of study

The main objective of the analytical study is to evaluate the behavior of structural steel tube infilled with steel fiber reinforced self-compacting concrete (SFRSCC) subjected to compressive load. Towards this aim, the first part started with applying four available codified formulations namely Eurocode 4 (2004), ACI 318 (2005), Japanese (AIJ) (2001), and Chinese (DL/T) (1999) so as to compute the axial load carrying capacity of circular CFST short columns. The calculation involved the use of set of data comprising the experimented compressive strength (results of 12 concrete mixtures tested experimentally at 28 and 90 days), three different column outer diameters and three steel yield strengths. Moreover, to study the structural responses of CFST column under compression forces, different aspects have been employed. The interaction between both of diameter to thickness (D/t) ratio and core concrete strength and the variance of axial capacity have been graphically presented. Despites, the same parameters included in the experimental research- nano silica (nS), steel fiber (SF), metakaolin (MK) and curing period – have been also discussed with respect to their actions on the performance of CFST column. The test configuration taken into account is uniaxial compression test which is schematically described in Figure 3.12.

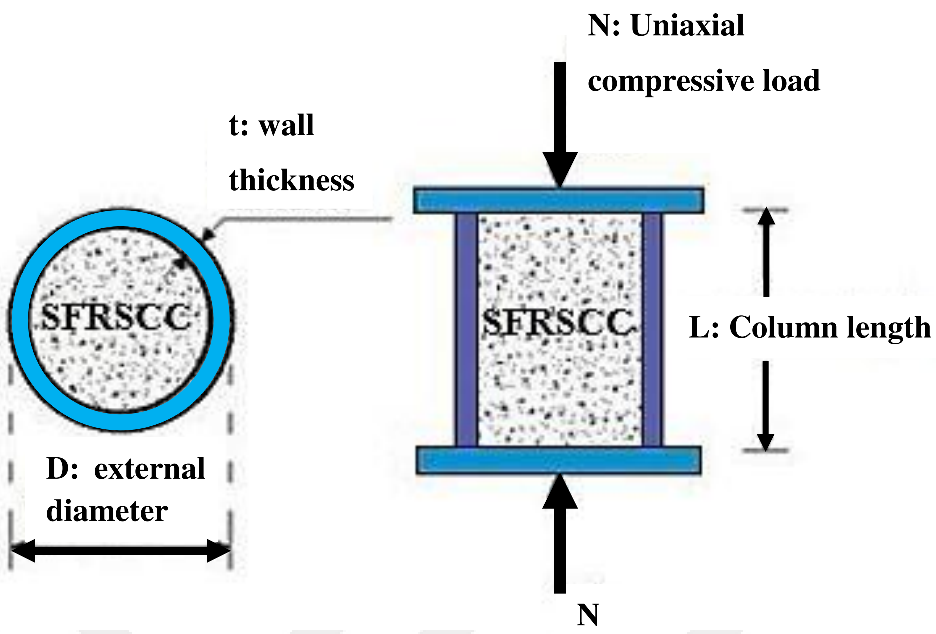

Figure 3.12 Presentation of load applied to the section of circular CFST column

3.2.3 Design code formulas

3.2.3.1 Eurocode 4

One the most reasonable treatment to date is that which is modeled by the Eurocode 4 (2004) (EC4). In this relation, the contributions of the concrete core and the steel tube as well as the confinement effect of the steel tube are considered. In this regard, the confinement coefficients for the steel (η_a) and core of concrete (η_c) are involved. Therefore, both of the steel and concrete strengths are influenced in such a way that the triaxial state of stress condition leads to increase strength of concrete core by η_c, whereas the hoop stresses yield a decrement in the steel yield strength by η_a.

The equations recommended by EC4 for computing axial capacity of a circular CFST column ($N_{u,\,EC4}$) are proposed as:

$$N_{u,EC4} = \left(1 + \eta_c \frac{t}{D} \frac{f_y}{f'_{cyl,150}}\right) f_c' A_c + \eta_a f_y A_s \qquad (3.5)$$

Where

$$\eta_a = 0.25(3 + 2\bar{\lambda}) \qquad (\eta_a \leq 1.0) \qquad (3.6)$$

$$\eta_c = 4.9 - 18.52\bar{\lambda} + 17\bar{\lambda}^2 \quad (\eta_c \geq 0) \tag{3.7}$$

in which the relative slenderness ($\bar{\lambda}$) of CFST column can be calculated from following equation:

$$\bar{\lambda} = \sqrt{\frac{N_{pIR}}{N_{cr}}} \tag{3.8a}$$

Where:

N_{pIR} is the cross-section plastic resistance of the CFST column, given as:

$$N_{pIR} = f_y A_s + f'_{cyl,150} A_c \tag{3.8b}$$

N_{cr} is the Euler buckling load of the pin-ended CFST column, represented by:

$$N_{cr} = \frac{\pi^2 (EI)_{eff^2}}{l^2} \tag{3.8c}$$

Where:

$(EI)_{eff^2}$ is the effective flexural stiffness of CFST and can be computed as:

$$(EI)_{eff^2} = E_s I_s + K_e E_{c2} I_c \tag{3.8d}$$

Where:

E_s and E_{c2} is the elastic modulus of steel and concrete, respectively. The elastic modulus of concrete = $22000[(f'_{cyl,150} + 8)]^{0.3}$

Typically, when $\bar{\lambda} = 0$, the sectional capacity (the zero length strength), $P_{0;EC4}$ can be simplified as

$$P_{0,EC4} = \left(1 + 4.9\frac{t}{D}\frac{f_y}{f'_{cyl,150}}\right) f'_{cyl,150} A_c + 0.75 f_y A_s \tag{3.9}$$

3.2.3.2 ACI 318R code

The American Concrete Institute (ACI-318R, 2005) for calculating the ultimate axial capacity of the circular CFST column was designated as $N_{u,\,ACI}$ in calculations. This relation does not contain the interaction between the steel tube and concrete core and the effectiveness of the concrete confinement. The steel tube limiting thickness to prevent buckling is based on realizing yield stress in a hollow tube under the action of monotonic axial loading which is not a significantly requirement for CFST columns. The equation for axial capacity of a circular CFST column, N_u is expressed by following formulae:

$$N_{u,ACI} = 0.85\, f'_{cyl,150}\, A_c + f_y A_s \tag{3.10}$$

Where $f'_{cyl,150}$ is the concrete cylinder compressive strength (150×300 mm), A_c is the concrete specimen core cross-sectional area, f_y is the yield stress of steel, and A_s is the cross sectional area of steel.

3.2.3.3 AIJ

AIJ (1997) (Architectural Institute of Japan. Recommendations for design and construction of concrete filled steel tubular structures, 1997) is another international code used for determining the capacity of the composite columns. In particular, AIJ conservatively estimate the confinement effects, which provide considerable underestimations on the sectional capacity of CFST columns. Thus, when using different CFST design codes to predict the sectional capacity of CFST columns, the predictions by AIJ compared with the test results are expected to be more conservative (Wang et al., 2015). The equation for axial capacity of a circular CFST column, $N_{u,\,AIJ}$ is expressed by following equation:

$$N_{u,AIJ} = 0.85\, f_{cyl,100}\, A_c + (1.0 + \eta) f_y A_s \quad \left(\frac{l_k}{D} \leq 4\right) \tag{3.11}$$

where l_k is the effective length of a CFST column; and η is the confinement factor which is equal to 0.27. According to this formula, the composite action represented by the confinement factor improves the load carrying capacity which is independent of the material strength and the cross section geometry of the column (Lu and Zhao, 2010).

3.2.3.4 Chinese code DL/T

The formulae proposed by Chinese code DL/T (1999) considered CFST column has one material not as a composite with a total area of A_{sc} with a nominal yielding strength of f_{scy}. Moreover, Chinese code DL/T (1999) introduces a factor of ξ for the confinement effect to describe the action between the concrete and steel tube. The equations for axial capacity of a circular CFST column ($N_{DL/T}$) are given as:

$$N_{u,DL/T} = f_{scy}A_{sc} = f_{scy}(A_s + A_c) \tag{3.12}$$

In which:

$$f_{scy} = (1.212 + B\xi + C\xi^2)f_{ck} \tag{3.13a}$$

$$B = 0.1759\frac{f_y}{235} + 0.974 \tag{3.13b}$$

$$C = -0.1038\frac{f_{ck}}{20} + 0.0309 \tag{3.13c}$$

$$\xi = \frac{A_s f_y}{A_c f_{ck}} \tag{3.13d}$$

$$f_{ck} = 0.67 f_{cu} \tag{3.13e}$$

Where: ξ the confinement factor; A_{sc} and f_{scy} the area of composite section and the nominal yielding strength of the composite section respectively, f_{cu} the compressive strength of 150 mm cube, and f_{ck} the characteristic concrete strength.

3.2.4 Summary of main computation steps

The computation of ultimate axial capacities of the circular self-compacting concrete-filled steel tubular by using the four codes (EC4, ACI 318, AIJ and DL/T) which have been illustrated earlier in section 3.2.3 conducted as follows:

- The experimental results of compressive strength at 28 and 90 days have been employed.
- So as to comprise different specification regarded steel material characteristics, yield strength of the steel tube f_y selected as 150, 300 and 450 MPa.
- Three different diameter-to-thickness (D/t) ratios of the CFST column cross section of 25, 55 and 90 were utilized in all computations.
- The length to diameter ratio of short composite columns was 3 to ensure that they would be with a small slenderness effect and would not fail in overall buckling. At the same time wall thickness of the steel tube was 2.5 mm.

It should be mentioned that the conversion of compressive strength of standard concrete cylinders 150*300 mm (f_c') to compressive strength of 150 mm cubes (f_{cu}) calculated by using Table 3.4 (Eurocode 2, 2004).

Table 3.4 Conversions between f_c' and f_{cu} (Eurocode 2, 2004)

Compressive strength of concrete cylinder (150*300 mm) (MPa)	Compressive strength of 150 mm cube (MPa)
12	15
16	20
20	25
25	30
30	37
35	45
40	50
45	55
50	60
55	67
60	75
70	85
80	95
90	105

CHAPTER 4

RESULTS AND DISCUSSION OF EXPERIMENTAL STUDY

4.1 Analysis of fresh property

The four essential properties that may determine the filling ability and stabilization of fresh self-compacting concrete (SCC) are the passing ability, liquidity, resistance towards segregation, and viscosity. Every one of these properties may be dealt with through one test method or a set of them EFNARC (2005). Slump flow test, for example, is utilized to measure the fluidity; whereas, V-shaped funnel flow time examinations and the T_{50} slump flow time are utilized to determine the viscosity. It is required for the fresh SCC to fulfill at least one of aforementioned four essential characteristics. The level or intended value shown in Table 4.1 must be specified by the mixtures.

Table 4.1 Limitations according to EFNARC (2005)

Class		**Slump flow diameter (mm)**
Slump flow classes		
SF1		550-650
SF2		660-750
SF3		760-850
Class	T 50 (s)	V-funnel time (s)
Viscosity classes		
VS1/VF1	≤2	≤8
VS2/VF2	>2	9-25
Passing ability classes		
PA1	≥0.8 with two rebar	
PA2	≥0.8 with three rebar	

The steel fiber reinforced SCC (SFRSCC) mixtures manufactured for this research had the slump flow diameter ranging from 630 mm to 750 mm, which were found by calculating the rate of two observed diameters of tested concrete as illustrated in Figure 4.1. Figure 4.2 demonstrates the final diameters of the slump flow of the mixes. The findings prove that the presence of nano silica (nS) reduced the diameter of the slump flow. nS has big surface area and represents minuscule particles. This property of nS raises the need for water when nS is utilized in manufacturing concrete. In this experiment, we maintained an unchanging water amount but the HRWRA content was raised so as to fulfill the conditions for the fiber reinforced SCC. Although, the reduction in the final diameter of the slump flow was noted when an extra amount of nS was used. In addition, the prior research demonstrated that using nS in the SCC preparation reduces the final diameter of the slump flow (Güneyisi et al., 2015; Jalal et al., 2012).

However, the reference mixture slump flow is decreased when metakaolin (MK) is introduced at the percentage 10%. This result could be attributed to the larger surface area of the particles of MK in comparison to Portland cement (PC). This result corroborates the finding of Güneyisi and Gesoglu (2008). HRWRA amount was raised to attain agreeable slump flow diameter and to lower the reduction in slump flow diameter because of the use of MK. Another result is that the mixtures including dual use of (nS and MK) resulted in an accumulative effect compared to mixtures having merely nS or MK. This can be clearly seen in the mixtures nS2MK10SF0 and nS4MK10SF0.

It is worth mentioning that steel fiber inclusion results in lowering concrete workability to a great extent. As an example, the mixtures nS0MK0SF0, nS0MK0SF1, nS4MK10SF0, and nS4MK10SF1. This has been attributed to the fact that fiber cause jamming of concrete particles throughout flow. Moreover, no segregation between aggregates and cement was detected in any of the samples. As can be seen in Table 4.1, most the SCC mixes may be categorized as SF2, which is convenient for several usual uses like columns and walls. 750 mm, the highest diameter of the slump flow was attained in nS0MK0SF0 mix; whereas, 630 mm, the lowest diameter was achieved in nS4MK10SF1. The diameter decrease was shown in the research of (Beigi et al, 2013). Siddique et al (2013) reported that the slump flow diameter was within the range of 650–720 mm. According to them, the addition of fiber at the ratios of 0.5%, 1%, and 1.5% by volume in SCC decreases the diameter from 720 to 690, 670, 650 mm, respectively.

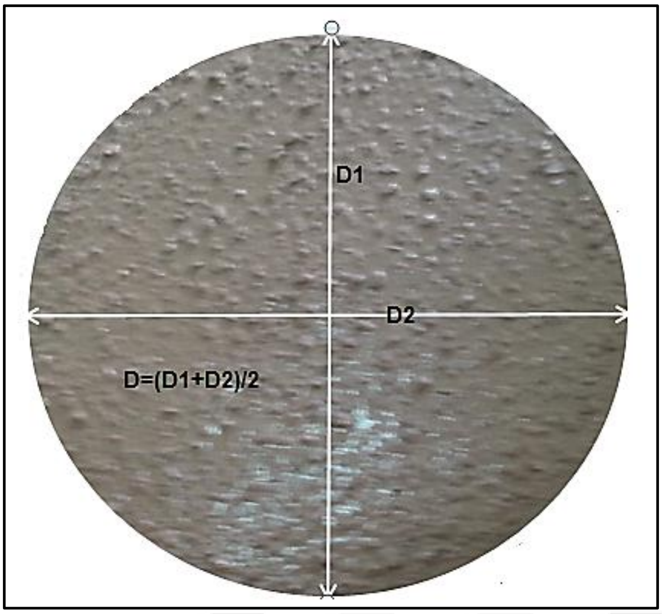

Figure 4.1 Slump flow diameter measurement for fiber reinforced SCC

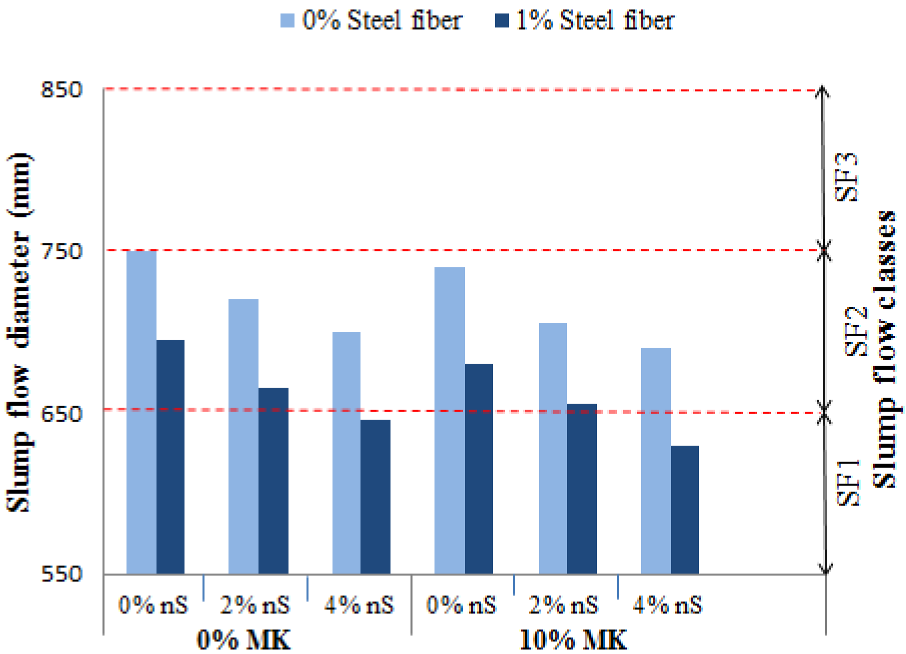

Figure 4.2 Slump flow diameter and slump classes of fiber reinforced SCC

Figures 4.3 and 4.4 demonstrates T_{50} slump flow and V-funnel slump flow time of SFRSCC mixes with and without nS or/and MK. Additionally, Figure 4.5 illustrates T_{50} slump flow time in relation to V-funnel flow time of every mix based on viscosity level according to EFNARC (2005). The findings ravealed that T_{50} slump flow and V-funnel flow times were influenced by the amount of nS or MK utilization. Raising the amount of nS, or using MK negatively affected the fresh properties. As seen in Figure 4.3, the mixture nS0MK0SF0 had the minimal slump flow time; whereas, the largest one was observed in nS4MK10SF1 mix.

Another outcome is that the flow time of SCCs in the fresh state rises as the usage of nS in binary blended MK in the SCC leads to more viscosity and cohesiveness in the fresh concrete. Moreover, steel fiber inclusion has an immediate impact on the T_{50} slump flow. The T_{50} slump flow time decreases with the incorporation of steel fiber because of steel fiber restrict the free flow of the mixtures. Thus, the T_{50} slump flow for SFRSCC was higher than the T_{50} slump flow for plain SCC.

Figure 4.4 shows the variation in SCC V-funnel slump flow time. The values ranged between 8.3 and 24.5 S. The findings demonstrated that incorporating nS had influence on the V-funnel flow time of plain SCCs. Additionally, the results presented in Figure 4.4 also revealed that the V-funnel flow time tends to rise with MK utilization. This supports that the inclusion of nS or MK made the SCC more viscous. As previously mentioned, the employment of both NS and MK in the same mixture causes an additional increase in V-funnel time rather than singly using nS or MK.

Moreover, the influence of steel fiber can be clearly seen in Figure 4.4. The utilization of steel fiber, the higher the increase in V-funnel slump flow time was observed in comparison to similar mixtures of plain SCC. This increase may be attributed to the friction taking place between fiber and aggregates; as well as friction of fiber together which protracts the time needed to entirely exit the V-funnel. For instance, the plain SCC mixture produced with 4%nS and 10MK had 13.3 S V-funnel slump flow time. However, SCC with steel fiber had 24.2 S in comparison to its plain SCC couterpart. Similar effects of nS, MK and steel fiber utilization were observed (Güneyisi et al, 2015; Jalal et al, 2012; Beigi et al, 2013; Siddique et al, 2013).

The relationship between V-funnel time and slump flow time of the mixtures was drawn in Figure 4.5. As shown in Figure 4.5, all SCCs mixtures were categorized as VS2/VF2. The concrete with viscosity level of VS2/VF2 can be used in the walls/columns and ramps with slump flow diameter class SF2.

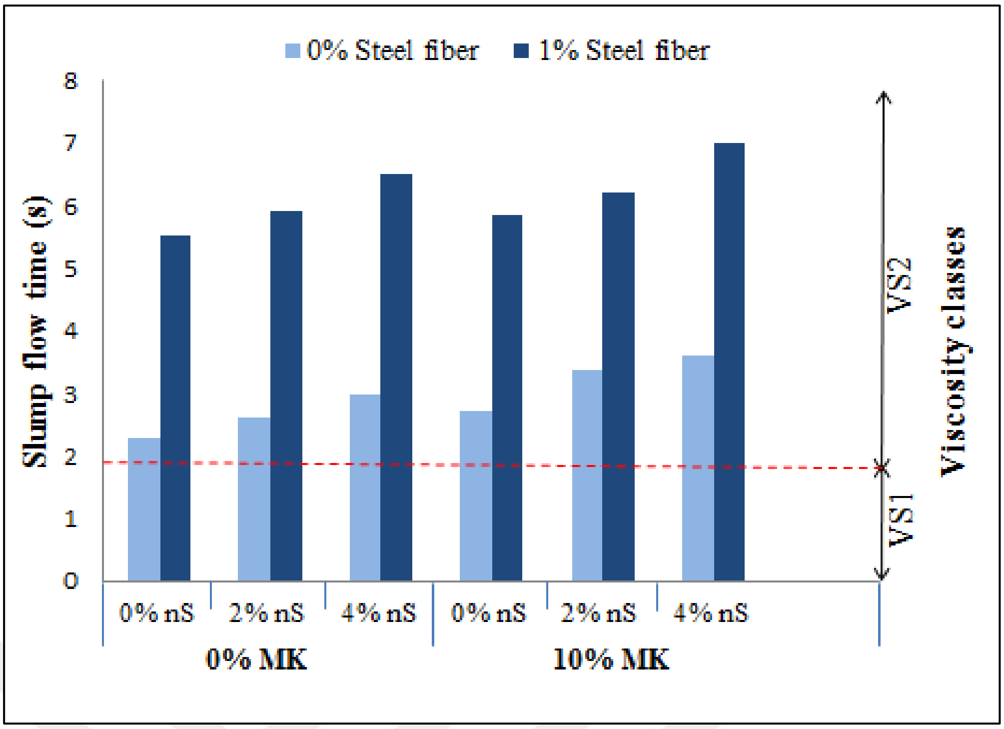

Figure 4.3 T_{50} slump flow time and viscosity classes of fiber reinforced SCC

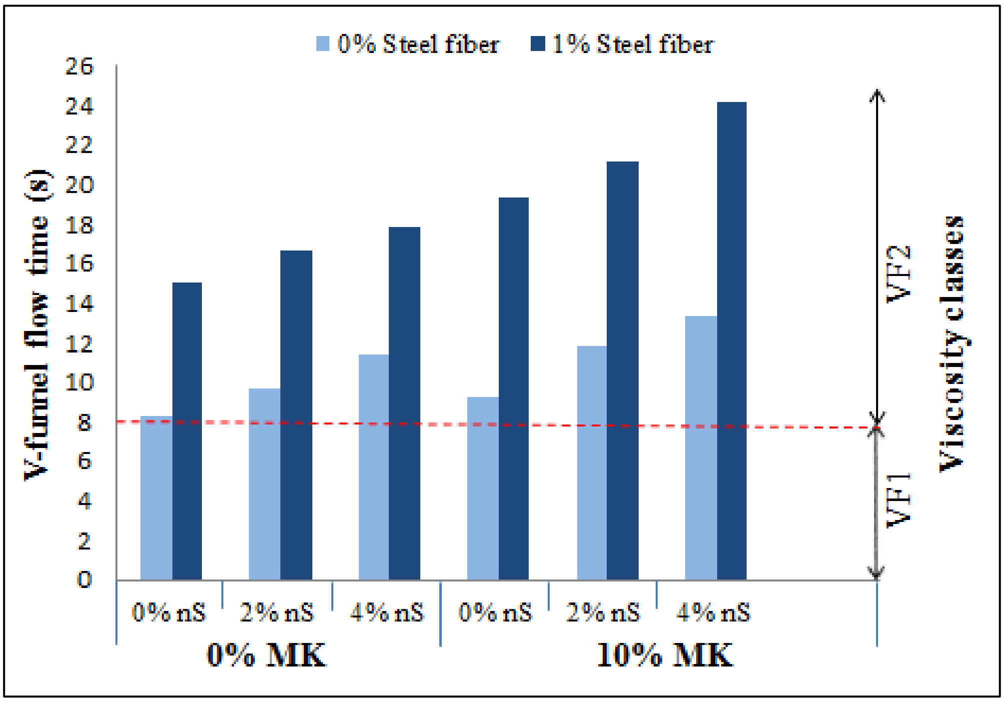

Figure 4.4 V-funnel flow time and viscosity classes of fiber reinforced SCC

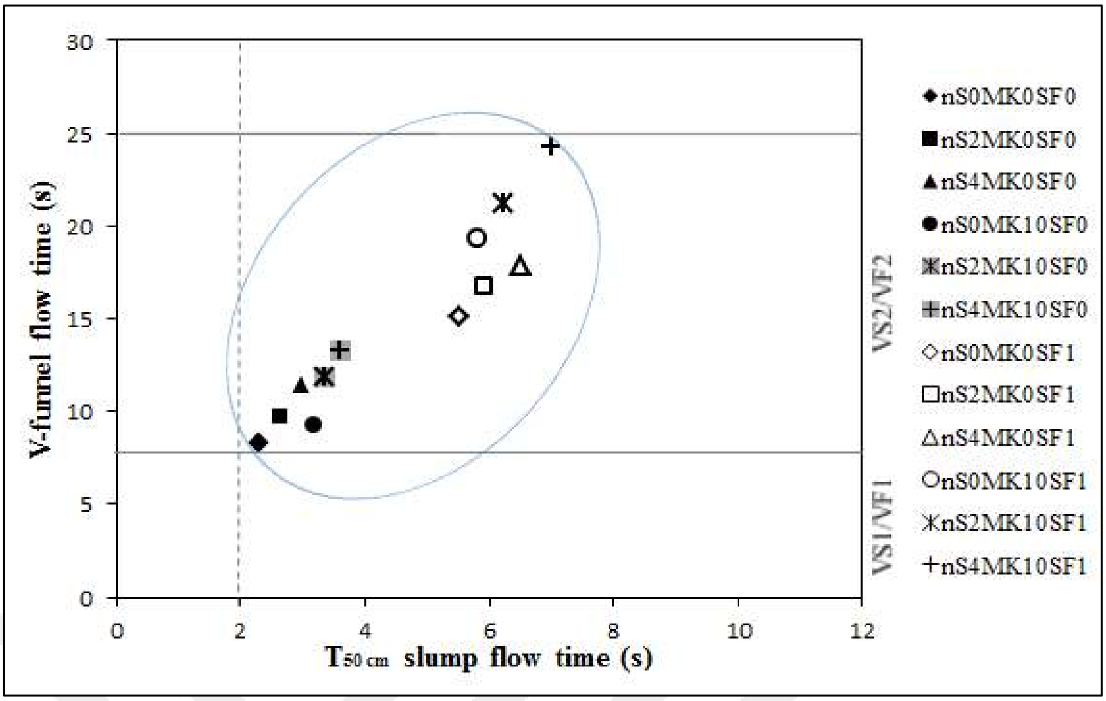

Figure 4.5 T_{50} slump flow time vs. V-funnel flow time

To determine the passing ability of the SCC mixes, L-box height ratio in terms of H2/H1 was measured. Examinations with an L-box having three bars, simulating more dense reinforcement EFNARC (2005), were conducted to carry out this test and the observations attained from this test are illustrated in Figure 4.6. The height ratio of the L-box needs to be equal to 0.8 or above to attest that the mixture fulfills the passing ability and whenever the height ratio of the L-box is 1.0, it may be said that a perfect fluid conduct of the concretes is achieved EFNARC (2005).

The findings showed that all of the mixes prepared in this research meet the EFNARC standards. It can be obviously observed in Figure 4.6, that L-box height ratios of all mixes were above 0.8, and particularly for nS0MK0SF0, nS2MK0SF0, nS4MK0SF0, nS0MK10SF0, and nS2MK10SF0 mixtures, had L-box height ratio greater than 0.9. Even though there was a decrease in L-box height ratio when nS used as singly or binery blended MK.

Moreover, T_{20} and T_{40}, the span of 20 and 40 cm with the horizontal portion from the gliding gate of the L-box which the mixes need to reach as in Figure 4.7, were likewise observed in the laboratory research. T_{20} as well as T_{40} are L-box flow times and they refer to the mixes ease of flow. The findings are shown in Figure 4.7 for T_{20} and T_{40} flow time. It was noted that both of nS or/and MK resulted in higher T_{20} and

T_{40} flow time. Based on L-box test findings, it was clear that incorporating steel fiber made the, L-box height ratios of SFRSCCs less than of SCC mixtures that have same amount nS and MK. addition of fiber to SCC led to an increase in T_{20} and T_{40} L-box flow times, indicating that fiber do not allow concrete to move freely and made blockage against flow.

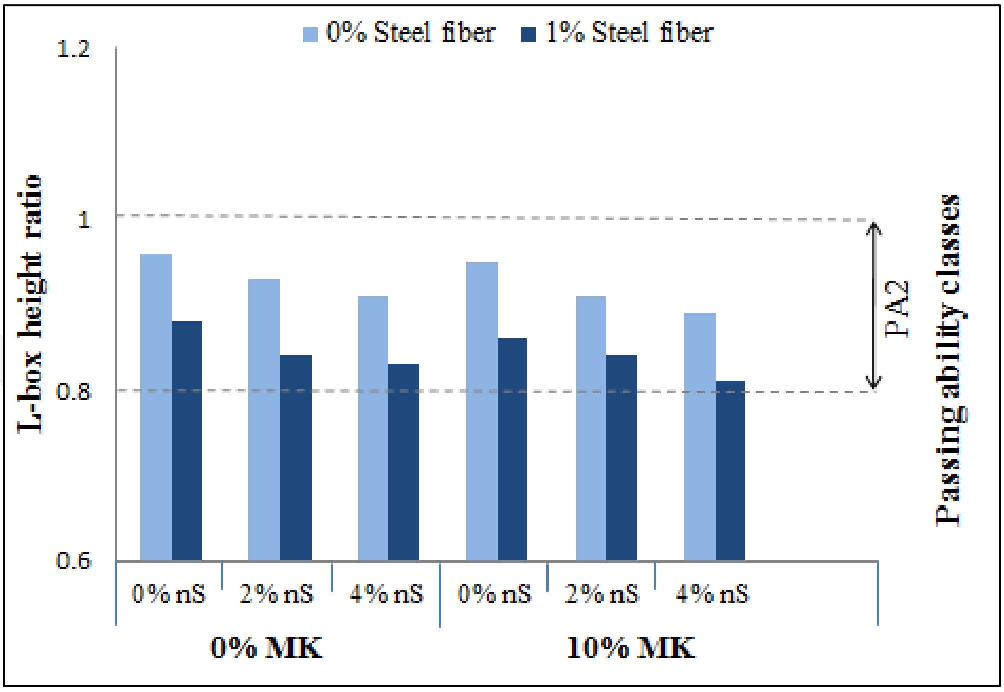

Figure 4.6 L-box height ratio and passing ability classes of fiber reinforced SCC

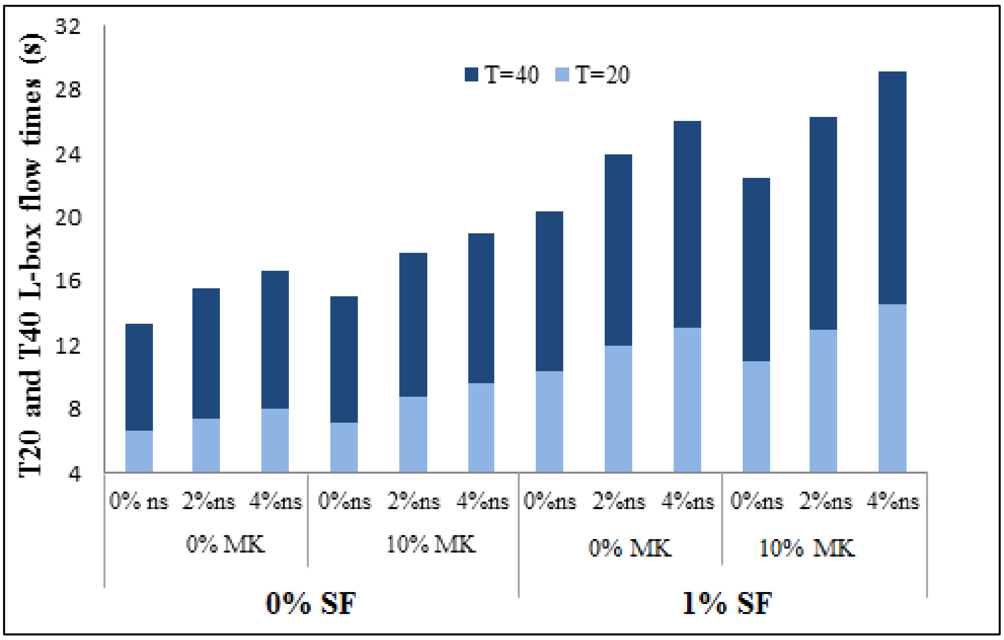

Figure 4.7 L-box height ratio and passing ability classes of fiber reinforced SCC

4.2 Analysis of mechanical property

The hardened samples were tested to find out compressive strength, splitting tensile strength, net flextural strength, modulus of elasticity, fracture energy and pullout test.

4.2.1 Compressive strength (*fc*)

It has been established that the weakness of concrete is related to tension while its strength is related to compression. consequently, concrete compressive strength is mainly viewed as the most interesting feature of concrete, and is the most universal indicator to assess the level of concrete in hardened state (Mather and Ozyildirim, 2002). The strength is known as a measure of the stress required fracturing a material, and is measured by calculating the utmost stress (fc′) that the sample bears under the effect of uni-axial compressive strength. Compression test of SCC sample was carried out with respect to ASTM C39 (2012) at 28 and 90 days old. The results for compressive strength of SCC were given as the average of three samples. The compressive strength at the ages of 28 and 90 days of mixtures is given in Figures 4.8a and b. The compressive strength values of 28 day ranging from 67.5 to 78.2 MPa while compressive strength values of 90 day ranging from 76.4 to 88.7 MPa was achieved in the current research. The lowest compressive strength result was obtained from the control mixture, and a systematic increase of compressive strength was observed as the nS, MK and steel fiber were used separately or together.

In this study, to better understand the effect of nS, MK, and steel fiber on SCC compressive strength, the results are compared in different groups, which are (single factor effect, dual factors effect, and triple factors effect) as presented in the following part.

1.Single factor effect:

The single factor influence of additives on the compressive strength of the mixtures at 28 and 90 day are presented in Figures 4.8a and b. Similarly to the results shown in other studies, the addition of nS (2% and 4%) improves the compressive force of the SCCs. This should be explained by the nucleation and pozzolanic effect of nS. Hence, the interface between the matrix and aggregate could become much stronger and the concrete strength could be simultaneously high. Güneyisi et al. (2015)

aproved that the increase in the amount of nS led to incease in the compressive strength at various levels of FA.

Additionally, the impact of MK on SCCs compressive strength showed clearly that introducing MK can improve the compressive strength of the designed SCCs. For instance, the compressive strength of the sample with 10% MK was 70.3 MPa at 28 days and 85.5 MPa at 90 days, which is obviously larger than the one without MK (67.5 and 76.4 MPa). Considerable enhancement in hardened strength of SCC was observed at 10% replacement of cement by MK (Chandrakantu et al., 2014). The compressive strength of SCC increases for 7 days to 28 days of curing, with replacement levels of 10%, 20%, 30 % of cement by MK. Likewise, it is clear that compressive strength, flexural strength, split tensile strength is the maximum for 10% replacement as compared to 20% and 30 % (Chandrakant et al., 2014). However, the incorporation of steel fiber can slightly increase the compressive strength of SCCs. For mixtures containing 1% of steel fiber, the value of compressive strength was 68.5 MPa at 28 days and 78.6 MPa at 90 days while for the same ages without steel fiber, these values were 67.5, and 76.4 MPa respectively. The impact of steel fiber on the compressive strength of SCC is based on the extent steel fiber influence on the concrete fluidity and the mix features of SCCs exercises a remarkable influence and the fiber characteristics. Siddique et al. (2016) found that the compressive strength increased with 1% steel fiber inclusions in SCC mixtures.

2. Dual factors effect:

Figure 4.8a and b shows the dual effect from nS and MK on the compressive strength of SCCs. It is noteworthy that the compressive strength of the sample with both nS and MK are much larger than that of the reference sample. Especially for the specimen with nS (4%) and MK (10%), the compressive strength is about 76.5, and 88.7 Mpa at 28 and 90 days, respectively. This should be attributed to the multiple effects of materials. The results of compressive strength obtained from the multiple effects of nS and steel fiber referred to that the addition of this materials can further improve the compressive strength of the reference mixture. For example, the strength of the sample with steel fiber (1 vol.%) nS (4%) of is about 74.2 MPa, which is clearly larger than the one without nS and steel fiber 67.5 MPa. Moreover, it was similarly noted that the compressive strength increased with the use of MK and steel fiber in tandem in SCC. Its clear that the utilization of MK and steel fiber in the mixture resulted in compressive strength higher than that without either MK, steel fiber, or both of them. For example, the mixture containing MK (10%) and steel fiber (1%) had a compressive strength of 86.8 MPa while the SCC strength with MK (0%) and steel fiber (0%) was 76.4 Mpa.

3. Triple factors effect:

The triple effect from used materials on the compressive strength of the designed SCCs is depicted in Figure 4.8a and b. It is important to notice that, for example, the compressive strength of the sample with nS (4%), MK (10%), and steel fiber (1%) is around 78.2 and 88.7 MPa, which is comparable to the control mixture (67.5 MPa at 28 days and 76.4 MPa at 90 days). Its clear that there is an improvement in compressive strength. This should be explained by the multiple influence of additives.

Moreover, it was observed that concerning the results achieved at 28 and 90 days, the value of the compressive strength of the mix included 2% of nS was nearly approximate to that having 10% of MK. For example, the mixture with 10% MK had strengths of 70.3 MPa at 28 days, and 85.5 MPa at 90 days. The corresponding values of the strength for the 2% nS mixtures were 70.5 MPa at 28 days, and 84 MPa at 90 days.

Strength improvement due to nS may be explained by a mechanism consisting of 4 stages that enhances the infrastructure and therefore improves the mechanical characteristics of the concrete. Due to this mechanism the points below are abstracted:

1. Pozzolanic reaction (Li et al, 2005; Ji, 2005; Bahadori and Hosseini, 2012): A great deal of calcium hydroxide crystals is formed during the chemical reaction between the cement and the water (Eqs. (4.1) and (4.2). Crystals of $Ca(OH)_2$ are hexagonal crystals in the transition zone between the cement paste matrix and the aggregates. These crystal are detrimental to both of the durability and strength of the concrete.

Because of its vast special surface area, nS is highly active chemically, and it forms C-S-H dense gel due to reaction with $Ca(OH)_2$. Consequently, crystals of $Ca(OH)_2$, in the pozzolanic reaction, decrease and a very strong condensed gel C-S-H, an outcome of the pozzolanic reaction (Eq. (4.3)) raises the concentation of the transition zone by filling in the voids and thus it boosts the strength.

$$2C_3S + 11H_2O \rightarrow C-S-H + 3Ca(OH)_2 \quad (4.1)$$

$$2C_3S + 9H_2O \rightarrow C-S-H + Ca(OH)_2 \quad (4.2)$$

$$2SiO_2 + 3Ca(OH)_2 \rightarrow 3CaO.2SiO_2.H_2O \quad (4.3)$$

To provide more interpretation for the rapid reaction of nS particles it could be claimed that for nS with unsaturated bonds the reaction between SiO_2 is show in the following equasions (Li and Zhao, 2003).

$$\equiv Si-O- + H-OH \rightarrow \equiv Si-OH \quad (4.4)$$

$$\equiv Si- + H-OH \rightarrow \equiv Si-OH \quad (4.5)$$

$$\equiv Si-OH + Ca\,(OH)_2 \rightarrow C-S-H \quad (4.6)$$

Thus nS partical goes through fast reactions.

2. Nano-filling feature (Qing et al, 2007; Li et al, 2005; Ji, 2005; Bahadori and Hosseini, 2012): The hydration productions contain 70% C-S-H. The medium particle diameter of C-S-H gel is about 10 nm (Bahadori and Hosseini, 2012). Nanoparticles, which have a filling capability characteristic, fill in the voids in C-S-H gel and create a more condensed adherent cement paste.

3. Acting as a nucleus (Bahadori and Hosseini, 2012; Bosiljkov, 2003; Nehdi et al, 1998): In the C-S-H gel structure, nano-sized particles may function as nuclei creating a very strong bond with the particles of the C-S-H gel. Thus, stability of the hydration products rises and hardened characteristics as well as concrete durability are predicted to become better.

4. Crystalization control (Li et al, 2005; Bahadori and Hosseini, 2012; Li, et al, 2006): If the quantity of nano-sized particles and their distribution is convenient for the crystallization process for crystals such as $Ca(OH)_2$ in the transition zone shrinks and the cement paste matrix, this way, becomes slicker and more condensed.

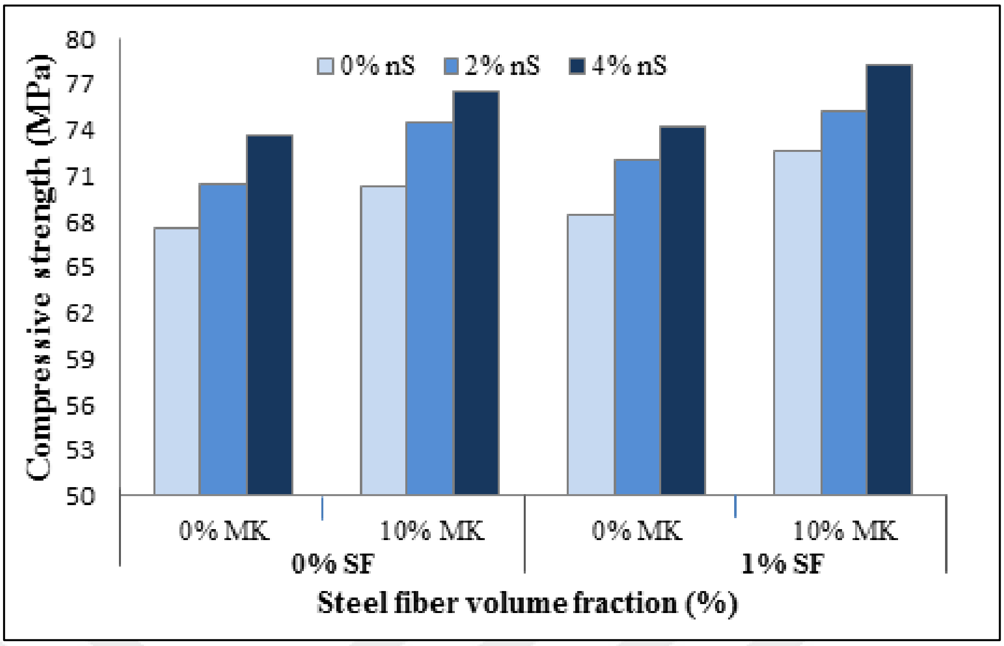

a)

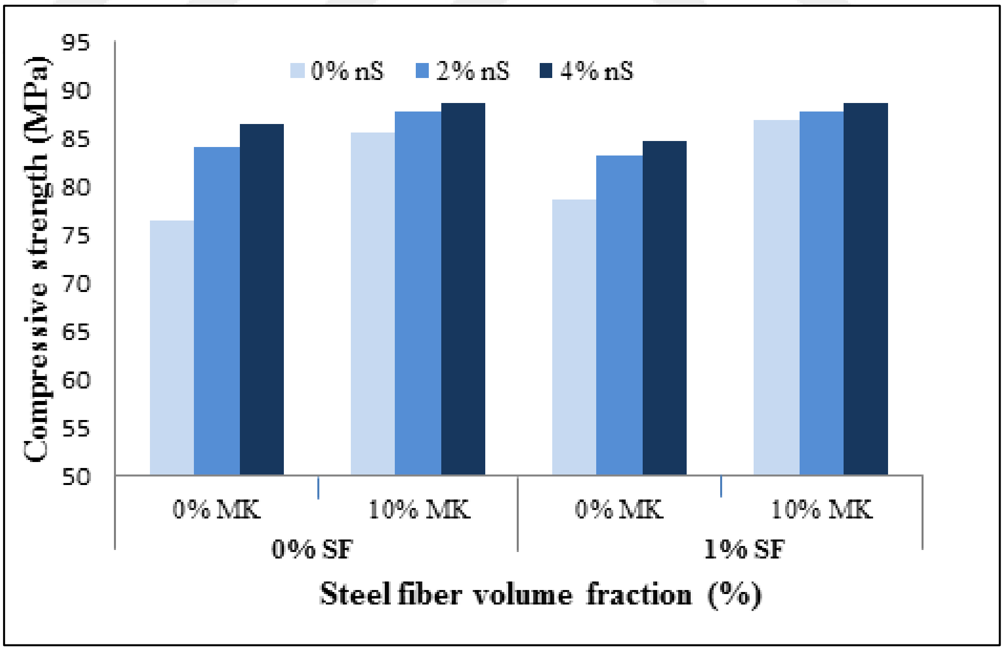

b)

Figure 4.8 Variations in: a) 28 days and b) 90 days compressive strength of fiber reinforced SCC

4.2.2 Splitting tensile strength (f_{st})

When tensile stress is loaded onto concrete, initially micro cracks and then macro cracks are created. The additional load instigates critical crack growth at the ends of macro-cracks. This process eventually causes failure (Banthia, 1994). The splitting tensile examination is the simplest method to measure a tensile strength of concrete in an indirect manner. Studying tensile strength is vital for providing data about the ultimate tensile load that concrete may bear prior to crack formation. The variation in splitting tensile strength of SCC with nS and MK with steel fiber different volume fractions 0% and 1% are shown in Figure 4.9a and b. The splitting tensile strength values ranging from 3.95 and 4.3 MPa to 5.84 and 6.3 MPa were achieved in this study at 28 and 90 days, respectively.

Clearly, the increase in the quantity of nS could increase the splitting tensile strength of the SCCs. For instance, the splitting tensile strength of the samples without nS fluctuates around 4 MPa, while the splitting tensile strength of the mixtures referred to as (nS2MK0SF0) and (nS4MK0SF0) increases to about 4.37 and 4.42 MPa respectively, at 28 days. Furthermore, with the addition of MK, the splitting tensile strength of concrete also increases. Over and above, with the increment of steel fiber quantity, the splitting tensile strength highly improves. The increment in the ratio of steel fiber from 0% (i.e. plain concrete) to 1% (i.e. reinforced concrete) has led to an enhancement in splitting tensile strength of nearly 25.8%. SFRSCC has better tensile characteristics in comparison to the reference mixture. The crack growth in splitting tensile test was either because steel fiber broke or because they pulled out of the matrix.

A summary of the effect of nS, MK and steel fiber on the splitting tensile strength of the SCCc is shown in Figure 4.9a and b. It is clear that with the inclusion of either nS with MK, nS with steel fiber, or MK with steel fiber in SCC, the splitting tensile strength dramatically improved compared with the mixture coded nS0MK0SF0.

However, the simultaneous inclusion of all additives can significantly improve the splitting tensile strength of the SCCs. The control mixture had a splitting tensile strength of 3.95, 4.30 MPa, while the splitting tensile strength of concrete containing 4% nS, 10% MK and 1% steel fiber with each other was 5.84 and 6.3 MPa at 28 and 90 day, respectively.

It has been established that steel fiber enhances the splitting tensile strength rather than the compressive strength, due to the crack arresting effect of steel fiber. For instance, the mixture coded nS0MK0SF1 made an increase of 25.8% while the one coded nS4MK10SF0 made an increase of 21.27%. Additionally, we can observe that the enhancement of the splitting tensile strength resulting from the use of steel fiber alone is more than that resulting from the use of nS and MK together. Also we can notice that the other important advantage of steel fiber incorporating related to mode of failure. The plain SCC cylindrical samples abruptly fail and split entirely into two separate pieces; whereas, th failure type in cylindrical samples containing steel fiber is cracking without separation at failure (Figure 4.10a and b).

In applications where crack resistance and shear strength are a priority such as airfield slabs, and highway design, tensile strength is essential. The introduction of nS and MK to plain and fiber reinforced SCC improves this property as shown in Figure 4.9 where a general inclination towards enhancing tensile strength can be seen, which can be explained by the same factors influencing compressive strength. In the presence of steel fiber, the increase in splitting tensile strength is because of the crack arresting effect of steel fiber. The relation between splitting tensile strength and compressive strength is dominated by several terms such as particle size distribution, sort of aggregate, and age of curing (Mehta and Monteiro, 2006) in addition to the sort and quantity of powder and admixture.

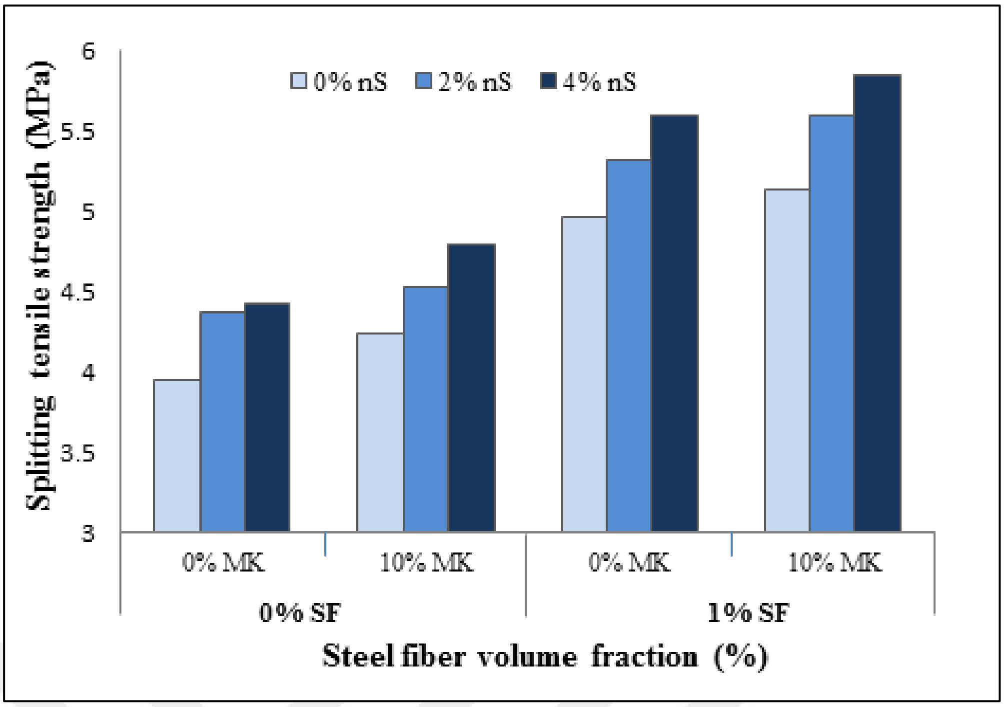

a)

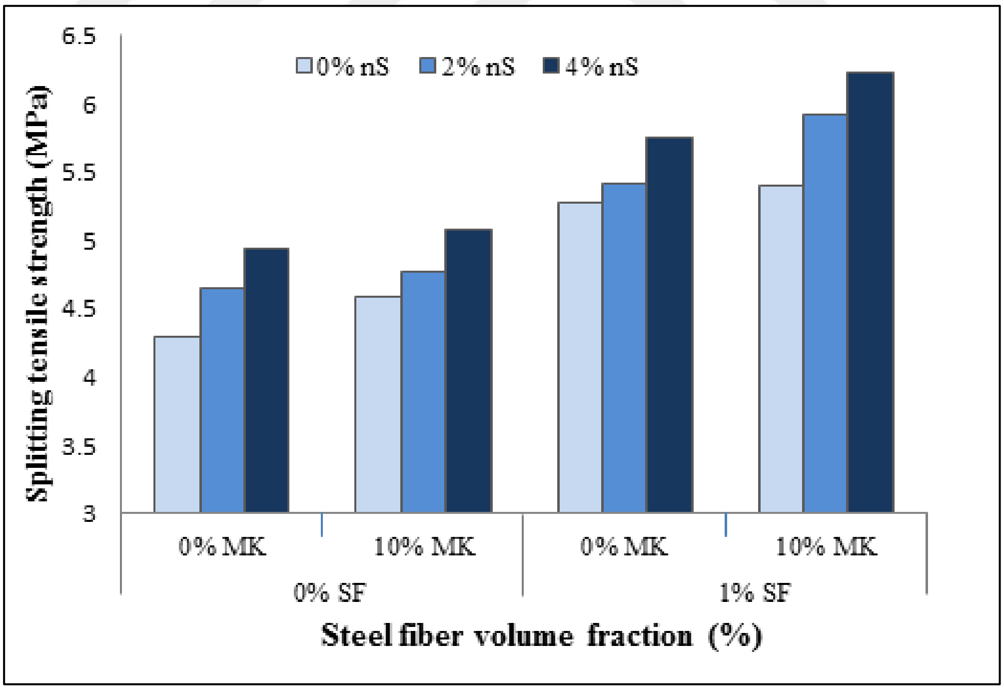

b)

Figure 4.9 Variations in: a) 28 days and b) 90 days splitting tensile strength of fiber reinforced SCC

a)

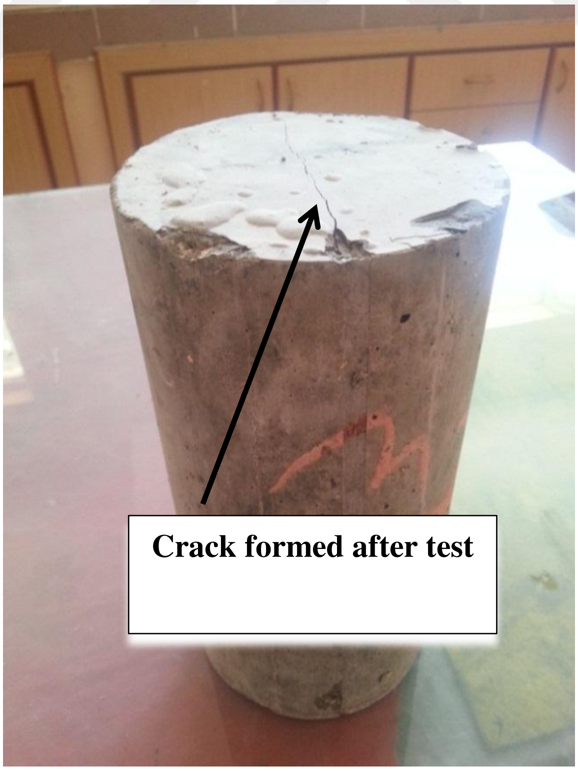

b)

Figure 4.10 Photoghraphic views of failure mode of: a) SCC and b) SFRSCC

4.2.3 Modulus of elasticity (E)

Inasmuch it provides useful information about the capability of concrete to deform elastically, modulus of elasticity is one of the most important material properties utilized in the design of concrete structures. It is a measure of stiffness of a component. The significance of the elastic limit in structural design lies in the fact that it represents the maximum allowable stress before the material undergoes permanent deformation. Due to concrete non-linearity, three methods are used to compute the modulus giving rise to three types of Moduli. These are the initial tangent modulus given by the slope of a line drawn tangent to the stress-strain (σ-ε) curve at any point on the curve, tangent modulus given by the slope of a line drawn from the origin to a point on the curve corresponding to a 40% stress at failure load and secant modulus given by the slope of a line drawn between two points on the σ-ε curve. Researchers investigated that a limited amount of silica nano particles giving a steeper slope in the stress–strain relationship curve by redistribution stress and reduced the localized strain (Gencel et al., 2011). It means that concrete with an optimized content of nanoparticles had better stiffness because the compactness of the paste bond with aggregates being better (Saloma et al., 2013).

Figure 4.11 demonstrated the 90 days static modulus of elasticity of the SFRSCC for different materials types and contents. The behavior herein was much similar to that seen the compressive strength. It was observed in Figure 4.11 that the effect of using nS was to increase the static elastic moduli of the concretes with and without MK. The rising tendency continued up to 4% nS content in SCC and SFRSCC. When a 4% nS was utilized, the concretes had higher elastic moduli by 12% for SCC containing 4% nS, 18% for SCC containing 4%nS10%MK, 9.5% for SCC containing 4%nS1%SF and 16.2% for SCC containing 4%nS10%MK1%SF. Moreover, test results suggested that the effect of 2% nS (nS2MK0SF0) on the modulus of elasticity was almost near to that of 10% MK (nS0MK10SF0). As seen also from the results, the impact of combined use of nS with MK or steel fiber was more pronounced with nano-individual replacement. This may be attributed to the better enhancement of binary effect on potential for the stress transfer during the initial elastic stage loading. It is worth mentioning that the highest outcome was in the mixes codded nS4MK10SF0 and nS4MK10SF1 because the combined effect results from the double and triple utilization of additives.

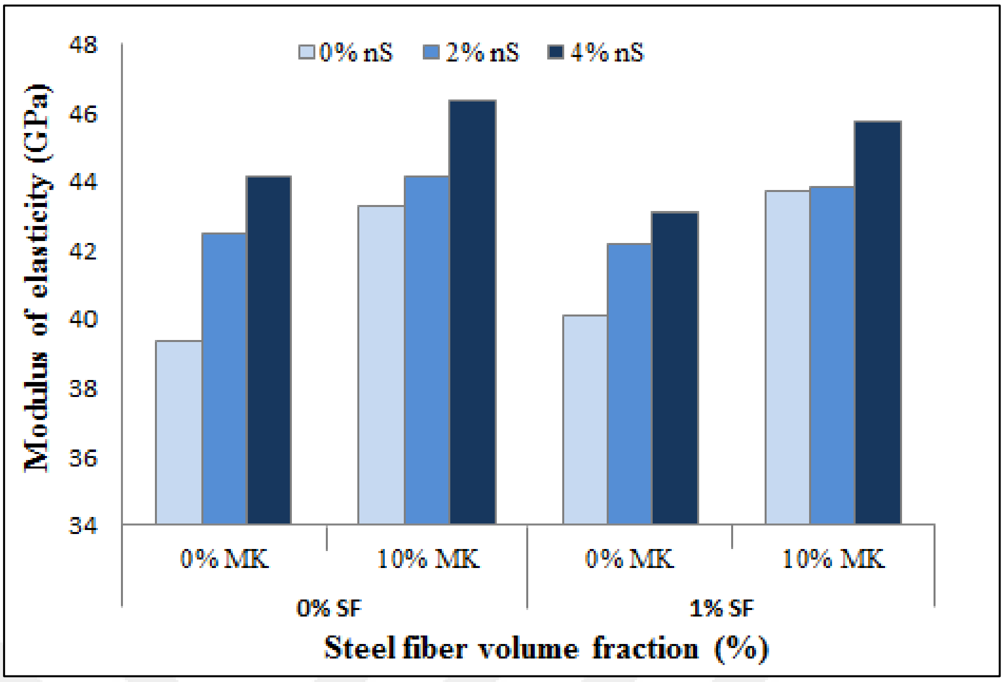

Figure 4.11 Variations in 90-day modulus of elasticity of fiber reinforced SCC

4.2.4 Bond strength (τ_b)

The transfer of axial force from reinforcing steel bar to the surrounding concrete produced from the development of tangential stress components along the contact surface. The stress acting parallel to the bar along the interface is called bond stress (Pillai and Kirk, 1983; Hadi, 2008).

The bond strength values were evaluated with the Equation 3.4 from cubic specimen including the Φ16-reinforcement bar subjected to tensile load. The bonding strength of the SFRSCC vs. the amount of the nS and MK is plotted in Figure 4.12. The lowest bond strength result was obtained from control mixture, and the systematical increasing of bond strength was observed as nS, MK and steel fiber content increased**.** The highest bond strength values have been measured on the nS4MK10SF1 mixture at the end of 90 days for the reason that the adhesion between matrix particles and surrounding cement paste is high. Increasing nS from 0 to 4%, MK from 0 to 10% and steel fiber from 0 to 1% resulted increasing the bond strength by up to 13.3, 7, and 21.2% respectively, while these rates (for the dual use of nS 4% with MK 10%, nS 4% with steel fiber 1%, and MK 10% with steel fiber 1%) resulted in increasing the bond strength by up to 14.9, 26 and 23.5%, respectively. Moreover, the triple effect of nS blended MK and steel fiber added more enhancement in the bond strength from the single effect or the dual effect. For instance, the mixture contaning nS 4% blended MK 10% and steel fiber 1% showed an increase of about 28.4%.

Baran et al. (2012) stated that steel fiber improve the pull-out resistance of strands by controlling the crack growth inside concrete blocks. They stated that, by this way, the level of confinement at the strand-concrete interface was increased, which resulted in improvements in both friction and mechanical bond components of the resistance. Their results also indicated that more than 30% increase was achieved in pull-out strength due to fiber reinforcement. However, the studies regarding the effect of inclusion of nS on the bonding strength between concrete and steel bars has not yet attracted the adequate attention. The previous results presented for MK incorporated steel fiber reinforced concretes may highlight the effectiveness of utilization of nS for this purpose. Güneyisi et al. (2014), observed the influence of MK on the bond property of steel fiber in matrix of concrete. They performed pullout tests in their experimental program, with the steel fiber content as the primary variable. They indicated that the incorporation of MK in concrete matrix greatly enhanced the fiber–matrix bond. Abu-Lebdeh et al. (2011) also revealed that the quality of matrix has prominent importance on the bonding and tensile strain capacity of steel fiber in high strength concrete. Consequently, owing to its superior enhancement in cement matrix as a result of pore size refinement (Wild et al., 1996) MK and nS provided improvement in the pullout capacity of the reinforced concretes.

Photographs of the pullout specimens tested in the current study are given in figure 4.13. As can be seen, after failure, the reinforcing steel bars were separated from the concrete samples without steel fiber, whereas SFRSCC samples did not release the steel bars.

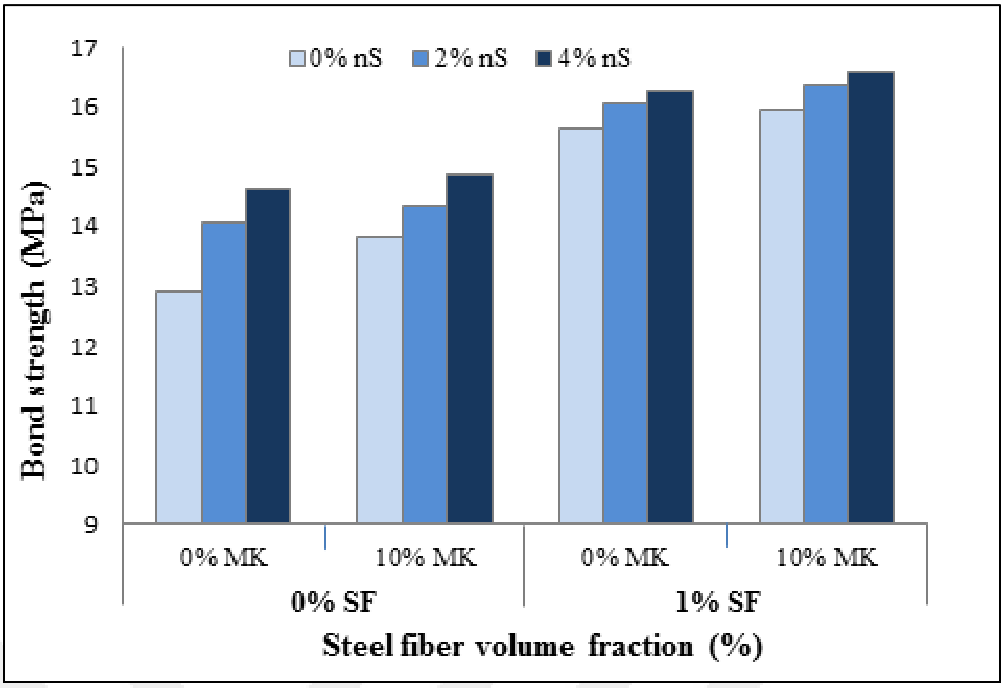

Figure 4.12 Variations in 90-day bond strength of fiber reinforced SCC

a)

b)

Figure 4.13 Failure mode of: a) SCC and b) SFRSCC

4.2.5 Net flexural strength (f_{flex})

The variation in the net flexural strength of SFRSCC are shown in Figure 4.14. The net flexural strength of SCC produced with nS (4%), MK (10%), and steel fiber (1%) was 7.53 MPa, which is the highest value while the SCC control mix gave the lowest net flextural strength. Its clear, for example, that increasing nS from 0% to 4% resulted in increasing the flextural strength from 5.0 to 5.9 MPa. At the same time, the mixture containing MK (10%) has resulted in increasing the flextural strength from 5.0 to 5.2 MPa while the increasing the flextural strength with mixed nS and MK was from 5.0 to 6.2 MPa. Same results were recently reported by the other researchers (Amin and Abu el-Hassan, 2015; Yu et al., 2014). The improving may be due to the quick consumption of calcium hydroxide associated with the nucleation of nS which helps in improving the bond between aggregate and cement mortar (Torgal et al., 2013). Then, more energy is needed to break SCC leading to superior energy absorption capacity under bending. Additionally, increasing the steel fiber fraction from 0% (plain concrete) to 1% has resulted in increasing the flexural strength from 5.0 to 6.3 MPa. Bayramov et al. (2003) have also achieved the best results with the aspect ratio of 80. The reason for increasing net flexural strength with utilization of steel fiber is that, after cracking of the matrix, the steel fiber will carry the load until the loss of the interfacial bond between the fiber and the matrix (Gao et al., 1997). Therefore, due to the efficient crack arrest by the steel fiber sudden failure is prevented and this situation results in increasing the load carrying capacity of concrete (Hassanpour et al., 2012). Finally, SCC mixes produced with (nS blended with MK, nS blended with steel fiber, and MK blended with steel fiber) resulted in increasing the flextural strength from the initial 5.0 to 6.2, to 7.0, and to 6.6 Mpa, respectively. It is noteworthy that when all materials were utilized in the same mixture, the result of net the flextural strength gave higher result as can seen that in mixture coded nS4MK10SF1, which had 7.53 MPa net flextural strength.

Its evidently from Figure 4.15, the different between mode of failure of sample without steel fiber and sample with steel fiber. The sample produced without steel fiber behaved as a brittle material while that produced with steel fiber behaved as a ductile material.

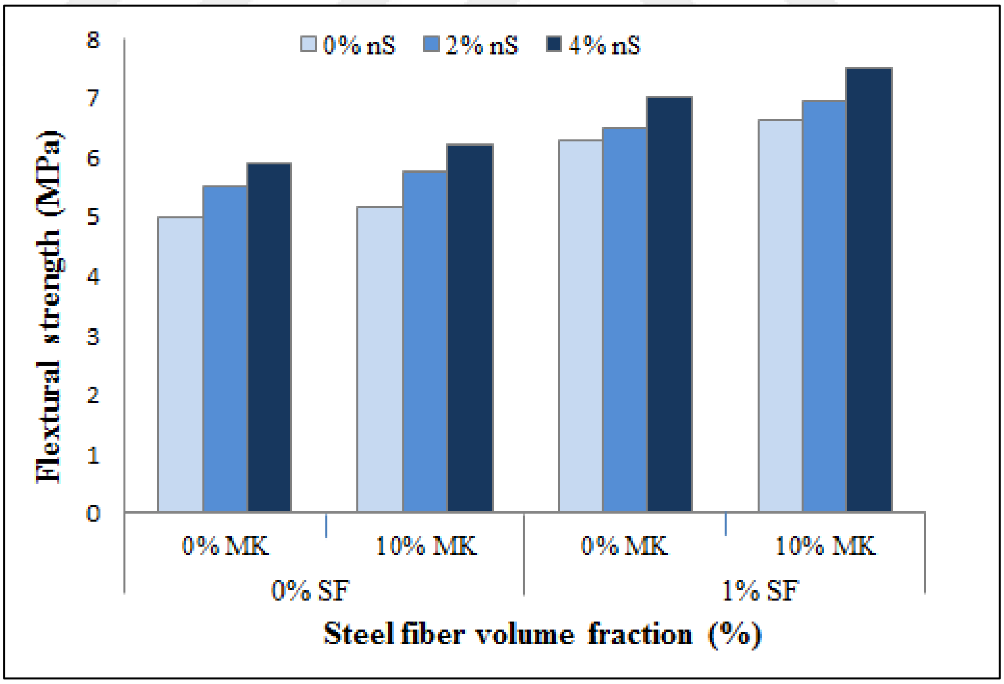

Figure 4.14 Variations in 90-day flexural strength of fiber reinforced SCC

a)

b)

Figure 4.15 mode of failure of: a) SCC and b) SFRSCC

4.2.6 Fracture energy (G_F) and ductility

Fracture energy (G_F), which is known as total energy or specific energy, is actually the energy required to create a crack with unit surface area and evaluated under three point-bending test. The variations in the fracture energy of the mixtures, are shown in Figures 4.16a and b, respectively. The calculation of fracture energy consists of two parts; energy supplied by the actuator and by the own weight of the beam. The area under the load versus displacement curve was used in the calculation of fracture energy as the energy supplied by the actuator, and the weight of the beam was used in the calculation as the energy supplied by own weight of the beam. While in the plain concretes, the final displacement of the specimens was used in the calculation of energy supplied by own weight, in SFRSCC, the 5 mm displacement was chosen as cut-off point and it is used in the calculation of energy supplied by the own weight of the beam (Güneyisi et al., 2015).

As seems in Figure 4.16a, the plain SCC with nS, irrespective the presence of MK, has higher the fracture energy than one with no nS. In the present study the total fracture energy of SCC was dependent on the amount of nS available in concrete mixes. It was expected like the other previous mechanical property tests that the SCC with 4% nS gave the highest value of the fracture energy regardless of the concrete groups. The fracture energy increased by 7.2% and 10% as well as 8% and 9.5% for the first and second group respectively, compared to the reference mixtures at 90 days, when 2% and 4% of nS were incorporated. The main reason behind this increase may be the fact that porosity in the cement paste and the ITZ zone being reduced due to filling properties of nS. As a result, the cement paste and ITZ zone would have a significant strength and subsequently, cracks were more likely to pass across the aggregates than cement paste and ITZ zone.

The utilization of steel fiber in concrete significantly increases the fracture energy shown in Figure 4.16b. However, the increasing rate in the ultimate load is not as much as increasing rate in fracture energy. Increasing the steel fiber volume fraction from 0 (plain) to 1% resulted in the increase of the fracture energy about 12 times, but it resulted in the increase of the ultimate load more than 0.25 times. The findings of this study are consistent with those obtained from Yardimci et al. (2014).

The second outcome is that the introduction of two materials gave a higher value of fracture energy compared with that produced with one material while the utilization of three materials in same mixture gave an even further increase of fracture energy than that produced with one or two materials. Considering the ranking from the highest to the lowest peak values, the SFRSCC were coded as nS4MK10SF1, nS2MK10SF1, nS4MK0SF1, nS2MK0SF1, nS0MK10SF1 and nS0MK0SF1.

In order to emphasize the increase in ductility of concrete by using steel fiber is calculated by the following formula and given in Table 4.2.

$$\text{Ductility ratio} = \frac{\text{GF (SFRSCC)}}{\text{GF (SCC)}} \tag{4.7}$$

Table 4.2 Fracture energy and ductility ratio

Mix code	90-day fracture energy (N/m)	Ductility ratio (%)
nS0MK0SF0	111.7	1
nS2MK0SF0	119.8	1
nS4MK0SF0	122.8	1
nS0MK10SF0	117.88	1
nS2MK10SF0	120.7	1
nS4MK10SF0	122.3	1
nS0MK0SF1	1355.5	12
nS2MK0SF1	1404.0	11.7
nS4MK0SF1	1434.8	11.7
nS0MK10SF1	1398.0	11.9
nS2MK10SF1	1408.0	11.7
nS4MK10SF1	1422.0	11.6

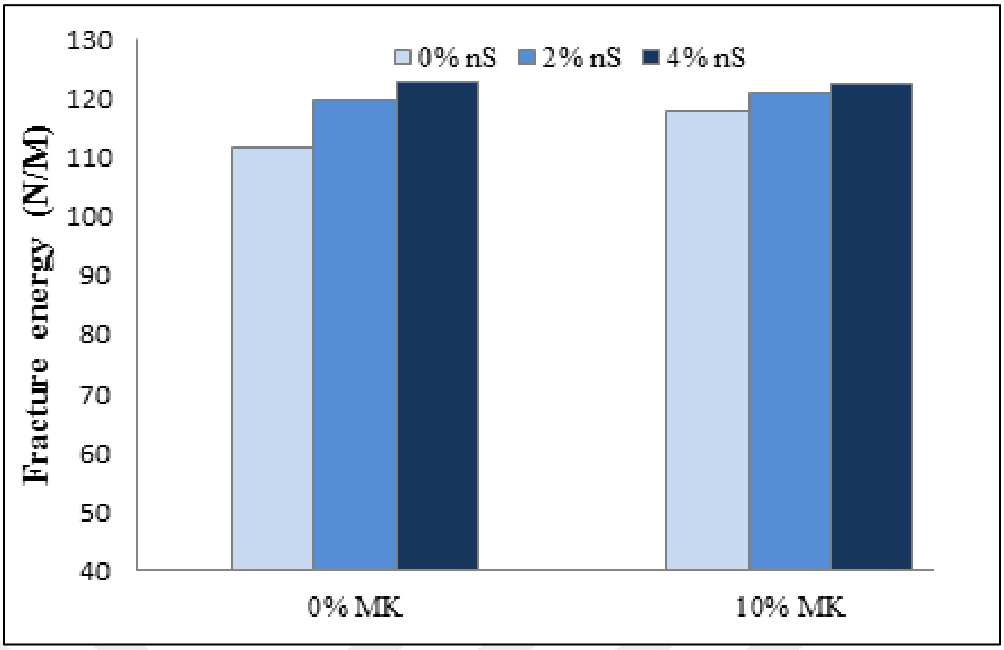

a)

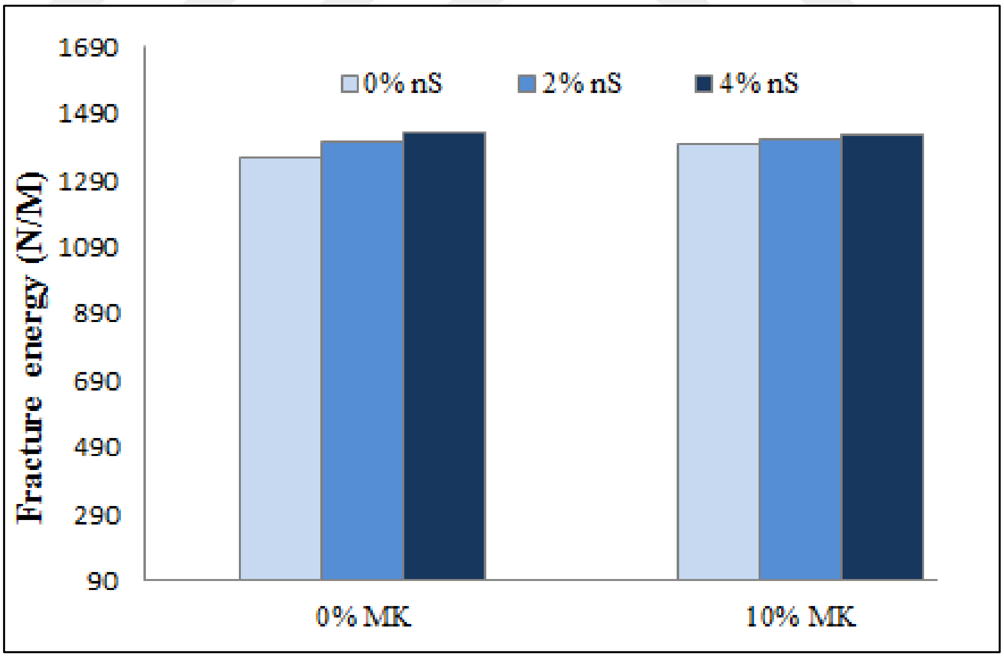

b)

Figure 4.16 Variations in 90-day fracture energy of: a) SCC and b) SFRSCC

CHAPTER 5

RESULTS AND DISCUSSION OF NUMERICAL STUDY

5.1 Axial capacity of CFST short columns

The axial capacity of short composite columns infilled with self-compacting concrete (SCC) or steel fiber reinforced self-compacting concrete (SFRSCC) calculated by using Eurocode 4 (2004), ACI 318R (2005), AIJ (2001) and DL/T (1999) are presented in Figures 5.1 and 5.2, 5.3 and 5.4, 5.5 and 5.6 and 5.7 and 5.8, respectively, with respect to nano silica (nS) content. These figures are contained all the parameters of numerical study which have been suggested to investigate the structural behavior of concrete filled steel tubular (CFST) circular short columns. For example, Figures 5.1a, 5.1b and 5.1c illustrate the Eurocode 4 ultimate axial capacity considering steel yield strength of 150 MPa, 300 MPa and 450 MPa, respectively, taking into account Figures 5.1 and 5.2 are related to sample tested at 28 and 90 days, respectively. The three different diameter to thickness (D/t) ratios of steel tube are also considered in each sub figure as it is presented for instance in Figure 5.1a. At each replacement level of nS, the value of axial capacity is presented as a column. Each column as can be seen merges four different types of concrete (MK10SF1, MK0SF1, MK10SF0 and MK0SF0), thus, in one figure it can be analyzed 12 composite columns according to the treated results.

The presented results of axial capacity in Figures 5.1 to 5.8 revealed that the enhancement of concrete core compressive strength due to the use of both MK and SF slightly increases the axial capacity of CFST column. For example, Figure 5.5a shows that by the use of concrete core incorporating 10% of MK and 1% of SF, the CFST column ultimate axial capacity calculated via AIJ (2001) increases by about 3.5%, 3.1% and 4.1%, 4.5%, 4.0% and 5.3%, and 5.0%, 4.5% and 5.8% for concretes made with nS content of 0%, 2% and 4% and with respect to the use of steel tubes having D/t ratio of 25, 55 and 90 and steel yield strength of 150 MPa, respectively, in comparison to the axial capacity of columns infilled with concrete free of MK and

SF. Generally similar behavior also can be observed for the effect of using different nS replacement levels except for some increments due to the interaction effect between efficiency of concrete constituents, age of concrete and composite column structural properties. In Figure 5.3a the part of plotted column which represents the 28 day ACI axial capacity of column infilled with concrete made with 10% MK and 0% SF (MK10SF0) can be an example to aforementioned observation. The axial capacity of this column enhanced due to the incorporation of 2% and 4% nS by about 2.2% and 4.4%, 2.8% and 5.6%, 3% and 6%, with respect to D/t ratio of 25, 55 and 90, respectively. Whilst, Figure 5.4a depicts an enhancement of 8% and 10%, 10.2% and 8.8%, 11% and 14.4% with respect to the same variables mentioned earlier but for curing period of 90 days.

As expected, the effect of D/t ratio on the variation of axial capacity seems to be very important irrespective of code type, age of curing, steel yield strength and type of concrete that used to fill steel tubular. For instance, with the increase of D/t ratio from 55 to 90 the predicted axial capacity of column infilled with plain concrete increases from 1505 to 3478 kN for plain concrete, respectively, Figure 5.6c. Apparently, this behavior agreed with previous research which it concluded that D/t ratio of circular steel tube has a significant effect on the ultimate axial capacity of CFST column due its influence on the composite action of such columns (Ellobody et al., 2006).

The present numerical investigation as mentioned in section 3.2.4 also involved the use of different kinds of steel grade (S150, S300 and S450) in the calculation of ultimate axial capacity of column infilled with SCC and SFRSCC. Considering various provision codes, the increase in the yield strength of composite column from 150 MPa to 300 MPa and from 300 to 450 MPa remarkably enhances the ultimate axial capacity regardless D/t ratio, kind of concrete and age of concrete. This confirms the observation by Liang and Fragomeni (2009), Lu and Zhao (2010), Patel et al. (2014) and Güneyisi et al. (2016) that increased steel yield strength is necessarily representative of improved CFST column axial capacity. Moreover, the variations in the predicted axial capacity are presented in Table 5.1. The results presented in this table comprise the minimum and maximum axial capacity irrespective the variation in D/t ratio, meaning that for each sub figure the range of ultimate axial capacity has been written in Table 5.1.

Table 5.1 Range of calculated ultimate axial capacity

Code provision	Testing age (days)	f_y (MPa)	Range of ultimate axial capacity (kN)
EC4	28	150	247 – 2771
		300	344 – 3130
		450	436 – 3480
	90	150	262 – 3165
		300	359 – 3519
		450	450 – 3865
ACI	28	150	193– 2302
		300	263 – 2564
		450	334 – 2826
	90	150	207 – 2643
		300	277 – 2904
		450	347 – 3167
AIJ	28	150	217 – 2458
		300	306 – 2791
		450	396 – 3124
	90	150	231 – 2813
		300	344 – 3146
		450	434 – 3479
DL/T	28	150	248 – 2812
		300	327 – 3145
		450	404 – 3522
	90	150	270 – 3152
		300	374 – 3485
		450	425 – 3862

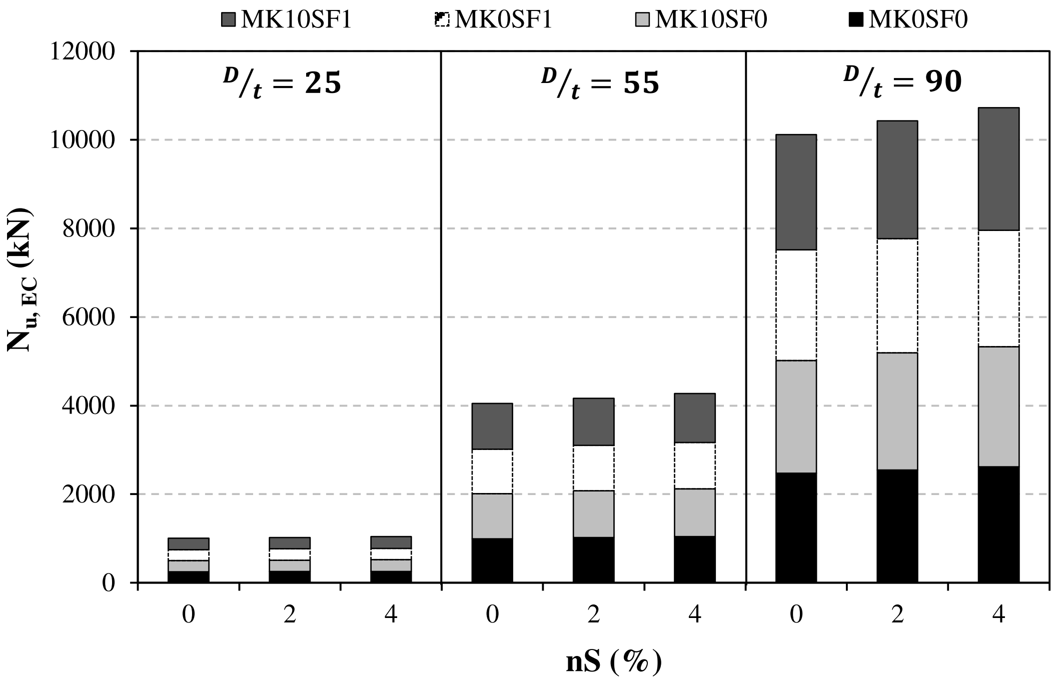
MK10SF1
MK0SF1
MK10SF0
MK0SF0
$^D/_t = 25$
$^D/_t = 55$
$^D/_t = 90$
$N_{u, EC}$ (kN)
nS (%)
0
2000
4000
6000
8000
10000
12000

a)

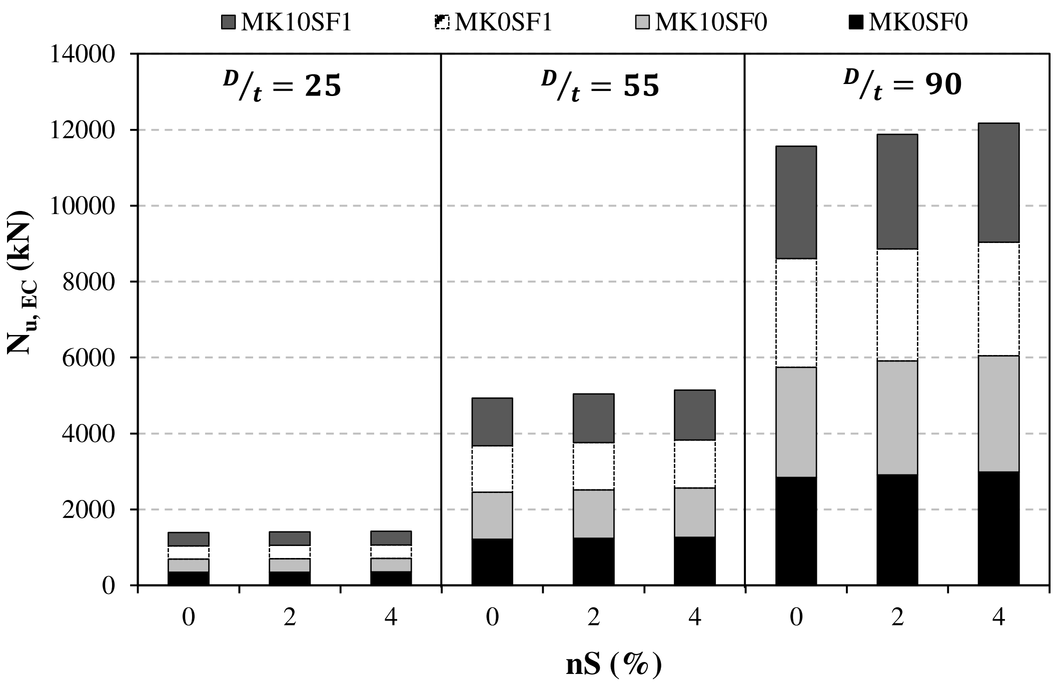
MK10SF1
MK0SF1
MK10SF0
MK0SF0
$^D/_t = 25$
$^D/_t = 55$
$^D/_t = 90$
$N_{u, EC}$ (kN)
nS (%)
0
2000
4000
6000
8000
10000
12000
14000

b)

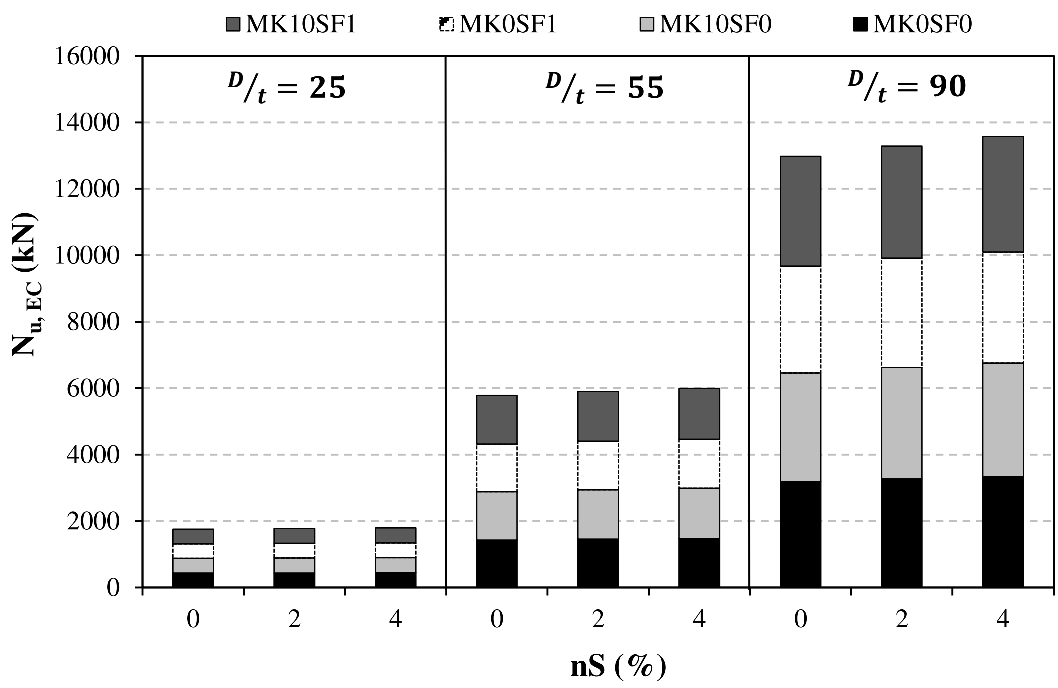

c)

Figure 5.1 Axial capacity calculated via Eurocode 4 at 28 days with respect to nS content for the steel yield strength of a) 150 MPa, b) 300 MPa and c) 450 MPa

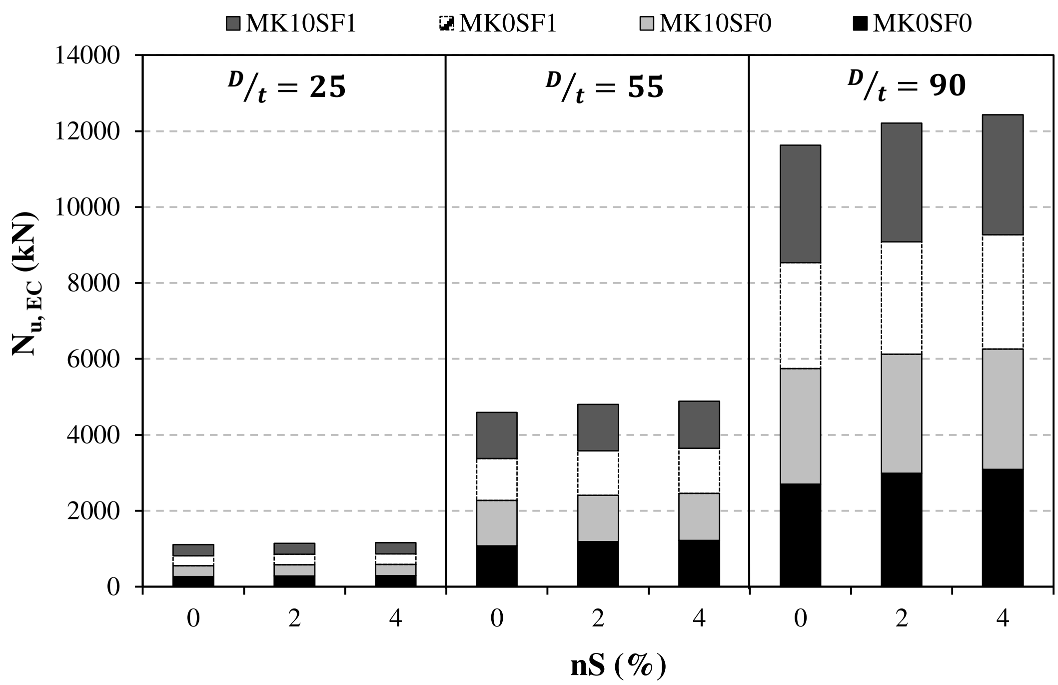

a)

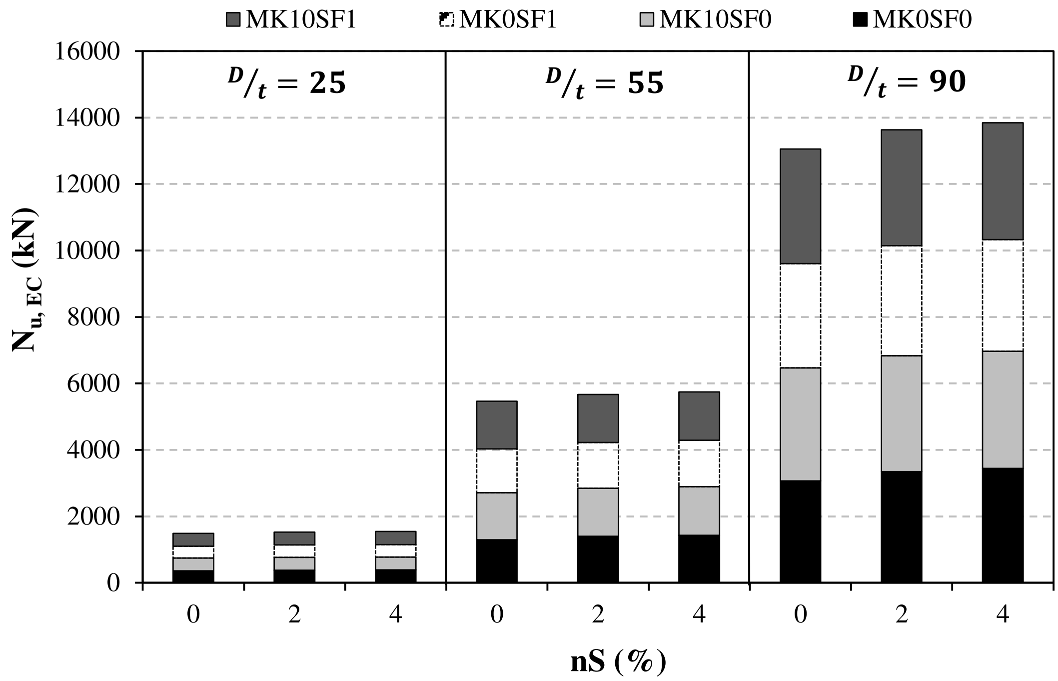

b)

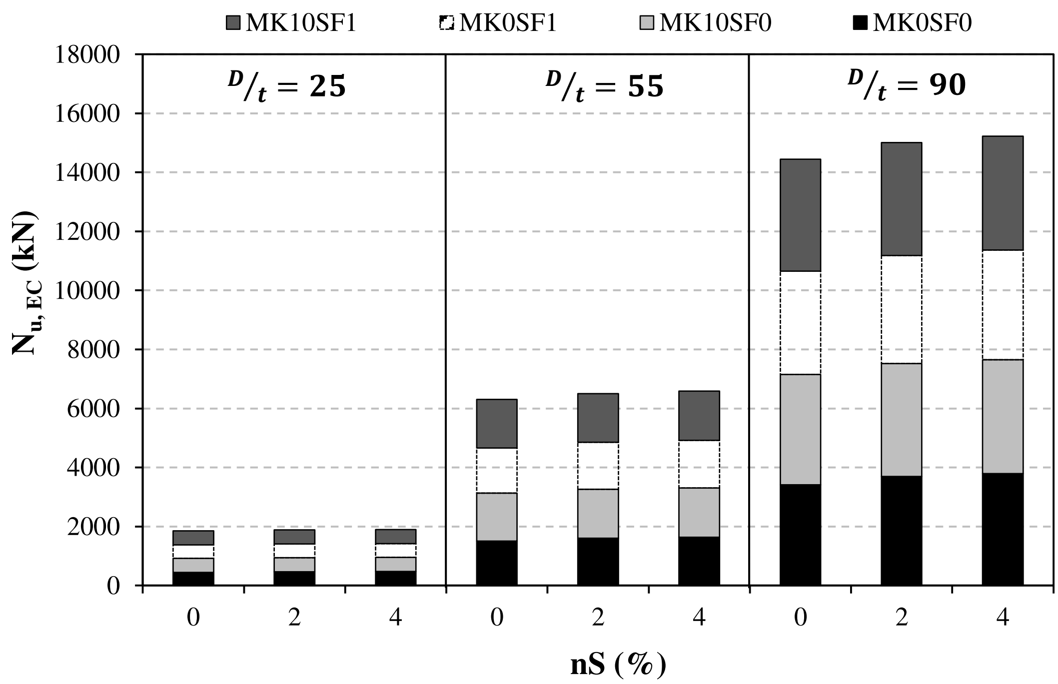

c)

Figure 5.2 Axial capacity calculated via Eurocode 4 at 90 days with respect to nS content for the steel yield strength of a) 150 MPa, b) 300 MPa and c) 450 MPa

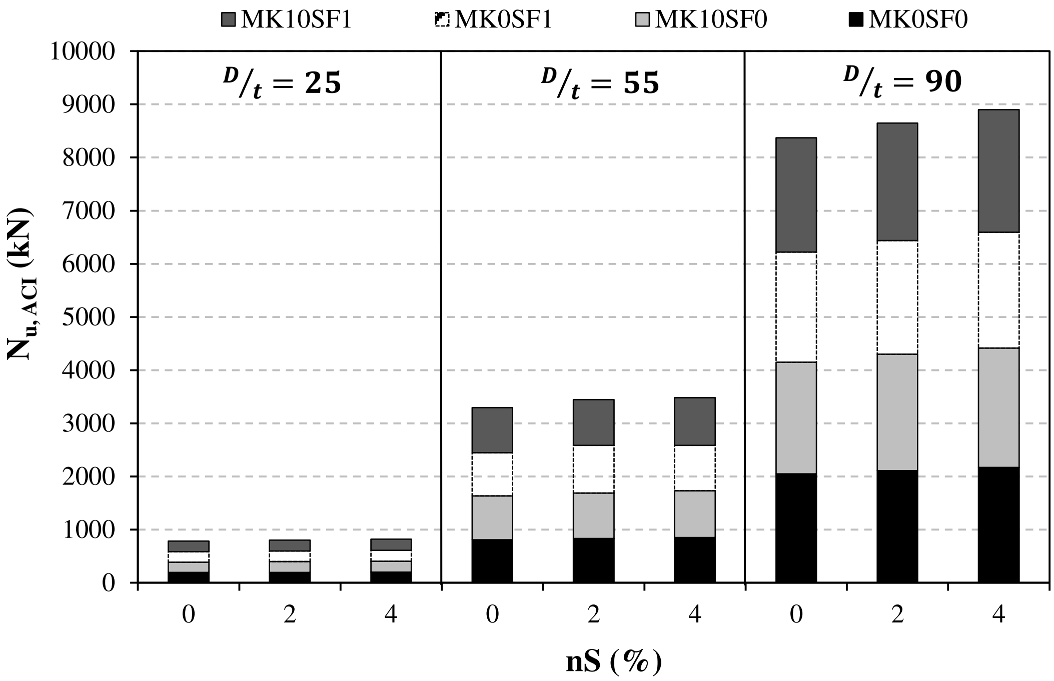
MK10SF1
MK0SF1
MK10SF0
MK0SF0
$^D/_t = 25$
$^D/_t = 55$
$^D/_t = 90$
$N_{u,ACI}$ (kN)
nS (%)
0
1000
2000
3000
4000
5000
6000
7000
8000
9000
10000
0
2
4

a)

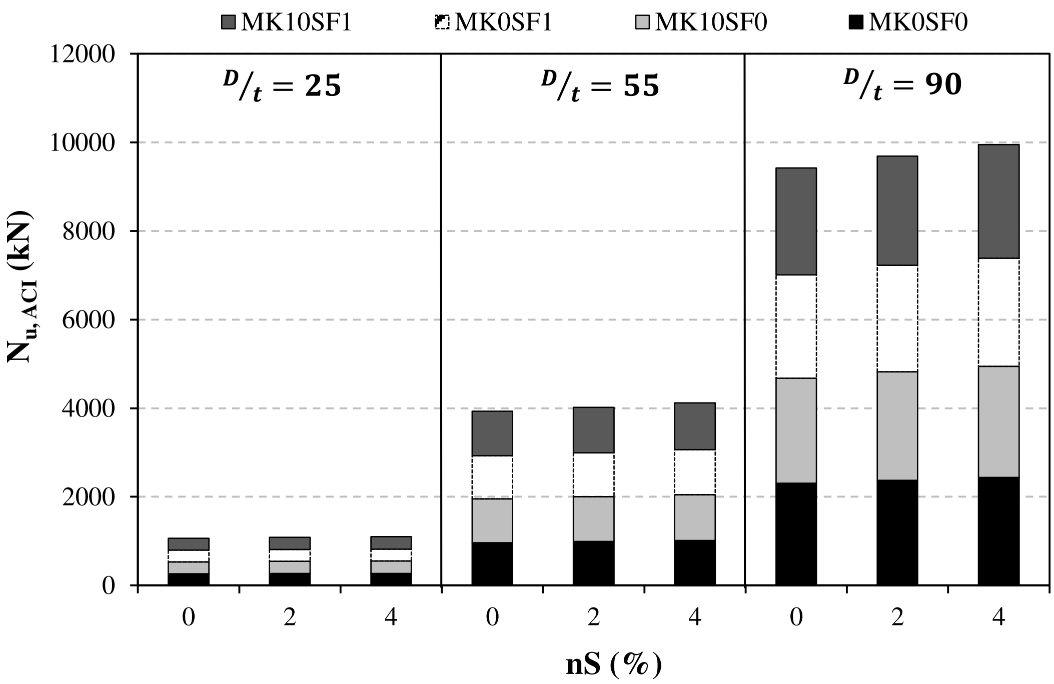
MK10SF1
MK0SF1
MK10SF0
MK0SF0
$^D/_t = 25$
$^D/_t = 55$
$^D/_t = 90$
$N_{u,ACI}$ (kN)
nS (%)
0
2000
4000
6000
8000
10000
12000
0
2
4

b)

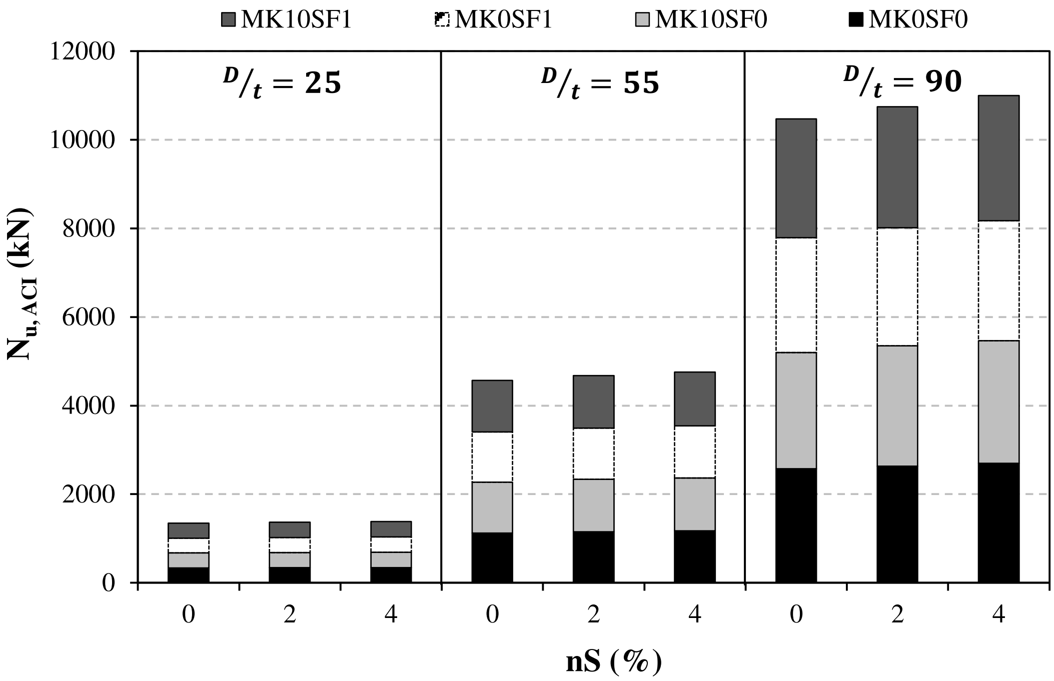

c)

Figure 5.3 Axial capacity calculated via ACI 318 at 28 days with respect to nS content for the steel yield strength of a) 150 MPa, b) 300 MPa and c) 450 MPa

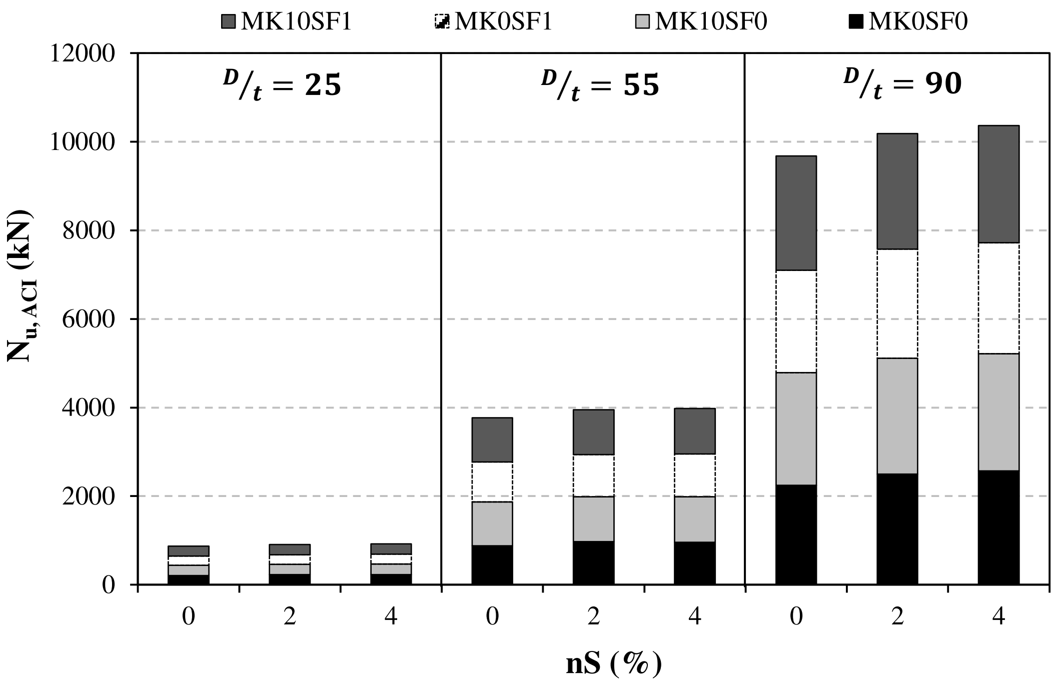

a)

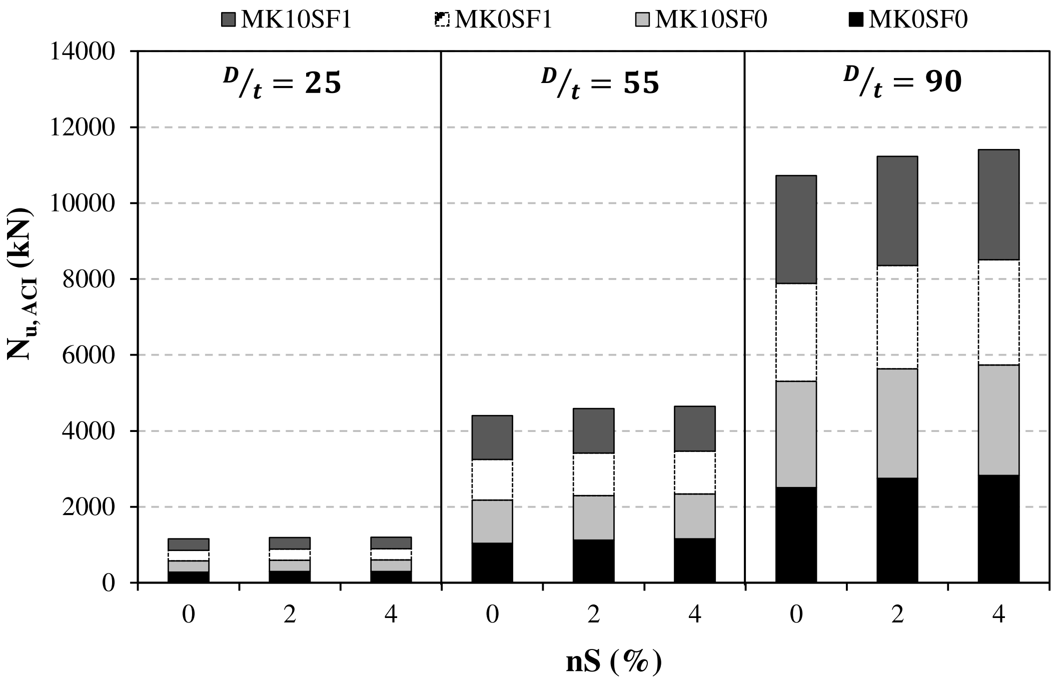

b)

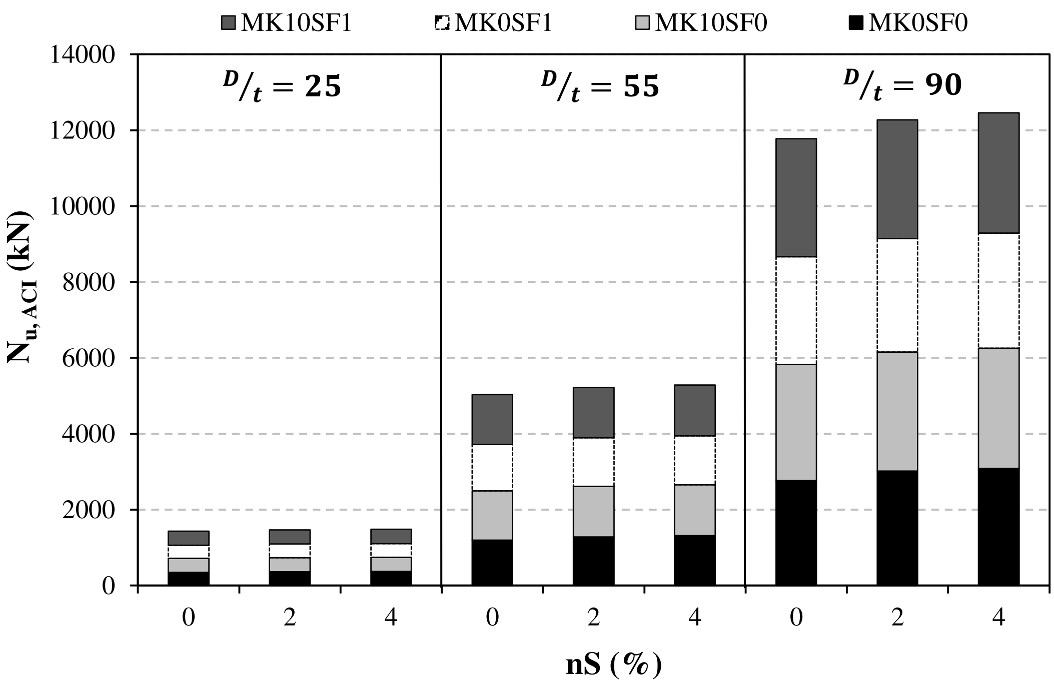

c)

Figure 5.4 Axial capacity calculated via ACI 318 at 90 days with respect to nS content for the steel yield strength of a) 150 MPa, b) 300 MPa and c) 450 MPa

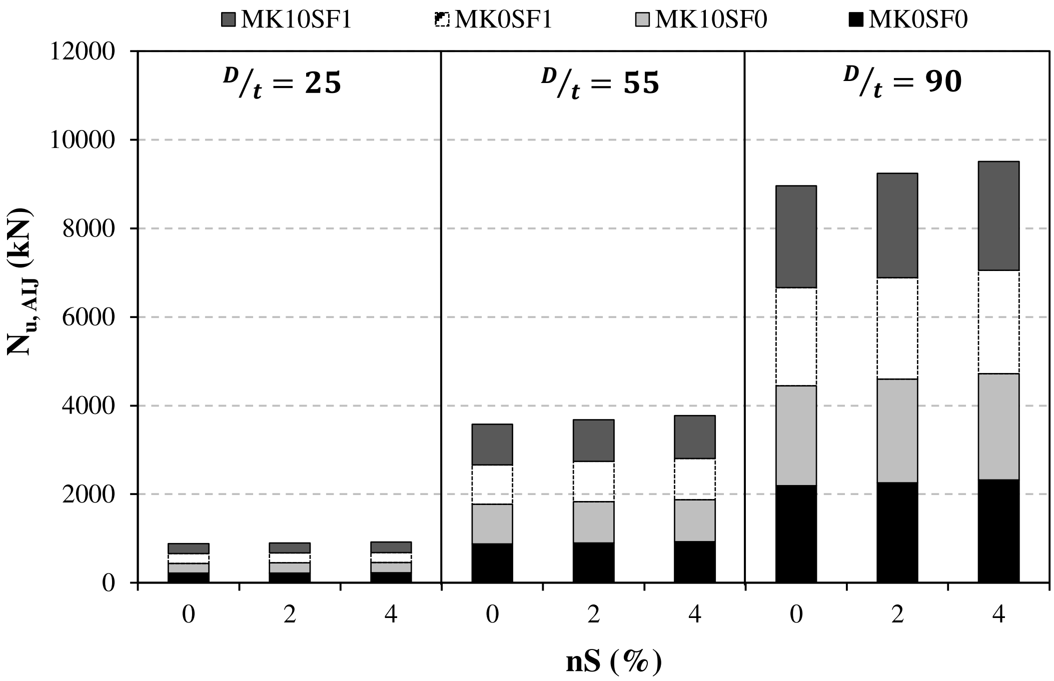
MK10SF1
MK0SF1
MK10SF0
MK0SF0
$^{D}/_{t} = 25$
$^{D}/_{t} = 55$
$^{D}/_{t} = 90$
$N_{u,AIJ}$ (kN)
12000
10000
8000
6000
4000
2000
0
0
2
4
0
2
4
0
2
4
nS (%)

a)

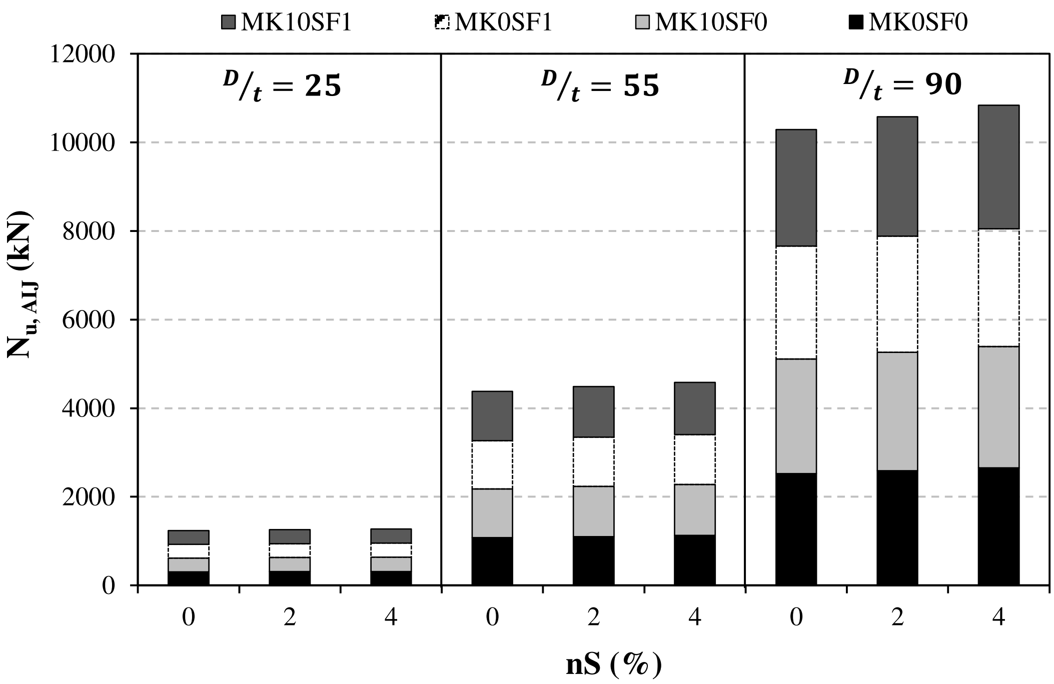
MK10SF1
MK0SF1
MK10SF0
MK0SF0
$^{D}/_{t} = 25$
$^{D}/_{t} = 55$
$^{D}/_{t} = 90$
$N_{u,AIJ}$ (kN)
12000
10000
8000
6000
4000
2000
0
0
2
4
0
2
4
0
2
4
nS (%)

b)

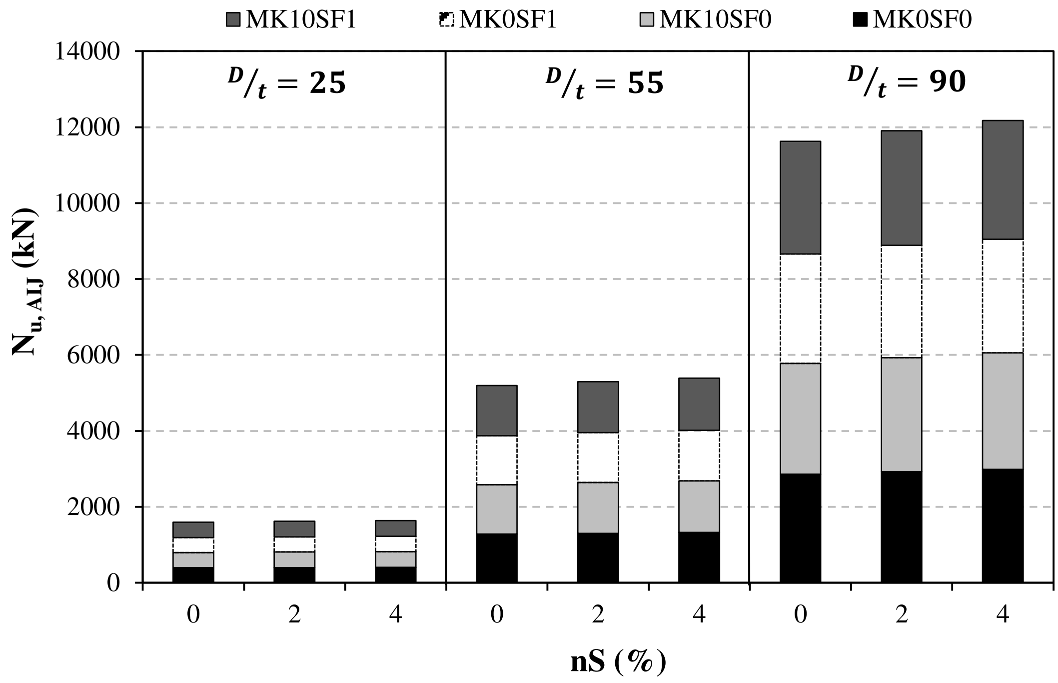

c)

Figure 5.5 Axial capacity calculated via AIJ at 28 days with respect to nS content for the steel yield strength of a) 150 MPa, b) 300 MPa and c) 450 MPa

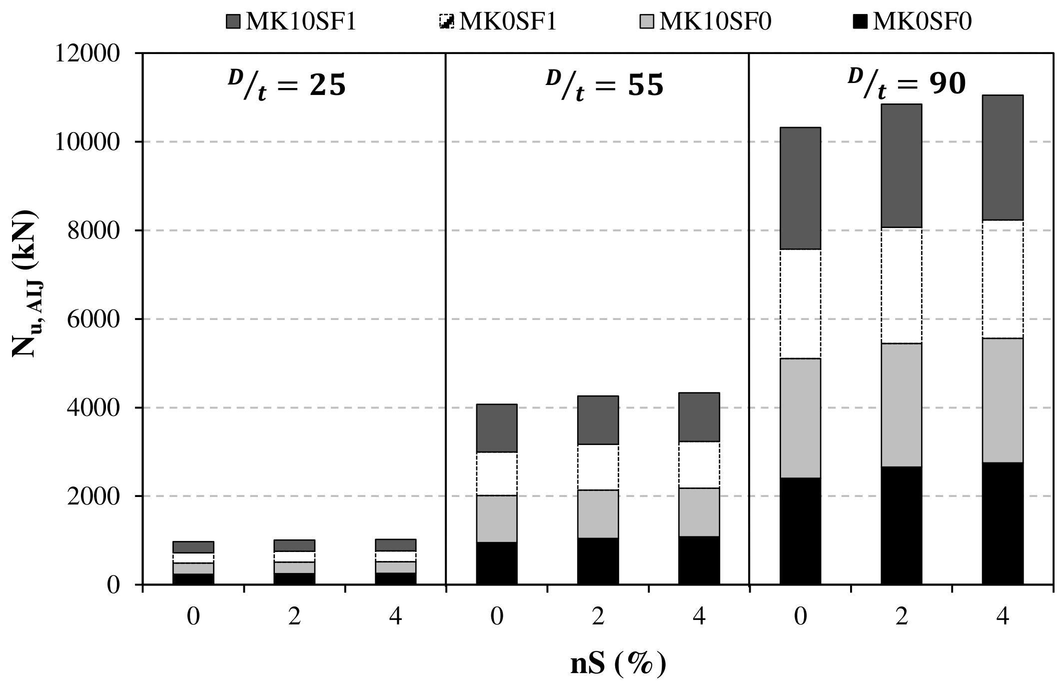

a)

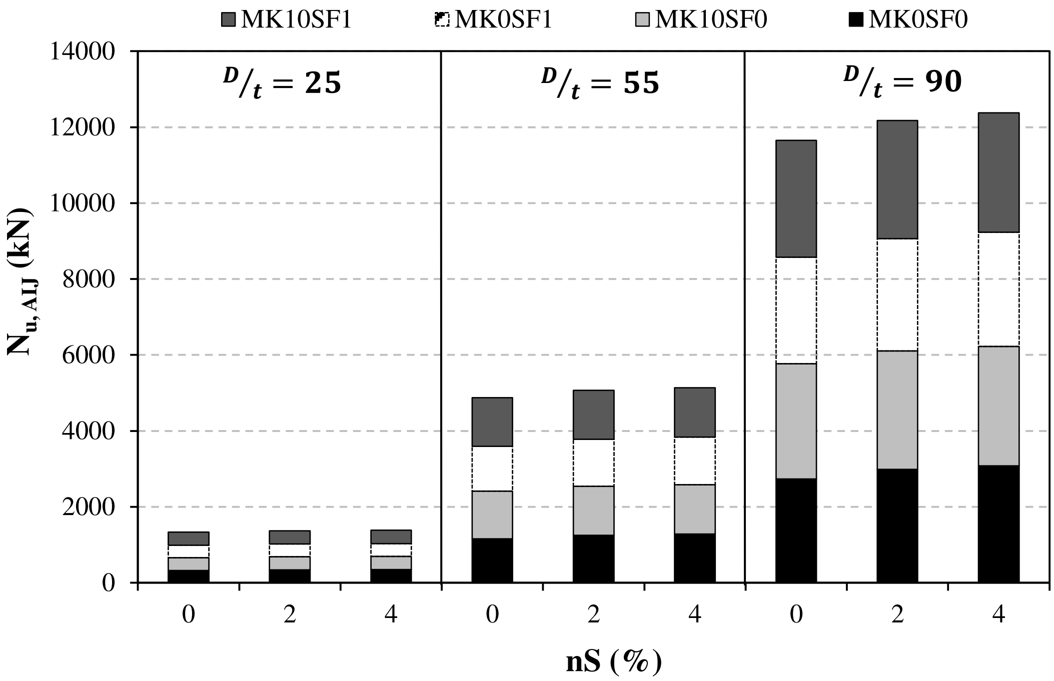

b)

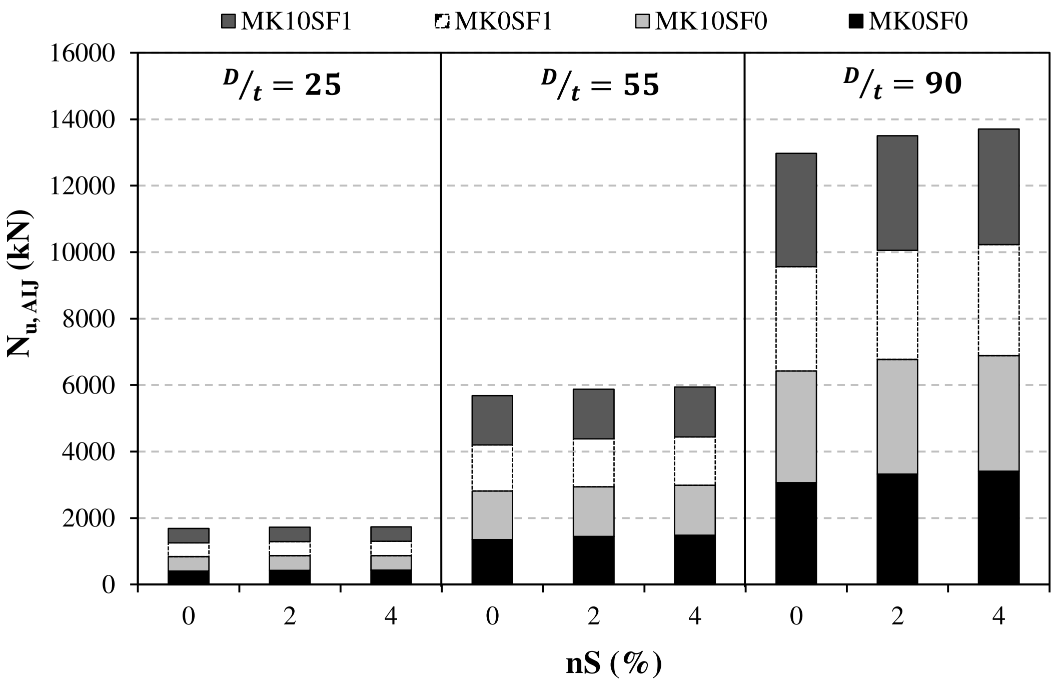

c)

Figure 5.6 Axial capacity calculated via AIJ at 90 days with respect to nS content for the steel yield strength of a) 150 MPa, b) 300 MPa and c) 450 MPa

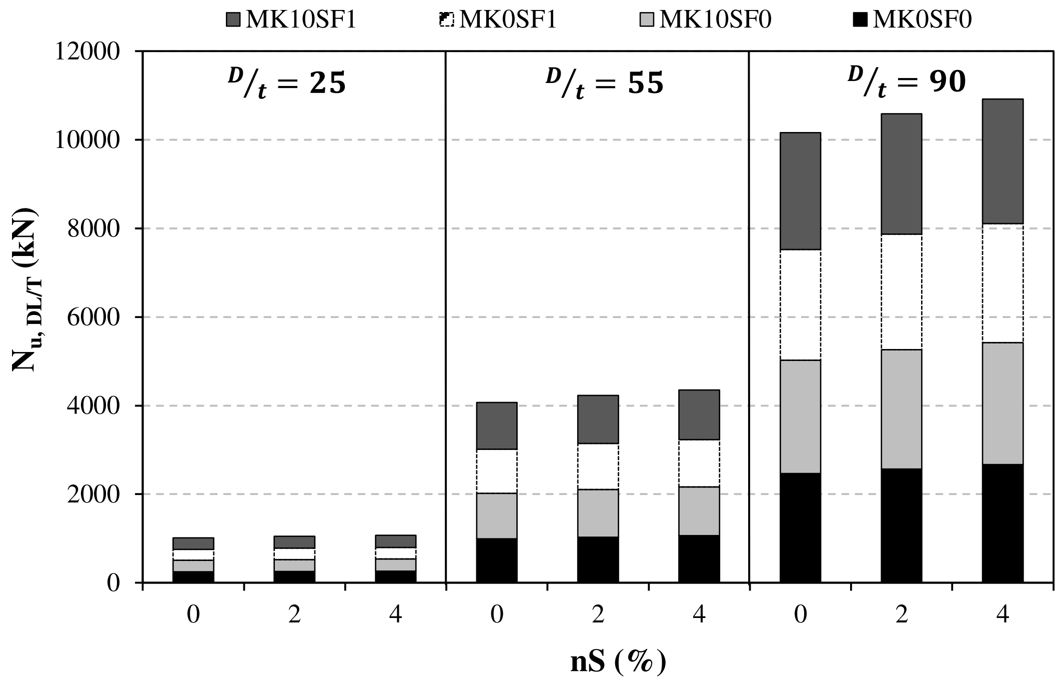
MK10SF1
MK0SF1
MK10SF0
MK0SF0
$^D/_t = 25$
$^D/_t = 55$
$^D/_t = 90$
$N_{u,\,DL/T}$ (kN)
nS (%)
0
2000
4000
6000
8000
10000
12000
0 2 4 0 2 4 0 2 4

a)

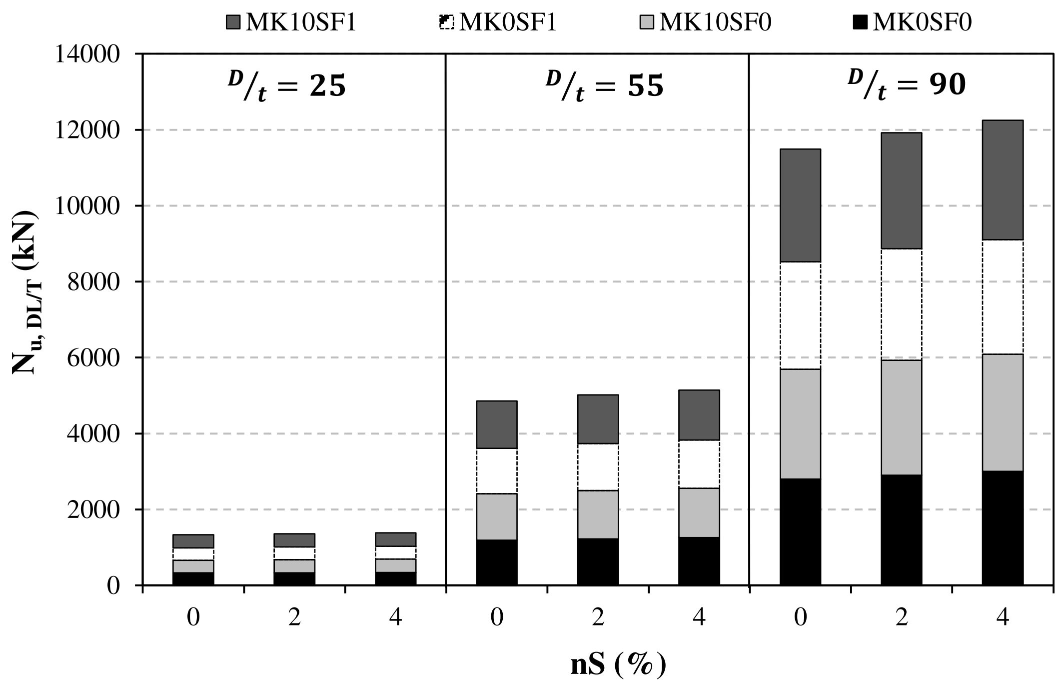
MK10SF1
MK0SF1
MK10SF0
MK0SF0
$^D/_t = 25$
$^D/_t = 55$
$^D/_t = 90$
$N_{u,\,DL/T}$ (kN)
nS (%)
0
2000
4000
6000
8000
10000
12000
14000
0 2 4 0 2 4 0 2 4

b)

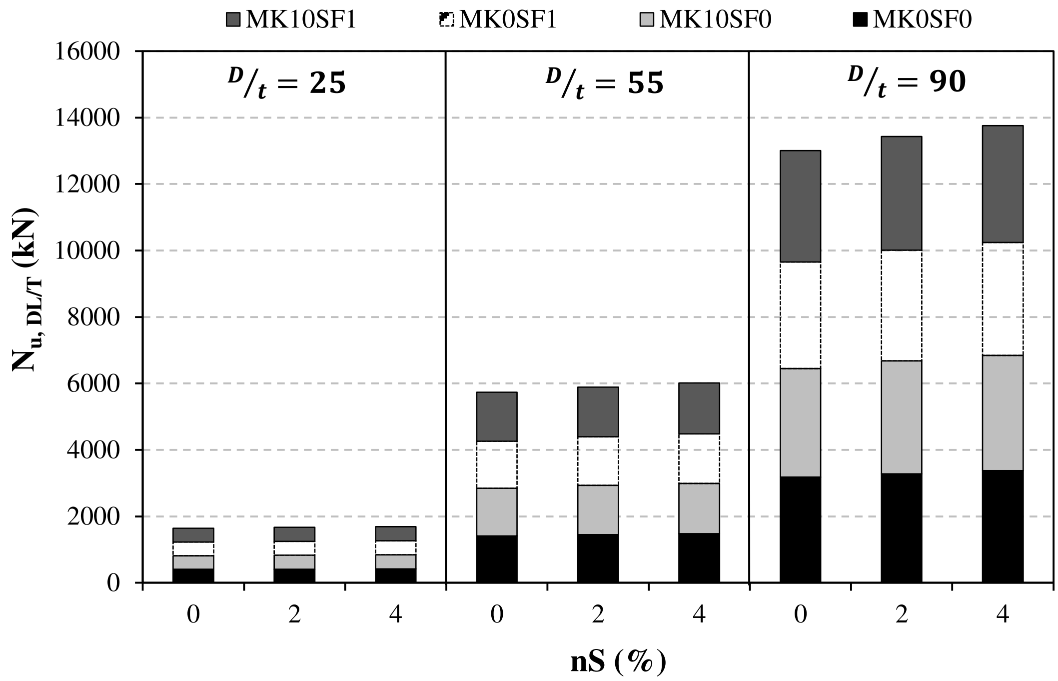

c)

Figure 5.7 Axial capacity calculated via DL/T at 28 days with respect to nS content for the steel yield strength of a) 150 MPa, b) 300 MPa and c) 450 MPa

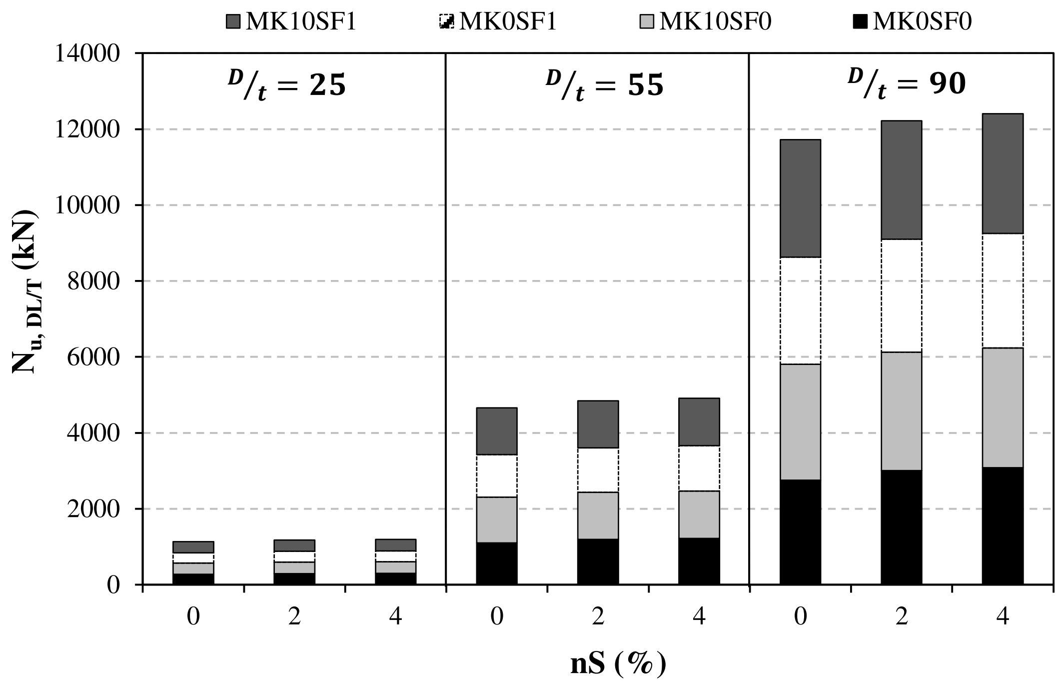

a)

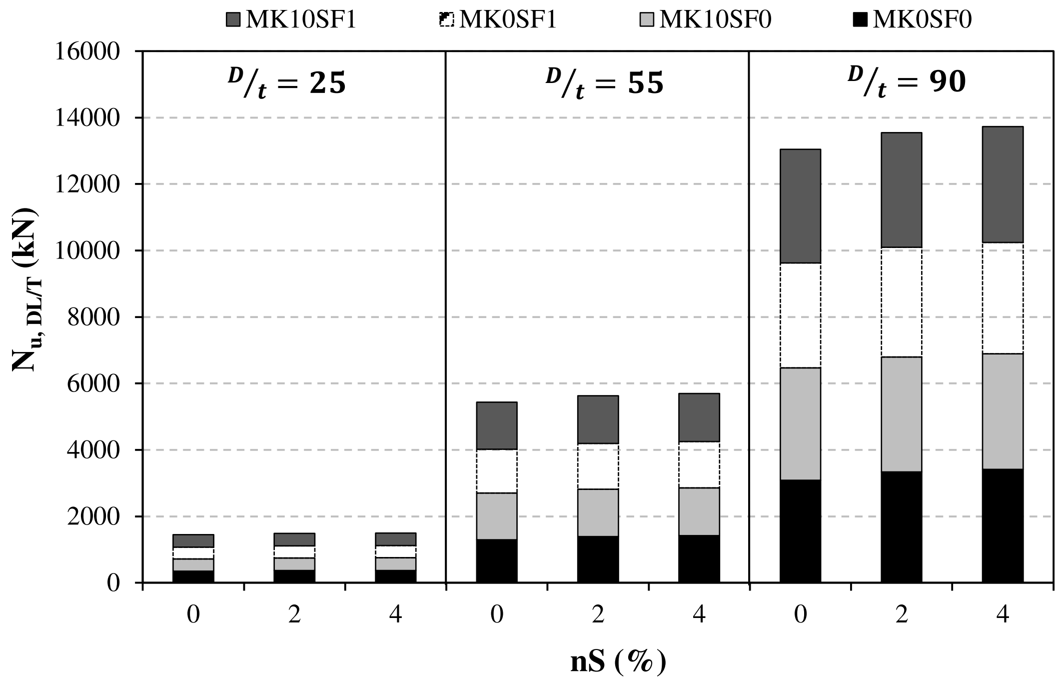

b)

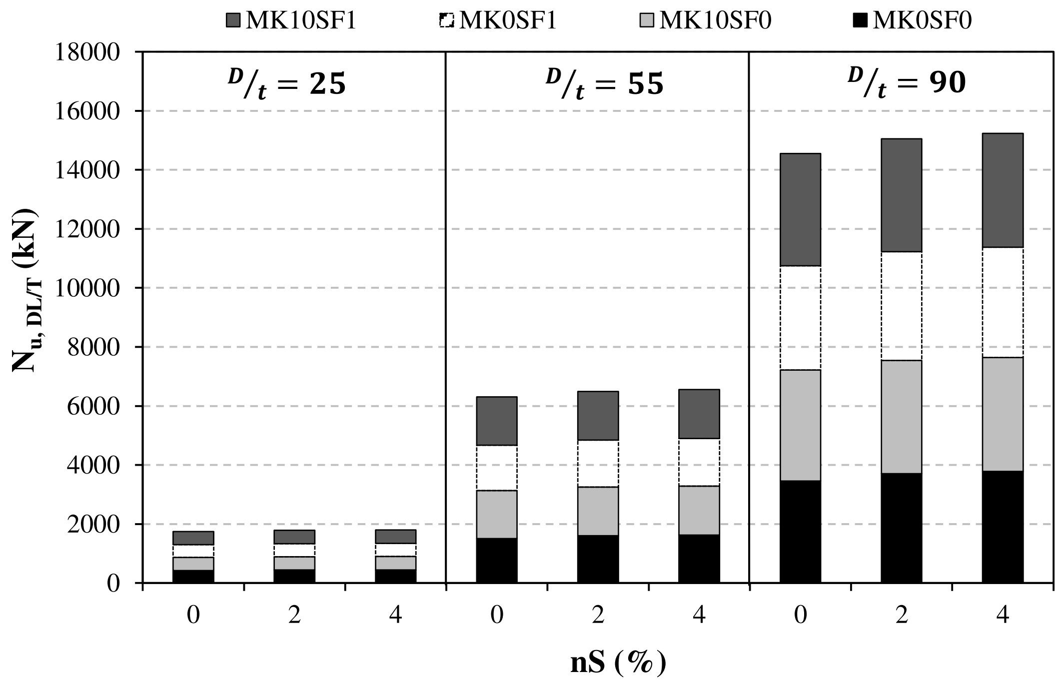

c)

Figure 5.8 Axial capacity calculated via DL/T at 90 days with respect to nS content for the steel yield strength of a) 150 MPa, b) 300 MPa and c) 450 MPa

5.2 Interaction between provision codes

5.2.1 Interaction analysis with D/t ratio

The interaction between computed axial capacity of Eurocode 4 and ACI, Eurocode 4 and AIJ and Eurocode 4 and DL/T versus D/t ratio relations are presented in Figures 5.9 to 5.14. Generally, the relation between axial capacity of Eurocode 4 and ACI computed by using the 28 days compressive strength of SCC and SFRSCC depicts that there are low differences resulted from the interaction action (interaction value close to 1) regarded the utilization of 0%, 2% and 4% nS , Figure 5.9a to c. Similar to this observation, the interaction action between Eurocode 4 and AIJ of 28 and 90 days curing period and between Eurocode 4 and DL/T but for 90 days can be clearly seen in Figure 5.11a to c and 5.14a to c, respectively. In spite of this, the effect of nS on the interaction between Eurocode 4 and ACI seems to be slightly affected at 90 days with the incorporation of nS in SCC and SFRSCC, Figure 5.10a to c. In this regard, it can be concluded that the interaction difference between the mentioned codes decreases continuously with the increases of nS from 0% to 2% and from 2% to 4%. At 28 days, the Eurocode 4 and DL/T interaction figure revealed comparable behaviour to those of Eurocode 4 and ACI at 90 days, Figure 5.13a to c and Figure 5.14a to c. However, the presented interaction curves in Figures 5.9 to 5.14 showed that at the same nS content and D/t ratio it is difficult to recognize clear behaviour between SCC free of steel fiber and those incorporated steel fiber.

The variation in the ratio of interaction are found to be at the range of 1-1.3, 1.1-1.14 and 0.97-1.08 for the ratio computed between Eurocode 4 and ACI, Eurocode 4 and AIJ and Eurocode and DL/T, respectively, irrespective of age and D/t ratio. Although from these light differences, it can be concluded that the most similar two codes are Eurocode 4 and DL/T. Wang et al. (2014) adopted the design guidelines specified by Eurocode 4 (2004) and Chinese code DL/T (1999) provisions to determine the test strength for the CFST column. It was directed that Eurocode 4 (2004) and Chinese code DL/T (1999) were closer to the test column strength than those by the other design guidelines.

Table 5.2 illustrates the details of CFST columns yielded lower interaction differences computed from employing two different codes in axial capacity predicting calculation.

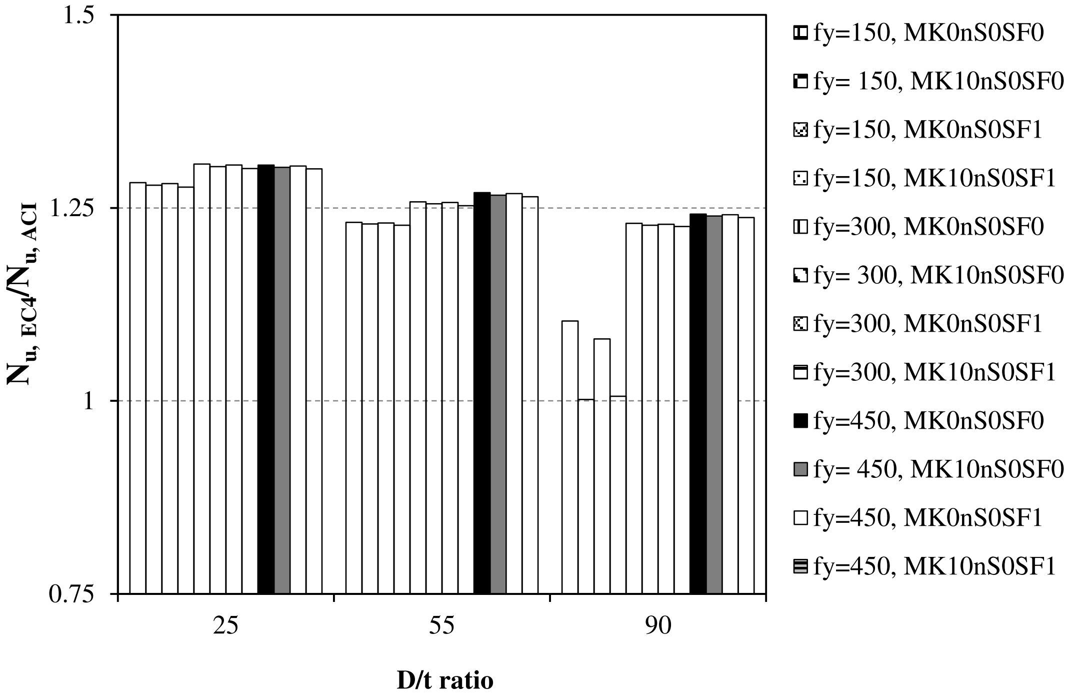
1.5
1.25
1
0.75
$N_{u,\ EC4}/N_{u,\ ACI}$
25
55
90
D/t ratio
fy=150, MK0nS0SF0
fy= 150, MK10nS0SF0
fy=150, MK0nS0SF1
fy=150, MK10nS0SF1
fy=300, MK0nS0SF0
fy= 300, MK10nS0SF0
fy=300, MK0nS0SF1
fy=300, MK10nS0SF1
fy=450, MK0nS0SF0
fy= 450, MK10nS0SF0
fy=450, MK0nS0SF1
fy=450, MK10nS0SF1

a)

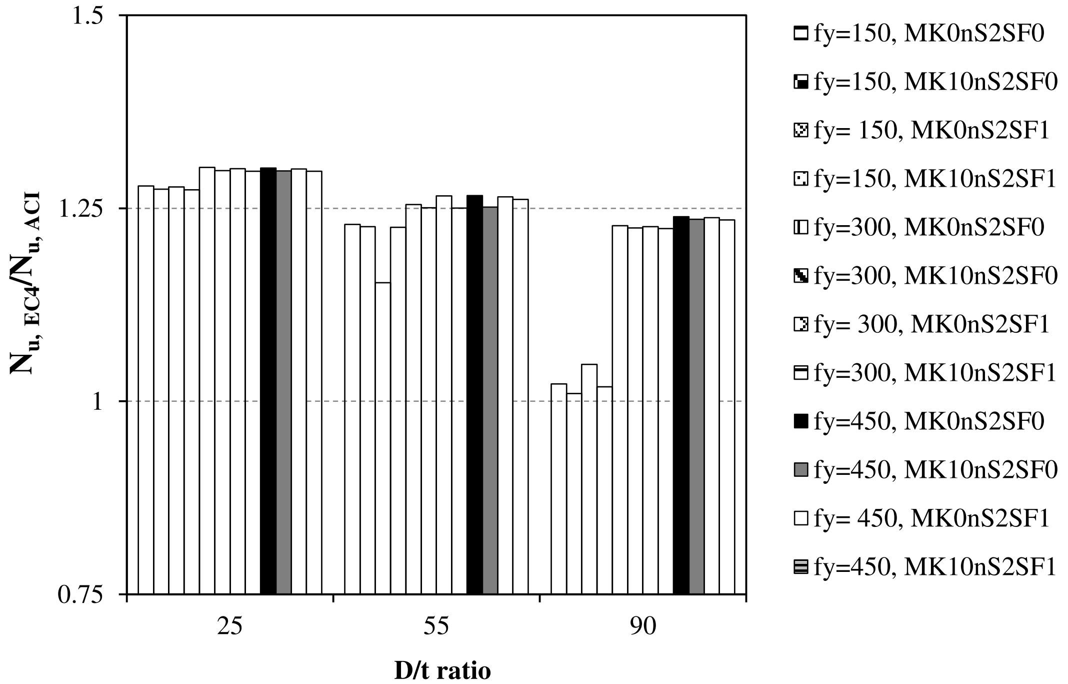
1.5
1.25
1
0.75
$N_{u,\ EC4}/N_{u,\ ACI}$
25
55
90
D/t ratio
fy=150, MK0nS2SF0
fy=150, MK10nS2SF0
fy= 150, MK0nS2SF1
fy=150, MK10nS2SF1
fy=300, MK0nS2SF0
fy=300, MK10nS2SF0
fy= 300, MK0nS2SF1
fy=300, MK10nS2SF1
fy=450, MK0nS2SF0
fy=450, MK10nS2SF0
fy= 450, MK0nS2SF1
fy=450, MK10nS2SF1

b)

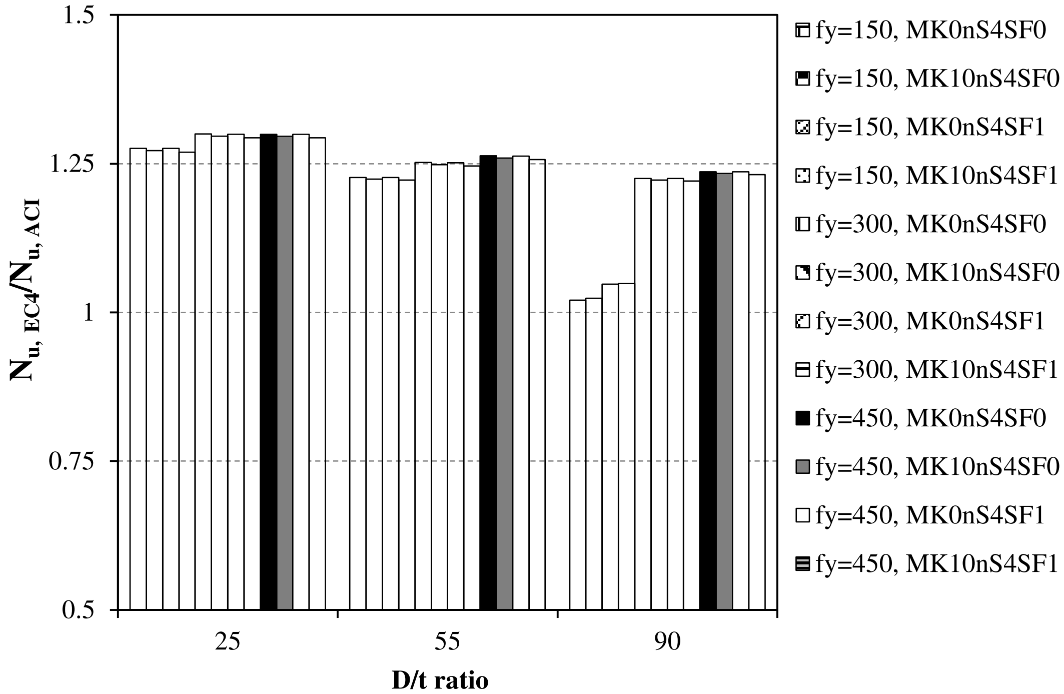

c)

Figure 5.9 Interaction between D/t and $N_{u,\ EC4}/N_{u,\ ACI}$ ratios at 28 days: a) nS0, b) nS2.0 and c) nS 4.0

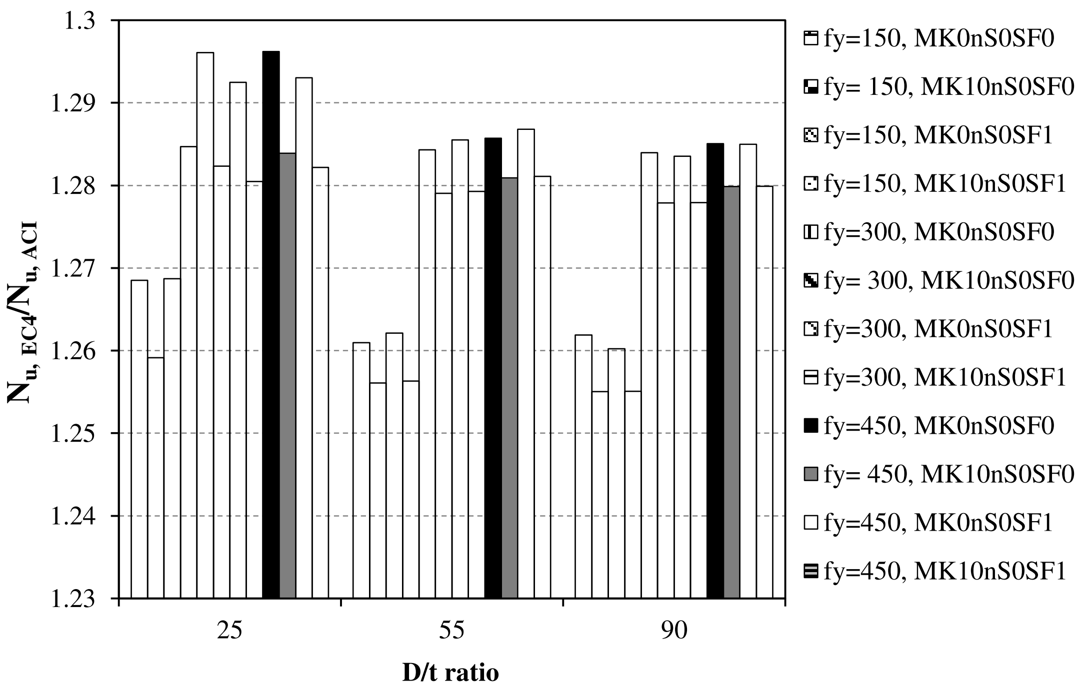

a)

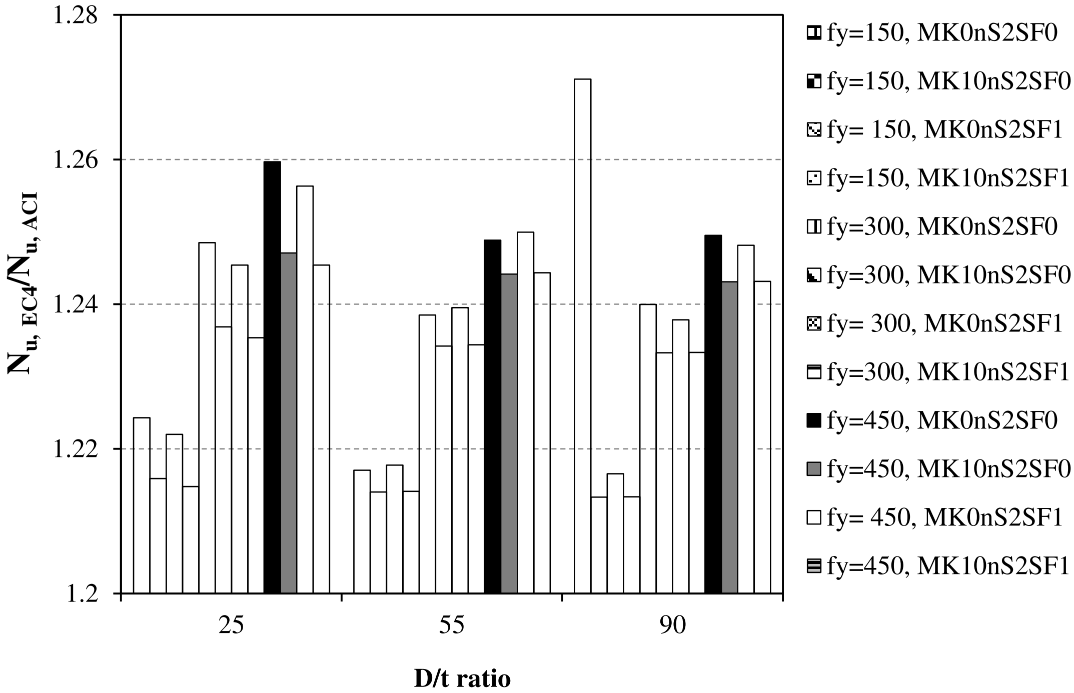

b)

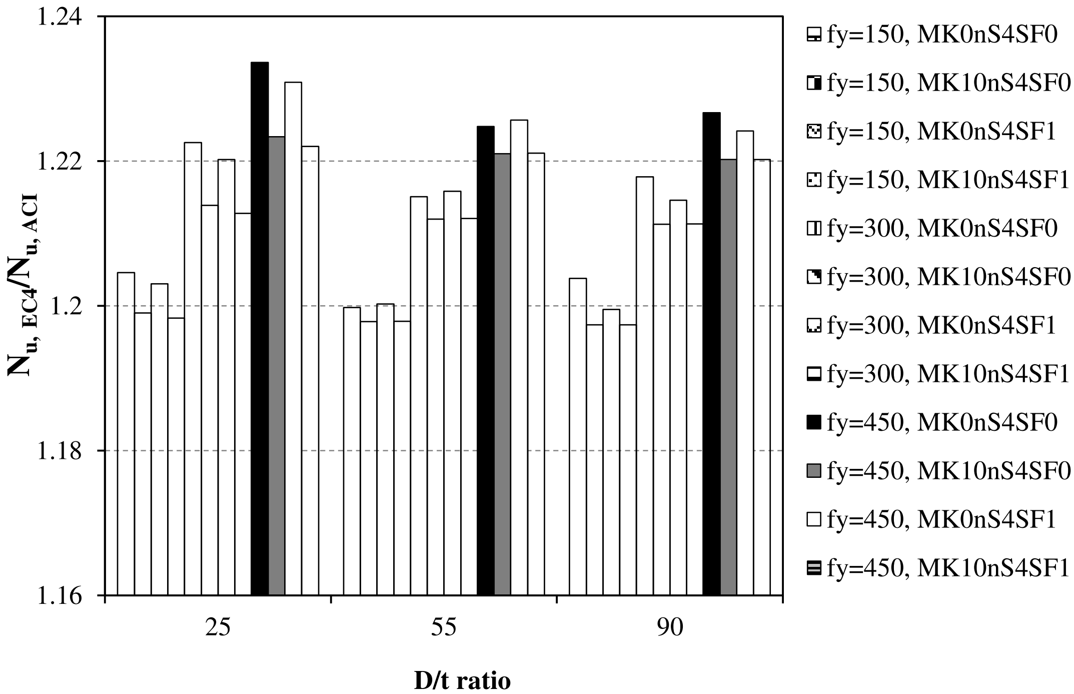

c)

Figure 5.10 Interaction between D/t and $N_{u,\ EC4}/N_{u,\ ACI}$ ratios at 90 days: a) nS0, b) nS2.0 and c) nS 4.0

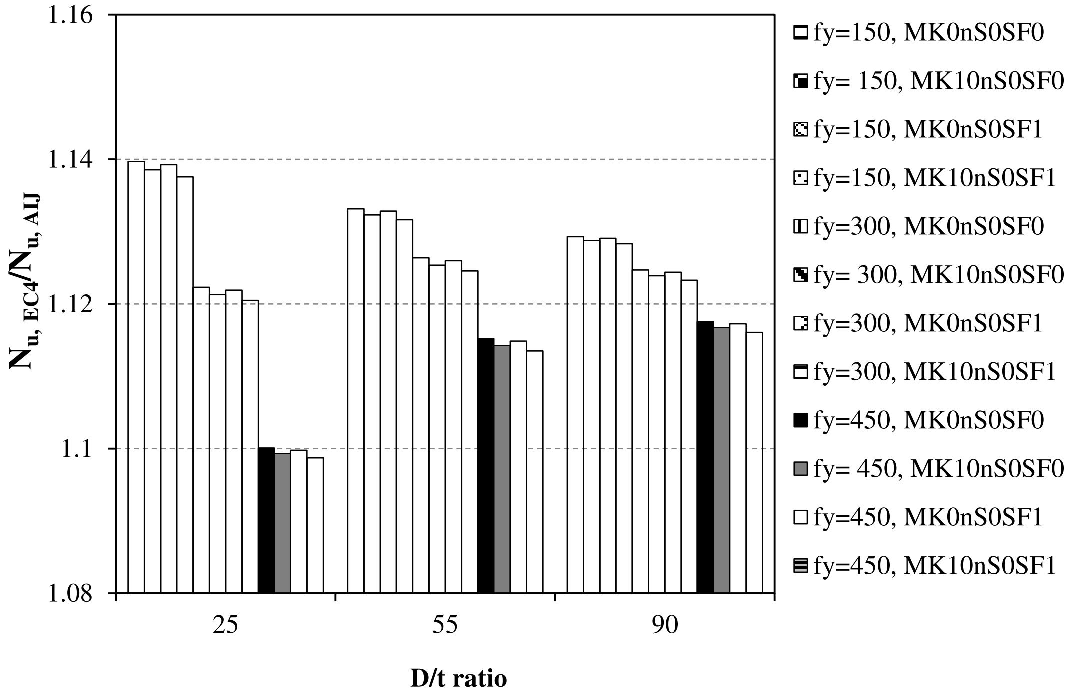
1.16
1.14
1.12
1.1
1.08
$N_{u, EC4}/N_{u, AIJ}$
25
55
90
D/t ratio
fy=150, MK0nS0SF0
fy= 150, MK10nS0SF0
fy=150, MK0nS0SF1
fy=150, MK10nS0SF1
fy=300, MK0nS0SF0
fy= 300, MK10nS0SF0
fy=300, MK0nS0SF1
fy=300, MK10nS0SF1
fy=450, MK0nS0SF0
fy= 450, MK10nS0SF0
fy=450, MK0nS0SF1
fy=450, MK10nS0SF1

a)

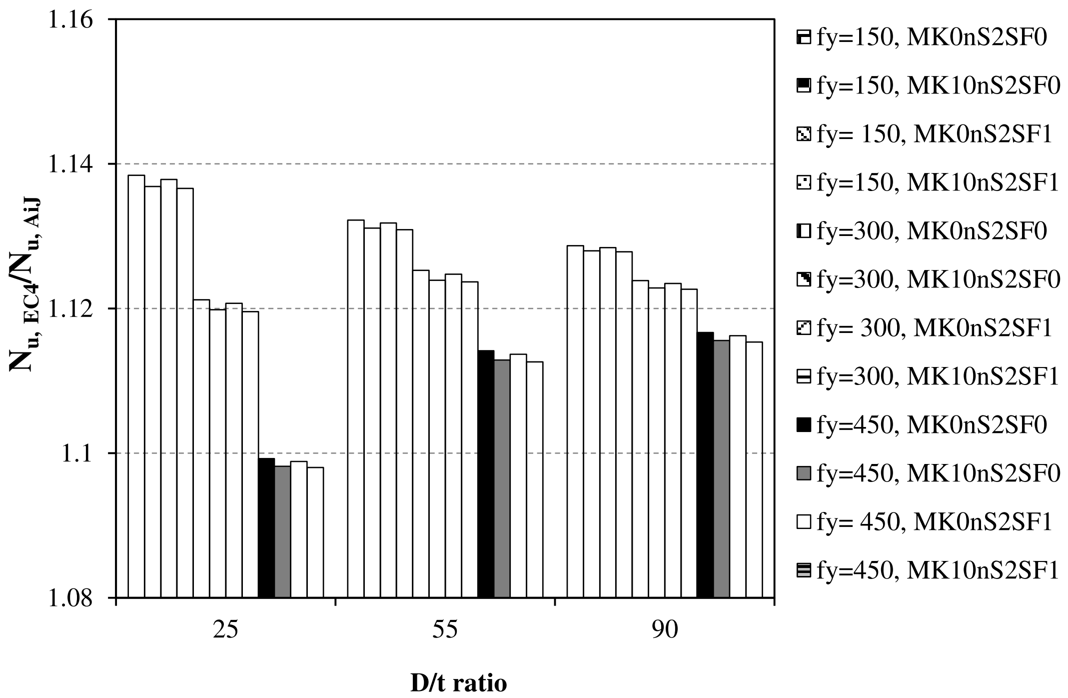
1.16
1.14
1.12
1.1
1.08
$N_{u, EC4}/N_{u, AiJ}$
25
55
90
D/t ratio
fy=150, MK0nS2SF0
fy=150, MK10nS2SF0
fy= 150, MK0nS2SF1
fy=150, MK10nS2SF1
fy=300, MK0nS2SF0
fy=300, MK10nS2SF0
fy= 300, MK0nS2SF1
fy=300, MK10nS2SF1
fy=450, MK0nS2SF0
fy=450, MK10nS2SF0
fy= 450, MK0nS2SF1
fy=450, MK10nS2SF1

b)

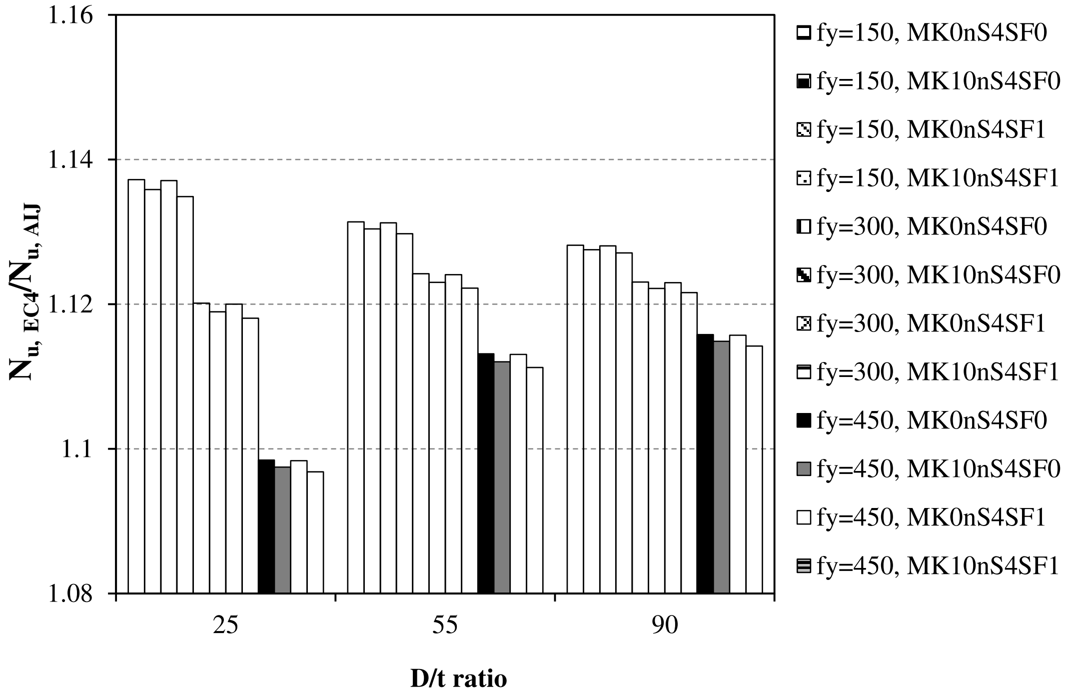

c)

Figure 5.11 Interaction between D/t and $N_{u,\ EC4}/N_{u,\ AIJ}$ ratios at 28 days: a) nS0, b) nS2.0 and c) nS 4.0

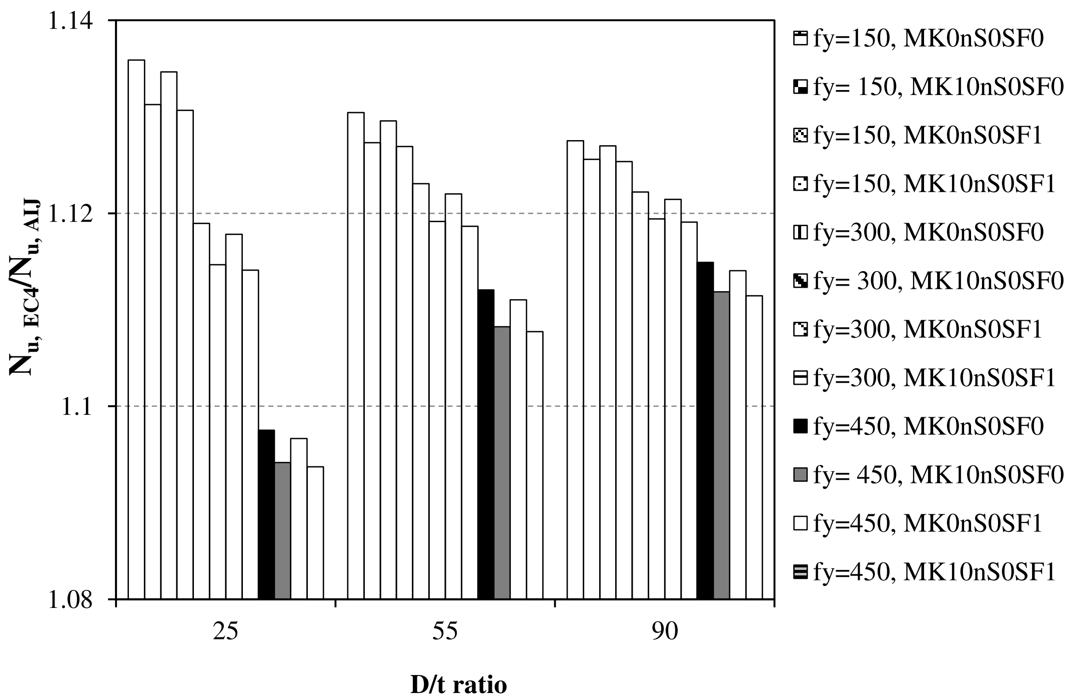

a)

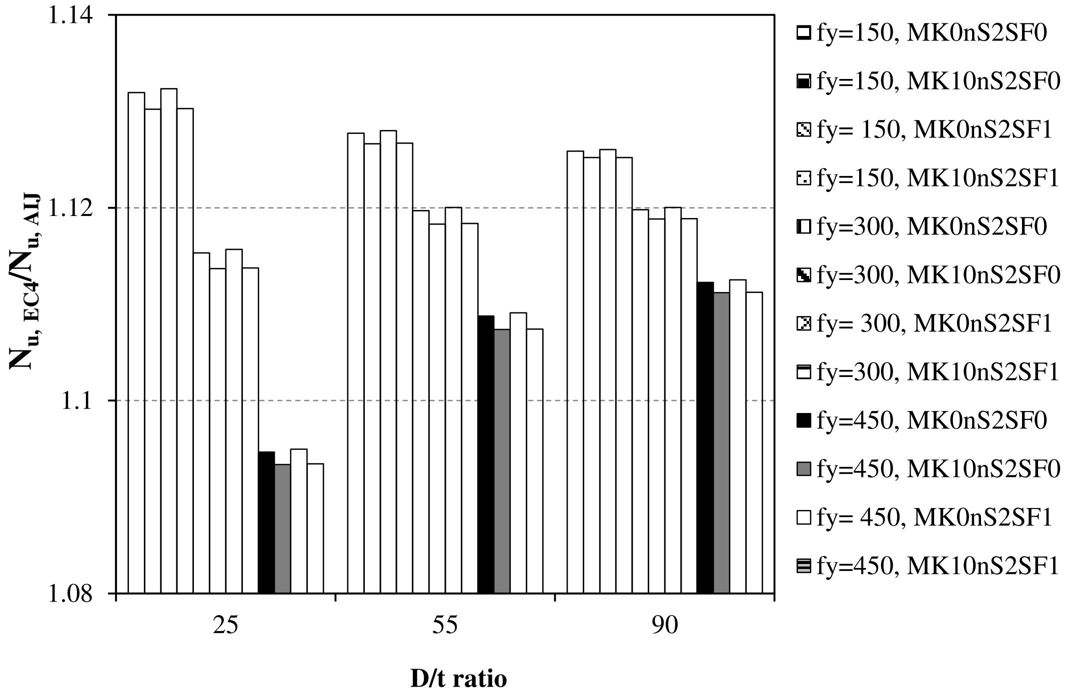

b)

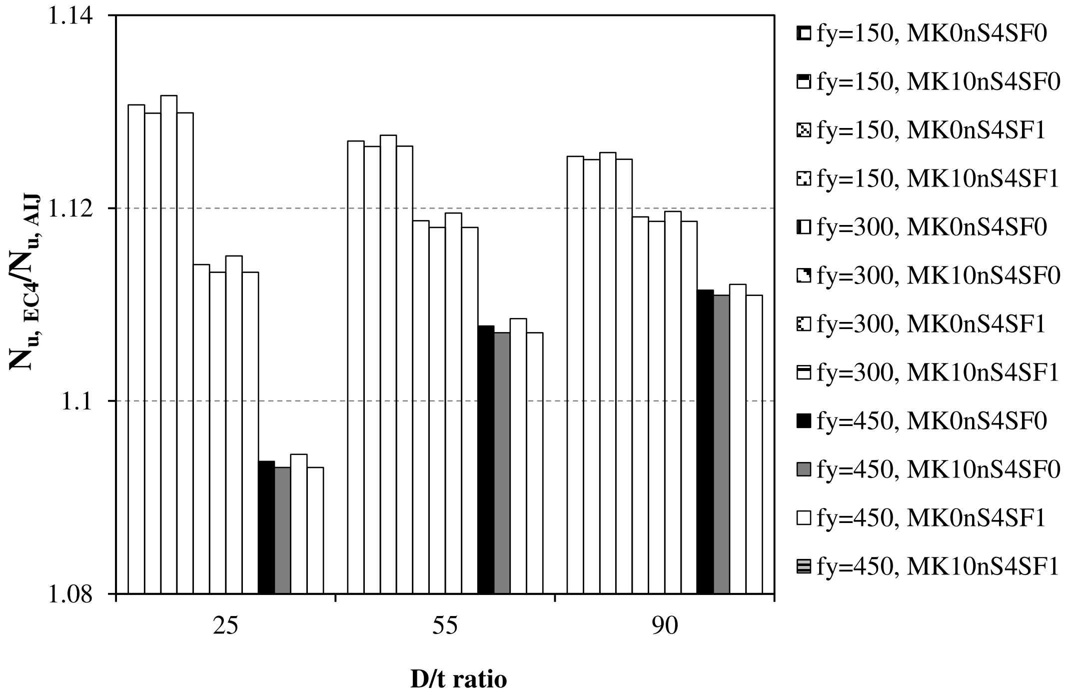

c)

Figure 5.12 Interaction between D/t and $N_{u,\ EC4}/N_{u,\ AIJ}$ ratios at 90 days: a) nS0, b) nS2.0 and c) nS 4.0

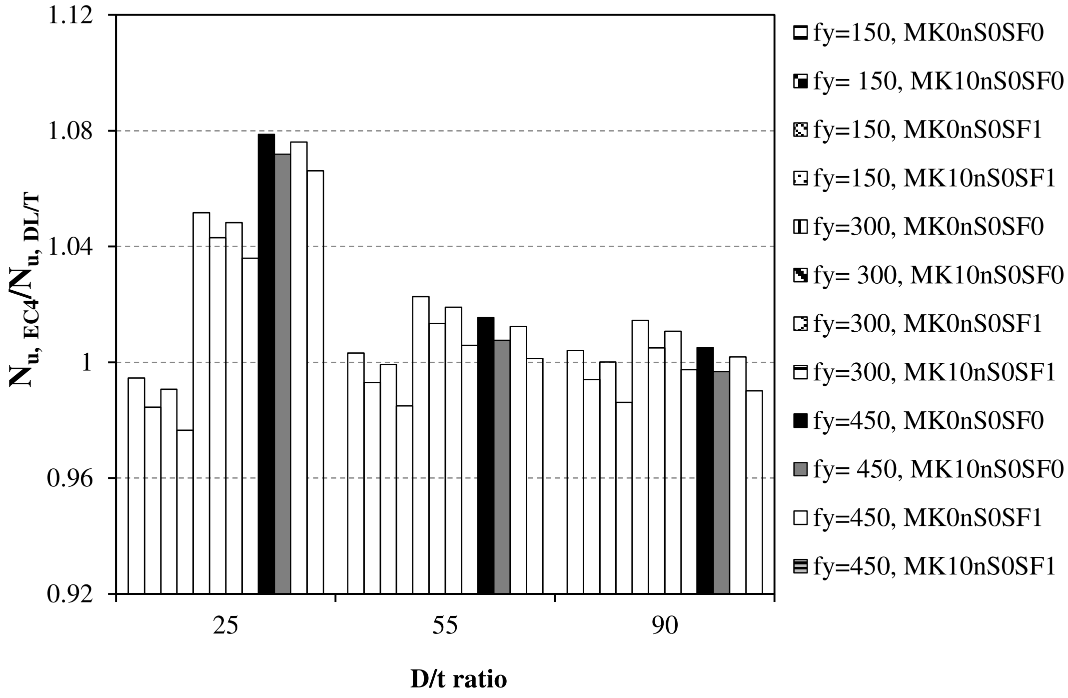
1.12
1.08
1.04
1
0.96
0.92
$N_{u, EC4}/N_{u, DL/T}$
25
55
90
D/t ratio
fy=150, MK0nS0SF0
fy= 150, MK10nS0SF0
fy=150, MK0nS0SF1
fy=150, MK10nS0SF1
fy=300, MK0nS0SF0
fy= 300, MK10nS0SF0
fy=300, MK0nS0SF1
fy=300, MK10nS0SF1
fy=450, MK0nS0SF0
fy= 450, MK10nS0SF0
fy=450, MK0nS0SF1
fy=450, MK10nS0SF1

a)

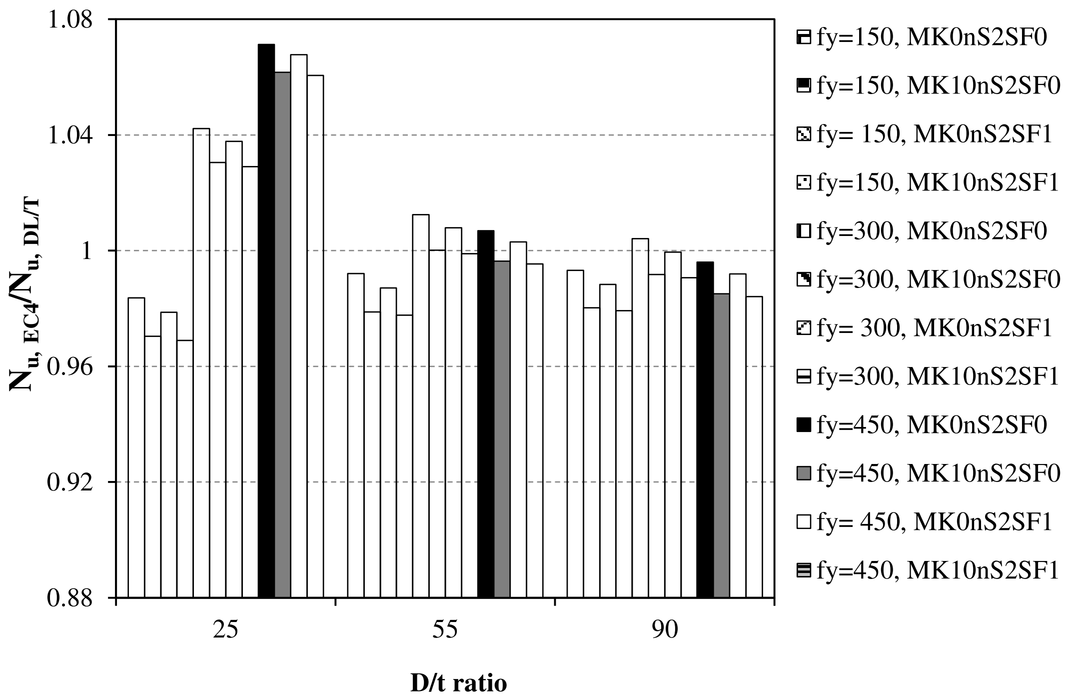
1.08
1.04
1
0.96
0.92
0.88
$N_{u, EC4}/N_{u, DL/T}$
25
55
90
D/t ratio
fy=150, MK0nS2SF0
fy=150, MK10nS2SF0
fy= 150, MK0nS2SF1
fy=150, MK10nS2SF1
fy=300, MK0nS2SF0
fy=300, MK10nS2SF0
fy= 300, MK0nS2SF1
fy=300, MK10nS2SF1
fy=450, MK0nS2SF0
fy=450, MK10nS2SF0
fy= 450, MK0nS2SF1
fy=450, MK10nS2SF1

b)

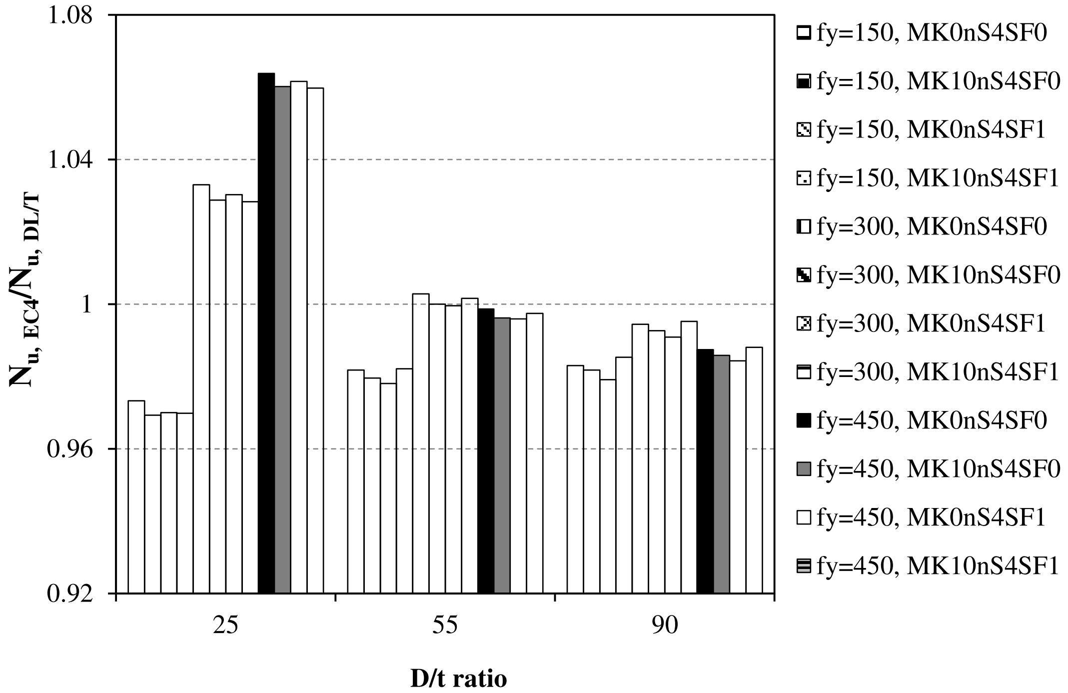

c)

Figure 5.13 Interaction between D/t and $N_{u, EC4}/N_{u, DL/T}$ ratios at 28 days: a) nS0, b) nS2.0 and c) nS 4.0

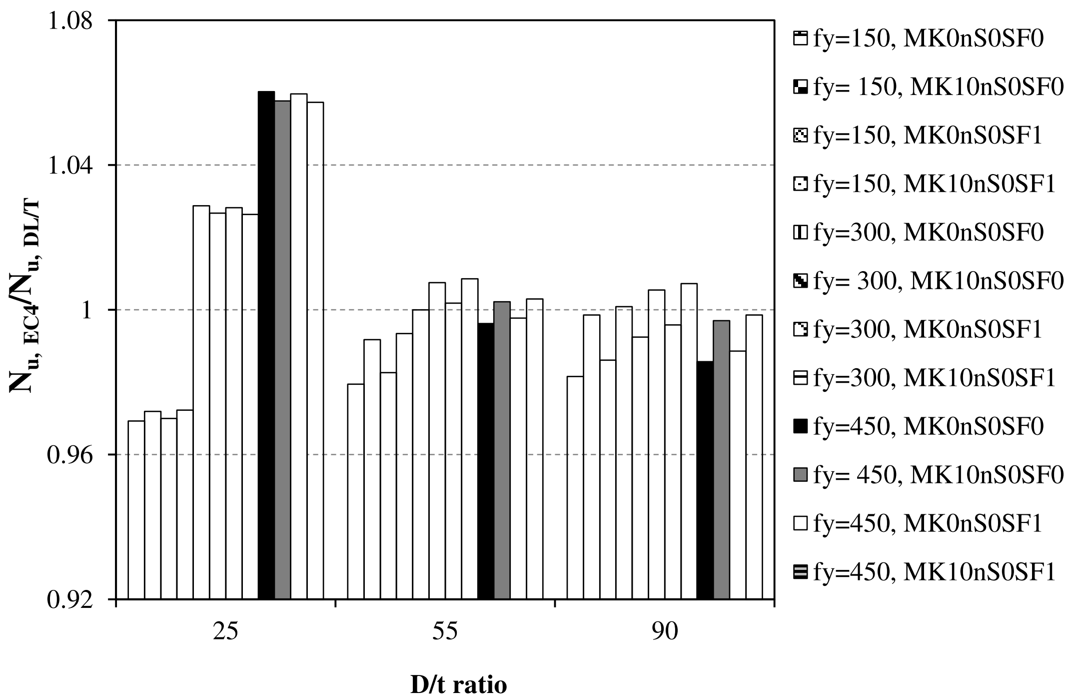

a)

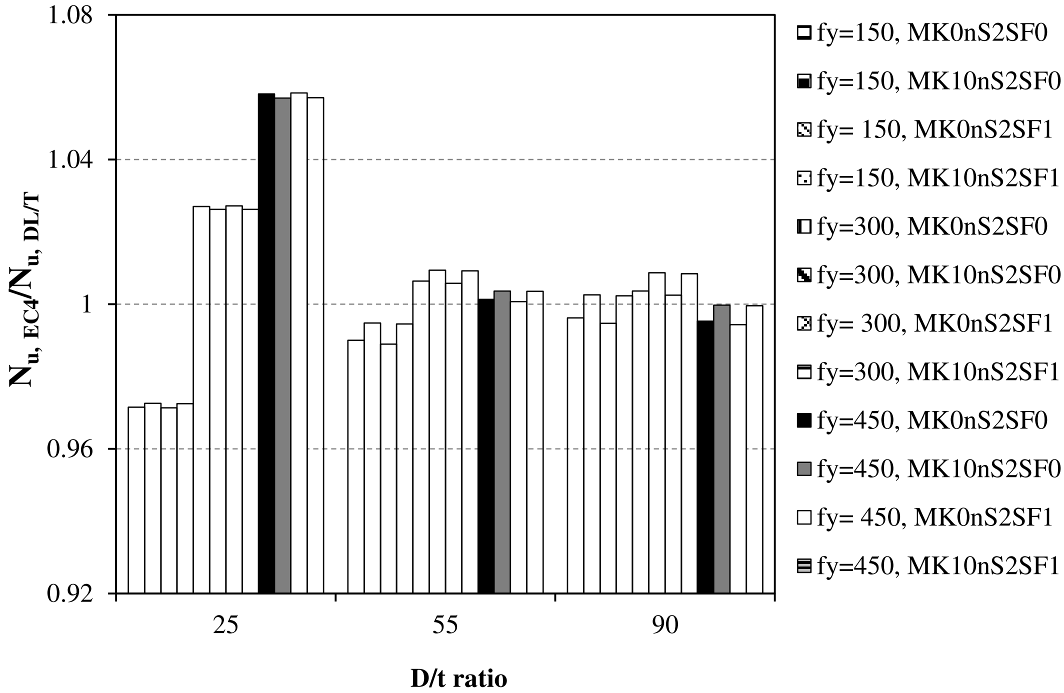

b)

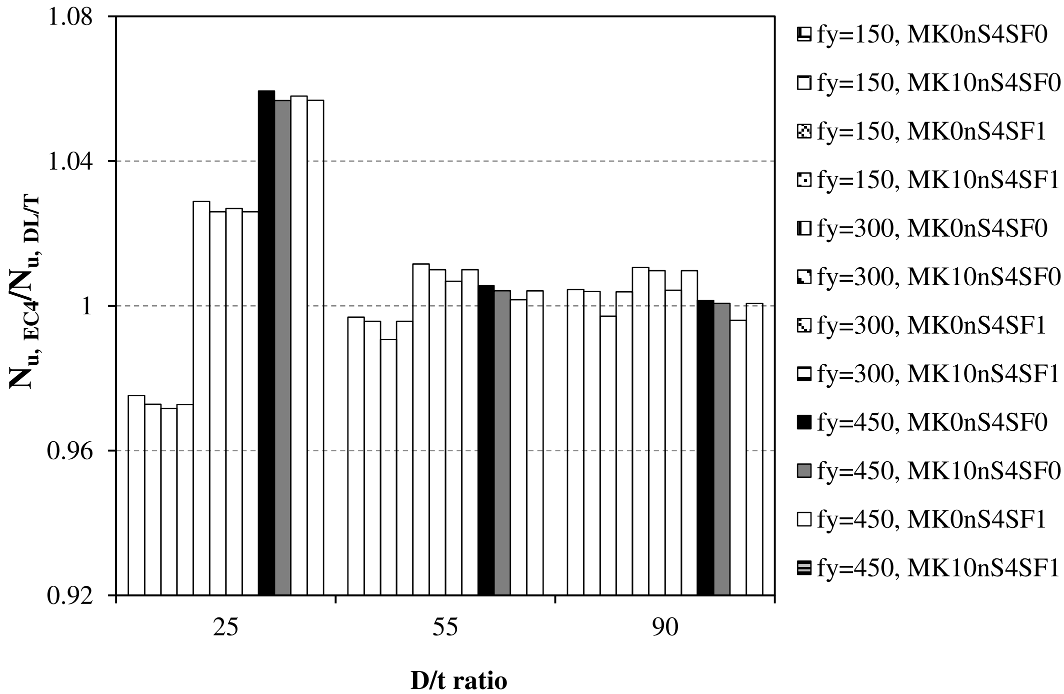

c)

Figure 5.14 Interaction between D/t and $N_{u,\ EC4}/N_{u,\ DL/T}$ ratios at 90 days: a) nS0, b) nS2.0 and c) nS 4.0

Table 5.2 Details of CFST columns having lower interaction effect

Intended codes	Type of concrete core	Age (days)	D/t ratio	Yield strength of steel (MPa)
EC4 and ACI	SCC+10%MK	28	90	150
EC4 and ACI	SFRSCC+10%MK	28	90	150
EC4 and ACI	SCC+10%MK+2%nS	28	90	150
EC4 and ACI	SFRSCC+10%MK+2%nS	28	90	150
EC4 and DL/T	SCC (plain)	28	25	150
EC4 and DL/T	SFRSCC	28	25	150
EC4 and DL/T	SCC (plain)	28	55	150
EC4 and DL/T	SCC+10%MK	28	55	150
EC4 and DL/T	SFRSCC	28	55	150
EC4 and DL/T	SFRSCC+10%MK	28	55	300
EC4 and DL/T	SCC+10%MK	28	55	450
EC4 and DL/T	SFRSCC+10%MK	28	55	450
EC4 and DL/T	SCC (plain)	28	90	150
EC4 and DL/T	SCC+10%MK	28	90	150
EC4 and DL/T	SFRSCC+10%MK	28	90	150
EC4 and DL/T	SCC+10%MK	28	90	300
EC4 and DL/T	SFRSCC	28	90	300
EC4 and DL/T	SFRSCC+10%MK	28	90	300
EC4 and DL/T	SCC (plain)	28	90	450
EC4 and DL/T	SCC+10%MK	28	90	450
EC4 and DL/T	SFRSCC	28	90	450
EC4 and DL/T	SFRSCC+10%MK	28	90	450
EC4 and DL/T	SCC (plain)+2%nS	28	55	150
EC4 and DL/T	SCC+10%MK+2%nS	28	55	300
EC4 and DL/T	SFRSCC+2%nS	28	55	300
EC4 and DL/T	SFRSCC+10%MK+2%nS	28	55	300
EC4 and DL/T	SCC (plain)+2%nS	28	55	450
EC4 and DL/T	SCC+10%MK+2%nS	28	55	450
EC4 and DL/T	SFRSCC+2%nS	28	55	450
EC4 and DL/T	SFRSCC+10%MK+2%nS	28	55	450
EC4 and DL/T	SCC (plain)+2%nS	28	90	150
EC4 and DL/T	SCC+2%nS	28	90	300
EC4 and DL/T	SCC+10%MK+2%nS	28	90	300
EC4 and DL/T	SFRSCC+2%nS	28	90	300
EC4 and DL/T	SFRSCC+10%MK+2%nS	28	90	300
EC4 and DL/T	SCC+2%nS	28	90	450
EC4 and DL/T	SFRSCC+2%nS	28	90	450
EC4 and DL/T	SCC+4%nS	28	55	300
EC4 and DL/T	SCC+10%MK+4%nS	28	55	300
EC4 and DL/T	SFRSCC+4%nS	28	55	300
EC4 and DL/T	SFRSCC+10%MK+4%nS	28	55	300
EC4 and DL/T	SCC+4%nS	28	55	450
EC4 and DL/T	SCC+10%MK+4%nS	28	55	450
EC4 and DL/T	SFRSCC+4%nS	28	55	450

Table 5.2 continued

Intended codes	Type of concrete core	Age (days)	D/t ratio	Yield strength of steel (MPa)
EC4 and DL/T	SFRSCC+10%MK+4%nS	28	55	450
EC4 and DL/T	SCC+4%nS	28	90	300
EC4 and DL/T	SCC+10%MK+4%nS	28	90	300
EC4 and DL/T	SFRSCC+4%nS	28	90	300
EC4 and DL/T	SFRSCC+10%MK+4%nS	28	90	300
EC4 and DL/T	SCC (plain)	90	55	300
EC4 and DL/T	SFRSCC	90	55	300
EC4 and DL/T	SCC (plain)	90	55	450
EC4 and DL/T	SCC+10%MK	90	55	450
EC4 and DL/T	SFRSCC	90	55	450
EC4 and DL/T	SFRSCC+10%MK	90	55	450
EC4 and DL/T	SCC+10%MK	90	90	150
EC4 and DL/T	SFRSCC+10%MK	90	90	150
EC4 and DL/T	SFRSCC	90	90	300
EC4 and DL/T	SCC+10%MK	90	90	450
EC4 and DL/T	SFRSCC+10%MK	90	90	450
EC4 and DL/T	SFRSCC+2%nS	55	90	300
EC4 and DL/T	SCC (plain)+2%ns	55	90	450
EC4 and DL/T	SCC+10%MK+2%nS	55	90	450
EC4 and DL/T	SFRSCC+2%nS	55	90	450
EC4 and DL/T	SFRSCC+10%MK+2%nS	55	90	450
EC4 and DL/T	SCC+10%MK+2%nS	90	90	150
EC4 and DL/T	SFRSCC+10%MK+2%nS	90	90	150
EC4 and DL/T	SCC (plain)+2%nS	90	90	300
EC4 and DL/T	SFRSCC+2%nS	90	90	300
EC4 and DL/T	SCC (plain)+2%nS	90	90	450
EC4 and DL/T	SCC+10%MK+2%nS	90	90	450
EC4 and DL/T	SFRSCC+2%nS	90	90	450
EC4 and DL/T	SFRSCC+10%MK+2%nS	90	90	450
EC4 and DL/T	SCC (plain)	55	90	150
EC4 and DL/T	SCC+10%MK	55	90	150
EC4 and DL/T	SFRSCC	55	90	150
EC4 and DL/T	SCC (plain)	55	90	450
EC4 and DL/T	SCC+10%MK	55	90	450
EC4 and DL/T	SFRSCC	55	90	450
EC4 and DL/T	SFRSCC+10%MK	55	90	450
EC4 and DL/T	SCC (plain)	90	90	150
EC4 and DL/T	SCC+10%MK	90	90	150
EC4 and DL/T	SFRSCC+10%MK	90	90	150
EC4 and DL/T	SFRSCC	90	90	300
EC4 and DL/T	SCC (plain)	90	90	450
EC4 and DL/T	SCC+10%MK	90	90	450
EC4 and DL/T	SFRSCC	90	90	450
EC4 and DL/T	SFRSCC+10%MK	90	90	450

5.2.2 Interaction analysis with concrete core strength

In this section the interaction between the ultimate axial capacity of Eurocode 4 and ACI, AIJ or DL/T with respect to 28 and 90 days concrete core compressive strength are graphically illustrated in Figures 5.15a and b, 5.16a and b and 5.17a and b, respectively.

Figure 5.15a and b depicts that the ratio of interaction ($N_{u,\ EC4}/N_{u,\ ACI}$) varied approximately between 1-1.3 and 1.2-1.3 for concrete tested at 28 and 90 days, respectively. In Figure 5.15b it can be seen that at the same value of steel yield strength and D/t ratio there is a tendency for reduction in the interaction action with the increase in concrete core compressive strength. For example, within CFST column having steel yield strength of 450 and D/t ratio of 25, the variation in compressive strength of concrete core of 78.6, 83.2 and 84.6 reduces interaction value slightly by 1.29, 1.26 and 1.23, respectively.

The relation between compressive strength of concrete core and ($N_{u,\ EC4}/N_{u,\ AIJ}$) indicates very low variation between the upper and lower estimated limit. Regardless the tested age, steel yield strength and D/t ratio the higher ratio has been observed for column infilled with concrete core has a 28 days compressive strength of 67.5 MPa of about 1.14, whereas the lower ratio is 1.093 resulted in CFST column has a concrete core compressive strength of 88.7 MPa. A distinguishable observation about the effect of using different steel yield strength and D/t ratio on the interaction analysis considering these two codes. Also can be reported herein that is at the same compressive strength value of concrete core and steel kind of hollow tube, the variation in D/t ratio cased to change the ration between the two codes. For example, Figure 5.16b shows that at 87.7 MPa of compressive strength and steel yield strength of 150 MPa, the D/t ratio of 25, 55 and 90 yields $N_{u,\ EC4}/N_{u,\ AIJ}$ ratio of 1.136, 1.13 and 1.127, respectively.

Finally, from relations presented in this section it can be said that the most comparable ratios have been resulted between the axial capacity computed via Eurocode 4 and DL/T, Figure 5.17a and b. The interaction between these two codes were found to be in the range of 0.968-1.079 and 0.969-1.06 with respect to 28 and 90 days.

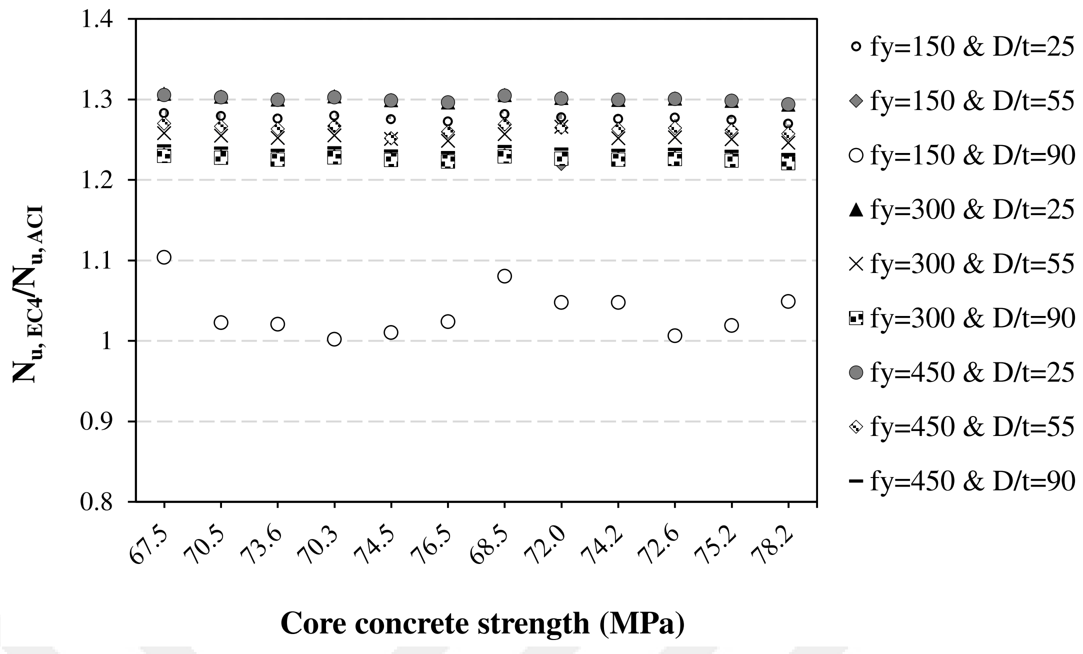

a)

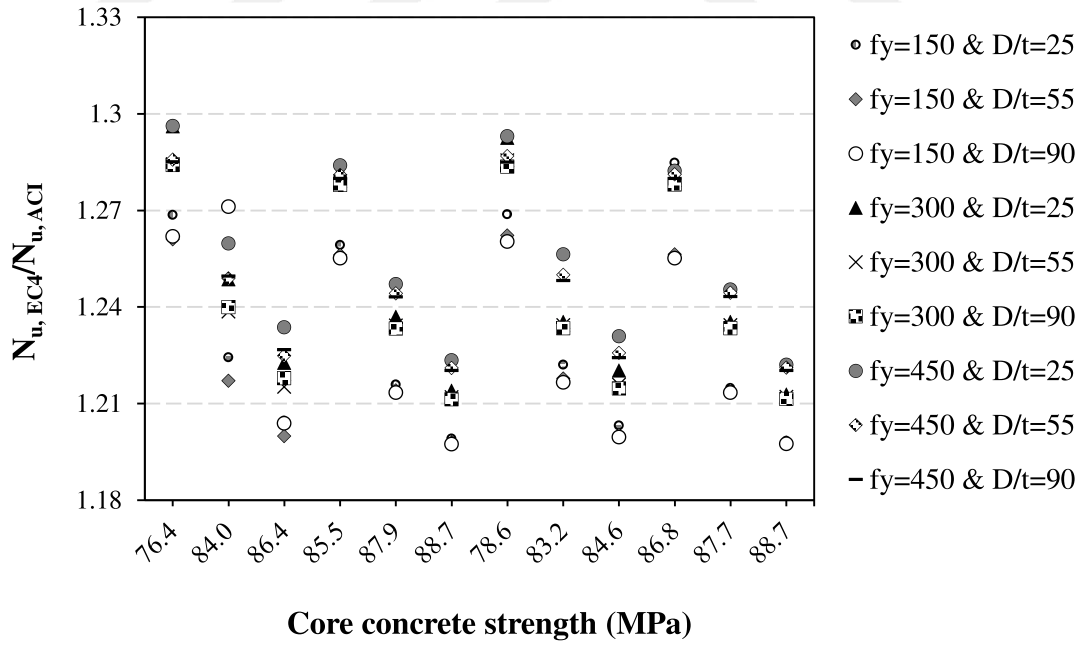

b)

Figure 5.15 Interaction between core concrete compressive strength and $N_{u, EC4}/N_{u, ACI}$:
a) 28 days and b) 90 days

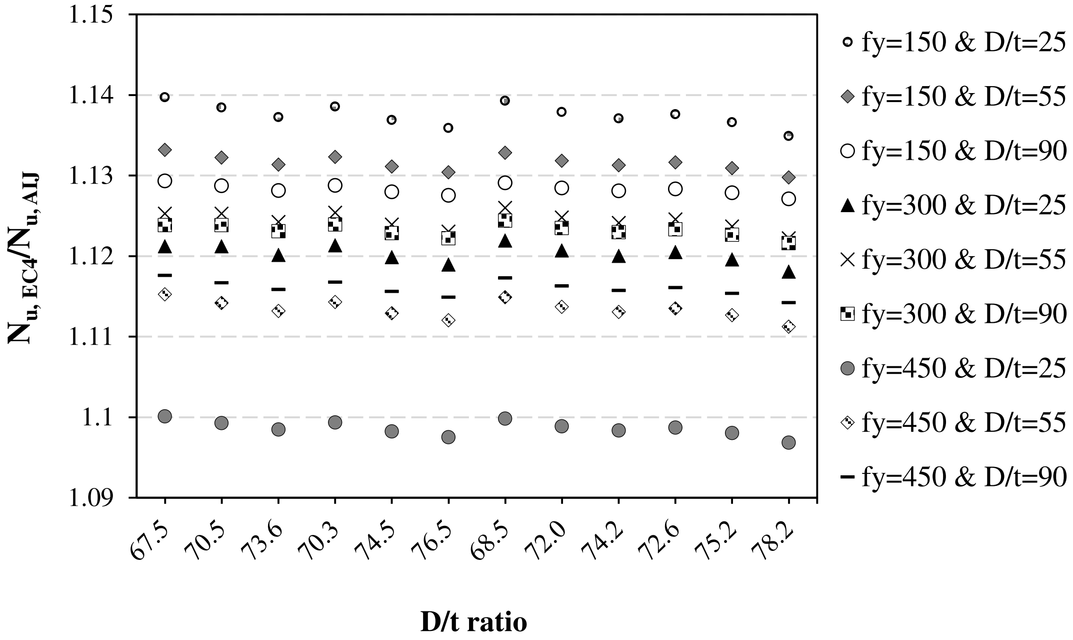

a)

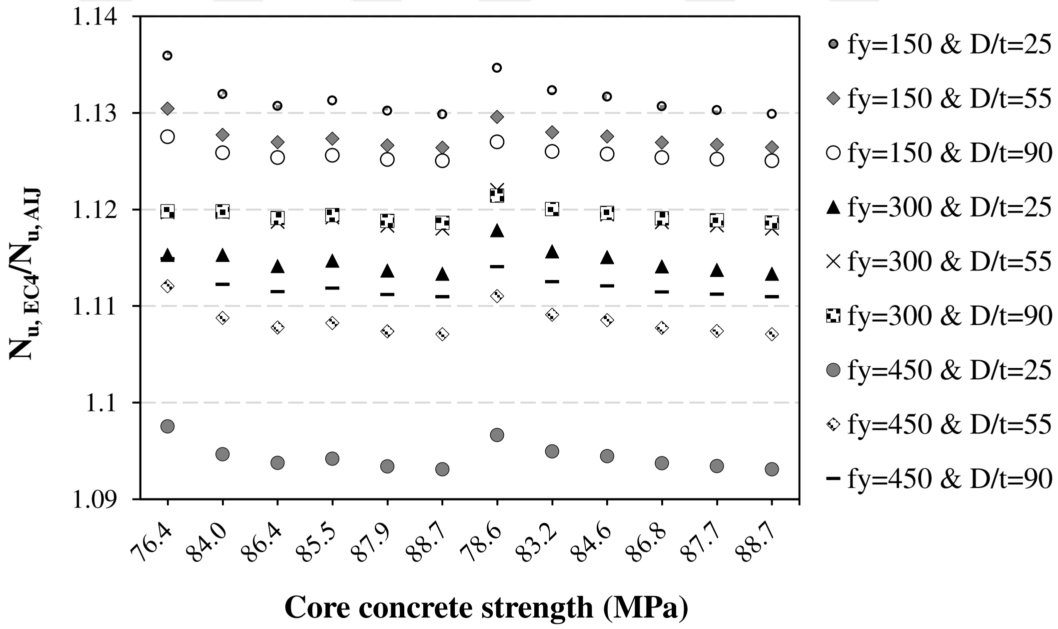

b)

Figure 5.16 Interaction between core concrete compressive strength and $N_{u, EC4}/N_{u, AIJ}$: a) 28 days and b) 90 days

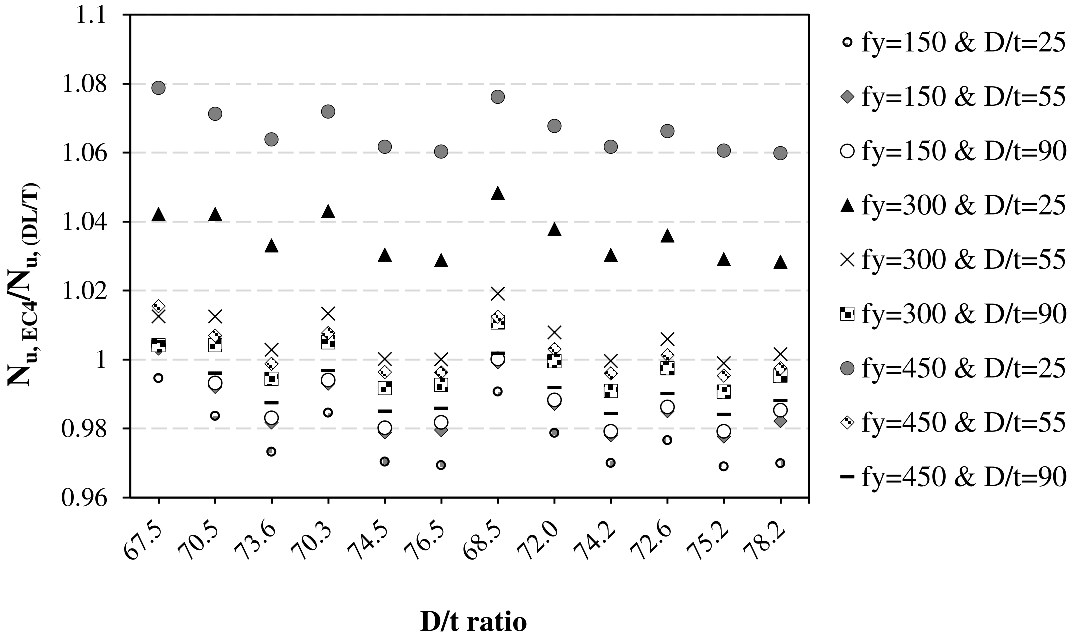

a)

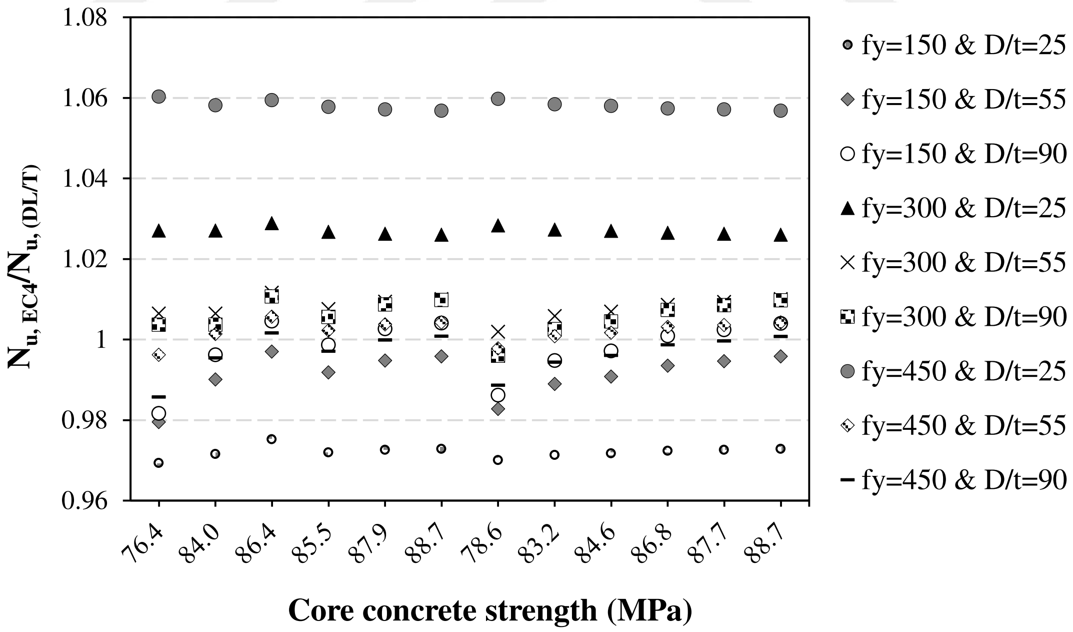

b)

Figure 5.17 Interaction between core concrete compressive strength and $N_{u, EC4}/N_{u, (DL/T)}$: a) 28 days and b) 90 days

5.3 Estimation of the overall CFST column performance

In order to estimate the structural performance of CFST short circular columns in terms of the predicted ultimate axial strength which is evaluated by the use of Eurocode 4 (2004), ACI-318R (2005), AIJ (2001) and Chinese code DL/T (1999) provisions, a comparative investigation of predictions of the evaluated data is conducted. To attain the objective of this section, three different special groups performed as follows:

A. The ultimate axial capacity of structural steel tube infilled with SCC or SFRSCC with its nS replacement level are presented in Figure 5.18 to Figure 5.21. These results regulated in such a way that the values of ultimate axial capacity of each curing period either 28 or 90 days are presented with respect to the total number of specimens. So, for each provision code two figures are performed and a total of eight figures can be found herein.
B. The ratios of $N_{u,\,EC4}$/ $N_{u,\,ACI}$, $N_{u,\,EC4}$/ $N_{u,\,AIJ}$, and $N_{u,\,EC4}$/ $N_{u,\,DL/T}$ versus the total number of CFST column specimens are shown in Figure 5.22 (a and b) to Figure 5.24 (a and b) for 28 and 90 days, respectively. For this, each mixture are presented by 27 ratios so as to comprise different D/t ratios and steel yield strengths proposed in this study.
C. The ultimate axial capacity computed by the utilize of Eurocode 4 are correlated to those resulted from ACI, AIJ and DL/T and represented in Figure 5.25, 5.26 and 5.27, respectively.

Regarding clause A, the estimation of structural performance of CFST column with respect to Eurocode 4 revealed that the axial capacity analysis of the first 36 specimens made with plain concrete were ranged from 247 to 3311 kN and from 262 to 3794 kN for samples tested at 28 and 90 days, Figure 5.18a and 5.18b, respectively. On the other side, the specimens which numbered as 37 to 72 and 73 to 108 are related to columns having concrete core made with 2% and 4% nS, respectively. Within these samples, it can be analyzed there is an increase in axial capacity due to the use of nS%, irrespective of curing period. For instance, Figure 5.18b shows the higher variation in axial capacity of about 283 to 3865 kN with respect to samples made with 4% nS (numbered as 73 to 108). However, for the other used codes similar trends can be observed. Ma and Wang (2012) reported nowadays the structures of CFST column are made with concrete incorporates supplementary cementitious materials (SCM) to improve the strength of concrete core, hence attaining better performance. CFST structural columns prepared in such a way can be considered as high strength concrete filled steel tube columns.

As presented above, figures of clause B represented the overall relation between axial capacity values in terms of the utilized codes. In general, one can easy to say there are slight differences due to the use of various international provision codes. The reason may be due to the presence of randomness concrete strength, different steel grade and various diameter to thickness ratio. However, the higher ratio can be found between Eurocode and ACI results, Figure 5.22a and b, whilst the lower ratio was observed between Eurocode and DL/T, Figure 5.24a and b. This behavior agrees well with Lu and Zhao (2010) on the relation between the Chinese code DL/T (1999) and ACI-318R (2005). They stated although the confinement effect is considered in the Chinese code DL/T (1999) formulas, it provided lesser predictions than those of ACI-318R (2005) for some specimens, particularly with very high-strength steel tube, which seems to be a deficiency of this code.

To investigate the relationship between axil capacities of CFST column, the regression analysis of data obtained by Eurocode 4, ACI, AIJ and DL/T are shown in Figure 5.25 to 5.27. It can be observed that there were considerably high relationship between the predicted values of Eurocode 4 (2004) and ACI-318R (2005), Eurocode 4 (2004) and AIJ (2001), and Eurocode 4 (2004) and Chinese code DL/T (1999), Figure 5.25a and b, Figure 5.26a and b and Figure 5.27a and b, respectively, so that a regression analysis provided correlation coefficient (R^2) of 0.99 for all codes and ages. Within the predicted axial capacity results by using the different provisions of this study, all models appeared to be well close to each other and provided higher prediction.

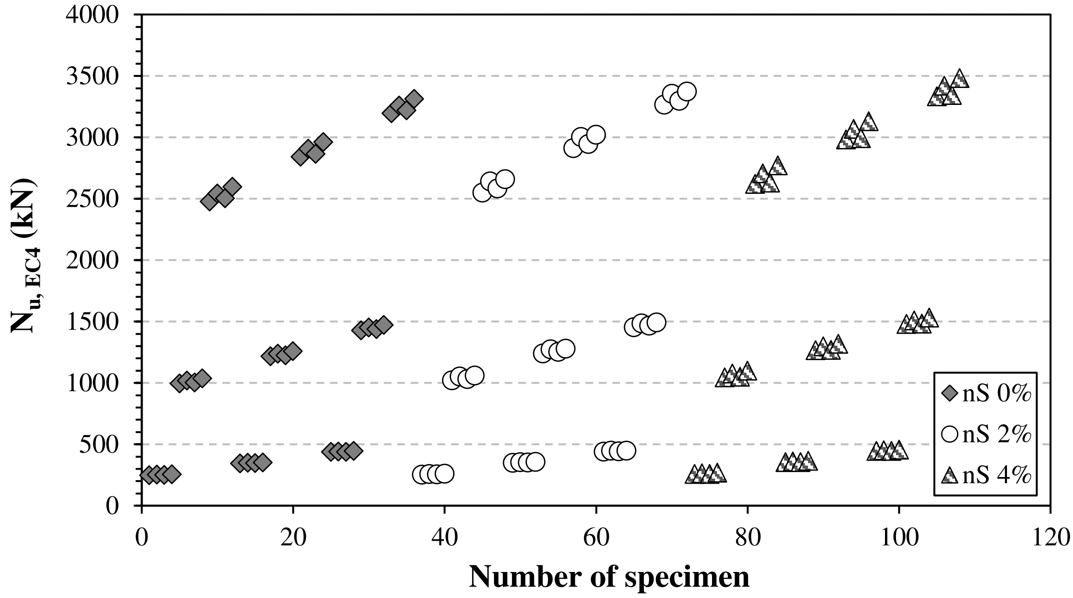

a)

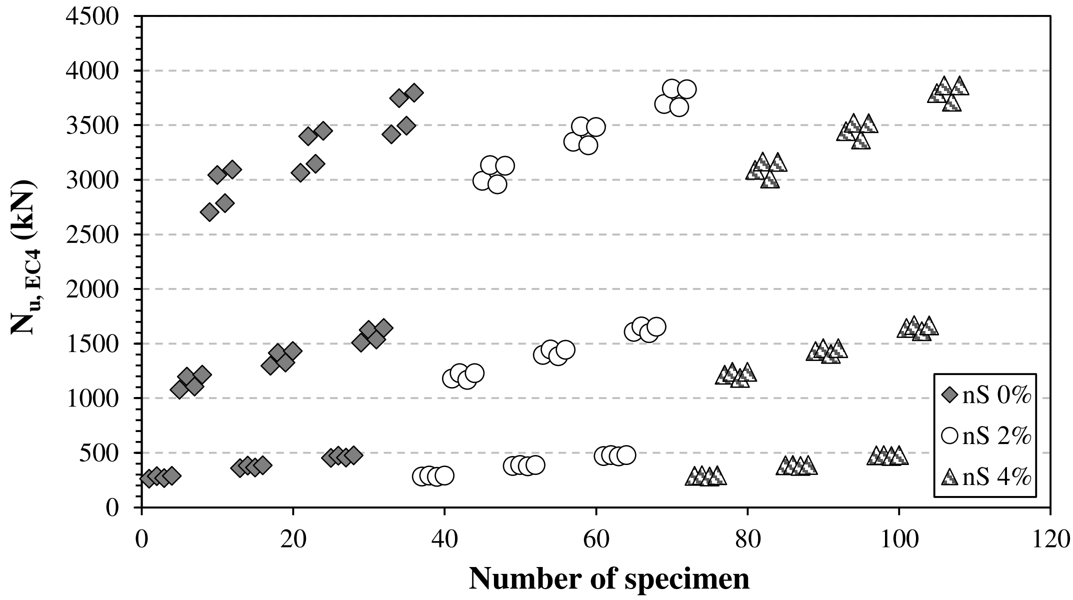

b)

Figure 5.18 Overall tendency of the capacity of the composite column having SFRSCC based on Eurocode 4: a) 28 days and b) 90 days

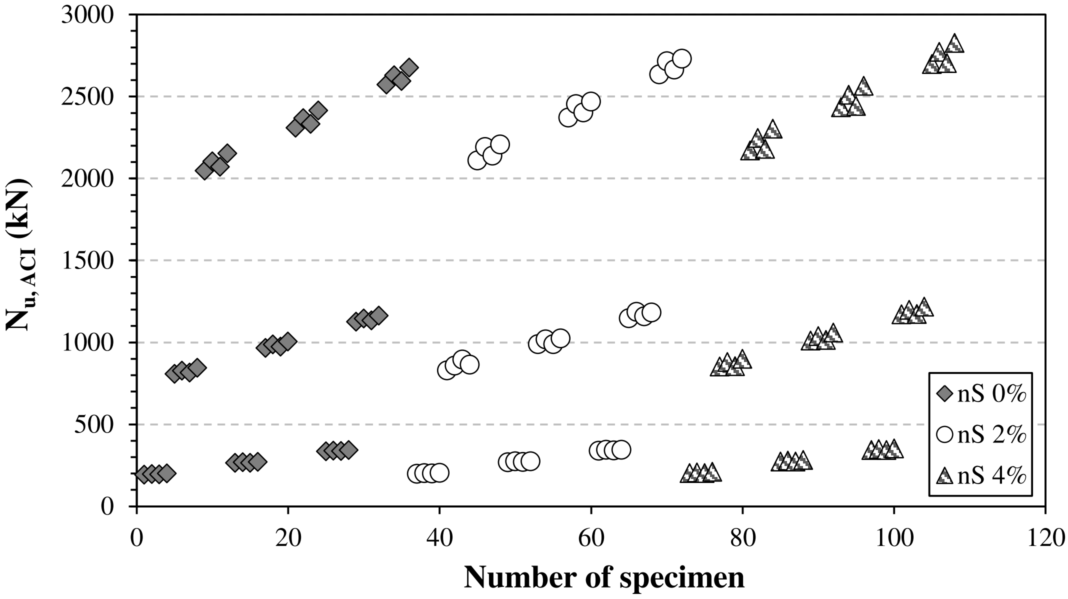

a)

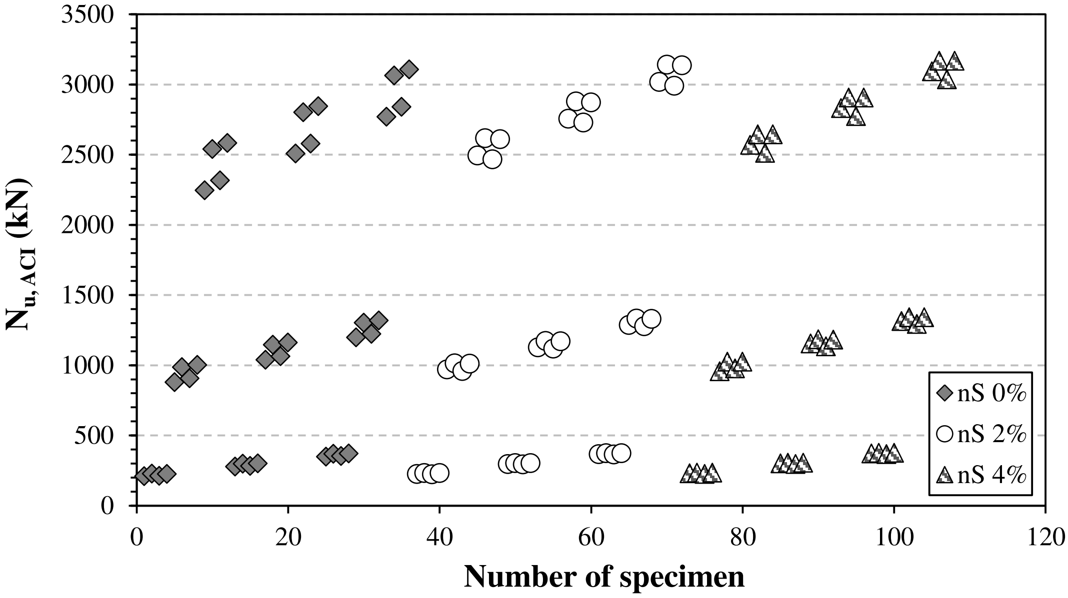

b)

Figure 5.19 Overall tendency of the capacity of the composite column having SFRSCC based on ACI 318: a) 28 days and b) 90 days

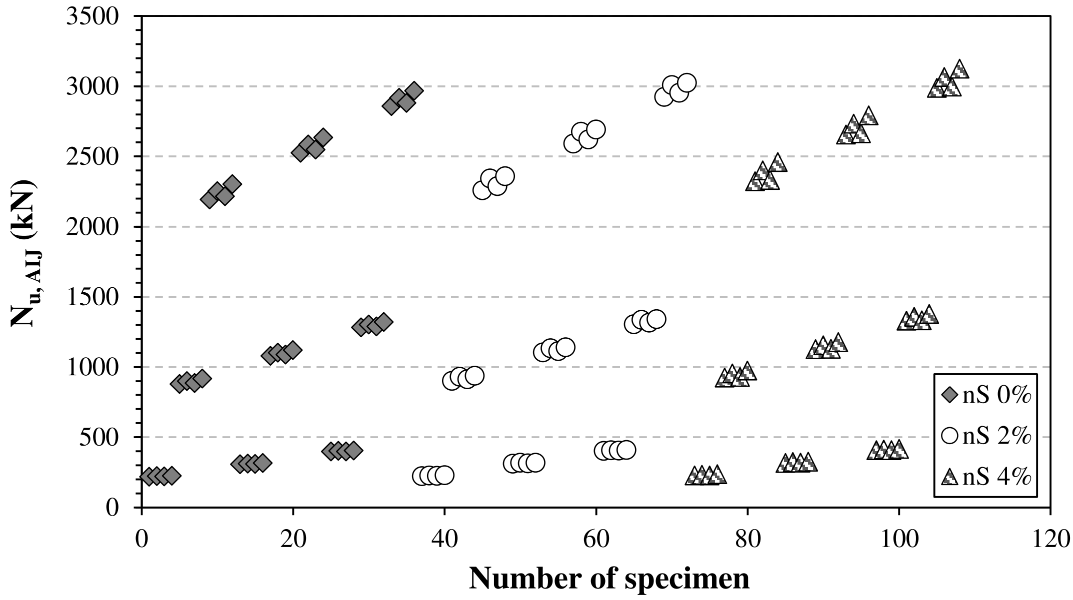

a)

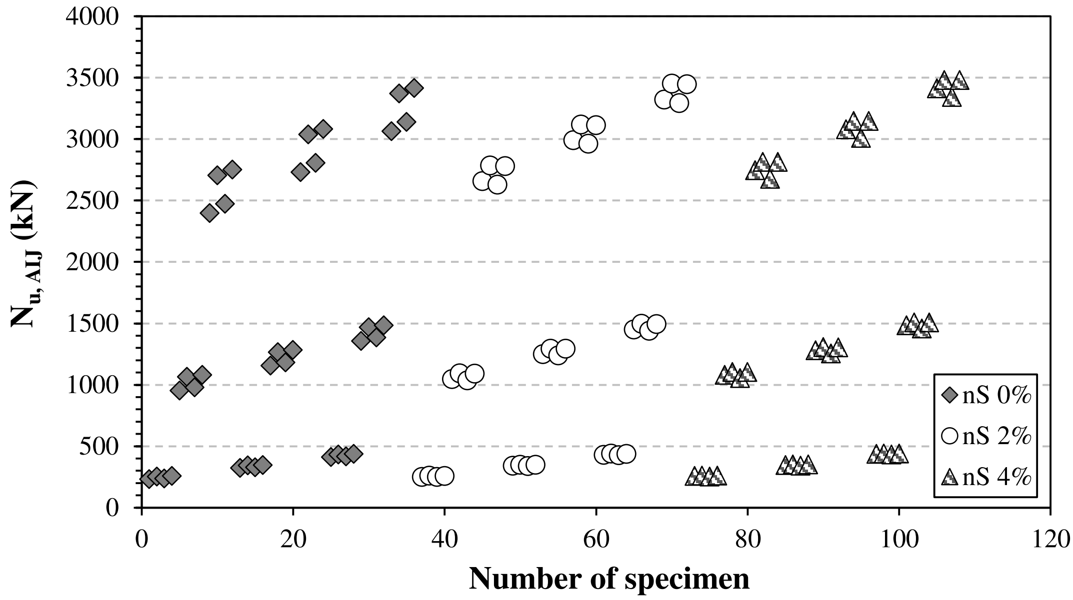

b)

Figure 5.20 Overall tendency of the capacity of the composite column having SFRSCC based on ACI 318: a) 28 days and b) 90 days

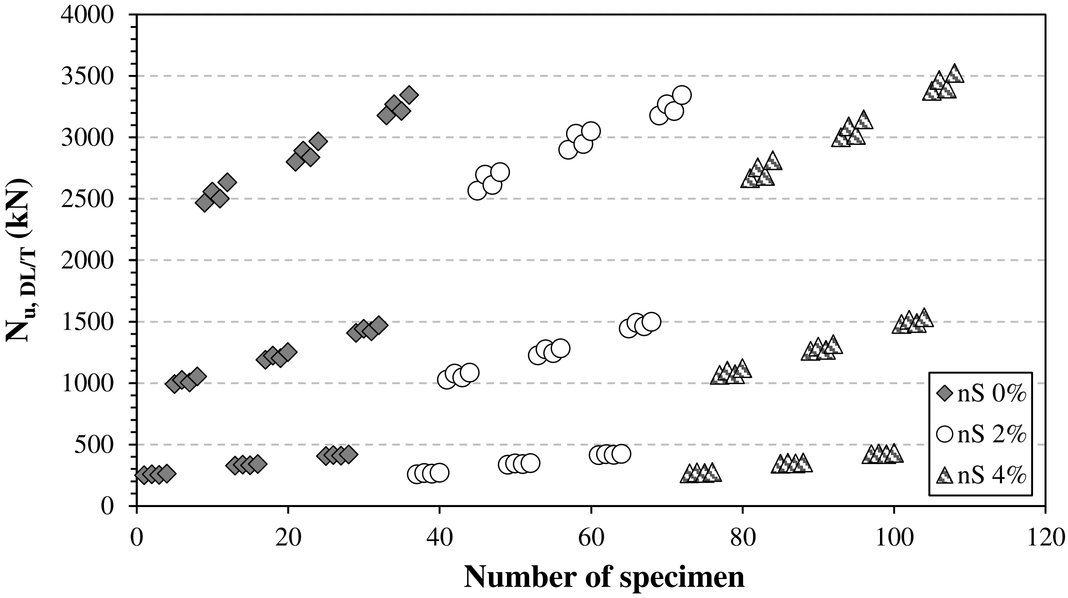

a)

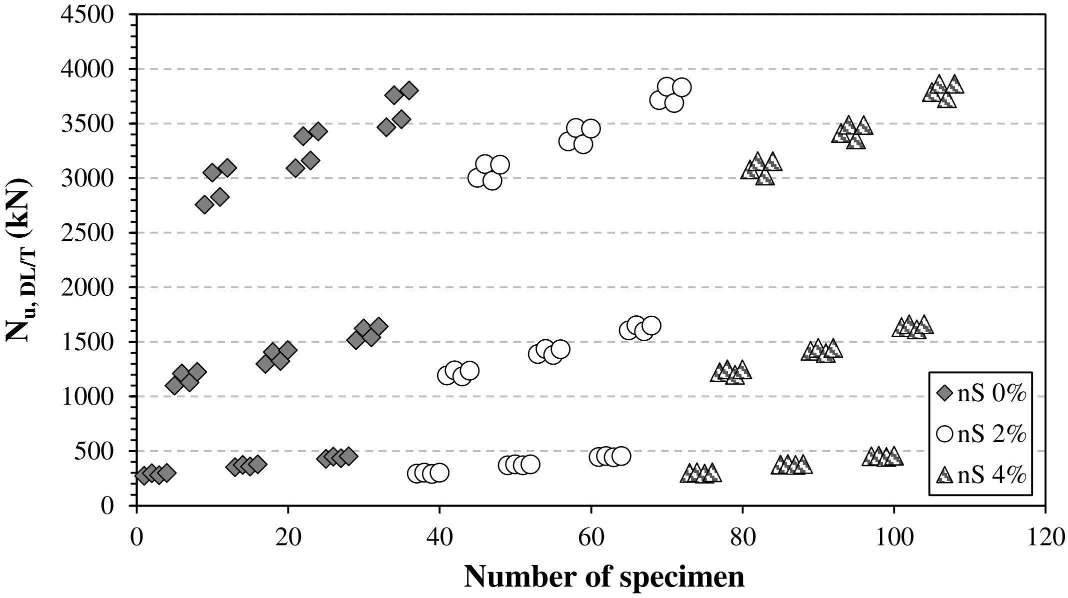

b)

Figure 5.21 Overall tendency of the capacity of the composite column having SFRSCC based on DL/T: a) 28 days and b) 90 days

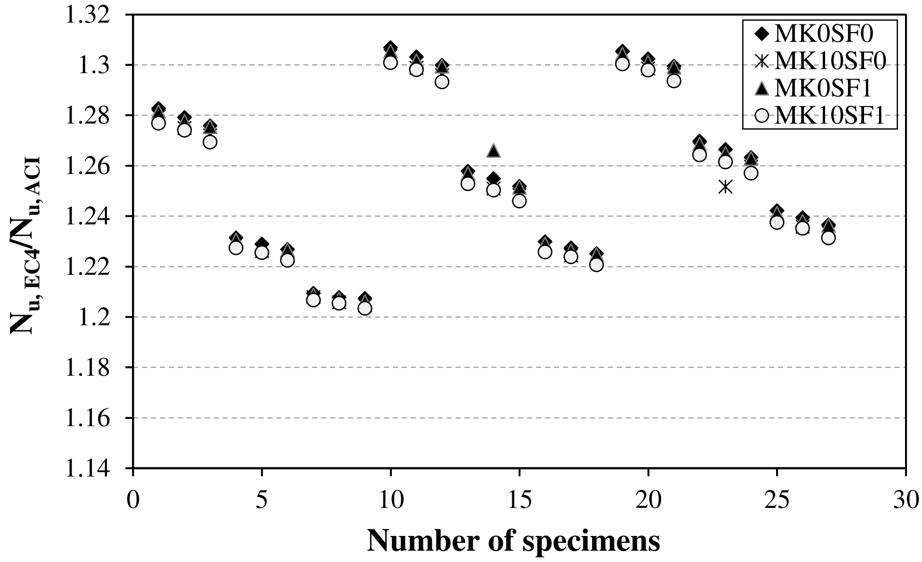

a)

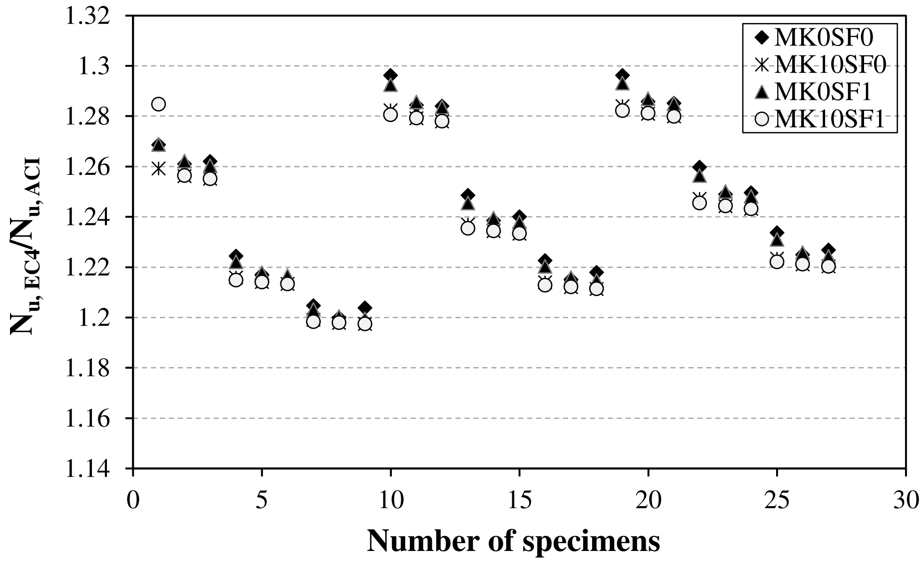

b)

Figure 5.22 Ratio of axial capacity results by using Eurocode 4 and ACI 318 provisions for SFRSCC: a) for 28 days and b) for 90 days

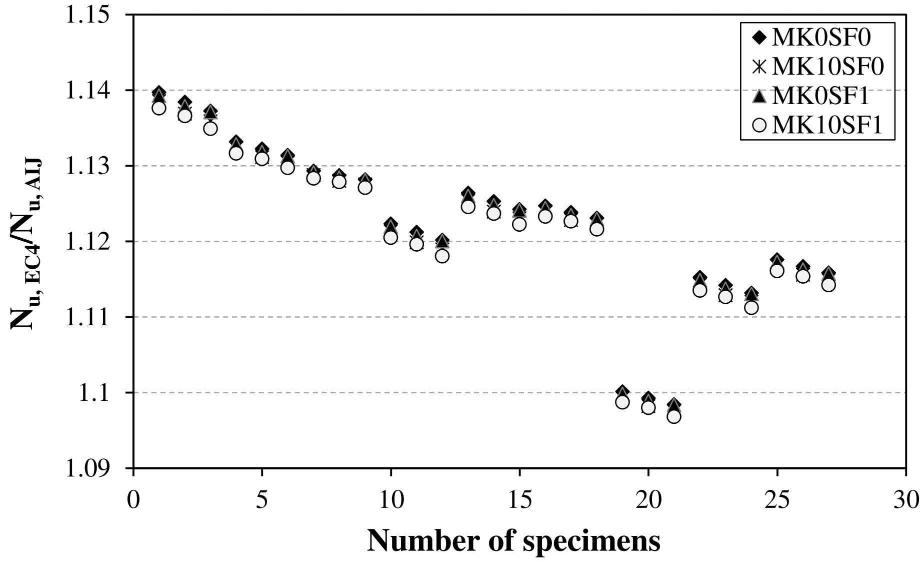

a)

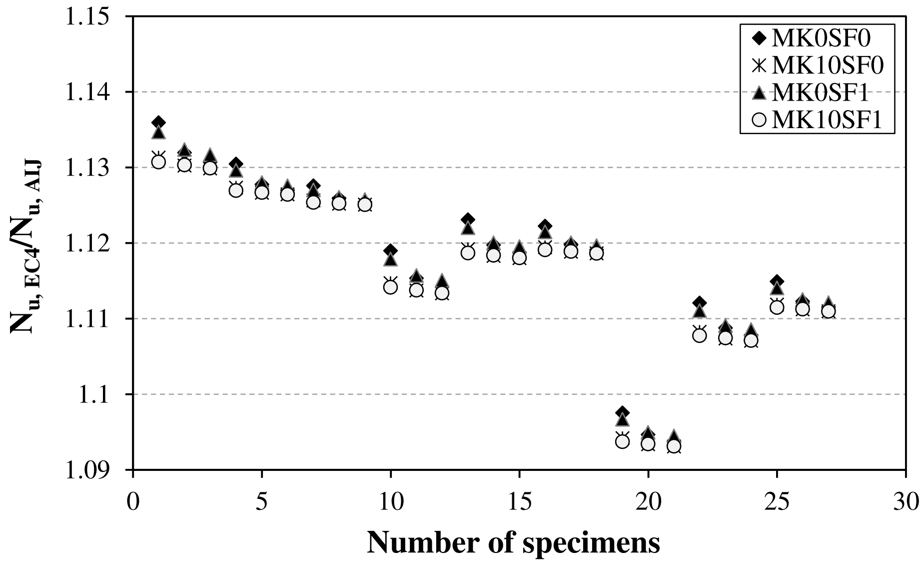

b)

Figure 5.23 Ratio of predicted axial capacity results by using Eurocode 4 and AIJ provisions for different SFRSCC: a) for 28 days and b) for 90 days

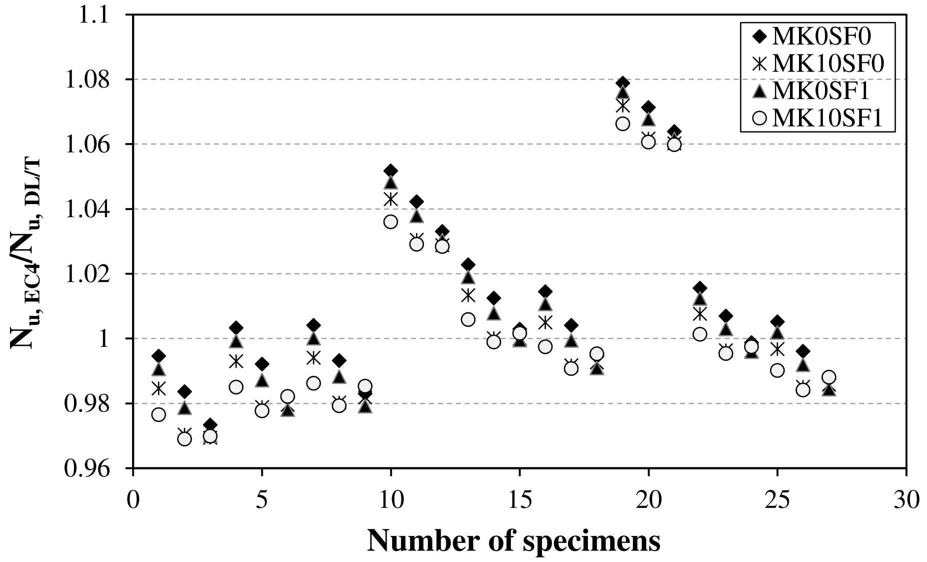

a)

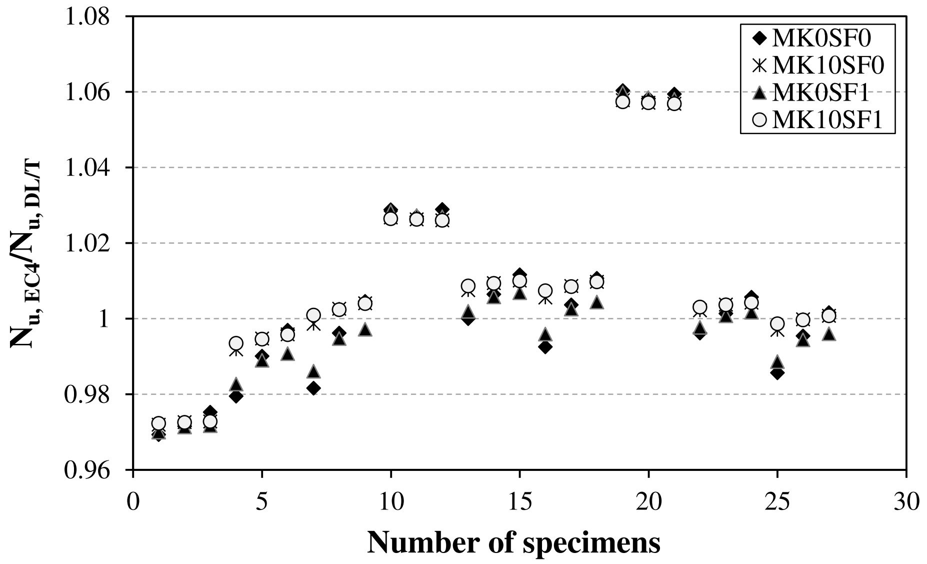

b)

Figure 5.24 Ratio of predicted axial capacity results by using Eurocode 4 and DL/T provisions for different SFRSCC: a) for 28 days and b) for 90 days

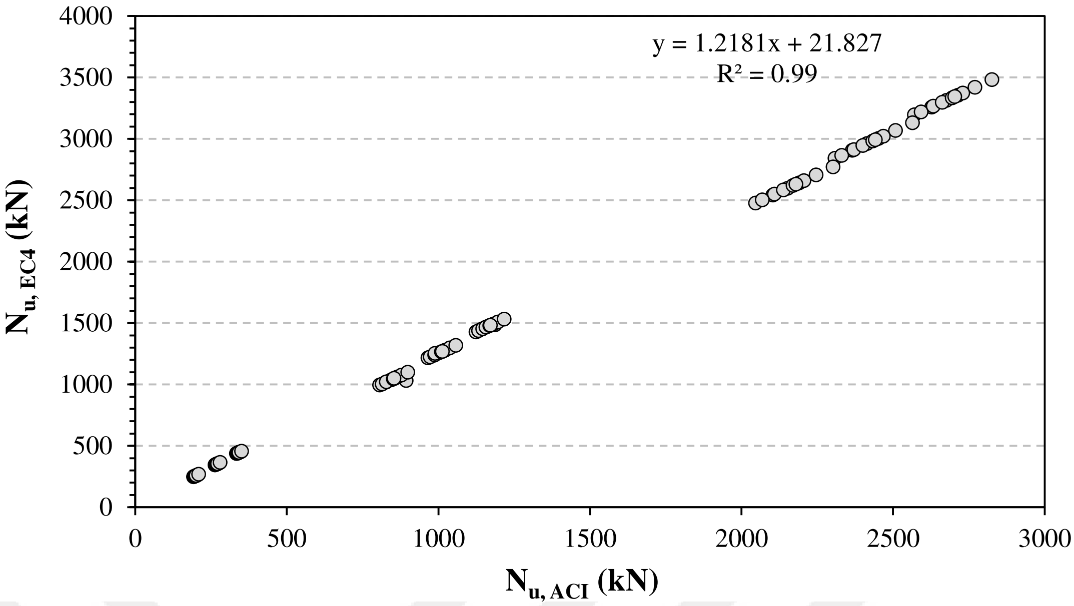

a)

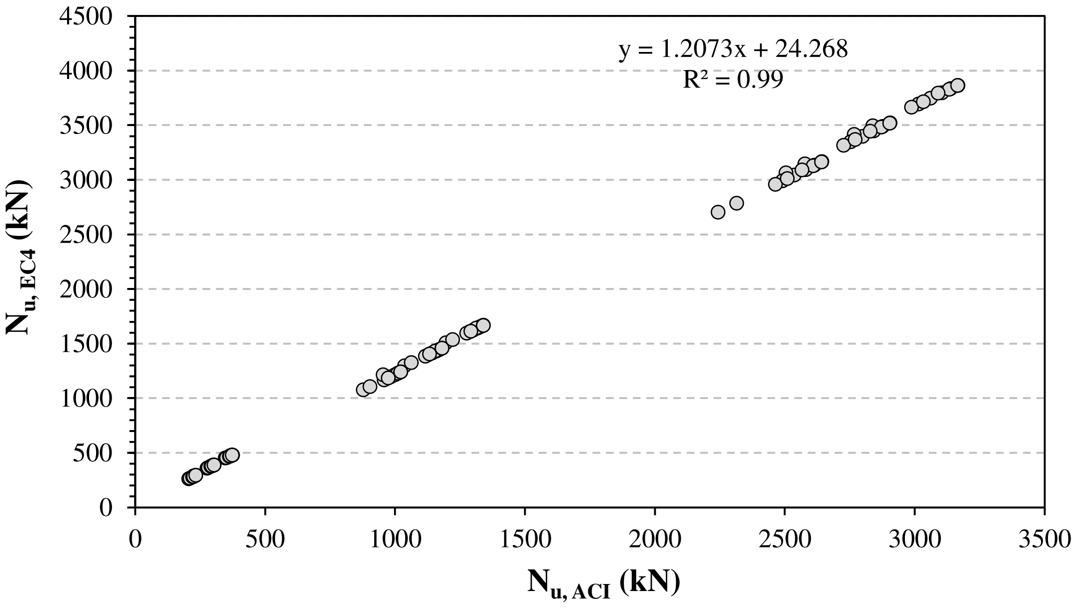

b)

Figure 5.25 Eurocode 4 and ACI regression model of predicted axial capacities of the composite columns: a) for 28 days and b) for 90 days

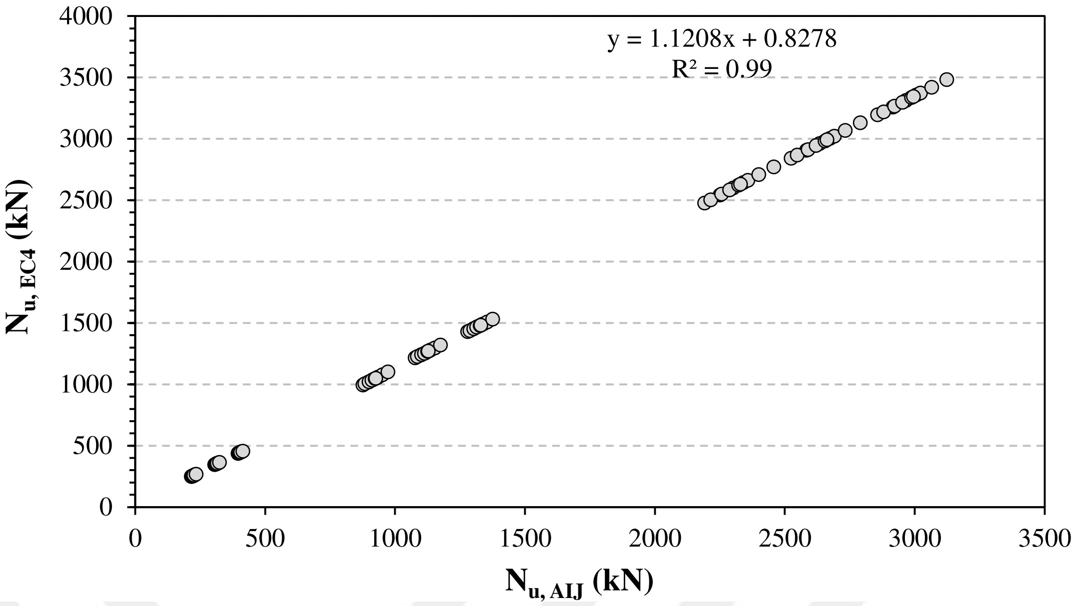

a)

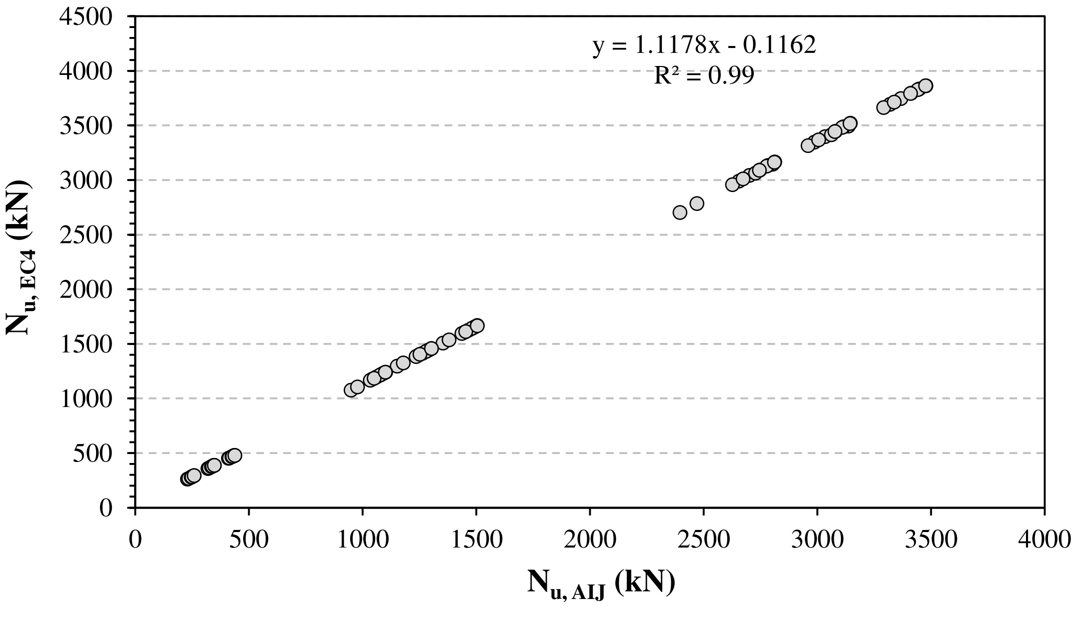

b)

Figure 5.26 Eurocode 4 and AIJ regression model of predicted axial capacities of the composite columns: a) for 28 days and b) for 90 days

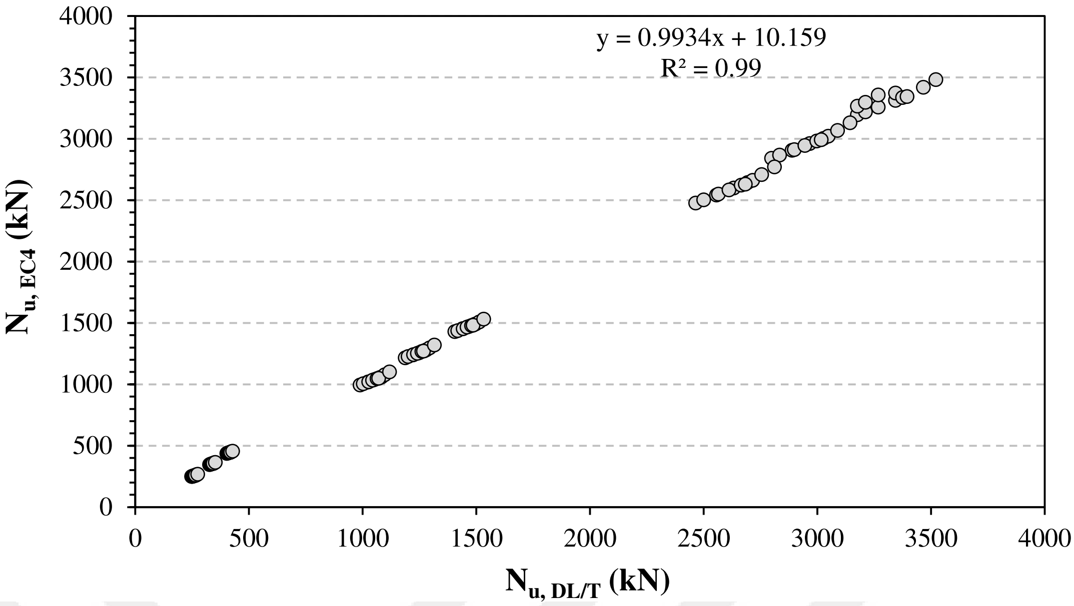

a)

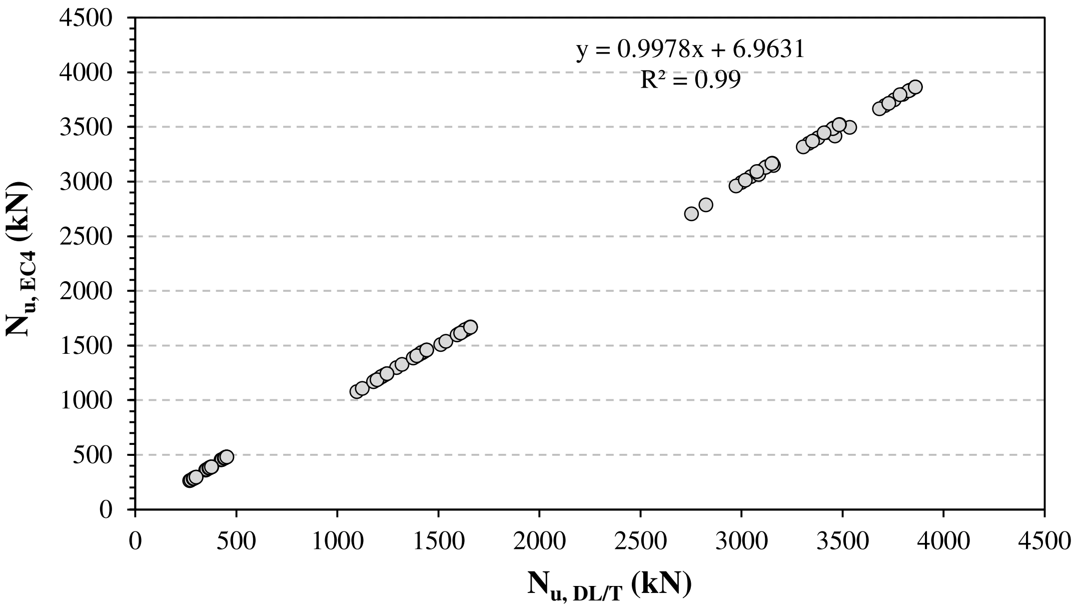

b)

Figure 5.27 Eurocode 4 and DL/T regression model of predicted axial capacities of the composite columns: a) for 28 days and b) for 90 days

CHAPTER 6

CONCLUSIONS

In the first part of the thesis, the fresh and mechanical performance of steel fiber reinforced self-compacting concrete (SFRSCC) were examined. In order to specify the flowability, viscosity and passing ability of the manufactured SFRSCC, slump flow diameter, T_{50} slump flow time, V-funnel flow time, L-box height ratio and L-box T_{20} and T_{40} flow times were measured as fresh properties. Additionally, mechanical properties was depicted by compressive strength, splitting tensile strength, modulus of elasticity, bond strength, net flexural strength, and fracture energy. In the second part of the thesis, the axial compressive behavior of SFRSCC filled steel tube columns having different diameter to thickness ratio and steel yield strengths have been analytically investigated by using Eurocode 4 (EC4), American code (ACI), Japanese code (AIJ) and Chinese design code (DL/T). Based on the comprehensive experimental program and the analytical study presented in this thesis, the following conclusions can be listed:

- The slump flow diameters ranging from 630 to 750 mm were obtained for the self-compacting concrete (SCC). Except for the mixtures coded nS4MK0SF1 and nS4MK10SF1, all the mixtures were in the SF2 class. Although increasing the nano silica (nS) content, regardless the concrete group, resulted in reducing the flow diameters. The results were acceptable for the many normal structural applications as per EFNARC (2005). The slump flow diameters of mixtures produced with 1% steel fiber was less than that of produced with no steel fiber. Mixture coded nS4MK10SF1 demonstrated the smallest flow diameter.
- Using nS or/and metakaolin (MK) with cement increased both T_{50} slump flow and V-funnel flow times. Additionally, replacing the steel fiber by volume of mixture so increased it. All mixtures can be categorized as VS2/VF2 viscosity class.

- The L-box height ratio was also affected by nS and MK. Increasing their contents caused systematical decreasing the ratio. However, all the mixtures had the height ratio more than 0.8 which is the lower limit determined by EFNARC (2005). Moreover, using these materials caused increasing of the L-box T_{20} and T_{40} flow times and replacement of mixture volume by 1% steel fiber caused increasing of flow times and decreasing of the height ratio.
- The compressive strength results indicated that the utilization of nS, MK and steel fiber (singly, binary and ternary) in concrete manufacturing resulted in increasing of the compressive strength.
- The lowest splitting tensile strength result was obtained from control mixture, and the incorporation of steel fiber significantly increased the 28 and 90 day tensile strength. The results indicated that the concrete produced with (4% nS, 10% MK and 1% steel fiber) together gave the highest tensile strength.
- The static elastic modulus increased in a fashion similar to that observed in compressive strengths. Their results indicated that the concretes produced with (4%nS, 10%MK and 1%SF) together gave the highest elastic modulus, those control mixture gave the lowest modulus.
- It was observed that the bond strength improved with increasing nS, MK and steel fiber content. The development of bond strength with binary blends was higher than that in the case of control mixture. Additionally, the mixture of ternary blends gave further improvement than that of control or binary system.
- The results obtained showed that the net flexural strength enhanced with using of nS, MK and steel fiber compared to the control mixture. Therefore, the net flexural strength of control mix is the lowest value while the mixture coded nS4MK10SF1 gave the highest net flexural strength.
- The lowest fracture energy (G_f) result was obtained from control mixture, and the systematical increasing was observed as nS content increased, regardless to MK utilization. The highest G_f value was obtained when the cement was replaced with (4% nS mixed 10% MK). The most efficient results for utilization of steel fiber was obtained from the fracture energy.
- The use of SFRSCC incorporating MK and/or nS to infill steel tubular yielded in an enhancement in the structural performance of composite

circular short columns compared to those made with SCC. The highest ultimate axial capacity values were predicted as 3863, 3166, 3478 and 3861 kN for CFST column of SFRSCC made with 10% MK and 4% nS computed via Eurocode 4 (2004), ACI 318R (2005), AIJ (2001) and DL/T (1999), respectively. Increasing period of curing upgraded the predicted resistance of CFST column under axial compression.

- The ultimate axial capacity of CFST columns were remarkably influenced by using different diameter to thickness (D/t) ratios and steel yield strengths. The use of D/t ratio of 90 and steel yield strength of 450 MPa recorded the higher axial capacity in this study, whilst the lower value of D/t ratio and yield strength of steel significantly reduced the axial capacity to its lesser limit.
- The use of different methods in the evaluated of ultimate axial capacity of CFST short circular column can be utilized to provide comparable results. The comparisons between the interaction ratios were found to be in the range of 1-1.3, 1.1-1.14 and 0.98-1.08 for the ratio computed between Eurocode 4 and ACI, Eurocode 4 and AIJ and Eurocode and DL/T, respectively. Moreover, the contribution of various parameters such as; SF, MK, nS, D/t ratio and steel grade can be used to optimize interaction response.
- In this thesis, the interaction between strength of concrete core and computed relative ultimate axial capacity (relative axial capacity is the ratio of Eurocode 4 value to ACI, AIJ or DL/T value) revealed the intensity of variation of relative axial capacity reduces with increasing SFRSCC core of composite column. The most comparable ratios have been resulted between the axial capacity computed via Eurocode 4 and DL/T.
- The key regression equations between Eurocode 4 and the others (ACI, AIJ and DL/T) are also performed at curing periods of 28 and 90 days to examine the relationship between them. Even though each design code used different parameters and followed different ways to calculate the capacity of the columns under axial compression, linear regression models with significantly high coefficient were observed between them in the current study.

REFERENCES

Abedi, K. (2008). A novel steel section for concrete-filled tubular columns. *Thin-Walled Structures*. **46**, 310-319.

Abu-Lebdeh, T., Hamoush, S., Heard, W., Zornig, B (2011). Effect of matrix strength on pullout behavior of steel fiber reinforced very-high strength concrete composites. *Construction Building Materials*. **25**,39–46.

ACI 544.1R. American Concrete Institute. (1996). State-of-the-art report on fiber reinforced concrete. Farmington Hills, Michigan, USA.

ACI Committee 408. American Concrete Institute. (2003). Bond and development of straight reinforcing bars in tension (ACI408-03). Farmington Hilss, Minchigan, USA, 49 p.

ACI Committee 544. (1996). State-of-the-Art Report on Fiber Reinforced Concrete. *AmericanConcrete Institute*.

ACI. American Concrete Institute. (2005). Building code requirements for structural concrete and commentary. *Manual of Concrete Practice*. ACI committee 318R, Farmington Hills, Michigan, U.S.A.

Ahin. Y.S., Köksal. F (2011). The influences of matrix and steel fiber tensile strengths on the fracture energy of high-strength concrete. *Construction and Building Materials*. **25**, 1801-1806.

AIJ. Standards for structural calculation of steel reinforced concrete structures. (2001). 5th edition. *Architectural Institute of Japan.* Tokyo, Japan (in Japanese).

AISC. American Institute of Steel Construction. (1999). Load and resistance factor design (LRFD) specification for structural steel buildings. Chicago, USA.

Akçay, B., (2007). Effects of Lightweight Aggregates on Autogenous Deformation and Fracture of High Performance Concrete. PhD Thesis. Istanbul, Istanbul Technical University.

Akcay, B., Tasdemir, M. A. (2012). Mechanical behaviour and fiber dispersion of hybrid steel fiber reinforced self-compacting concrete. *Construction and Building Materials.* **28**, 287–293.

Altoubat, S.A., and Lange, D.A. (2001). Creep, Shrinkage, and Cracking of Restrained Concrete at Early Age. *ACI Materials Journal*. American Concrete Institute, Farmington Hills, Michigan, 323-331.

Aslani, F., Uy, B., Hur, J., Carino, P. (2017). Behaviour and design of hollow and concrete-filled spiral welded steel tube columns subjected to axial compression. *Journal of Constructional Steel Research*. **128**, 261-288.

ASTM C 618-08 (2002). Standard Specification for Coal Fly Ash and Raw or Calcined Natural Pozzolan for use as a Mineral Admixture in Concrete. West Conshohocken, PA, Annual Book of ASTM Standard.

ASTM C39 (2012). American Society for Testing and Materials.Standard Test Method for Compressive Strength of Cylindrical Concrete Specimens, Annual Book of ASTM Standard. Philadelphia, Vol. **04**-02, 7 pages.

ASTM C469 (2010). American Society for Testing and Materials. 2010. Standard Test Method for Static Modulus of Elasticity and Poisson's Ratio of Concrete in Compression. Annual Book of ASTM Standard. Vol. **04**.02, 5 pages.

ASTM C496 (2011). American Society for Testing and Materials. Standard Test Method for Splitting Tensile Strength of Cylindrical Concrete Specimens, Annual Book of ASTM Standard. Philadelphia. Vol. **04**-02, 5 pages.

ASTM. American Society for Testing and Materials. (2011). Standard Specification for Steel Fibers for Fiber-Reinforced Concrete. ASTM A820. http://enterprise1.astm.org/DOWNLOAD/A820.1181661-1.pdf.

Badogiannis, E., Kakali, G., Tsivilis, S. (2005). Metakaolin as a supplementary cementitious material; optimization of kaolin to metakaolin conversion. *J of Ther Anal and Cal*, **81**, 457–62.

Bahadori, H., Hosseini, P. (2012). Reduction of cement consumption by the aid of silica nano-particles (investigation on concrete properties). *Journal of Civil Engineering and Management*. **18**:416-425.

Balaguru, P., Narahari, R., Patel, M. (1992). Flexural toughness of steel fibre reinforced concrete. *ACI Materials Journal*, **89**, 541-546.

Balaguru, P., Shah, S. (1992). Fiber Reinforced Cement Composites. *McGraw-Hill Inc*.

Banthia. N., Sappakittipakorn. M (2007). Toughness enhancement in steel fiber reinforced concrete through fiber hybridization. *Cement and Concrete Research*. **37**, 1366-1372.

Baran, E., Akis, T., Yesilmen, S (2012). Pull-out behavior of prestressing strands in steel fiber reinforced concrete. *Construction and Building Materials*.**28**,362-71.

Barnes, A. J. (2007). Uniaxial Compression and Flexural Behavior of High Performance Cementitious Composites (HPFRCC) "A Master thesis". University of Wisconsin.

Barnes, P., Bensted, J., Jones, T.R. (2003). Structure and performance of cements. 2nd edition. Metakaolin as pozzolanic addition to concrete. England. p. 372–98.

Barros, JAO., SenaCruz JM. (2011). Fracture energy of steel fibre reinforced concrete. *J Mech Compos Mater Struct*, **8**, 29–45.

Bayramov, F., Taşdemir, C., and Taşdemir, M.A. (2004). Optimisation of steel fibre reinforced concretes by means of statistical response surface method. *Cement and Concrete Compositess*, **26**, 665-675.

Bažant, Z.P. (1984). Size Effect in Blunt Fracture- Concrete, Rock, Metal, *ASCE Engineering Mechanics,* **110**, 518-535.

Bažant, Z.P. and Oh, B.H. (1983). Crack band theory for fracture of concrete, M*aterials and Structures,***16**, 155-157.

Beigi, M H., Berenjian, J., Omran, O L., Nik,A S., Nikbin, I M. An experimental survey on combined effects of fibers and nano silica on the mechanical, rheological, and durability properties of self-compacting concrete. *Materials and Design*, **50**, 1019–1029.

Benaicha, M., Jalbaud, O., Hafidi, A.A., Burtschell, Y. (2013). Rheological and Mechanical Characterization of Fiber-Reinforced Self-Compacting Concrete. *International Journal of Engineering and Innovative Technology*. **2**, 151-159.

Bernard. E (2001). Correlations in the behaviour of fibre reinforced shotcrete beam and panel specimens. *Material and Structure*. **35**, 156-164.

Bosfa. Dramix steel fiber seller. http://www.bosfa.com/docs/RC-80_60-BN_groen_GB.pdf. 16/12/2012.

Bosiljkov, V B (2003). SCC mixes with poorly graded aggregate and high volume of limestone filler. *Cement Concrete Research*. **33**,1279–86.

Buratti. N., Mazzotti. C., Savoia. M (2011). Post-cracking behaviour of steel and macrosynthetic fibre-reinforced concretes. *Construction and Building Materials*. **25**, 2713-2722.

Caldarone, M.A., Gruber, K.A., Burg, R.G. (1994). High-reactivity metakaolin: a new generation mineral admixture. *Concrete Internationa*, **16**, 37–40.

Cattaneo, S., Giussani, F., Mola, F. (2012). Flexural behaviour of reinforced, prestressed and composite self-consolidating concrete beams. *Construction and Building Materials*. **36(1)**, 826-837.

Chang, X., Lei, F., Zhao H.B., Zhang, Y.B. (2013). Behaviors of axially loaded circular concrete-filled steel tube (cft) stub columns with notch in steel tubes. *Thin-Walled Structures*. **73**, 273-280.

Chanrakantu., Mehetre, P. Urade, S., Mahure.,Ravi, K (2014). Comparative study of properties of self compacting concrete with metakaolin and cement kiln dust as mineral admixtures. *Impact: International Journal of Research in Engineering & Technology* (IMPACT: IJRET). **2**, 37-52.

Chen, W.F. (1997). Handbook of structural engineering. CRC Press LLC, USA.

Choudhary, C. (2017). Composite Construction of Buildings – Composite Beams. http://civildigital.com/composite-construction-buildings-composite-beams/.

Chu, K. (2014). Axial load behaviour of steel tube columns in-filled with various high-performance concretes. *MSc Thesis*. Ryerson University, Toronto, Ontario, Canada.

Collings, D. (2008). Composite construction. *ICE Manual of Bridge Engineering*. doi: 10.1680/mobe.34525.0283. 283-304.

Cracknell, D.W. (1963). The Runnymede bridge. *Proceedings of the ICE.* **25(3)**; 325-344.

Craig, R. J (1984). Structural applications of reinforced steel fibrous concrete. *Concrete International. Design and Construction*. **6**, 28-32.

Crisinel, M, & Marimon, F (2004). A new simplified method for the design of composite slabs. Journal of Constructional Steel Research, 60, 481-491.

Cui, Z.Q., Han, L.H., Song, T.Y. (2013). Behavior of concrete filled steel tubular (CFST) triple-limb laced columns subjected to ISO 834 Standard Fire. The 2013 world congress on Advances in Structural Engineering and Mechanics (ASEM13), Jeju, Korea, 2608-2618.

Dehn F., Holschemacher K., and Weibe D. (2000). Self-Compacting Concrete (SCC)¾ Time Development of the Material Properties and the Bond Behaviour. *LACER* No 5, pp 115-124.

Deutscher Ausschuß für Stahlbeton (DAfStb): Richtlinie Stahlfaserbeton (German Committee for Structural Concrete DAfStb guideline steel fibre concrete), Edition 2010.

Ding, F-X., Yu, Z-W., Bai, Y., Gong, Y-Z. (2011). Elasto-plastic analysis of circular concrete filled steel tube stub columns. *Journal of Constructional Steel Research*. **67,** 1567-1577.

DL/T. Chinese design code for steel-concrete composite structures. (1999). In: DL/T 5085-1999. *Chinese Electricity Press*. Beijing, China (in Chinese).

Duan, K., Hu, X.Z., Wittmann, F.H. (2003). Boundary effect on concrete fracture and non-constant fracture energy distribution. *Engineering Fracture Mechanics,* **70**, 2257-2268.

Dugdale, D.S. (1959). Yielding of steel sheets containing slits. *Journal of the Mechanics and Physics of Solids,* **8**, 100-104.

Dvorkin, L., Dvorkin, O. Basics of concrete science. <http://www.scribd.com/doc/ 6004561/Basics-of-Concrete-Science> [accessed 20.01.11].

EFNARC (2005). Specification and guidelines for self compacting concrete. May2005. Free pdf copy downloadable from http://www.efnarc.org

eHow. How to videos, articles and more. (2012). Uses of steel fiber reinforced concrete. http://www.ehow.com/about_5542383_uses-steel-fiber-reinforced-concrete. html#ixzz2FO8dVzEx. 28/11/2012.

El-Deib. A.S (2016). Performance of Reinforced Concrete Columns Using Ultra-High-Strength Fiber-Reinforced Self-Compacted Concrete (UHS-FRSCC). *MOJ Civil Engineering*. **1**, 1-5.

El-Dieb, A.S. (2009). Mechanical, durability and microstructural characteristics of ultra-high-strength self-compacting concrete incorporating steel fibers. *Material and Design*. **30(10)**, 4286-4292.

Eligehausen, R., Popov, E.P., and Bertero, V.V. (1983). Local bond stress-slip relationships of deformed bars under generalized excitations. Report No. UCB/EERC-82/ 23, *Earthquake Engineering Research Center*, University of California at Berkeley. California 169 pp.

Ellobody, E. (2013). Nonlinear behavior of eccentrically loaded FR concrete-filled stainless steel tubular columns. *Journal of Constructional Steel Research*. **90**, 1-12.

Ellobody, E., Young, B., Lam, D. (2006). Behaviour of normal and high strength concrete-filled compact steel tube circular stub columns. *Journal of Constructional Steel Research*. **62**, 706-715.

EN 1992-1-1:2004. Design of concrete structures. General rules and rules for buildings.

Eurocode 2. European Committee for Standardization: British Standards Institution. (2004). Design of concrete structures. Part 1-1: General rules and rules for buildings.

Eurocode 4. European Committee for Standardization: British Standards Institution. (2004). Design of composite steel and concrete structures. Part 1.1, General rules and rules for buildings.

Ferrara. L., Meda. A (2006). Relationships between fiber distribution, workability and the mechanical properties of SFRC applied to precast roof elements, *Materials and Structures*. **39**, 411-420.

Gambhir, M.L. 1985. Concrete technology. 2nd Edition. New Delhi, India: TataMcGraw-Hill.

Gao, J., Suqa, W., Morino, K. (1997). Mechanical properties of steel fiber-reinforced, high strength, lightweight concrete. *Cement and Concrete Composites*. **19**,307-313.

Giakoumelis, G., Lam, D. (2004). Axial capacity of circular concrete-filled tube columns. *Journal of Constructional Steel Research*. **60(7)**, 1049-1068.

Goto, Y. (1971). Crack formed in concrete around deformed tension bars. *ACI Journal*, **68**, 244-251.

Griffith, A.A., (1920). The phenomena of rupture and flow in solids. *Philosophical Transactions of Royal Society of London,* **221**, 163-198.

Guler, S., Lale, E., Aydogan, M. (2013). Behaviour of sfrc filled steel tube columns under axial load. *Advanced Steel Construction*. **9(1)**, 14-25.

Güneyisi, E. M., Gültekin A., Mermerdaş K. (2016). Ultimate capacity prediction of axially loaded. *International Journal of Steel Streuctures*. **16(1)**, 99-114.

Güneyisi, E., Gesoglu, M (2008). Properties of self-compacting mortars with binary and ternary cementitious blends of fly ash and metakaolin. *Matererials and Structeres*. **41**, 1519–1531.

Güneyisi, E., Gesoğlu, M., Akoi, A.M.O., Mermerdaş, K. (2014). Combined effect of steel fiber and metakaolin incorporation on mechanical properties of concrete. *Composites: Part B*. **56**, 83-91.

Güneyisi, E., Gesoglu, M., Al-Goody, A., Ipek, S.(2015). Fresh and rheological behavior of nano-silica and fly ash blended self-compacting concrete, *Construction and Building Materials*. **95**, 29–44.

Güneyisi, E., Gesoğlu, M., Karaboğa, F., Mermerdaş, K. (2013). Corrosion behavior of reinforcing steel embedded in chloride contaminated concretes with and without metakaolin. *Composites: Part B,* **45**, 1288–1295.

Güneyisi, E., Gesoğlu, M., Karaoğlu, S., Mermerdaş, K. (2012). Strength, permeability and shrinkage cracking of silica fume and metakaolin concretes. *Construction and Building Materials*, **34**, 120-130.

Güneyisi, E., Gesoğlu, M., Mermerdaş, K. (2008). Improving strength, drying shrinkage, and pore structure of concrete using metakaolin. *Materials and Structures*, **41**, 937-49.

Güneyisi, E., Gesoglu, M., Omer, A., Akoi, M., Mermerdas (2014). Combined effect of steel fiber and metakaolin incorporation on mechanical properties of concrete. *Composites: Part B*. **56**, 83-91.

Güneyisi, E., Gesoğlu, M., Özturan, T., İpek, S. (2015). Fracture behavior and mechanical properties of concrete with artificial lightweight aggregate and steel fiber. *Construction and Building Materials.* **84**, 156-168.

Güneyisi, E., Gesoğlu, M., Özturan, T., Mermerdaş, K. (2012). Microstructural properties and pozzolanic activity of calcined kaolins as supplementary cementing materials. *Canadian Journal Civil Engineering*, **39**, 1274-1284.

Güneyisi, E., Gesoglu., M (2008). Properties of self-compacting mortars with binary and ternary cementitious blends of fly ash and metakaolin. *Matererials and Structeres*. **41**, 1519–1531.

Gupta, P.K., Sarda, S.M., Kumar, M.S. (2007). Experimental and computational study of concrete filled steel tubular columns under axial loads. *Journal of Constructional Steel Research*. **63(2)**, 182-193.

Hadi, Mns. (2008). Bond of high strength concrete with high strength reinforcing steel, *The Open Civil Journal*, vol. **2**, 143-147.

Hajjar, J.F. (1998). A distributed plasticity model for concrete-filled steel tube beam columns with interlayer slip. *Engineering Structures*. **20(8)**, 663-676.

Han, L. H., Yao, G.H. (2004). Experimental behaviour of thin-walled hollow structural steel (HSS) columns filled with self-consolidating concrete (SCC). *Thin-Walled Structures*. **42(9)**, 1357-1377.

Han, L.H. (2007). Concrete filled steel tubular structures-theory and practice, Science Press, Beijing, China, in Chinese.

Han, L.H., Li, W., Bjorhovde, R. (2014). Developments and advanced applications of concrete-filled steel tubular (CFST) structures: Members. *Journal of Constructional Steel Research*. **100**, 211-228.

Han, L.H., Tao, Z., Huang, H., Zhao, X.L. (2004). Concrete-filled double-skin (SHS outer and CHS inner) steel tubular beam-columns. *Thin-Walled Structures*. **42(9)**, 1329-1355.

Han, L.H., Yao, G.H., Zhao, X.L. (2005). Tests and calculations for hollow structural steel (HSS) stub columns filled with self-consolidating concrete (SCC). *Journal of Constructional Steel Research*. **61(9)**, 1241-1269.

Hassanein, M.F., Kharoob, O.F., Liang, Q.Q. (2013). Circular concrete-filled double skin tubular short columns with external stainless steel tubes under axial compression. *Thin-Walled Structures.* **73**, 252-263.

Hassanein, M.F., O.F. Kharoob. (2014). Compressive strength of circular concrete-filled double skin tubular short columns. *Thin-Walled Structures*. **77,** 165-173.

Hassanpour, M., Shafigh, P., Mahmud, H B (2012). Lightweight aggregate concrete fiber reinforcement – a review. *Construction and Building Matererials*.**37**,452–61.

Hillerborg, A., Modeer, M. and Peterson, P.E. (1976). Analysis of crack formation and crack growth in concrete by means of fracture mechanics and finite elements. *Cement and Concrete Research,* **6**, 773-782.

Hu, X.Z., and Wittman, F.H. (2000). Size effect on toughness induced by crack close to free surface. *Engineering Fracture Mechanics,* **65**, 209-211.

Huang, C.S., Yeh, Y.-K. Liu, G.-Y., Hu, H.-T. (2002). Axial Load Behavior of Stiffened Concrete-Filled Steel Columns. *Journal of Structural Engineering, ASCE.* **128(9)**, 1222-1230.

Huang, H., Han, L.H., Tao, Z., Zhao, X.L. (2010). Analytical behavior of concrete-filled double skin steel tubular (CFDST) stub columns. *Journal of Constructional Steel Research*. **66(4)**, 542-555.

Huang, Y. (2015). Seismic behavior of concrete filled steel tubular built-up columns. *Ph.D Thesis*. University of Trento, Italia.

Hubertova, M., Hela, R. (2007). The effect of metakaolin and silica fume on the properties of lightweight self-consolidating concrete. ACI Publication SP-243- 3, Detroit: American Concrete Institute, 35-48.

Irwin, G.R. (1957). Analysis of stresses and strains near the end of a crack transversing a plate. *Journal of Applied Mechanics*, **24**, 361-364.

Jaffry, S.A.D. (2001). concrete filled glass fibre reinforced polymerr (GFRP) shells under concentric compression. *MSc Thesis*. University of Toronto, Canada.

Jalal, M., Mansouri, E., Sharifipour, M.,Pouladkhan, A. (2012). Mechanical, rheological, durability and microstructural properties of high performance self-compacting concrete containing SiO2 micro and nanopartic, *Materials and Design* **34**, 389–400.

Jamaluddin, N., Lam, D., Dai, X.H., Ye, J. (2013). An experimental study on elliptical concrete filled columns under axial compression. *Journal of Constructional Steel Research*. **87**, 6-16.

Jenq, Y. and Shah, S.P. (1985). Two parameter fracture model for concrete. *ASCE Journal of Engineering Mechanics,* **11**, 1227-1241.

Ji, T (2005). Preliminary study on the water permeability and microstructure of concrete incorporating nano-SiO2. *Cement Concrete Research*. **35**:1943–7.

Jo, B., Kim, C.H., Tae, G.H., Park, J.B. (2007). Characteristics of cement mortar with nano- SiO_2 particles. *Construction and Building Materials*, **21**, 1351–1355.

Johnson, R.P. (2004). Composite structures of steel and concrete beams, slabs, columns, and frames for buildings. Third Edition, Blackwell Publishing. ISBN 1-4051-0035-4.

Kaplan, M.E. (1961). Crack propagation and fracture of concrete. *Journal of American Concrete Institute*, **58**, 591-610.

Karihaloo, B.L. 1995. Fracture mechanics and structural concrete. Essex, England: Longman Group Ltd.

Khaloo, A., Raisi, E. M., Hosseini, P., Tahsin, H. (2014). Mechanical performance of self-compacting concrete reinforced with steel fibers. *Construction and Building Materials*. **51(1)**, 179-186.

Kilpatrick, A.E., Rangan, B.V. (1999). Influence of interfacial shear transfer on behavior of concrete-filled steel tubular columns, *ACI Structural Journal*. **96(4)**, 642-648.

Korpa, A., Kowald, T., Trettin, R. (2008). Hydration ahaviour, Structure and morphology of hydration phases in advanced cement-based systems containing micro and nanoscale pozzolanic additives. *Cement and Concrete Research*, **38**, 955–962.

Krauss, H.W., Budelmann, H. (2011). Hydration kinetics of cement paste with very fine inert mineral additives. *Proceedings RILEM*, **79**, 58–65.

Kumar, A., Bishnoi, S., Scrivener, K.L. (2012). Modelling early age hydration kinetics of alite. *Cement and Concrete Research*, **42**, 903–918.

Lachemi, M., Hossain, K.M., Lambros, V. (2006). Self-consolidating concrete filled steel tube columns – design equations for confinement and axial strength. *Structural Engineering and Mechanics*. **22(5)**, 541-562.

Lai, M.H., Ho, J.C.M. (2013). Uni-axial compression test of concrete-filled-steel-tube columns confined by tie bars. *Procedia Engineering*. **57**, 662-669.

Land, G., Stephan, D. (2012). The influence of nano-silica on the hydration of ordinary Portland cement. *J. Mater. Sci*, **47**, 1011–1017.

Lange-Kornbak, D., Karihaloo, B.L. (1998). Design of fibre-reinforced DSP mixes for minimum brittleness, *Adv Cem Based Mater*, **7**, 89– 101.

Lemond, J.F., Pielert, J.H (2006). Fiber-reinforced concrete. Signifigance of tests and properties of concrete making materials, STP 169D, ASTM international, West Conshohocken, Pennsylvania, U.S.A. pp 578-589.

Li, G. (2004). Properties of high volume fly ash concrete incorporating nano-silica. *Cement and Concrete Research*, **34**, 1043–9.

Li, G., Zhao, X (2003). Properties of concrete incorporating fly ash and ground granulated blast-furnace slage. *Cement Concrete Composite*. **25**, 293–9.

Li, H., Xiao, H G., Yuan, J., Ou, J (2005). Microstructure of cement mortar with nanoparticles.*Composites:* Part B. **35**:185–9.

Li, H., Zhang, M H, Ou, J P (2006). Abrasion resistance of concrete containing nanoparticles for pavement. Wear. **260**,1262–6.

Liang, Q. Q., Fragomenu, S. (2009). Nonlinear analysis of circular concrete-filled steel tubular short columns under axial loading. *Journal of Constructional Steel Research.* **65**, 2186-2196.

Liao, W.-C., Chao, S.-H., Park, S.-Y., Naaman, A. E. (2006). Self-Consolidating High Performance Fiber Reinforced Concrete (SCHPFRC) – Preliminary Investigation. Ann Arbor, USA: University of Michigan.

Library of Japanese Society of Civil Engineers, June 25, p. 107-120.

Lothenbach, B., Scrivener, K., Hooton, R.D. (2011). Supplementary cementitious materials. *Cement and Concrete Research*, **41**, 1244–1256.

Lu, F.W., Li, S.P., Sun, G. (2007). A study on the behavior of eccentrically compressed square concrete-filled steel tube columns. *Journal of Constructional Steel Research*. **63**, 941-948.

Lu, Z-H., Zhao, Y.G. (2010). Suggested empirical models for the axial capacity of circular CFT stub columns. *Journal of Constructional Steel Research*. **66(6)**, 850-862.

M. Amin, K. Abu el-hassan (2015). Effect of using different types of nano materials on mechanical properties of high strength concrete. *Construction and Building Materials*, **80**, 116–124.

Ma, Y. S., Wang, Y. F. (2012). Creep of high strength concrete filled steel tube columns. *Thin-Walled Structures*. **53**, 91-98.

Mather, B. and Ozyildirim C. (2002). Concrete Primer. Farmington Hills, American Concrete Institute.

Matsui, C., Tsuda, K., Ishibashi, Y. (1995). Slender concrete filled steel tubular columns under combined compression and bending. In: PSSC'95 4th pacific structural steel conference. *Steel–concrete composite structures*. **3**, 29-36.

McCormac, J.C., Brown, R.H. (2014). Design of reinforced concrete. 9th edition. John Wiley & Sons, Inc, USA.

Mehta, P.K., Monteiro, P.J.M. (2006). Concrete; microstructure, properties, and materials. 3rd edition. New York: McGraw-Hill.

Mehta; K.P., Monteiro, P.J.M. (2006). Concrete Microstructure, Properties, and Materials, Mc Graw-Hill, New York.

Mindess, S. and Diamond, S. (1982). The cracking and fracture of mortar. *Materials and Structures*, **15**, 107-113.

Minelli, F. (2005). Plain and Fiber Reinforced Concrete Beams under Shear LoadingStructural Behavior and Design Aspects *"A PhD dissertation"*. Italy: University of Brescia.

Moliner, V., Espinos, A., Romero, M.L., Hospitaler, A. (2013). Fire behavior of eccentrically loaded slender high strength concrete-filled tubular columns. *Journal of Constructional Steel Research*. **83(1)**, 137-146.

Muciaccia, G., Giussani, F., Rosati, G., Mola, F. (2011). Response of self-compacting concrete filled tubes under eccentric compression. *Journal of Constructional Steel Research.* **67**, 904-916.

MWM. Metal Wire Mesh. http://www.metalmesh.com.cn/news/Do-steel-fibers-affect-the-slump-of-concrete--9.html. 01/12/2012.

N. Banthia (1994). Fiber reinforced concrete. ACI SP-142ACI, Detroit, MI; 1994. p. 91–119.

Naaman, A.E. (1985). Fibre reinforcement for concretes. *Concrete International, Design and Construction*, **7**, 21-25.

Naaman, A.E. (2003). Engineered Steel Fibers with Optimal Properties for Reinforcement of Cement Composites. *Journal of Advanced Concrete Technology,***1**,241-252.

Nagamoto N., Ozawa K. (1997). Mixture properties of Self-Compacting, High-Performance Concrete, Proceedings, Third CANMET/ACI International Conferences on Design and Materials and Recent Advances in Concrete Technology, SP-172, V. M. Malhotra, American Concrete Institute, Farmington Hills, Mich,p. 623-637.

Nallathambi, P., and Karihaloo, B.L. (1990). Fracture of concrete: Application of effective crack model. *in 9th International Conference on Experimental Mechanics,* Volume. 4, *Lyngby,* Denmark, 20-24 August, 1413-1422.

Nanni, A. (1998). Splitting-tension test for fiber reinforced concrete. *ACI Material Journal*, **85**, 229-233.

Nehdi, M., Mindess, s., Aitcin P.- C. (1998). Rheology of high performance concrete: effect of ultra-fine particles. *Cement Concrete Ressearch*. **28**, 687–97.

Nili M, Afroughsabet V. (2012). Property assessment of steel–fibre reinforced concrete made with silica fume. *Construction and Building Materials*. **28:** 664-9.

O. Gencel, W. Brostow, T. Datashvili, M. Thedford (2011). Workability and mechanical performance of steel fiber-reinforced self-compacting concrete with fly ash. *Compos Interface*, **18(2)**, 169–84.

Oertel, T., Hutter, F., Tänzer, R. (2013). Primary particle size and agglomerate size effects of amorphous silica in ultra-high performance concrete. *Cement Concrete Composite*, **37**, 61–67.

Oh, J.Y., Lee, D.H., Lee, J., Kim, K.S., Kim, S.B. (2016). Experimental study on reinforced concrete column incased in prefabricated permanent thin-walled steel form. *Advances in Materials Science and Engineering*. doi:10.1155/2016/3806549.

Okamura H., ozawa K. (1995). Mix Design for Self-Compacting Concrete, Concrete

Olivito. R.S., Zuccarello. F.A (2010). An experimental study on the tensile strength of steel fiber reinforced concrete. *Composites: Part B.* **41**, 246-255.

Orbe. A., Cuadrado. J., Losada. R., Roj. E (2012). Framework for the design and analysis of steel fiber reinforced self-compacting concrete structures. *Construction and Building Materials*. **35**, 676-686.

Ozyurt, N. (2005). Connecting fiber dispersion, rheology and mechanical performance for fiber reinforced cement based materials. PhD Thesis, Istanbul Technical University, Turkey.

P.F. Torgal, S. Miraldo, Y. Ding, J.A. Labrincha (2013). Targeting HPC with the help of nanoparticles: an overview. *Constr Build Mater*, **38**, 365–370.

Park, R., Paulay, T. (1975). Reidorced Concrete Structures. *John Wiley and Sons, New York*.

Patel, V. I., Liang, Q. Q., Hadi, M. N. S. (2014). Behavior of biaxially-loaded rectangular concrete-filled steel tubular slender beam-columns with preload effects. *Thin-Walled Structures.* **79**, 166-177.

Petrus, C., Abdul Hamid, H., Ibrahim, A., Parke, G. (2010). Experimental behaviour of concrete filled thin walled steel tubes with tab stiffeners. *Journal of Constructional Steel Research.* **66**, 915-922.

Pillai, S.U., Kirk, D.W. (1983). Reinforced concrete design in Canada. 2nd Edition. Canada: McGraw-Hill.

Pillai, SU., Kirk, DW (1983). Reinforced concrete design in Canada. McGraw-hill.

Pires, T.A.C., Rodrigues, J.P.C., Silva, J.J.R. (2012). Fire resistance of concrete filled circular hollow columns with restrained thermal elongation. *Journal of Constructional Steel Research*. **77(1)**, 82-94.

Prion, H.G.L., Boehme, J. (1989). Beam-column behavior of steel tubes filled with high strength concrete. In: Fourth international colloquium. SSRC. 439–49.

Qing, Y., Zenan, Z., Deyu, K., Rongshen, K (2007). Influence of nano-SiO_2 addition on properties of hardened cement paste as compared with silicafume. *Construction Building Materials*. **21**,539–545.

Qing, Y., Zenan, Z., Deyu, K., Rongshen, C. (2007). Influence of nano- SiO_2 addition on properties of hardened cement paste as compared with silica fume. *Construction and Building Materials*, **21**, 539–45.

R. Yu, P. Spiesz, H.J.H. Brouwers (2014). A study of multiple effects of nano-silica and hybrid fibres on the properties of Ultra-High Performance Fibre Reinforced Concrete (UHPFRC) incorporating waste bottom ash (WBA). *Constr Build Mater*. **60**, 98–110.

Richart, F.E., Brandzaeg, A., Brown, R.L. (1928). A study of the failure of concrete under combined compressive stresses. Bull. 185. Champaign (IL, USA): University of Illinois Engineering Experimental Station.

RILEM 50-FMC. (1985). Committee of fracture mechanics of concrete. Determination of fracture energy of mortar and concrete by means of three-point bend tests on notched beams. *Materials and Structures,***18**, 285–290.

RILEM RC6. (1996). Recommendations for the testing and use of constructions materials bond test for reinforcement steel. 2. Pull-out test, 3 pages.

RILEM TC 162 TDF, Design of Steel fibre reinforced concrete – Method, recommendations, Material and Structures, March 2001.

Ritchie, A., Rahman, T. (1973). The effect of fiber reinforcements on the rheological Properties of concrete mixes. *American Concrete Institute*, 29-44.

Roeder, C.W., Cameron, B., Brown, C.B. (1999). Composite action in concrete filled tubes. *Journal of Structural Engineering ASCE*. **125(5)**, 477-484.

Ross, A. (2008). Steel fibre reinforced concrete (SFRC) – Quality, performance and specification. BOSFA (Bekaert one steel fibres australasia).

Rteil, A., (2007). Fatigue bond behaviour of corroded reinforcement a CFRP confined concrete. PhD thesis. Canada, University of Waterloo.

Sabir, B.B., Wild, S., Bai, J. (2001). Metakaolin and calcined clays as pozzolans for concrete: a review, *Cement Concrete Composite*, **23**, 441-454.

Sakino, K, Tomii, M., Watanabe, K. (1985). Sustaining load capacity of plain concrete stub columns by circular steel tubes. In: Proc. int. spec. conf. on concrete-filled steel tubular struct. 112-118.

Sakino, K., Nakahara, H., Morino, S., Nishiyama, I. (2004). Behavior of centrally loaded concrete-filled steel-tube short columns. *Journal of Structural Engineering. ASCE.* **130(2)**, 180-188.

Saloma, A. Nasution, I. Imran, M. Abdullah (2013). Experimental investigation on nanomaterial concrete. *Int J Civ Environ Eng*, **13**, 15–20.

Şamhâl, E. (2005). Lecture 1.1: Composite Construction. http://web.itu.edu.tr/~haluk/COMPOSITE%201.pdf.

Schneider, S.P. (1998). Axially loaded concrete-filled steel tubes. *Journal of Structural Engineering*. **124(10)**, 1125-1138.

Shah, S.P., Naaman, A.E. (1976). Mechanical properties of glass and steel fibre reinfoced mortar. *ACI Journal*. **73**, 50-53.

Shah, S.P., Swartz, S.E., and Ouyang, C. (1995). Fracture mechanics of concrete: applications of fracture mechanics to concrete, rock, and other quasi-brittle materials. John Wiley & Sons, Inc., New York.

Shaikh, F.U.A., Supit, S. (2014). Mechanical and durability properties of high volume fly ash (HVFA) concrete containing calcium carbonate (CaCO3) nanoparticles. *Construction and Building Materials*, **70**, 309–321.

Shikoku Island Concrete Research Association. (2000 - 2002). Report by Self-Compacting Concrete Research Committee, Self-Compacting Concrete in Shikoku Island.

Shvarzman, A., Kovler, K., Grader, G.S., Shter, G.E. (2003). The effect of dehyroxylation/amorphization degree on pozzolanic activity of kaolinite. *Cement Concrete Research*, **31**, 405-416.

Siddique, R., Kaur, G., Kunal (2013). Strength and permeation properties of self-compacting concrete containing fly ash and hooked steel fibres. *Construction and Building Materials*. **103**, 15–22.

Simoes. T., Costa. H., Dias-da-Costa. D., Julio. E (2017). Influence of fibers on the mechanical behaviour of fibre reinforced concrete matrixes. Construction and Building Materials. 137, 548-556.

Song. P., Hwang. S (2004). Mechanical properties of high-strength steel fiber reinforced concrete. *Construction and Building Materials*. **18**, 669-673.

Sorelli. L., Meda. A., Plizzari. G (2006). Steel fiber concrete slabs on ground: a structural matter. *Aci Structural Jornal*, **103**, 551-558.

Stracturae-International database for civil and structural engineering. New Applications for Steel Fibre Reinforced Concrete and Combined Reinforcement. www.Structurae.net.

Sucharda, O., Pajak, M., Ponikiewski, T., Konecny, P (2017). Identification of mechanical and fracture properties of self-compacting concrete beams with different types of steel fibres using inverse analysis. *Construction and building materials*. **138**, 263-275.

Supit, S., Shaikh, F.U A., Sarker, P.K. (2013). Effect of nano silica and ultrafine fly ash on compressive strength of high volume fly ash mortar. *Appl Mech Mater*, **106**, 1–5.

Svensson, H.S. (2005). Modern composite bridges in Germany. *The Structural Engineer*. **83(4)**, 21–28.

Tao, Z., Han, L.H. (2006). Behaviour of concrete-filled double skin rectangular steel tubular beam–columns. *Journal of Constructional Steel Research*. **62**, 631-664.

Tao, Z., Han, L.H., Wang, D.Y. (2008). Strength and ductility of stiffened thin-walled hollow steel structural stub columns filled with concrete. Thin-Walled Structures. **10(46)**, 1113-1128.

Tao, Z., Song, T-Y., Uy, B., Han, L-H. (2016). Bond behavior in concrete-filled steel tubes. *Journal of Constructional Steel Research*. **120**, 81-93.

Tao, Z., Uy, B., Han, L.H., Wang, Z.B. (2009). Analysis and design of concrete-filled stiffened thin-walled steel tubular columns under axial compression. *Thin-Walled Structures*. **47(12)**, 1544-1556.

Taşdemir, C., and Taşdemir, M.A. (1996). Effects of silica fume and aggregate size on the brittleness of concrete. *Cement and Concrete Research*, **26**, 63-68.

Taşdemir, M.A. and Karihaloo, B.L. (2001). Effect of aggregate volume fraction on the parameters of concrete: A meso-mechanical approach. *Magazine of Concrete Research*, **53**, 405-415.

Thomas, J.J., Jennings, H.M., Chen, J.J. (2009). Influence of nucleation seeding on the hydration mechanisms of tricalcium silicate and cement. *The jornal of physical chemistry C*, **113**, 4327–4334.3.

Thomas. J., Ramaswamy. A (2007). Mechanical properties of steel fiber-reinforced concrete. *Jornal of Materials in Civil Engineering*. **19**, 385–392.

Tokgoz, S., Dundar, C. (2010). Experimental study on steel tubular columns in-filled with plain and steel fiber reinforced concrete. *Thin-Walled Structures.* **48,** 414-422.

Tu, Y.Q., Shen, Y.F., Li, P. (2014). Behaviour of multi-cell composite T-shaped concrete-filled steel tubular columns under axial compression. *Thin-Walled Structures*. **85**, 57-70.

Turkish Standard TS EN 197-1. (2002). Çimento-bölüm 1: genel cimentolar-bilesim, ozellikler ve uygunluk kriterleri. UM, the University of Memphis.

Uenaka, K., Kitoh, H., Sonoda, K. (2010). Concrete filled double skin circular stub columns under compression. *Thin-Walled Structures*. **48**,19-24.

UM, The University of Memphis. http://www.ce.memphis.edu/1101/notes/concrete/PCA_manual/Chap03.pdf.12/12/2012.

Uy, B., Tao, Z., Han, L.H. (2011). Behaviour of short and slender concrete-filled stainless steel tubular columns. *Journal of Constructional Steel Research*. **67(3)**, 360-378.

Uy, B., Wright, H.D., Bradford, M.A. (2001). Combined axial and flexural strength of profiled composite walls. *Structures and Buildings*. **146(2)**, 129-139.

Varma, A.H., Ricles, J.M., Sause, R., Lu, L.W. (2002). Experimental behavior of high strength square concrete-filled steel tube beam-columns. *Journal of Structural Engineering*, *ASCE*. **128(3)**, 309-318.

Wafa, F.F., Ashour, S.A. (1992). Mechanical properties of high-strength fibre reinforced concrete. *ACI Materials Journal*, **89**, 449-455.

Wang, Y., Chen, J., Geng, Y. (2015). Testing and analysis of axially loaded normal-strength recycled aggregate concrete filled steel tubular stub columns. *Engineering Structures*. **86**, 192-212.

Wang, Y.C. (2014). Design guide for concrete filled hot finished structural hollow section (SHS) columns. www.steelconstruction.info/File:CFT_Design_Guide_March_2014.pdf? internal_link

Wang. S., Zhang. M-H., Quek. S.T (2012). Mechanical behavior of fiber-reinforced high strength concrete subjected to high strain-rate compressive loading. *Construction and Building Materials*. **31**, 1–11.

Wardenier, J., Packer, J.A., Zhao, X.L., Van der Vegte, G.J. (2010). Hollow sections in structural applications. CIDECT, Geneva, Switzerland.

Warner, R.F., Rangam, B.V., Hall, A.S., Faulkes, K.A. (1998). Concrete structures, Longman, Australia. *The Open Civil Engineering Journal*, **2**, 143-147.

Weiler, B., Grosse, C. (2010). Pullout behaviour of fibers in steel fiber reinforced concrete. MSc thesis. Malaysia, Universiti Technologi Malaysia.

Wikipedia (2016) https://en.wikipedia.org/wiki/SEG_Plaza

Wild, S., Khatip, J M., Jones, A (1996). Relative strength, pozzolanic activity and cement hydration in superplasticized metakaolin concrete. *Cement and Concrete Research*. **26**:1537–44.

Wild, S., Khatip, J.M., Jones, A. (1996). Relative strength, pozzolanic activity and cement hydration in superplasticized metakaolin concrete. *Cement and Concrete Research,* **26**, 1537-1544.

www.Amvicsystem.com

Yan, P.Y. and Yu, C.H. (2009). Application of self consolidating concrete in Beijing." In: Shi, Yu, Khayat, and Yan, eds., *RILEM Proceedings, PRO 65, Design, performance and use of self-consolidating concrete,SCC'2009* , Beijing, pp. 817–822.

Yardimci, M Y., Baradan, B and Tasdemir, M A., (2014). Effect of fine to coarse aggregate ratio on the rheology and fracture energy of steel fibre reinforced self-compacting concretes. *Sadhana.* **39**, 1447–1469. Indian Academy of Sciences.

Yin, J., Zha, X., Li, L. (2006). Fire resistance of axially loaded concrete filled steel tube columns. *Journal of Constructional Steel Research*. **62**, 723-729.

Yi-yan, L., Na, L., Shan, L., Hong-jun, L. (2015). Experimental investigation of axially loaded steel fiber reinforced high strength concrete-filled steel tube columns. *Journal of Central South University of Technology*. **22**, 2287-2296.

Yu, Q., Tao, Z., Wu, Y. (2008). Experimental behaviour of high performance concrete-filled steel tubular columns. *Thin-Walled Structures.* **46(4)**, 362-370.

Yuan, W.B, and Yang J.J. (2013). Experimental and numerical studies of short concrete-filled double skin composite tube columns under axially compressive loads. *Journal of Constructional Steel Research*. **80**, 23-31.

PERSONAL INFORMATION

Name and Surname: JAMEEL, Ghassan Subhi

Nationality: Iraqi

Birth place and date: Iraq-Anbar/01-January-1980

Marital status: married

Phone number: +90 5368870681

Email: gsj_alkubaisi@yahoo.com

EDUCATION

Master degree: Civil Engineering Dep., College of engineering, AL-Anbar University (2009)

Bachelor's degree: Civil Engineering Dep., College of engineering, AL-Anbar University (2002)

High School: AL-Romaila (1998)

Work experience

2003-2009: Civil Engineer, Dams and Water Recourse, College Of Engineering, AL-Anbar University

2009-2013: Assist Lecturer, Dams and Water Recourse, College Of Engineering, AL-Anbar University

2013-Present: Lecturer, Dams and Water Recourse, College of Engineering, AL-Anbar University

PUBLICATIONS

[1] Ghassan Subhi Jameel (2013). Study The Effect Of Waste Plastic On Compressive And Tensile Strengths Of Structural Lightweight Concrete Containing Broken Bricks As A Coarse Aggregate. *International Journal Of Civil Engineering And Technology*. **4**, 415-432.

[2] Abdulkader Ismail Al – Hadithi, Ahmed Tareq Al–Ejbari, Ghassan subhi jameel (2013). Behaviour of Waste Fiber Concrete Slabs Under Low Velocity Impact. *Iraqi Journal Of Civil Engineering*. **9**, 135-148.

FOREIGN LANGUAGE

Arabic (Mother Language), English and Turkish